

To appear in
FRONTIERS IN NUMBER THEORY, PHYSICS, AND GEOMETRY VOL.I,
P. Cartier; B. Julia; P. Moussa; P. Vanhove (Editors),
Springer Verlag, 2006.

Flat Surfaces

Anton Zorich

IRMAR, Université de Rennes 1, Campus de Beaulieu, 35042 Rennes, France
`Anton.Zorich@univ-rennes1.fr`

Summary. Various problems of geometry, topology and dynamical systems on surfaces as well as some questions concerning one-dimensional dynamical systems lead to the study of closed surfaces endowed with a flat metric with several cone-type singularities. Such flat surfaces are naturally organized into families which appear to be isomorphic to moduli spaces of holomorphic one-forms.

One can obtain much information about the geometry and dynamics of an individual flat surface by studying both its orbit under the Teichmüller geodesic flow and under the linear group action. In particular, the Teichmüller geodesic flow plays the role of a time acceleration machine (renormalization procedure) which allows to study the asymptotic behavior of interval exchange transformations and of surface foliations.

This survey is an attempt to present some selected ideas, concepts and facts in Teichmüller dynamics in a playful way.

57M50, 32G15 (37D40, 37D50, 30F30)

Key words: Flat surface, billiard in polygon, Teichmüller geodesic flow, moduli space of Abelian differentials, asymptotic cycle, Lyapunov exponent, interval exchange transformation, renormalization, Teichmüller disc, Veech surface

1	Introduction	3
1.1	Flat Surfaces	4
1.2	Very Flat Surfaces	5
1.3	Synopsis and Reader's Guide	7
1.4	Acknowledgments	12
2	Eclectic Motivations	12
2.1	Billiards in Polygons	12
2.2	Electron Transport on Fermi-Surfaces	17
2.3	Flows on Surfaces and Surface Foliations	20

3	Families of Flat Surfaces and Moduli Spaces of Abelian Differentials	21
3.1	Families of Flat Surfaces	22
3.2	Toy Example: Family of Flat Tori	23
3.3	Dictionary of Complex-Analytic Language	25
3.4	Volume Element in the Moduli Space of Holomorphic One-Forms	27
3.5	Action of $SL(2, \mathbb{R})$ on the Moduli Space	28
3.6	General Philosophy	30
3.7	Implementation of General Philosophy	31
4	How Do Generic Geodesics Wind Around Flat Surfaces	33
4.1	Asymptotic Cycle	33
4.2	Deviation from Asymptotic Cycle	35
4.3	Asymptotic Flag and “Dynamical Hodge Decomposition”	37
5	Renormalization for Interval Exchange Transformations. Rauzy–Veech Induction	39
5.1	First Return Maps and Interval Exchange Transformations	39
5.2	Evaluation of the Asymptotic Cycle Using an Interval Exchange Transformation	41
5.3	Time Acceleration Machine (Renormalization): Conceptual Description	44
5.4	Euclidean Algorithm as a Renormalization Procedure in Genus One	48
5.5	Rauzy–Veech Induction	50
5.6	Multiplicative Cocycle on the Space of Interval Exchanges	54
5.7	Space of Zippered Rectangles and Teichmüller geodesic flow	58
5.8	Spectrum of Lyapunov Exponents (after M. Kontsevich, G. Forni, A. Avila and M. Viana)	63
5.9	Encoding a Continued Fraction by a Cutting Sequence of a Geodesic	67
6	Closed Geodesics and Saddle Connections on Flat Surfaces	69
6.1	Counting Closed Geodesics and Saddle Connections	70
6.2	Siegel–Veech Formula	75
6.3	Simplest Cusps of the Moduli Space	79
6.4	Multiple Isometric Geodesics and Principal Boundary of the Moduli Space	81
6.5	Application: Billiards in Rectangular Polygons	87
7	Volume of Moduli Space	90
7.1	Square-tiled Surfaces	91
7.2	Approach of A. Eskin and A. Okounkov	97
8	Crash Course in Teichmüller Theory	99
8.1	Extremal Quasiconformal Map	99
8.2	Teichmüller Metric and Teichmüller Geodesic Flow	101

9	Hope for a Magic Wand and Recent Results	102
9.1	Complex Geodesics	102
9.2	Geometric Counterparts of Ratner's Theorem	103
9.3	Main Hope	104
9.4	Classification of Connected Components of the Strata	106
9.5	Veech Surfaces	111
9.6	Kernel Foliation	115
9.7	Revolution in Genus Two (after K. Calta and C. McMullen)	121
9.8	Classification of Teichmüller Discs of Veech Surfaces in $\mathcal{H}(2)$	129
10	Open Problems	132
A	Ergodic Theorem	135
B	Multiplicative Ergodic Theorem	137
B.1	A Crash Course of Linear Algebra	137
B.2	Multiplicative Ergodic Theorem for a Linear Map on the Torus	138
B.3	Multiplicative Ergodic Theorem	139
	References	141

1 Introduction

These notes correspond to lectures given first at Les Houches and later, in an extended version, at ICTP (Trieste). As a result they keep all blemishes of oral presentations. I rush to announce important theorems as facts, and then I deduce from them numerous corollaries (which in reality are used to prove these very keystone theorems). I omit proofs or replace them by conceptual ideas hiding under the carpet all technicalities (which sometimes constitute the main value of the proof). Even in the choice of the subjects I poach the most fascinating issues, ignoring those which are difficult to present no matter how important the latter ones are. These notes also contain some philosophical discussions and hopes which some emotional speakers like me include in their talks and which one, normally, never dares to put into a written text.

I am telling all this to warn the reader that this playful survey of some selected ideas, concepts and facts in this area cannot replace any serious introduction in the subject and should be taken with reservation.

As a much more serious accessible introduction I can recommend a collection of introductory surveys of A. Eskin [E], G. Forni [For2], P. Hubert and T. Schmidt [HuSdt5] and H. Masur [Ma7], organized as a chapter of the Handbook of Dynamical Systems. I also recommend recent surveys of H. Masur and S. Tabachnikov [MaT] and of J. Smillie [S]. The part concerning renormalization and interval exchange transformations is presented in the article of J.-C. Yoccoz [Y] of the current volume in a much more responsible way than my introductory exposition in Sec. 5.

1.1 Flat Surfaces

There is a common prejudice which makes us implicitly associate a metric of constant positive curvature to a sphere, a metric of constant zero curvature to a torus, and a metric of constant negative curvature to a surface of higher genus. Actually, any surface can be endowed with a flat metric, no matter what the genus of this surface is... with the only reservation that this flat metric will have several singular points. Imagine that our surface is made from plastic. Then we can flatten it from the sides pushing all curvature to some small domains; making these domains smaller and smaller we can finally concentrate all curvature at several points.

Consider the surface of a cube. It gives an example of a perfectly flat sphere with eight conical singularities corresponding to eight vertices of the cube. Note that our metric is nonsingular on edges: taking a small neighborhood of an interior point of an edge and unfolding it we get a domain in a Euclidean plane, see Fig. 1. The illusion of degeneration of the metric on the edges comes from the singularity of the embedding of our flat sphere into the Euclidean space \mathbb{R}^3 .

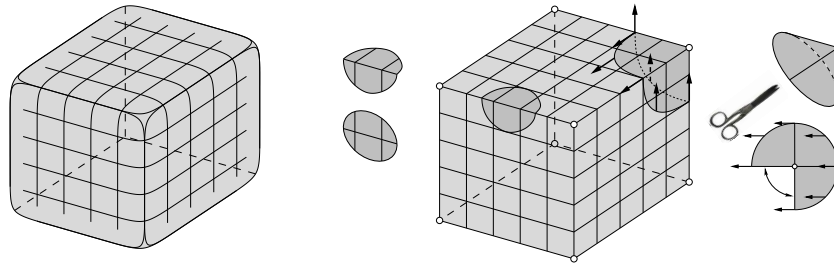


Fig. 1. The surface of the cube represents a flat sphere with eight conical singularities. The metric *does not* have singularities on the edges. After parallel transport around a conical singularity a vector comes back pointing to a direction different from the initial one, so this flat metric has nontrivial *holonomy*.

However, the vertices of the cube correspond to actual *conical singularities* of the metric. Taking a small neighborhood of a vertex we see that it is isometric to a neighborhood of the vertex of a cone. A flat cone is characterized by the *cone angle*: we can cut the cone along a straight ray with an origin at the vertex of the cone, place the resulting flat pattern in the Euclidean plane and measure the angle between the boundaries, see Fig. 1. Say, any vertex of the cube has cone angle $3\pi/2$ which is easy to see since there are three squares adjacent to any vertex, so a neighborhood of a vertex is glued from three right angles.

Having a manifold (which is in our case just a surface) endowed with a metric it is quite natural to study *geodesics*, which in a flat metric are locally isometric to straight lines.

General Problem. *Describe the behavior of a generic geodesic on a flat surface. Prove (or disprove) that the geodesic flow is ergodic¹ on a typical (in any reasonable sense) flat surface.*

Does any (almost any) flat surface has at least one closed geodesic which does not pass through singular points?

If yes, are there many closed geodesics like that? Namely, find the asymptotics for the number of closed geodesics shorter than L as the bound L goes to infinity.

Believe it or not there has been no (even partial) advance in solving this problem. The problem remains open even in the simplest case, when a surface is a sphere with only three conical singularities; in particular, it is not known, whether any (or even almost any) such flat sphere has *at least one* closed geodesic. Note that in this particular case, when a flat surface is a flat sphere with three conical singularities the problem is a reformulation of the corresponding billiard problem which we shall discuss in Sect. 2.1.

1.2 Very Flat Surfaces

A general flat surface with conical singularities much more resembles a general Riemannian manifold than a flat torus. The reason is that it has nontrivial *holonomy*.

Locally a flat surface is isometric to a Euclidean plane which defines a *parallel transport* along paths on the surface with punctured conical points. A parallel transport along a path homotopic to a trivial path on this punctured surface brings a vector tangent to the surface to itself. However, if the path is not homotopic to a trivial one, the resulting vector turns by some angle. Say, a parallel transport along a small closed path around a conical singularity makes a vector turn exactly by the cone angle, see Fig. 1. (Exercise: perform a parallel transport of a vector around a vertex of a cube.)

Nontrivial linear holonomy forces a generic geodesic to come back and to intersect itself again and again in different directions; geodesics on a flat torus (which has trivial linear holonomy) exhibit radically different behavior. Having chosen a direction to the North, we can transport it to any other point of the torus; the result would not depend on the path. A geodesic on the torus emitted in some direction will forever keep going in this direction. It will either close up producing a regular closed geodesic, or will never intersect itself. In the latter case it will produce a dense irrational winding line on the torus.

¹In this context “*ergodic*” means that a typical geodesic will visit any region in the *phase space* and, moreover, that in average it will spend a time proportional to the volume of this region; see Appendix A for details.

Fortunately, the class of flat surfaces with trivial linear holonomy is not reduced to flat tori. Since we cannot advance in the General Problem from the previous section, from now on we confine ourselves to the study of these *very flat* surfaces (often called *translation surfaces*): that is, to closed orientable surfaces endowed with a flat metric having a finite number of conical singularities and having trivial linear holonomy.

Triviality of linear holonomy implies, in particular, that all cone angles at conical singularities are integer multiples of 2π . Locally a neighborhood of such a conical point looks like a “*monkey saddle*”, see Fig. 2.

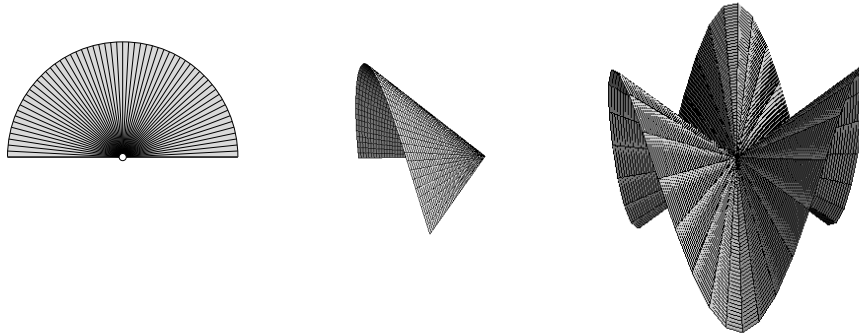


Fig. 2. A neighborhood of a conical point with a cone angle 6π can be glued from six metric half discs

As a first example of a nontrivial very flat surface consider a regular octagon with identified opposite sides. Since identifications of the sides are isometries, we get a well-defined flat metric on the resulting surface. Since in our identifications we used only parallel translations (and no rotations), we, actually, get a very flat (translation) surface. It is easy to see (check it!) that our gluing rules identify all vertices of the octagon producing a single conical singularity. The cone angle at this singularity is equal to the sum of the interior angles of the octagon, that is to 6π .

Figure 3 is an attempt to convince the reader that the resulting surface has genus two. We first identify the vertical sides and the horizontal sides of the octagon obtaining a torus with a hole of the form of a square. To simplify the drawing we slightly cheat: namely, we consider another torus with a hole of the form of a square, but the new square hole is turned by $\pi/4$ with respect to the initial one. Identifying a pair of horizontal sides of the hole by an isometry we get a torus with two holes (corresponding to the remaining pair of sides, which are still not identified). Finally, isometrically identifying the pair of holes we get a surface of genus two.

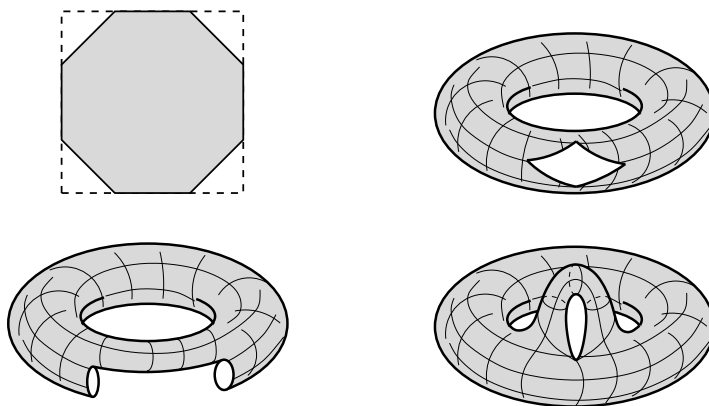


Fig. 3. Gluing a pretzel from a regular octagon

Convention 1. From now on by a *flat surface* we mean a closed oriented surface with a flat metric having a finite number of conical singularities, such that the metric has trivial linear holonomy. Moreover, we always assume that the flat surface is endowed with a distinguished direction; we refer to this direction as the “direction to the North” or as the “*vertical direction*”.

The convention above implies, in particular, that if we rotate the octagon from Fig. 3 (which changes the “direction to the North”) and glue a flat surface from this rotated octagon, this will give us a different flat surface.

We make three exceptions to Convention 1 in this paper: billiards in general polygons considered at the beginning Sec. 2.1 give rise to flat metrics with nontrivial linear holonomy. In Sec. 3.2 we consider flat tori forgetting the direction to the North.

Finally, in Sec. 8.1 we consider *half-translation surfaces* corresponding to flat metrics with holonomy group $\mathbb{Z}/2\mathbb{Z}$. Such flat metric is a slight generalization of a *very flat* metric: a parallel transport along a loop may change the direction of a vector, that is a vector \mathbf{v} might return as $-\mathbf{v}$ after a parallel transport.

1.3 Synopsis and Reader’s Guide

These lectures are an attempt to give some idea of what is known (and what is not known) about flat surfaces, and to show what an amazing and marvellous object a flat surface is: problems from dynamical systems, from solid state physics, from complex analysis, from algebraic geometry, from combinatorics, from number theory, ... (the list can be considerably extended) lead to the study of flat surfaces.

Section 2. Motivations

To give an idea of how flat surfaces appear in different guises we give some motivations in Sec. 2. Namely, we consider billiards in polygons, and, in particular, billiards in rational polygons (Sec. 2.1) and show that the consideration of billiard trajectories is equivalent to the consideration of geodesics on the corresponding flat surface. As another motivation we show in Sec. 2.2 how the electron transport on Fermi-surfaces leads to study of foliation defined by a closed 1-form on a surface. In Sec. 2.3 we show that under some conditions on the closed 1-form such a foliation can be “straightened out” into an appropriate flat metric. Similarly, a Hamiltonian flow defined by the corresponding multivalued Hamiltonian on a surface follows geodesics in an appropriate flat metric.

Section 3. Basic Facts

A reader who is not interested in motivations can proceed directly to Sec. 3 which describes the basic facts concerning flat surfaces. For most of applications it is important to consider not only an individual flat surface, but an entire family of flat surfaces sharing the same topology: genus, number and types of conical singularities. In Sec. 3.1 we discuss deformations of flat metric inside such families. As a model example we consider in Sec. 3.2 the family of flat tori. In Sec. 3.3 we show that a flat structure naturally determines a complex structure on the surface and a holomorphic one-form. Reciprocally, a holomorphic one-form naturally determines a flat structure. The dictionary establishing correspondence between geometric language (in terms of the flat metrics) and complex-analytic language (in terms of holomorphic one-forms) is very important for the entire presentation; it makes Sec. 3.3 more charged than an average one. In Sec. 3.4 we continue establishing correspondence between families of flat surfaces and strata of moduli spaces of holomorphic one-forms. In Sec. 3.5 we describe the action of the linear group $SL(2, \mathbb{R})$ on flat surfaces – another key issue of this theory.

We complete Sec. 3 with an attempt to present the following general principle in the study of flat surfaces. In order to get some information about an individual flat surface it is often very convenient to find (the closure of) the orbit of corresponding element in the *family* of flat surfaces under the action of the group $SL(2, \mathbb{R})$ (or, sometimes, under the action of its diagonal subgroup). In many cases the structure of this orbit gives comprehensive information about the initial flat surface; moreover, this information might be not accessible by a direct approach. These ideas are expressed in Sec. 3.6. This general principle is illustrated in Sec. 3.7 presenting Masur’s criterion of unique ergodicity of the directional flow on a flat surface. (A reader not familiar with the ergodic theorem can either skip this last section or read an elementary presentation of ergodicity in Appendix A.)

Section 4. Topological Dynamics of Generic Geodesics

This section is independent from the others; a reader can pass directly to any of the further ones. However, it gives a strong motivation for renormalization discussed in Sec. 5 and in the lectures by J.-C. Yoccoz [Y] in this volume. It can also be used as a formalism for the study of electron transport mentioned in Sec. 2.2.

In Sec. 4.1 we discuss the notion of *asymptotic cycle* generalizing the *rotation number* of an irrational winding line on a torus. It describes how an “irrational winding line” on a surface of higher genus winds around a flat surface in average. In Sec. 4.2 we heuristically describe the further terms of approximation, and we complete with a formulation of the corresponding result in Sec. 4.3.

In fact, this description is equivalent to the description of the deviation of a directional flow on a flat surface from the ergodic mean. Sec. 4.3 involves some background in ergodic theory; it can be either omitted in the first reading, or can be read accompanied by Appendix B presenting the multiplicative ergodic theorem.

Section 5. Renormalization

This section describes the relation between the Teichmüller geodesic flow and *renormalization* for *interval exchange transformations* discussed in the lectures of J.-C. Yoccoz [Y] in this volume. It is slightly more technical than other sections and can be omitted by a reader who is not interested in the proof of the Theorem from Sec. 4.3.

In Sec. 5.1 we show that interval exchange transformations naturally arise as the *first return map* of a directional flow on a flat surface to a transversal segment. In Sec. 5.2 we perform an explicit computation of the *asymptotic cycle* (defined in Sec. 4.1) using interval exchange transformations. In Sec. 5.3 we present a conceptual idea of *renormalization*, a powerful technique of acceleration of motion along trajectories of the directional flow. This idea is illustrated in Sec. 5.4 in the simplest case where we interpret the Euclidean algorithm as a renormalization procedure for rotation of a circle.

We develop these ideas in Sec. 5.5 describing a concrete geometric renormalization procedure (called *Rauzy–Veech induction*) applicable to general flat surfaces (and general interval exchange transformations). We continue in Sec. 5.6 with the elementary formalism of *multiplicative cocycles* (see also Appendix B). Following W. Veech we describe in Sec. 5.7 *zippered rectangles* coordinates in a family of flat surfaces and describe the action of the Teichmüller geodesic flow in a fundamental domain in these coordinates. We show that the first return map of the Teichmüller geodesic flow to the boundary of the fundamental domain corresponds to the Rauzy–Veech induction. In Sec. 5.8 we present a short overview of recent results of G. Forni, M. Kontsevich, A. Avila and M. Viana concerning the spectrum of *Lyapunov exponents* of the corresponding cocycle (completing the proof of the Theorem from Sec. 4.3). As

an application of the technique developed in Sec. 5 we show in Sec. 5.9 that in the simplest case of tori it gives the well-known encoding of a continued fraction by a cutting sequence of a geodesic on the upper half-plane.

Section 6. Closed geodesics

This section is basically independent of other sections; it describes the relation between closed geodesics on individual flat surfaces and “cusps” on the corresponding moduli spaces. It might be useful for those who are interested in the global structure of the moduli spaces.

Following A. Eskin and H. Masur we formalize in Sec. 6.1 the counting problems for closed geodesics and for saddle connections of bounded length on an individual flat surface. In Sec. 6.2 we present the Siegel–Veech Formula and explain a relation between the counting problem and evaluation of the volume of a tubular neighborhood of a “cusp” in the corresponding moduli space. In Sec. 6.3 we describe the structure of a simplest cusp. We describe the structure of general “cusps” (the structure of *principal boundary* of the moduli space) in Sec. 6.4. As an illustration of possible applications we consider in Sec. 6.5 billiards in rectangular polygons.

Section 7 Volume of the Moduli Space

In Sec. 7.1 we consider very special flat surfaces, so called *square-tiled surfaces* which play a role of *integer points* in the moduli space. In Sec. 7.2 we present the technique of A. Eskin and A. Okounkov who have found an asymptotic formula for the number of square-tiled surfaces glued from a bounded number of squares and applied these results to evaluation of volumes of moduli spaces.

As usual, Sec. 7 is independent of others; however, the notion of a square-tiled surface appears later in the discussion of *Veech surfaces* in Sec. 9.5–9.8.

Section 8. Crash Course in Teichmüller Theory

We proceed in Sec. 8 with a very brief overview of some elementary background in Teichmüller theory. Namely, we discuss in Sec. 8.1 the *extremal quasiconformal map* and formulate the *Teichmüller theorem*, which we use in Sec. 8.2 we to define the distance between complex structures (*Teichmüller metric*). We finally explain why the action of the diagonal subgroup in $SL(2; \mathbb{R})$ on the space of flat surfaces should be interpreted as the *Teichmüller geodesic flow*.

Section 9. Main Conjecture and Recent Results

In this last section we discuss one of the central problems in the area – a conjectural structure of *all* orbits of $GL^+(2, \mathbb{R})$. The main hope is that the closure of *any* such orbit is a nice complex subvariety, and that in this sense the moduli spaces of holomorphic 1-forms and the moduli spaces of quadratic differentials resemble homogeneous spaces under an action of a unipotent group. In this

section we also present a brief survey of some very recent results related to this conjecture obtained by K. Calta, C. McMullen and others.

We start in Sec. 9.1 with a geometric description of the $GL^+(2, \mathbb{R})$ -action in Sec. 9.1 and show why the projections of the orbits (so-called *Teichmüller discs*) to the moduli space \mathcal{M}_g of complex structures should be considered as *complex geodesics*. In Sec. 9.2 we present some results telling that analogous “complex geodesics” in a homogeneous space have a very nice behavior. It is known that the moduli spaces are *not* homogeneous spaces. Nevertheless, in Sec. 9.3 we announce one of the main hopes in this field telling that in the context of the closures of “complex geodesics” the moduli spaces behave as if they were.

We continue with a discussion of two extremal examples of $GL^+(2, \mathbb{R})$ -invariant submanifolds. In Sec. 9.4 we describe the “largest” ones: the connected components of the strata. In Sec. 9.5 we consider flat surfaces S (called *Veech surfaces*) with the “smallest” possible orbits: the ones which are closed. Since recently the list of known Veech surfaces was very short. However, K. Calta and C. McMullen have discovered an infinite family of Veech surfaces in genus two and have classified them. Developing these results C. McMullen has proved the main conjecture in genus two. These results of K. Calta and C. McMullen are discussed in Sec. 9.7. Finally, we consider in Sec. 9.8 the classification of Teichmüller discs in $\mathcal{H}(2)$ due to P. Hubert, S. Lelièvre and to C. McMullen.

Section 10. Open Problems

In this section we collect open problems dispersed through the text.

Appendix A. Ergodic Theorem

In Appendix A we suggest a two-pages exposition of some key facts and constructions in ergodic theory.

Appendix B. Multiplicative Ergodic Theorem

Finally, in Appendix B we discuss the Multiplicative Ergodic Theorem which is mentioned in Sec. 4 and used in Sec. 5.

We start with some elementary linear-algebraic motivations in Sec. B.1 which we apply in Sec. B.2 to the simplest case of a “linear” map of a multi-dimensional torus. This examples give us intuition necessary to formulate in Sec. B.3 the *multiplicative ergodic theorem*. Morally, we associate to an ergodic dynamical system a matrix of *mean differential* (or of *mean monodromy* in some cases). We complete this section with a discussion of some basic properties of *Lyapunov exponents* playing a role of logarithms of eigenvalues of the “mean differential” (“mean monodromy”) of the dynamical system.

1.4 Acknowledgments

I would like to thank organizers and participants of the workshop “*Frontiers in Number Theory, Physics and Geometry*” held at Les Houches, organizers and participants of the activity on *Algebraic and Topological Dynamics* held at MPI, Bonn, and organizers and participants of the workshop on *Dynamical Systems* held at ICTP, Trieste, for their interest, encouragement, helpful remarks and for fruitful discussions. In particular, I would like to thank A. Avila, C. Boissy, J.-P. Conze, A. Eskin, G. Forni, P. Hubert, M. Kontsevich, F. Ledrappier, S. Lelièvre, H. Masur, C. McMullen, Ya. Pesin, T. Schmidt, M. Viana, Ya. Vorobets and J.-C. Yoccoz.

These notes would be never written without tactful, friendly and persistent pressure and help of B. Julia and P. Vanhove.

I would like to thank MPI für Mathematik at Bonn and IHES at Bures-sur-Yvette for their hospitality while preparation of these notes. I highly appreciate the help of V. Solomatina and of M.-C. Vergne who prepared several most complicated pictures. I am grateful to M. Duchin and to G. Le Floc’h for their kind permission to use the photographs. I would like to thank the The State Hermitage Museum and Succession H. Matisse/VG Bild-Kunst for their kind permission to use “La Dance” of H. Matisse as an illustration in Sec. 6.

2 Eclectic Motivations

In this section we show how flat surfaces appear in different guises: we consider billiards in polygons, and, in particular, billiards in rational polygons. In Sec. 2.1 we show that consideration of billiard trajectories is equivalent to the consideration of geodesics on the corresponding flat surface. As another motivation we show in Sec. 2.2 how the electron transport on Fermi-surfaces leads to the study of foliation defined by a closed 1-form on a surface. In Sec. 2.3 we show, that under some conditions on the closed 1-form such foliation can be “straightened up” in an appropriate flat metric. Similarly, a Hamiltonian flow defined by the corresponding multivalued Hamiltonian on a surface follows geodesics in an appropriate flat metric.

2.1 Billiards in Polygons

Billiards in General Polygons

Consider a *polygonal billiard table* and an ideal billiard ball which reflects from the walls of the table by the “optical” rule: the angle of incidence equals the angle after the reflection. We assume that the mass of our ideal ball is concentrated at one point; there is no friction, no spin.

We mostly consider *regular trajectories*, which do not pass through the corners of the polygon. However, one can also study trajectories emitted from one corner and trapped after several reflections in some other (or the same) corner. Such trajectories are called the *generalized diagonals*.

To simplify the problem let us start our consideration with billiards in *triangles*. A triangular billiard table is defined by angles α, β, γ (proportional rescaling of the triangle does not change the dynamics of the billiard). Since $\alpha + \beta + \gamma = \pi$ the family of triangular billiard tables is described by two real parameters.

It is difficult to believe that the following Problem is open for many decades.

Problem (Billiard in a Polygon).

1. Describe the behavior of a generic regular billiard trajectory in a generic triangle, in particular, prove (or disprove) that the billiard flow is ergodic²;
2. Does any (almost any) billiard table has at least one regular periodic trajectory? If the answer is affirmative, does this trajectory survive under deformations of the billiard table?
3. If a periodic trajectory exists, are there many periodic trajectories like that? Namely, find the asymptotics for the number of periodic trajectories of length shorter than L as the bound L goes to infinity.

It is easy to find a special closed regular trajectory in an acute triangle: see the left picture at Fig. 4 presenting the *Fagnano trajectory*. This periodic trajectory is known for at least two centuries. However, it is not known whether any (or at least almost any) obtuse triangle has a periodic billiard trajectory.

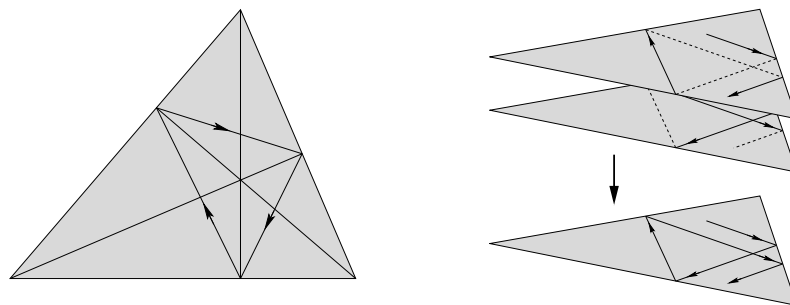


Fig. 4. Fagnano trajectory and Fox–Kershner construction

Obtuse triangles with the angles $\alpha \leq \beta < \gamma$ can be parameterized by a point of a “simplex” Δ defined as $\alpha + \beta < \pi/2$, $\alpha, \beta > 0$. For some obtuse triangles the existence of a regular periodic trajectory is known. Moreover, some

²On behalf of the Center for Dynamics and Geometry of Penn State University, A. Katok promised a prize of 10.000 euros for a solution of this problem.

of these periodic trajectories, called *stable periodic trajectories*, survive under small deformations of the triangle, which proves existence of periodic trajectories for some regions in the parameter space Δ (see the works of G. Galperin, A. M. Stepin, Ya. Vorobets and A. Zemliakov [GaStVb1], [GaStVb2], [GaZe], [Vb1]). It remains to prove that such regions cover the entire parameter space Δ . Currently R. Schwartz is in progress of extensive computer search of stable periodic trajectories hoping to cover Δ with corresponding computer-generated regions.

Now, following Fox and Kershner [FxKr], let us see how billiards in polygons lead naturally to geodesics on flat surfaces.

Place two copies of a polygonal billiard table one atop the other. Launch a billiard trajectory on one of the copies and let it jump from one copy to the other after each reflection (see the right picture at Fig. 4). Identifying the boundaries of the two copies of the polygon we get a connected path ρ on the corresponding topological sphere. Projecting this path to any of the two “polygonal hemispheres” we get the initial billiard trajectory.

It remains to note that our topological sphere is endowed with a flat metric (coming from the polygon). Analogously to the flat metric on the surface of a cube which is nonsingular on the edges of the cube (see Sec. 1.1 and Fig. 1), the flat metric on our sphere is nonsingular on the “equator” obtained from the identified boundaries of the two equal “polygonal hemispheres”. Moreover, let x be a point where the path ρ crosses the “equator”. Unfolding a neighborhood of a point x on the “equator” we see that the corresponding fragment of the path ρ unfolds to a straight segment in the flat metric. In other words, the path ρ is a geodesic in the corresponding flat metric.

The resulting flat metric is *not very flat*: it has nontrivial linear holonomy. The conical singularities of the flat metric correspond to the vertices of the polygon; the cone angle of a singularity is twice the angle at the corresponding vertex of the polygon.

We have proved that every geodesic on our flat sphere projects to a billiard trajectory and every billiard trajectory lifts to a geodesic. This is why General Problem from Sec. 1.1 is so closely related to the Billiard Problem.

Two Beads on a Rod and Billiard in a Triangle

It would be unfair not to mention that billiards in polygons attracted a lot of attention as (what initially seemed to be) a simple model of a Boltzman gas. To give a flavor of this correspondence we consider a system of two elastic beads confined to a rod placed between two walls, see Fig. 5. (Up to the best of my knowledge this construction originates in lectures of Ya. G. Sinai [Sin].)

The beads have different masses m_1 and m_2 they collide between themselves, and also with the walls. Assuming that the size of the beads is negligible we can describe the configuration space of our system using coordinates $0 < x_1 \leq x_2 \leq a$ of the beads, where a is the distance between the walls. Rescaling the coordinates as

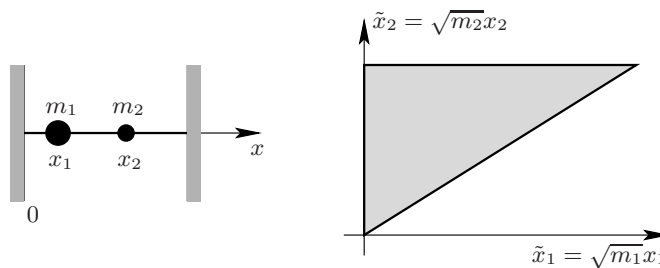


Fig. 5. Gas of two molecules in a one-dimensional chamber

$$\begin{cases} \tilde{x}_1 = \sqrt{m_1}x_1 \\ \tilde{x}_2 = \sqrt{m_2}x_2 \end{cases}$$

we see that the configuration space in the new coordinates is given by a right triangle Δ , see Fig. 5. Consider now a trajectory of our dynamical system. We leave to the reader the pleasure to prove the following elementary Lemma:

Lemma. *In coordinates $(\tilde{x}_1, \tilde{x}_2)$ trajectories of the system of two beads on a rod correspond to billiard trajectories in the triangle Δ .*

Billiards in Rational Polygons

We have seen that taking two copies of a polygon we can reduce the study of a billiard in a general polygon to the study of geodesics on the corresponding flat surface. However, the resulting flat surface has *nontrivial* linear holonomy, it is *not* “very flat”.

Nevertheless, a more restricted class of billiards, namely, billiards in *rational polygons*, lead to “very flat” (translation) surfaces.

A polygon is called *rational* if all its angles are rational multiples of π . A billiard trajectory emitted in some direction will change direction after the first reflection, then will change direction once more after the second reflection, etc. However, for any given billiard trajectory in a rational billiard the set of possible directions is *finite*, which make billiards in rational polygons so different from general ones.

As a basic example consider a billiard in a rectangle. In this case a generic trajectory at any moment goes in one of four possible directions. Developing the idea with the general polygon we can take *four* (instead of two) copies of our billiard table (one copy for each direction). As soon as our trajectory hits the wall and changes the direction we make it jump to the corresponding copy of the billiard – the one representing the corresponding direction.

By construction each side of every copy of the billiard is identified with exactly one side of another copy of the billiard. Upon these identifications the four copies of the billiard produce a closed surface and the unfolded billiard trajectory produces a connected line on this surface. We suggest to the reader

to check that *the resulting surface is a torus and the unfolded trajectory is a geodesic on this flat torus*, see Fig. 6.

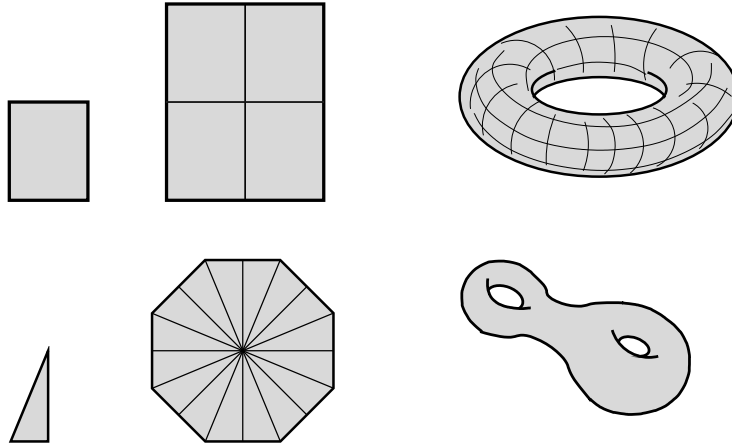


Fig. 6. Billiard in a rectangle corresponds to directional flow on a flat torus. Billiard in a right triangle $(\pi/8, 3\pi/8, \pi/2)$ leads to directional flow on a flat surface obtained from the regular octagon.

A similar unfolding construction (often called *Katok–Zemliakov construction*) works for a billiard in any rational polygon. Say, for a billiard in a right triangle with angles $(\pi/8, 3\pi/8, \pi/2)$ one has to take 16 copies (corresponding to 16 possible directions of a given billiard trajectory). Appropriate identifications of these 16 copies produce a regular octagon with identified opposite sides (see Fig. 6). We know from Sec. 1.2 and from Fig. 3 that the corresponding flat surface is a “very flat” surface of genus two having a single conical singularity with the cone angle 6π .

Exercise. What is the genus of the surface obtained by Katok–Zemliakov construction from an isosceles triangle $(3\pi/8, 3\pi/8, \pi/4)$? How many conical points does it have? What are the cone angles at these points? Hint: this surface *can not* be glued from a regular octagon.

It is quite common to unfold a rational billiard in two steps. We first unfold the billiard table to a polygon, and then identify the appropriate pairs of sides of the resulting polygon. Note that the polygon obtained in this intermediate step is not canonical.

Show that a generic billiard trajectory in the right triangle with angles $(\pi/2, \pi/5, 3\pi/10)$ has 20 directions. Show that both polygons at Fig. 7 can be obtained by Katok–Zemliakov construction from 20 copies of this triangle. Verify that after identification of parallel sides of these polygons we obtain isometric very flat surfaces (see also [HuSdt5]). What genus, and what conical points do they have? What are the cone angles at these points?

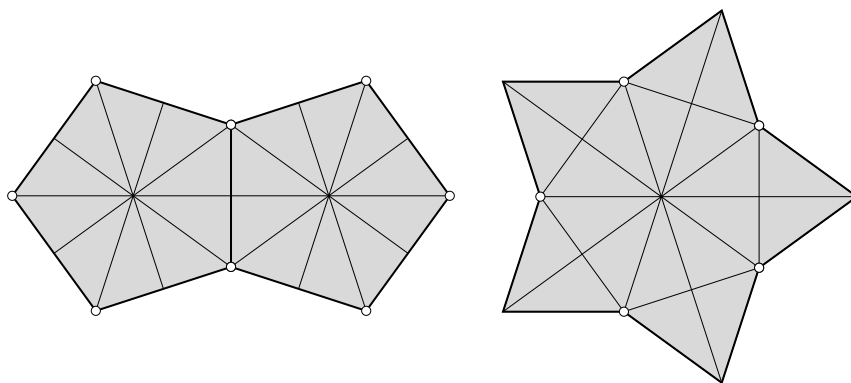


Fig. 7. We can unfold the billiard in the right triangle $(\pi/2, \pi/5, 3\pi/10)$ into different polygons. However, the resulting very flat surfaces are the same (see also [HuSdt5]).

Note that in comparison with the initial construction, where we had only two copies of the billiard table we get a more complicated surface. However, what we gain is that in this new construction our flat surface is actually “very flat”: it has trivial linear holonomy. It has a lot of consequences; say, due to a Theorem of H. Masur [Ma4] it is possible to find a regular periodic geodesic on *any* “very flat” surface. If the flat surface was constructed from a billiard, the corresponding closed geodesic projects to a regular periodic trajectory of the corresponding billiard which solves part of the Billiard Problem for billiards in rational polygons.

We did not intend to present in this section any comprehensive information about billiards, our goal was just to give a motivation for the study of flat surfaces. A reader interested in billiards can get a good idea on the subject from a very nice book of S. Tabachnikov [T]. Details about billiards in polygons (especially rational polygons) can be found in the surveys of E. Gutkin [Gu1], P. Hubert and T. Schmidt [HuSdt5], H. Masur and S. Tabachnikov [MaT] and J. Smillie [S].

2.2 Electron Transport on Fermi-Surfaces

Consider a periodic surface \tilde{M}^2 in \mathbb{R}^3 (i.e. a surface invariant under translations by any integer vector in \mathbb{Z}^3). Such a surface can be constructed in a fundamental domain of a cubic lattice, see Fig. 8, and then reproduced repeatedly in the lattice. Choose now an affine plane in \mathbb{R}^3 and consider an intersection line of the surface by the plane. This intersection line might have some closed components and it may also have some unbounded components. The question is *how does an unbounded component propagate in \mathbb{R}^3 ?*

The study of this subject was suggested by S. P. Novikov about 1980 (see [N]) as a mathematical formulation of the corresponding problem concern-

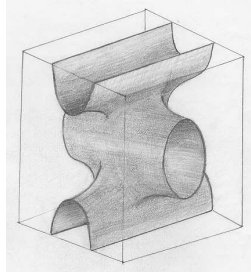


Fig. 8. Riemann surface of genus 3 embedded into a torus \mathbb{T}^3

ing electron transport in metals. A periodic surface represents a *Fermi-surface*, affine plane is a plane orthogonal to a magnetic field, and the intersection line is a trajectory of an electron in the so-called *inverse lattice*.

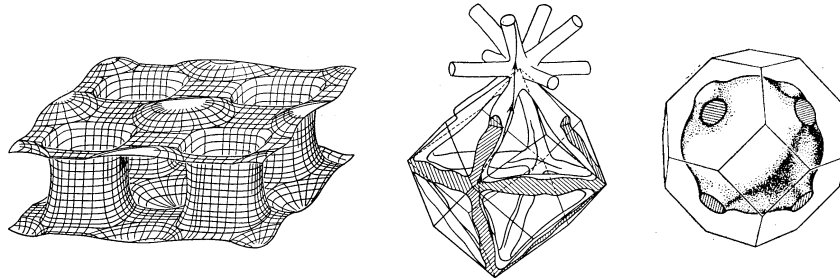


Fig. 9. Fermi surfaces of tin, iron and gold correspond to Riemann surfaces of high genera. (Reproduced from [AzLK] which cites [AGLP] and [WYa] as the source)

It was known since extensive experimental research in the 50s and 60s that Fermi-surfaces may have fairly complicated shape, see Fig. 9; it was also known that open (i.e. unbounded) trajectories exist, see Fig. 10, however, up to the beginning of the 80s there were no general results in this area.

In particular, it was not known whether open trajectories follow (in a large scale) the same direction, whether there might be some scattering (trajectory comes from infinity in one direction and then after some scattering goes to infinity in some other direction, whether the trajectories may even exhibit some chaotic behavior?

Let us see now how this problem is related to flat surfaces.

First note that passing to a quotient $\mathbb{R}^3/\mathbb{Z}^3 = \mathbb{T}^3$ we get a closed orientable surface $M^2 \subset \mathbb{T}^3$ from the initial periodic surface \tilde{M}^2 . Say, identifying the opposite sides of a unit cube at Fig. 8 we get a closed surface M^2 of genus $g = 3$.

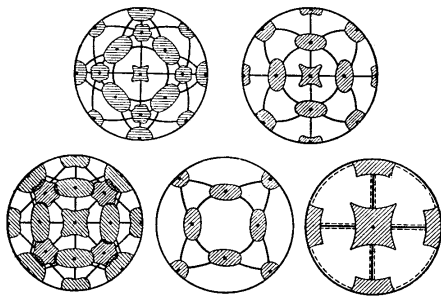


Fig. 10. Stereographic projection of the magnetic field directions (shaded regions and continuous curves) which give rise to open trajectories for some Fermi-surfaces (experimental results in [AzLK]).

We are interested in plane sections of the initial periodic surface \tilde{M}^2 . This plane sections can be viewed as level curves of a linear function $f(x, y, z) = ax + by + cz$ restricted to \tilde{M}^2 .

Consider now a closed differential 1-form $\tilde{\omega} = a dx + b dy + c dz$ in \mathbb{R}^3 and its restriction to \tilde{M}^2 . A closed 1-form defines a codimension-one foliation on a manifold: locally one can represent a closed one-form as a differential of a function, $\tilde{\omega} = df$; the foliation is defined by the levels of the function f . We prefer to use the 1-form $\tilde{\omega} = a dx + b dy + c dz$ to the linear function $f(x, y, z) = ax + by + cz$ because we cannot push the function $f(x, y, z)$ into a torus \mathbb{T}^3 while the 1-form $\omega = a dx + b dy + c dz$ is well-defined in \mathbb{T}^3 . Moreover, after passing to a quotient over the lattice $\mathbb{R}^3 \rightarrow \mathbb{R}^3/\mathbb{Z}^3$ the plane sections of \tilde{M}^2 project to the leaves of the foliation defined by restriction of the closed 1-form ω in \mathbb{T}^3 to the surface M^2 .

Thus, our initial problem can be reformulated as follows.

Problem (Novikov’s Problem on Electron Transport). *Consider a foliation defined by a linear closed 1-form $\omega = a dx + b dy + c dz$ on a closed surface $M^2 \subset \mathbb{T}^3$ embedded into a three-dimensional torus. How do the leaves of this foliation get unfolded, when we unfold the torus \mathbb{T}^3 to its universal cover \mathbb{R}^3 ?*

The foliation defined by a closed 1-form on a surface is a subject of discussion of the next section. We shall see that under some natural conditions such a foliation can be “straightened up” to a geodesic foliation in an appropriate flat metric.

The way in which a geodesic on a flat surface gets unfolded in the universal Abelian cover is discussed in detail in Sec. 4.

To be honest, we should admit that 1-forms as in the Problem above usually do not satisfy these conditions. However, a surface as in this Problem can be decomposed into several components, which (after some surgery) already satisfy the necessary requirements.

References for Details

There is a lot of progress in this area, basically due to S. Novikov’s school, and especially to I. Dynnikov, and in many cases Novikov’s Problem on electron transport is solved.

In [Zo1] the author proved that for a given Fermi-surface and for an open dense set of directions of planes any open trajectory is bounded by a pair of parallel lines inside the corresponding plane.

In a series of papers I. Dynnikov applied a different approach: he fixed the direction of the plane and deformed a Fermi-surface inside a family of level surfaces of a periodic function in \mathbb{R}^3 . He proved that for all but at most one level any open trajectory is also bounded between two lines.

However, I. Dynnikov has constructed a series of highly elaborated examples showing that in some cases an open trajectory can “fill” the plane. In particular, the following question is still open. Consider the set of directions of those hyperplanes which give “nontypical” open trajectories. Is it true that this set has measure zero in the space $\mathbb{R}P^2$ of all possible directions? What can be said about Hausdorff dimension of this set?

For more details we address the reader to papers [D1], [D2] and [NM].

2.3 Flows on Surfaces and Surface Foliations

Consider a closed 1-form on a closed orientable surface. Locally a closed 1-form ω can be represented as the differential of a function $\omega = df$. The level curves of the function f locally define the leaves of the closed 1-form ω . (The fact that the function f is defined only up to a constant does not affect the structure of the level curves.) We get a foliation on a surface.

In this section we present a necessary and sufficient condition which tells when one can find an appropriate flat metric such that the foliation defined by the closed 1-form becomes a foliation of parallel geodesics going in some fixed direction on the surface. This criterion was given in different context by different authors: [Clb], [Kat1], [HbMa]. We present here one more formulation of the criterion. Morally, it says that *the foliation defined by a closed 1-form ω can be “straightened up” in an appropriate flat metric if and only if the form ω does not have closed leaves homologous to zero*. In the remaining part of this section we present a rigorous formulation of this statement.

Note that a closed 1-form ω on a closed surface necessarily has some critical points: the points where the function f serving as a “local antiderivative” $\omega = df$ has critical points.

The first obstruction for “straightening” is the presence of minima and maxima: such critical points should be forbidden. Suppose now that the closed 1-form has only isolated critical points and all of them are “saddles” (i.e. ω does not have minima and maxima). Say, a form defined in local coordinates as df , where $f = x^3 + y^3$ has a saddle point in the origin $(0, 0)$ of our coordinate chart, see Fig. 11.

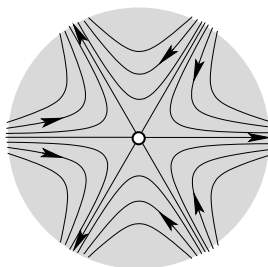


Fig. 11. Horizontal foliation in a neighborhood of a saddle point. Topological (nonmetric) picture

There are several singular leaves of the foliation landing at each saddle; say, a saddle point from Fig. 11 has six prongs (separatrices) representing the critical leaves. Sometimes a critical leaf emitted from one saddle can land to another (or even to the same) saddle point. In this case we say that the foliation has a *saddle connection*.

Note that the foliation defined by a closed 1-form on an oriented surface gets natural orientation (defined by $\text{grad}(f)$ and by the orientation of the surface). Now we are ready to present a rigorous formulation of the criterion.

Theorem. *Consider a foliation defined on a closed orientable surface by a closed 1-form ω . Assume that ω does not have neither minima nor maxima but only isolated saddle points. The foliation defined by ω can be represented as a geodesic foliation in an appropriate flat metric if and only if any cycle obtained as a union of closed paths following in the positive direction a sequence of saddle connections is not homologous to zero.*

In particular, if there are no saddle connections at all (provided there are no minima and maxima) it can always be straightened up. (In slightly different terms it was proved in [Kat1] and in [HbMa].)

Note that saddle points of the closed 1-form ω correspond to conical points of the resulting flat metric.

One can consider a closed 1-form ω as a multivalued Hamiltonian and consider corresponding Hamiltonian flow along the leaves of the foliation defined by ω . On the torus \mathbb{T}^2 it was studied by V. I. Arnold [Ald2] and by K. Khanin and Ya. G. Sinai [KhSin].

3 Families of Flat Surfaces and Moduli Spaces of Abelian Differentials

In this section we present the generalities on flat surfaces. We start in Sec. 3.1 with an elementary construction of a flat surface from a polygonal pattern. This construction explicitly shows that any flat surface can be deformed inside an appropriate *family* of flat surfaces. As a model example we consider

in Sec. 3.2 the family of flat tori. In Sec. 3.3 we show that a flat structure naturally determines a complex structure on the surface and a holomorphic one-form. Reciprocally, a holomorphic one-form naturally determines a flat structure. The dictionary establishing correspondence between geometric language (in terms of the flat metrics) and complex-analytic language (in terms of holomorphic one-forms) is very important for the entire presentation; it makes Sec. 3.3 more charged than an average one. In Sec. 3.4 we continue with establishing correspondence between families of flat surfaces and strata of moduli spaces of holomorphic one-forms. In Sec. 3.5 we describe the action of the linear group $SL(2, \mathbb{R})$ on flat surfaces – another key issue of this theory.

We complete Sec. 3 with an attempt to present the following general principle in the study of flat surfaces. In order to get some information about an individual flat surface it is often very convenient to find (the closure of) the orbit of the corresponding element in the *family* of flat surfaces under the action of the group $SL(2, \mathbb{R})$ (or, sometimes, under the action of its diagonal subgroup). In many cases the structure of this orbit gives a comprehensive information about the initial flat surface; moreover, this information might be not accessible by a direct approach. These ideas are expressed in Sec. 3.6. This general principle is illustrated in Sec. 3.7 presenting Masur’s criterion of unique ergodicity of the directional flow on a flat surface. (A reader not familiar with ergodic theorem can either skip this last section or read an elementary presentation of ergodicity in Appendix A.)

3.1 Families of Flat Surfaces

In this section we present a construction which allows to obtain a large variety of flat surfaces, and, moreover, allows to continuously deform the resulting flat structure. Later on we shall see that this construction is even more general than it may seem at the beginning; it allows to get *almost all* flat surfaces in any *family* of flat surfaces sharing the same geometry (i.e. genus, number and types of conical singularities). The construction is strongly motivated by an analogous construction in the paper of H. Masur [Ma3].

Consider a collection of vectors $\mathbf{v}_1, \dots, \mathbf{v}_n$ in \mathbb{R}^2 and construct from these vectors a broken line in a natural way: a j -th edge of the broken line is represented by the vector \mathbf{v}_j . Construct another broken line starting at the same point as the initial one by taking the same vectors but this time in the order $v_{\pi(1)}, \dots, v_{\pi(n)}$, where π is some permutation of n elements.

By construction the two broken lines share the same endpoints; suppose that they bound a polygon as in Fig. 12. Identifying the pairs of sides corresponding to the same vectors v_j , $j = 1, \dots, n$, by parallel translations we obtain a flat surface.

The polygon in our construction depends continuously on the vectors \mathbf{v}_i . This means that the topology of the resulting flat surface (its genus g , the number m and the types of the resulting conical singularities) do not change under small deformations of the vectors \mathbf{v}_i . Say, we suggest to the reader to

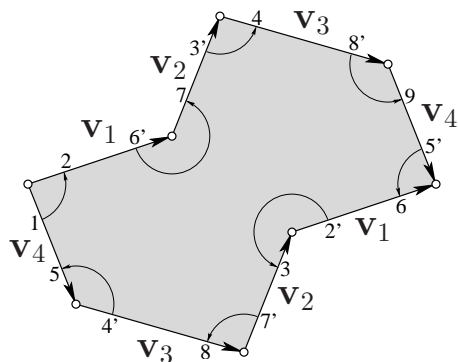


Fig. 12. Identifying corresponding pairs of sides of this polygon by parallel translations we obtain a flat surface.

check that the flat surface obtained from the polygon presented in Fig. 12 has genus two and a single conical singularity with cone angle 6π .

3.2 Toy Example: Family of Flat Tori

In the previous section we have seen that a flat structure can be deformed. This allows to consider a flat surface as an element of a *family* of flat surfaces sharing a common geometry (genus, number of conical points). In this section we study the simplest example of such family: we study the family of flat tori. This time we consider the family of flat surfaces *globally*. We shall see that it has a natural structure of a noncompact complex-analytic manifold (to be more honest – *orbifold*). This “baby family” of flat surfaces, actually, exhibits all principal features of any other family of flat surfaces, except that the family of flat tori constitutes a homogeneous space endowed with a nice hyperbolic metric, while general families of flat surfaces *do not* have the structure of a homogeneous space.

To simplify consideration of flat tori as much as possible we make two exceptions from the usual way in which we consider flat surfaces. Temporarily (only in this section) we forget about the choice of the direction to North: in this section two isometric flat tori define the same element of the family of all flat tori. Another exception concerns normalization. Almost everywhere below we consider the area of any flat surface to be normalized to one (which can be achieved by a simple homothety). In this section it would be more convenient for us to apply homothety in the way that the shortest closed geodesic on our flat torus would have length 1. Find the closed geodesic which is next after the shortest one in the length spectrum. Measure the angle ϕ , where $0 \leq \phi \leq \pi$ between these two geodesics; measure the length r of the second geodesic and mark a point with polar coordinates (r, ϕ) on the upper half-plane. This point encodes our torus.

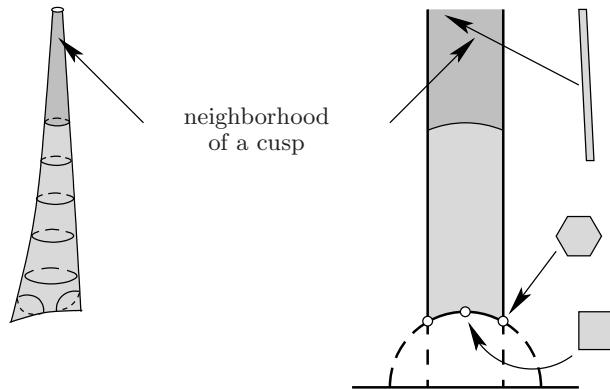


Fig. 13. Space of flat tori

Reciprocally, any point of the upper half-plane defines a flat torus in the following way. (Following the tradition we consider the upper half-plane as a complex one.) A point $x + iy$ defines a parallelogram generated by vectors $\mathbf{v}_1 = (1, 0)$ and $\mathbf{v}_2 = (x + iy)$, see Fig. 13. Identifying the opposite sides of the parallelogram we get a flat torus.

To make this correspondence bijective we have to be sure that the vector \mathbf{v}_1 represents the shortest closed geodesic. This means that the point $(x + iy)$ representing \mathbf{v}_2 cannot be inside the unit disc. The condition that \mathbf{v}_2 represents the geodesic which is next after the shortest one in the length spectrum implies that $-1/2 \leq x \leq 1/2$, see Fig. 13. Having mentioned these two hints we suggest to the reader to prove the following Lemma.

Lemma 1. *The family of flat tori is parametrized by the shadowed fundamental domain from Fig. 13, where the parts of the boundary of the fundamental domain symmetric with respect to the vertical axis $(0, iy)$ are identified.*

Note that topologically we obtain a sphere punctured at one point: the resulting surface has a *cusp*. Tori represented by points close to the cusp are “disproportional”: they are very narrow and very long. In other words they have an abnormally short geodesic.

Note also that there are two special points on our modular curve: they correspond to points with coordinates $(0 + i)$ and $\pm 1/2 + i\sqrt{3}/2$. The corresponding tori have extra symmetry, they can be represented by a square and by a regular hexagon with identified opposite sides correspondingly. The surface glued from the fundamental domains has “corners” at these two points.

There is an alternative more algebraic approach to our problem. Actually, the fundamental domain constructed above is known as a *modular curve*, it parameterizes the *space of lattices of area one* (which is isomorphic to the space of flat tori). It can be seen as a double quotient

$$SO(2, \mathbb{R}) \backslash SL(2, \mathbb{R}) / SL(2, \mathbb{Z}) = \mathbb{H} / SL(2, \mathbb{Z})$$

3.3 Dictionary of Complex-Analytic Language

We have seen in Sec. 3.1 how to construct a flat surfaces from a polygon as on Fig. 12.

Note that the polygon is embedded into a complex plane \mathbb{C} , where the embedding is defined up to a parallel translation. (A rotation of the polygon changes the vertical direction and hence, according to Convention 1 it changes the corresponding flat surface.)

Consider the natural coordinate z in the complex plane. In this coordinate the parallel translations which we use to identify the sides of the polygon are represented as

$$z' = z + \text{const} \quad (1)$$

Since this correspondence is holomorphic, it means that our flat surface S with punctured conical points inherits the complex structure. It is an exercise in complex analysis to check that the complex structure extends to the punctured points.

Consider now a holomorphic 1-form dz in the initial complex plane. When we pass to the surface S the coordinate z is not globally defined anymore. However, since the changes of local coordinates are defined by the rule (1) we see that $dz = dz'$. Thus, the holomorphic 1-form dz on \mathbb{C} defines a holomorphic 1-form ω on S which in local coordinates has the form $\omega = dz$. Another exercise in complex analysis shows that the form ω has *zeroes* exactly at those points of S where the flat structure has conical singularities.

In an appropriate local coordinate w in a neighborhood of zero (different from the initial local coordinate z) a holomorphic 1-form can be represented as $w^d dw$, where d is called the *degree* of zero. The form ω has a zero of degree d at a *conical point* with cone angle $2\pi(d + 1)$.

Recall the formula for the sum of degrees of zeroes of a holomorphic 1-form on a Riemann surface of genus g :

$$\sum_{j=1}^m d_j = 2g - 2$$

This relation can be interpreted as the formula of Gauss–Bonnet for the flat metric.

Vectors \mathbf{v}_j representing the sides of the polygon can be considered as complex numbers. Let \mathbf{v}_j be joining vertices P_j and P_{j+1} of the polygon. Denote by ρ_j the resulting path on S joining the points $P_j, P_{j+1} \in S$. Our interpretation of \mathbf{v}_j as of a complex number implies the following obvious relation:

$$\mathbf{v}_j = \int_{P_j}^{P_{j+1}} dz = \int_{\rho_j} \omega \quad (2)$$

Note that the path ρ_j represents a *relative cycle*: an element of the relative homology group $H_1(S, \{P_1, \dots, P_m\}; \mathbb{Z})$ of the surface S relative to the finite

collection of conical points $\{P_1, \dots, P_m\}$. Relation (2) means that \mathbf{v}_j represents a *period* of ω : an integral of ω over a relative cycle ρ_j .

Note also that the flat area of the surface S equals the area of the original polygon, which can be measured as an integral of $dx \wedge dy$ over the polygon. Since in the complex coordinate z we have $dx \wedge dy = \frac{i}{2} dz \wedge d\bar{z}$ we get the following formula for the flat area of S :

$$\text{area}(S) = \frac{i}{2} \int_S \omega \wedge \bar{\omega} = \frac{i}{2} \sum_{j=1}^g (A_j \bar{B}_j - \bar{A}_j B_j) \quad (3)$$

Here we also used the Riemann bilinear relation which expresses the integral $\int_S \omega \wedge \bar{\omega}$ in terms of *absolute periods* A_j, B_j of ω , where the absolute periods A_j, B_j are the integrals of ω with respect to some symplectic basis of cycles.

An individual flat surface defines a pair: (complex structure, holomorphic 1-form). A family of flat surfaces (where the flat surfaces are as usual endowed with a choice of the vertical direction) corresponds to a *stratum* $\mathcal{H}(d_1, \dots, d_m)$ in the *moduli space of holomorphic 1-forms*. Points of the stratum are represented by pairs (point in the moduli space of complex structures, holomorphic 1-form in the corresponding complex structure having zeroes of degrees d_1, \dots, d_m).

The notion “stratum” has the following origin. The moduli space of pairs (holomorphic 1-form, complex structure) forms a natural vector bundle over the moduli space \mathcal{M}_g of complex structures. A fiber of this vector bundle is a vector space \mathbb{C}^g of holomorphic 1-forms in a given complex structure. We already mentioned that the sum of degrees of zeroes of a holomorphic 1-form on a Riemann surface of genus g equals $2g - 2$. Thus, the total space \mathcal{H}_g of our vector bundle is stratified by subspaces of those forms which have zeroes of degrees exactly d_1, \dots, d_m , where $d_1 + \dots + d_m = 2g - 2$. Say, for $g = 2$ we have only two partitions of number 2, so we get two strata $\mathcal{H}(2)$ and $\mathcal{H}(1, 1)$. For $g = 3$ we have five partitions, and correspondingly five strata $\mathcal{H}(4), \mathcal{H}(3, 1), \mathcal{H}(2, 2), \mathcal{H}(2, 1, 1), \mathcal{H}(1, 1, 1, 1)$.

$$\begin{array}{ccc} \mathcal{H}(d_1, \dots, d_m) & \subset & \mathcal{H}_g \\ & & \downarrow \\ & & \mathcal{M}_g \end{array} \quad (4)$$

Every stratum $\mathcal{H}(d_1, \dots, d_m)$ is a complex-analytic orbifold of dimension

$$\dim_{\mathbb{C}} \mathcal{H}(d_1, \dots, d_m) = 2g + m - 1 \quad (5)$$

Note, that an individual stratum $\mathcal{H}(d_1, \dots, d_m)$ does not form a fiber bundle over \mathcal{M}_g . For example, according to our formula, $\dim_{\mathbb{C}} \mathcal{H}(2g - 2) = 2g$, while $\dim_{\mathbb{C}} \mathcal{M}_g = 3g - 3$.

We showed how the geometric structures related to a flat surface define their complex-analytic counterparts. Actually, this correspondence goes in two directions. We suggest to the reader to make the inverse translation: to start with complex-analytic structure and to see how it defines the geometric one. This correspondence can be summarized in the following dictionary.

Table 1. Correspondence of geometric and complex-analytic notions

Geometric language	Complex-analytic language
flat structure (including a choice of the vertical direction)	complex structure + a choice of a holomorphic 1-form ω
conical point with a cone angle $2\pi(d + 1)$	zero of degree d of the holomorphic 1-form ω (in local coordinates $\omega = w^d dw$)
side \mathbf{v}_j of a polygon	relative period $\int_{P_j}^{P_{j+1}} \omega = \int_{\mathbf{v}_j} \omega$ of the 1-form ω
area of the flat surface S	$\frac{i}{2} \int_S \omega \wedge \bar{\omega} = \frac{i}{2} \sum_{j=1}^g (A_j \bar{B}_j - \bar{A}_j B_j)$
family of flat surfaces sharing the same types $2\pi(d_1 + 1), \dots, 2\pi(d_m + 1)$ of cone angles	stratum $\mathcal{H}(d_1, \dots, d_m)$ in the moduli space of Abelian differentials
coordinates in the family: vectors \mathbf{v}_i defining the polygon	coordinates in $\mathcal{H}(d_1, \dots, d_m)$: collection of relative periods of ω , i.e. cohomology class $[\omega] \in H^1(S, \{P_1, \dots, P_m\}; \mathbb{C})$

3.4 Volume Element in the Moduli Space of Holomorphic One-Forms

In the previous section we have considered vectors $\mathbf{v}_1, \dots, \mathbf{v}_n$ determining the polygon from which we glue a flat surface S as on Fig. 12. We have identified these vectors $\mathbf{v}_j \in \mathbb{R}^2 \sim \mathbb{C}$ with complex numbers and claimed (without proof) that under this identification $\mathbf{v}_1, \dots, \mathbf{v}_n$ provide us with local coordinates in the corresponding family of flat surfaces. We identify every such family with a stratum $\mathcal{H}(d_1, \dots, d_m)$ in the moduli space of holomorphic 1-forms. In complex-analytic language we have locally identified a neighborhood of a “point” (complex structure, holomorphic 1-form ω) in the corresponding stratum with a neighborhood of the cohomology class $[\omega] \in H^1(S, \{P_1, \dots, P_m\}; \mathbb{C})$.

Note that the cohomology space $H^1(S, \{P_1, \dots, P_m\}; \mathbb{C})$ contains a natural integer lattice $H^1(S, \{P_1, \dots, P_m\}; \mathbb{Z} \oplus \sqrt{-1}\mathbb{Z})$. Consider a linear volume element $d\nu$ in the vector space $H^1(S, \{P_1, \dots, P_m\}; \mathbb{C})$ normalized in such a way that the volume of the fundamental domain in the “cubic” lattice

$$H^1(S, \{P_1, \dots, P_m\}; \mathbb{Z} \oplus \sqrt{-1}\mathbb{Z}) \subset H^1(S, \{P_1, \dots, P_m\}; \mathbb{C})$$

is equal to one. In other terms

$$d\nu = \frac{1}{J} \frac{1}{(2\sqrt{-1})^n} d\mathbf{v}_1 d\bar{\mathbf{v}}_1 \dots d\mathbf{v}_n d\bar{\mathbf{v}}_n,$$

where J is the determinant of a change of the basis $\{\mathbf{v}_1, \dots, \mathbf{v}_n\}$ considered as a basis in the first relative *homology* to some “symplectic” basis in the first relative homology.

Consider now the real hypersurface

$$\mathcal{H}_1(d_1, \dots, d_m) \subset \mathcal{H}(d_1, \dots, d_m)$$

defined by the equation $area(S) = 1$. Taking into consideration formula (3) for the function $area(S)$ we see that the hypersurface $\mathcal{H}_1(d_1, \dots, d_m)$ defined as $area(S) = 1$ can be interpreted as a “unit hyperboloid” defined in local coordinates as a level of the indefinite quadratic form (3).

The volume element $d\nu$ can be naturally restricted to a hyperplane defined as a level hypersurface of a function. We denote the corresponding volume element on $\mathcal{H}_1(d_1, \dots, d_m)$ by $d\nu_1$.

Theorem (H. Masur. W. A. Veech). *The total volume*

$$\int_{\mathcal{H}_1(d_1, \dots, d_m)} d\nu_1$$

of every stratum is finite.

The values of these volumes were computed only recently by A. Eskin and A. Okounkov [EOk], twenty years after the Theorem above was proved in [Ma3], [Ve3] and [Ve8]. We discuss this computation in Sec. 7.

3.5 Action of $SL(2, \mathbb{R})$ on the Moduli Space

In this section we discuss a property of flat surfaces which is, probably, the most important in our study: we show that the linear group acts on every family of flat surfaces, and, moreover, acts *ergodically* (see Append. A for discussion of the notion of ergodicity). This enables us to apply tools from dynamical systems and from ergodic theory.

Consider a flat surface S and consider a polygonal pattern obtained by unwrapping it along some geodesic cuts. For example, one can assume that our flat surface S is glued from a polygon $\Pi \subset \mathbb{R}^2$ as on Fig. 12. Consider a linear transformation $g \in GL^+(2, \mathbb{R})$ of the plane \mathbb{R}^2 . It changes the shape of the polygon. However, the sides of the new polygon $g\Pi$ are again arranged into pairs, where the sides in each pair are parallel and have equal length (different from initial one), see Fig. 14. Thus, identifying the sides in each pair by a parallel translation we obtain a new flat surface gS .

It is easy to check that the surface gS does not depend on the way in which S was unwrapped to a polygonal pattern Π . It is clear that all topological characteristics of the new flat surface gS (like genus, number and types

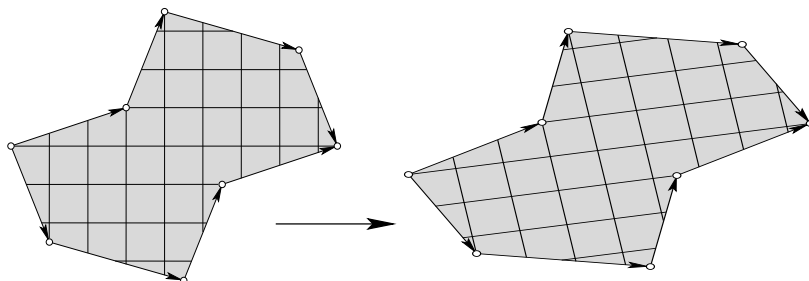


Fig. 14. Action of the linear group on flat surfaces

of conical singularities) are the same as those of the initial flat surface S . Hence, we get a continuous action of the group $GL^+(2, \mathbb{R})$ on each stratum $\mathcal{H}(d_1, \dots, d_m)$.

Considering the subgroup $SL(2, \mathbb{R})$ of area preserving linear transformations we get the action of $SL(2, \mathbb{R})$ on the “unit hyperboloid” $\mathcal{H}_1(d_1, \dots, d_m)$. Considering the diagonal subgroup $\begin{pmatrix} e^t & 0 \\ 0 & e^{-t} \end{pmatrix} \subset SL(2, \mathbb{R})$ we get a continuous action of this one-parameter subgroup on each stratum $\mathcal{H}(d_1, \dots, d_m)$. This action induces a natural flow on the stratum, which is called the *Teichmüller geodesic flow*.

Key Theorem (H. Masur. W. A. Veech). *The action of the groups $SL(2, \mathbb{R})$ and $\begin{pmatrix} e^t & 0 \\ 0 & e^{-t} \end{pmatrix}$ preserves the measure dv_1 . Both actions are ergodic with respect to this measure on each connected component of every stratum $\mathcal{H}_1(d_1, \dots, d_m)$.*

This theorem might seem quite surprising. Consider almost any flat surface S as in Fig. 12. “Almost any flat surface” is understood as “corresponding to a set of parameters $\mathbf{v}_1, \dots, \mathbf{v}_4$ of full measure; here the vectors \mathbf{v}_i define the polygon Π from Fig. 12.

Now start contracting the polygon Π in the vertical direction and expanding it in the horizontal direction with the same coefficient e^t . The theorem says, in particular, that for an appropriate $t \in \mathbb{R}$ the deformed polygon will produce a flat surface $g_t S$ which would be arbitrary close to the flat surface S_0 obtained from the regular octagon as on Fig. 3 since a trajectory of almost any point under an ergodic flow is everywhere dense (and even “well distributed”). However, it is absolutely clear that acting on our initial polygon Π from Fig. 12 with expansion-contraction we never get close to a regular octagon... Is there a contradiction?..

There is no contradiction since the statement of the theorem concerns flat surfaces and not polygons. In practice this means that we can apply expansion-contraction to the polygon Π , which does not change too much the shape of the polygon, but radically changes the flat structure. Then we can change

the way in which we unwrap the flat surface $g_t S$ (see Fig. 15). This radically changes the shape of the polygon, but *does not change at all* the flat structure!

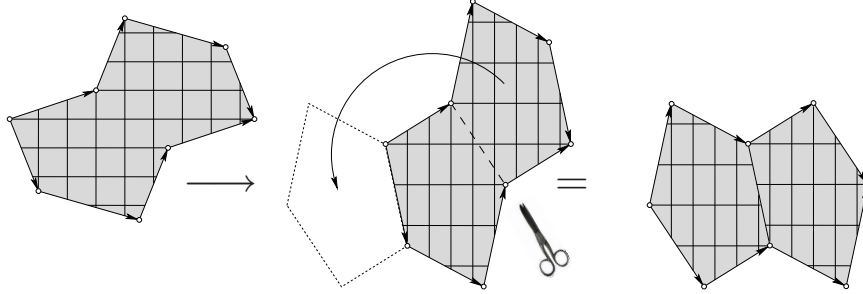


Fig. 15. The first modification of the polygon changes the flat structure while the second one just changes the way in which we unwrap the flat surface

3.6 General Philosophy

Now we are ready to describe informally the basic idea of our approach to the study of flat surfaces. Of course it is not universal; however, in many cases it appears to be surprisingly powerful.

Suppose that we need some information about geometry or dynamics of an individual flat surface S . Consider the element S in the corresponding family of flat surfaces $\mathcal{H}(d_1, \dots, d_m)$. Denote by $\mathcal{C}(S) = GL^+(2, \mathbb{R}) S \subset \mathcal{H}(d_1, \dots, d_m)$ the closure of the $GL^+(2, \mathbb{R})$ -orbit of S in $\mathcal{H}(d_1, \dots, d_m)$. *In numerous cases knowledge about the structure of $\mathcal{C}(S)$ gives a comprehensive information about geometry and dynamics of the initial flat surface S . Moreover, some delicate numerical characteristics of S can be expressed as averages of simpler characteristics over $\mathcal{C}(S)$.*

The remaining part of this survey is an attempt to show some implementations of this general philosophy. The first two illustrations would be presented in the next section.

We have to confess that we do not tell all the truth in the formulation above. Actually, there is a hope that this philosophy extends much further. A closure of an orbit of an abstract dynamical system might have extremely complicated structure. According to the most optimistic hopes, the closure $\mathcal{C}(S)$ of the $GL^+(2, \mathbb{R})$ -orbit of *any* flat surface S is a nice complex-analytic variety. Moreover, according to the most daring conjecture it would be possible to classify all these $GL^+(2, \mathbb{R})$ -invariant subvarieties. For genus two the latter statements were recently proved by C. McMullen (see [McM2] and [McM3]) and partly by K. Calta [Clt].

We discuss this hope in more details in Sec. 9, in particular, in Sec. 9.3. We complete this section by a Theorem which supports the hope for some nice and simple description of orbit closures.

Theorem (M. Kontsevich). *Suppose that a closure $\mathcal{C}(S)$ in $\mathcal{H}(d_1, \dots, d_m)$ of a $GL^+(2, \mathbb{R})$ -orbit of some flat surface S is a complex-analytic subvariety. Then in cohomological coordinates $H^1(S, \{P_1, \dots, P_m\}; \mathbb{C})$ it is represented by an affine subspace.*

3.7 Implementation of General Philosophy

In this section we present two illustrations showing how the “general philosophy” works in practice.

Consider a directional flow on a flat surface S . It is called *minimal* when the closure of any trajectory gives the entire surface. When a directional flow on a flat torus is minimal, it is necessarily ergodic, in particular, any trajectory in average spends in any subset $U \subset \mathbb{T}^2$ a time proportional to the area (measure) of the subset U . Surprisingly, for surfaces of higher genera a directional flow can be minimal but not ergodic! Sometimes it is possible to find some special direction with the following properties. The flow in this direction is minimal. However, the flat surface S might be decomposed into a disjoint union of several subsets V_i of positive measure in such a way that some trajectories of the directional flow prefer one subset to the others. In other words, the average time spent by a trajectory in the subset V_i is not proportional to the area of V_i anymore. (The original ideas of such examples appear in [Ve1], [Kat1], [Sat] [Kea2]; see also [MaT] and especially [Ma7] for a very accessible presentation of such examples.)

Suppose that we managed to find a direction on the initial surface S_0 such that the flow in this direction is minimal but not ergodic (with respect to the natural Lebesgue measure). Let us apply a rotation to S_0 which would make the corresponding direction vertical. Consider the resulting flat surface S (see Convention 1 in Sec. 1.2). Consider the corresponding “point” $S \in \mathcal{H}(d_1, \dots, d_m)$ and the orbit $\{g_t S\}_{t \in \mathbb{R}}$ of S under the action of the diagonal subgroup $g_t = \begin{pmatrix} e^t & 0 \\ 0 & e^{-t} \end{pmatrix}$.

Recall that the stratum (or, more precisely, the corresponding “unit hyperboloid”) $\mathcal{H}_1(d_1, \dots, d_m)$ is never compact, it always contains “cusps”: regions where the corresponding flat surfaces have very short saddle connections or very short closed geodesics (see Sec. 3.2).

Theorem (H. Masur). *Consider a flat surface S . If the vertical flow is minimal but not ergodic with respect to the natural Lebesgue measure on the flat surface then the trajectory $g_t S$ of the Teichmüller geodesic flow is divergent, i.e. it eventually leaves any fixed compact subset $K \subset \mathcal{H}_1(d_1, \dots, d_m)$ in the stratum.*

Actually, this theorem has an even stronger form.

A stratum $\mathcal{H}_1(d_1, \dots, d_m)$ has “cusps” of two different origins. A flat surface may have two distinct zeroes get very close to each other. In this case S has a short saddle connection (or, what is the same, a short relative period). However, the corresponding Riemann surface is far from being degenerate. The cusps of this type correspond to “simple noncompactness”: any stratum $\mathcal{H}_1(d_1, \dots, d_m)$ is adjacent to all “smaller” strata $\mathcal{H}_1(d_1 + d_2, d_3, \dots, d_m), \dots$

Another type of degeneration of a flat surface is the appearance of a short closed geodesic. In this case the underlying Riemann surface is close to a degenerate one; the cusps of this second type correspond to “essential noncompactness”.

To formulate a stronger version of the above Theorem consider the natural projection of the stratum $\mathcal{H}(d_1, \dots, d_m)$ to the moduli space \mathcal{M}_g of complex structures (see (4) in Sec. 3.3). Consider the image of the orbit $\{g_t S\}_{t \in \mathbb{R}}$ in \mathcal{M}_g under this natural projection. By the reasons which we explain in Sec. 8 it is natural to call this image a *Teichmüller geodesic*.

Theorem (H. Masur). *Consider a flat surface S . If the vertical flow is minimal but not ergodic with respect to the natural Lebesgue measure on the flat surface then the “Teichmüller geodesic” $g_t S$ is divergent, i.e. it eventually leaves any fixed compact subset $K \subset \mathcal{M}$ in the moduli space of complex structures and never visits it again.*

This statement (in a slightly different formulation) is usually called *Masur’s criterion of unique ergodicity* (see Sec. A for discussion of the notion *unique ergodicity*).

As a second illustrations of the “general philosophy” we present a combination of *Veech criterion* and of a Theorem of J. Smillie.

Recall that closed regular geodesics on a flat surface appear in families of parallel closed geodesics. When the flat surface is a flat torus, any such family covers all the torus. However, for surfaces of higher genera such families usually cover a cylinder filled with parallel closed geodesic of equal length. Each boundary of such a cylinder contains a conical point. Usually a geodesic emitted in the same direction from a point outside of the cylinder is dense in the complement to the cylinder or at least in some nontrivial part of the complement. However, in some rare cases, it may happen that the entire surface decomposes into several cylinders filled with parallel closed geodesics going in some fixed direction. This is the case for the vertical or for the horizontal direction on the flat surface glued from a regular octagon, see Fig. 3 (please check). Such direction is called *completely periodic*.

Theorem (J. Smillie; W. A. Veech). *Consider a flat surface S . If its $GL^+(2, \mathbb{R})$ -orbit is closed in $\mathcal{H}(d_1, \dots, d_m)$ then a directional flow in any direction on S is either completely periodic or uniquely ergodic.*

(see Sec. A for the notion of *unique ergodicity*). Note that unique ergodicity implies, in particular, that any orbit which is not a *saddle connection*, (i.e.

which does not hit the singularity both in forward and in backward direction) is everywhere dense. We shall return to this Theorem in Sec. 9.5 where we discuss *Veech surfaces*.

4 How Do Generic Geodesics Wind Around Flat Surfaces

In this section we study geodesics on a flat surface S going in generic directions on S . Such geodesics are dense on S ; moreover, it is possible to show that they wind around S in a relatively regular manner. Namely, it is possible to find a cycle $c \in H_1(S; \mathbb{R})$ such that in some sense a long piece of geodesic pretends to wind around S repeatedly following this *asymptotic cycle* c .

In Sec. 4.1 we study the model case of the torus and give a rigorous definition of the asymptotic cycle. Then we study the asymptotic cycles on general flat surfaces. In Sec. 4.2 we study “further terms of approximation”. The asymptotic cycle describes the way in which a geodesic winds around the surface in average. In Sec. 4.2 we present an empirical description of the deviation from average. The corresponding rigorous statements are formulated in Sec. 4.3. Some ideas of the proof of this statement are presented in Sec. 5.

4.1 Asymptotic Cycle

Asymptotic Cycle on a Torus

As usual we start from the model case of the torus. We assume that our flat torus is glued from a square in the natural way. Consider an irrational direction on the torus; any geodesic going in this direction is dense in the torus.

Fix a point x_0 on the torus and emit a geodesic in the chosen direction. Wait till it winds for some time around the torus and gets close to the initial point x_0 . Join the endpoints of the resulting piece of geodesic by a short path. We get a closed loop on the torus which defines a cycle c_1 in the first homology group $H_1(\mathbb{T}^2; \mathbb{Z})$ of the torus. Now let the initial geodesic wind around the torus for some longer time; wait till it get close enough to the initial point x_0 and join the endpoints of the longer piece of geodesic by a short path. We get a new cycle $c_2 \in H_1(\mathbb{T}^2; \mathbb{Z})$. Considering longer and longer geodesic segments we get a sequence of cycles $c_i \in H_1(\mathbb{T}^2; \mathbb{Z})$.

For example, we can choose a short segment X going through x_0 orthogonal (or just transversal) to the direction of the geodesic. Each time when the geodesic crosses X we join the crossing point with the point x_0 along X obtaining a closed loop. Consecutive return points x_1, x_2, \dots define a sequence of cycles c_1, c_2, \dots , see Fig. 16.

For the torus case we can naturally identify the universal covering space $\mathbb{R}^2 \rightarrow \mathbb{T}^2$ with the first homology group $H_1(\mathbb{T}^2; \mathbb{R}) \simeq \mathbb{R}^2$. Our irrational

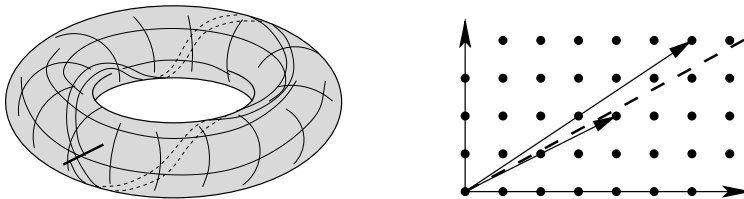


Fig. 16. A sequence of cycles approximating a dense geodesic on a torus

geodesic unfolds to an irrational straight line \mathcal{V}_1 in \mathbb{R}^2 and the sequence of cycles c_1, c_2, \dots becomes a sequence of integer vectors $\mathbf{v}_1, \mathbf{v}_2, \dots \in \mathbb{Z}^2 \subset \mathbb{R}^2$ approximating \mathcal{V}_1 , see Fig. 16.

In particular, it is not surprising that there exists the limit

$$\lim_{n \rightarrow \infty} \frac{c_n}{\|c_n\|} = c \quad (6)$$

Under our identification $H_1(\mathbb{T}^2; \mathbb{R}) \simeq \mathbb{R}^2$ the cycle c represents a unit vector in direction \mathcal{V}_1 .

Let the area of the torus be normalized to one. Let the interval X , which we use to construct the sequence c_1, c_2, \dots , be orthogonal to the direction of the geodesic. Denote by $|X|$ its length. The following limit also exists and is proportional to the previous one:

$$\lim_{n \rightarrow \infty} \frac{1}{n} c_n = \frac{1}{|X|} \cdot c \quad (7)$$

The cycles obtained as limits (6) and (7) are called *asymptotic cycles*. They show how the corresponding irrational geodesic winds around the torus *in average*. It is easy to see that they do not depend on the starting point x .

The notion “asymptotic cycle” was introduced by S. Schwartzman [Schw].

Asymptotic Cycle on a Surface of Higher Genus

We can apply the same construction to a geodesic on a flat surface S of higher genus. Having a geodesic segment $X \subset S$ and some point $x \in X$ we emit from x a geodesic orthogonal to X . From time to time the geodesic would intersect X . Denote the corresponding points as x_1, x_2, \dots . Closing up the corresponding pieces of the geodesic by joining the endpoints x_0, x_j with a path going along X we again get a sequence of cycles c_1, c_2, \dots .

Proposition 1. *For any flat surface S of area one and for almost any direction α on it any geodesic going in direction α is dense on S and has an asymptotic cycle which depends only on α .*

In other words, for almost any direction the limit

$$\lim_{n \rightarrow \infty} \frac{1}{n} c_n = \frac{1}{|X|} \cdot c$$

exists and the corresponding asymptotic cycle c does not depend on the starting point $x_0 \in S$.

This proposition is an elementary corollary from the following theorem of S. Kerckhoff, H. Masur and J. Smillie [KMaS] (which is another Key Theorem in this area).

Theorem (S. Kerckhoff, H. Masur, J. Smillie). *For any flat surface S the directional flow in almost any direction is ergodic.*

In this case the asymptotic cycle has the same dynamical interpretation as for the torus: it shows how a geodesic going in the chosen direction winds around the surface S in average.

Remark. Note that the asymptotic cycle $c \in H_1(S, \mathbb{R})$ also has a topological interpretation. Assume for simplicity that c corresponds to the vertical direction. Let ω be the holomorphic 1-form corresponding to the flat structure on S (see Sec. 3.3). Then the closed 1-form $\omega_0 = \operatorname{Re}(\omega)$ defines the vertical foliation and $c = D[\omega_0]$ is Poincaré dual to the cohomology class of ω_0 . Choosing other ergodic directions on the flat surface S we get asymptotic cycles in the two-dimensional subspace $\langle D[\omega_0], D[\omega_1] \rangle_{\mathbb{R}} \subset H_1(S, \mathbb{R})$ spanned by homology classes dual to cocycles $\omega_0 = \operatorname{Re}(\omega)$ and $\omega_1 = \operatorname{Im}(\omega)$.

4.2 Deviation from Asymptotic Cycle

We have seen in the previous section that a sequence of cycles c_1, c_2, \dots approximating long pieces of an “irrational” geodesic on a flat torus \mathbb{T}^2 and on a flat surface S of higher genus exhibit similar behavior: their norm grows (approximately) linearly in n and their direction approaches the direction of the asymptotic cycle c . Note, however, that for the torus the cycles c_n live in the two-dimensional space $H_1(\mathbb{T}^2; \mathbb{R}) \simeq \mathbb{R}^2$, while for the surface of higher genus $g \geq 2$ the cycles live in the larger space $H_1(S; \mathbb{R}) \simeq \mathbb{R}^{2g}$. In particular, they have “more room” for deviation from the asymptotic direction.

Namely, observing the right part of Fig. 16 we see that all vectors c_n follow the line \mathcal{V}_1 spanned by the asymptotic cycle c rather close: the norm of projection of c_n to the line orthogonal to \mathcal{V}_1 is uniformly bounded (with respect to n and to the choice of the starting point x_0).

The situation is different for surfaces of higher genera. Choose a hyperplane $\mathcal{S} \perp c$ in $H_1(S, \mathbb{R})$ as a screen orthogonal (transversal) to the asymptotic cycle c and consider a projection to this screen parallel to c . Projections of cycles c_n would not be uniformly bounded anymore. There is no contradiction since if the norms of these projections grow sublinearly, then the directions of the cycles c_n still tend to direction of the asymptotic cycle c .

Let us observe how the projections are distributed in the screen \mathcal{S} . Figure 17 shows results of numerical experiments where we take a projection of

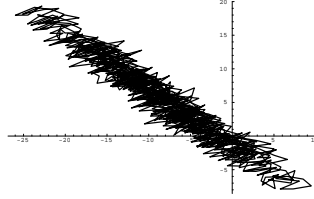


Fig. 17. Projection of a broken line joining the endpoints of $c_1, c_2, \dots, c_{100000}$ to a screen orthogonal to the asymptotic cycle. Genus $g = 3$

a broken line joining the endpoints of $c_1, c_2, \dots, c_{100000}$ and we take a two-dimensional screen orthogonal to c to make the picture more explicit.

We see that the distribution of projections of cycles c_n in the screen \mathcal{S} is anisotropic: the projections accumulate along some line. This means that in the original space \mathbb{R}^{2g} the vectors c_n deviate from the asymptotic direction \mathcal{V}_1 not arbitrarily but along some two-dimensional subspace $\mathcal{V}_2 \supset \mathcal{V}_1$, see Fig. 18.

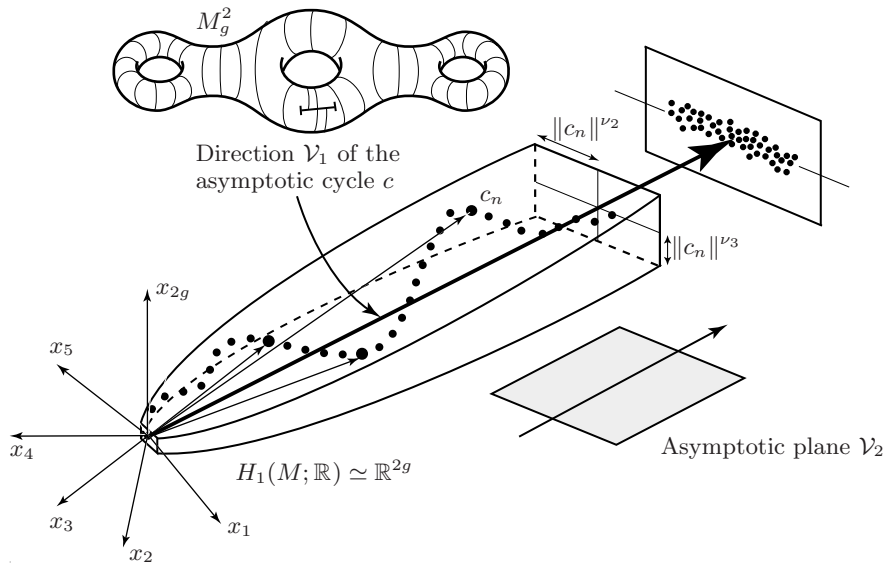


Fig. 18. Deviation from the asymptotic direction

Moreover, measuring the norms of the projections $proj(c_n)$ to the screen \mathcal{S} orthogonal to $\mathcal{L}_1 = \langle c \rangle_{\mathbb{R}}$, we get

$$\limsup_{n \rightarrow \infty} \frac{\log \|proj(c_n)\|}{\log n} = \nu_2 < 1$$

In other words the vector c_n is located approximately in the subspace \mathcal{V}_2 , and the distance from its endpoint to the line $\mathcal{V}_1 \subset \mathcal{V}_2$ is bounded by $\text{const} \cdot \|c_n\|^{\nu_2}$, see Fig. 18.

Consider now a new screen $\mathcal{S}_2 \perp \mathcal{V}_2$ orthogonal to the plane \mathcal{V}_2 . Now the screen \mathcal{S}_2 has codimension two in $H_1(S, \mathbb{R}) \simeq \mathbb{R}^{2g}$. Considering the projections of c_n to \mathcal{S}_2 we eliminate the asymptotic directions \mathcal{V}_1 and \mathcal{V}_2 and we see how do the vectors c_n deviate from \mathcal{V}_2 . On the screen \mathcal{S}_2 we see the same picture as in Fig. 17: the projections are located along a one-dimensional subspace.

Coming back to the ambient space $H_1(S, \mathbb{R}) \simeq \mathbb{R}^{2g}$, this means that in the first term of approximation all vectors c_n are aligned along the one-dimensional subspace \mathcal{V}_1 spanned by the asymptotic cycle. In the second term of approximation, they can deviate from \mathcal{V}_1 , but the deviation occurs mostly in the two-dimensional subspace \mathcal{V}_2 , and has order $\|c\|^{\nu_2}$ where $\nu_2 < 1$. In the third term of approximation we see that the vector c_n may deviate from the plane \mathcal{V}_2 , but the deviation occurs mostly in a three-dimensional space \mathcal{V}_3 and has order $\|c\|^{\nu_3}$ where $\nu_3 < \nu_2$.

Going on we get further terms of approximation. However, getting to a subspace \mathcal{V}_g which has half the dimension of the ambient space we shall see that, in a sense, there is no more deviation from \mathcal{V}_g : the distance from any c_n to \mathcal{V}_g is uniformly bounded.

Note that the intersection form endows the space $H_1(S, \mathbb{R}) \simeq \mathbb{R}^{2g}$ with a natural symplectic structure. It can be checked that the resulting g -dimensional subspace \mathcal{V}_g is a *Lagrangian* subspace for this symplectic form.

4.3 Asymptotic Flag and “Dynamical Hodge Decomposition”

A rigorous formulation of phenomena described in the previous section is given by the following Theorem proved³ by the author in [Zo3] and [Zo4].

Following Convention 1 we always consider a flat surface together with a choice of direction which by convention is called the *vertical direction*, or *direction to the North*. Using an appropriate homothety we normalize the area of S to one, so that $S \in \mathcal{H}_1(d_1, \dots, d_m)$.

We chose a point $x_0 \in S$ and a horizontal segment X passing through x_0 ; by $|X|$ we denote the length of X . We consider a geodesic ray γ emitted from x_0 in the vertical direction. (If x_0 is a saddle point, there are several outgoing vertical geodesic rays; choose any of them.) Each time when γ intersects X we join the point x_n of intersection and the starting point x_0 along X producing a closed path. We denote the homology class of the corresponding loop by c_n .

Let ω be the holomorphic 1-form representing S ; let g be genus of S . Choose some Euclidean metric in $H_1(S; \mathbb{R}) \simeq \mathbb{R}^{2g}$ which would allow to measure a distance from a vector to a subspace. Let by convention $\log(0) = -\infty$.

³Actually, the theorem was initially proved under certain hypothesis on the Lyapunov exponents of the Teichmüller geodesic flow. These conjectures were proved later by G. Forni and in the most complete form by A. Avila and M. Viana; see the end of this section and especially Sec. 5.8

Theorem. For almost any flat surface S in any stratum $\mathcal{H}_1(d_1, \dots, d_m)$ there exists a flag of subspaces

$$\mathcal{V}_1 \subset \mathcal{V}_2 \subset \dots \subset \mathcal{V}_g \subset H_1(S; \mathbb{R})$$

in the first homology group of the surface with the following properties.

Choose any starting point $x_0 \in X$ in the horizontal segment X . Consider the corresponding sequence c_1, c_2, \dots of cycles.

— The following limit exists

$$|X| \lim_{n \rightarrow \infty} \frac{1}{n} c_n = c,$$

where the nonzero asymptotic cycle $c \in H_1(M_g^2; \mathbb{R})$ is Poincaré dual to the cohomology class of $\omega_0 = \operatorname{Re}[\omega]$, and the one-dimensional subspace $\mathcal{V}_1 = \langle c \rangle_{\mathbb{R}}$ is spanned by c .

— For any $j = 1, \dots, g-1$ one has

$$\limsup_{n \rightarrow \infty} \frac{\log \operatorname{dist}(c_n, \mathcal{V}_j)}{\log n} = \nu_{j+1}$$

and

$$|\operatorname{dist}(c_n, \mathcal{V}_g)| \leq \operatorname{const},$$

where the constant depends only on S and on the choice of the Euclidean structure in the homology space.

The numbers $2, 1 + \nu_2, \dots, 1 + \nu_g$ are the top g Lyapunov exponents of the Teichmüller geodesic flow on the corresponding connected component of the stratum $\mathcal{H}(d_1, \dots, d_m)$; in particular, they do not depend on the individual generic flat surface S in the connected component.

A reader who is not familiar with *Lyapunov exponents* can either read about them in Appendix B or just consider the numbers ν_j as some abstract constants which depend only on the connected component $\mathcal{H}^{\operatorname{comp}}(d_1, \dots, d_m)$ containing the flat surface S .

It should be stressed, that the theorem above was initially formulated in [Zo4] as a conditional statement: under the conjecture that $\nu_g > 0$ there exist a Lagrangian subspace \mathcal{V}_g such that the cycles are in a bounded distance from \mathcal{V}_g ; under the further conjecture that all the exponents ν_j , for $j = 1, 2, \dots, g$, are distinct, there is a *complete* Lagrangian flag (i.e. the dimensions of the subspaces \mathcal{V}_j , where $j = 1, 2, \dots, g$, rise each time by one). These two conjectures were later proved by G. Forni [For1] and by A. Avila and M. Viana [AvVi]. We discuss their theorems in Sec. 5.8.

Another remark concerns the choice of the horizontal segment X . By convention it is chosen in such way that the trajectories emitted in the vertical direction (in direction to the North) from the endpoints of X hit the conical points before the first return to X . Usually we just place the left endpoint of X at the conical point.

Omitting this condition and considering a continuous family of horizontal subintervals X_t of variable length (say, moving continuously one of the endpoints), the theorem stays valid for a subset of X_t of full measure.

5 Renormalization for Interval Exchange Transformations. Rauzy–Veech Induction

In this section we elaborate a powerful time acceleration machine which allows to study the asymptotic cycles described in Sec. 4. Following the spirit of this survey we put emphasis on geometric ideas and omit proofs. This section can be considered as a geometric counterpart of the article of J.-C. Yoccoz [Y] in the current volume.

I use this opportunity to thank M. Kontsevich for numerous ideas and conjectures which were absolutely crucial for my impact in this theory: without numerous discussions with M. Kontsevich papers [Zo2] and [Zo3], probably, would be never written.

5.1 First Return Maps and Interval Exchange Transformations

Our goal is to study cycles obtained from long pieces of “irrational” geodesic on a flat surface by joining their endpoints along a transversal segment X . To perform this study we elaborate some simple machine which generates the cycles, and then we accelerate this machine to obtain very long cycles in a rather short time.

Consider *all* geodesics emitted from a transverse segment X in the same generic direction and let each of them come back to X for the first time. We get a *first return map* $T : X \rightarrow X$ which is interesting by itself and which deserves a separate discussion. Its properties play a crucial role in our study. (See Appendix A for general properties of the first return map.)

As usual let us start with a model case of a flat torus. Take a meridian of the torus as a transversal X and emit from X a directional flow. Every geodesic comes back to X inducing the *first return map* $T : X \rightarrow X$, which in this case isometrically rotates the meridian X along itself by an angle which depends on the direction of the flow, see Fig. 19.

Assume that our flat torus \mathbb{T}^2 is glued from a unit square. Let us replace now a meridian of the torus by a generic geodesic segment X orthogonal to the direction of the flow. From every point of X we emit a geodesic in direction orthogonal to X and wait till it hits X for the first time. We again obtain a first return map $T : X \rightarrow X$, but this time the map T is slightly more complicated.

To study this map it is convenient to unfold the torus into a plane. The map T is presented at Fig. 20. It chops X into three pieces and then shuffles them sending the left subinterval to the right, the right subinterval to the left

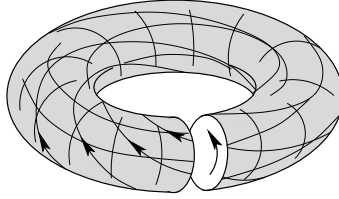


Fig. 19. The first return map of a meridian to itself induced by a directional flow is just a twist

and keeping the middle one in the middle but shifting it a bit. The map T gives an example of an *interval exchange transformation*.

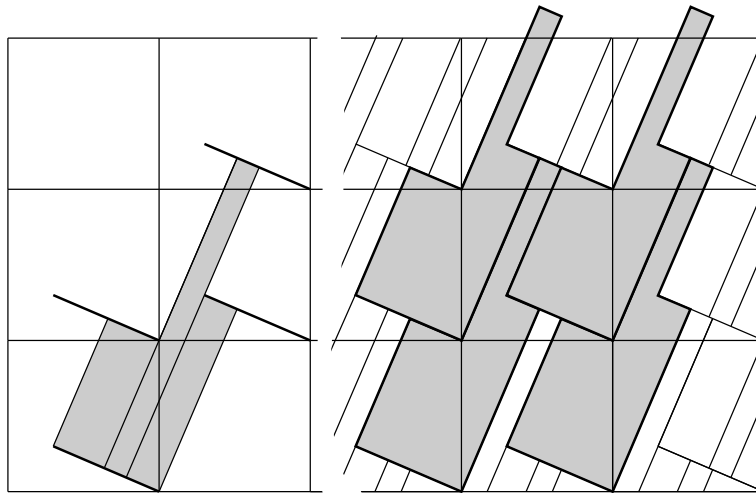


Fig. 20. Directional flow on a torus. The first return map of a segment to itself is an interval exchange transformation of three subintervals

Note that when the direction of the flow is *irrational*, the geodesics emitted from X again cover the entire torus \mathbb{T}^2 before coming back to X . The torus is get ripped into three rectangles based on the three subintervals in which T chops X . The corresponding building of three rectangles gives a new fundamental domain representing the torus: one can see at Fig. 20 that it tiles the plane. Initially we glued our flat torus from a square; the building under consideration gives another way to unwrap \mathbb{T}^2 into a polygon. We recommend to the reader to check that identifying the two pairs of corresponding vertical sides of the building and gluing the top horizontal sides of the rectangles to the bottom of X as prescribed by the interval exchange transformation T we get the initial torus.

Consider now a flat surface of genus higher than one. Say, consider a flat surface of genus $g = 2$ as on Fig. 21. We suggest to the reader to check that this flat surface has a single conical singularity with a cone angle 6π (see Fig. 2). To study a directional flow choose as before a geodesic segment $X \subset S$ orthogonal to the direction of the flow and consider the first return map $T : X \rightarrow X$ induced by the flow; see Fig. 21. We see that X is chopped into a larger number of subintervals (in comparison with the torus case), namely, for our choice of X it is chopped into four subintervals.

Now we observe a new phenomenon: trajectories emitted from some points of X hit the conical point and our directional flow splits at this point. Since in our particular case the cone angle at the conical point is $6\pi = 3 \cdot 2\pi$ there are *three* trajectories in direction \mathbf{v} which hit it. The corresponding points at which X is chopped are marked with bold dots. The remaining discontinuity point of X corresponds to a trajectory which hits the endpoint of X .

Our construction with a segment X transversal to the flow and with trajectories of the flow emitted from X and followed till their first return to X trims a braid from the flow. Conical points play the role of a comb which splits the flow into several locks and then trims them in a different order. Note, however, that if we follow the flow till the second return to X it will pass through the comb twice, and thus will be generically split already into seven locks. (If you are interested in details, think why this second return has *seven* and not *eight* locks and what sort of genericity we need).

Similarly, the interval exchange transformation T of the base interval X can be compared to a shuffling machine. Imagine that X represents a stock of cards. We split the stock into n parts of fixed widths and shuffle the parts in a different order (given by some permutation π of n elements). At the second iteration we again split the new stock in the parts of the same widths as before and shuffle the parts according to the same permutation π , etc. Note, that even if the permutation π is such that $\pi^2 = id$, say, $\pi = (4, 3, 2, 1)$, the second iteration T^2 is not an identical transformation provided the widths $\lambda_1, \dots, \lambda_4$ are not symmetric: for a generic choice of $\lambda_1, \dots, \lambda_4$ the interval exchange transformation T^2 has 6 discontinuities (and hence 7 subintervals under exchange).

Exercise. Consider an interval exchange transformation $T(\lambda, \pi)$ corresponding to the permutation $\pi = (4, 3, 2, 1)$. Choose some generic values of the lengths $\lambda_1, \dots, \lambda_4$ of subintervals and construct T^2 and T^3 .

5.2 Evaluation of the Asymptotic Cycle Using an Interval Exchange Transformation

Now we can return to our original problem. We want to study long pieces of leaves of the vertical foliation. Fix a horizontal segment X and emit a vertical trajectory from some point $x \in X$. When the trajectory intersects X for the first time join the corresponding point $T(x)$ to the original point x

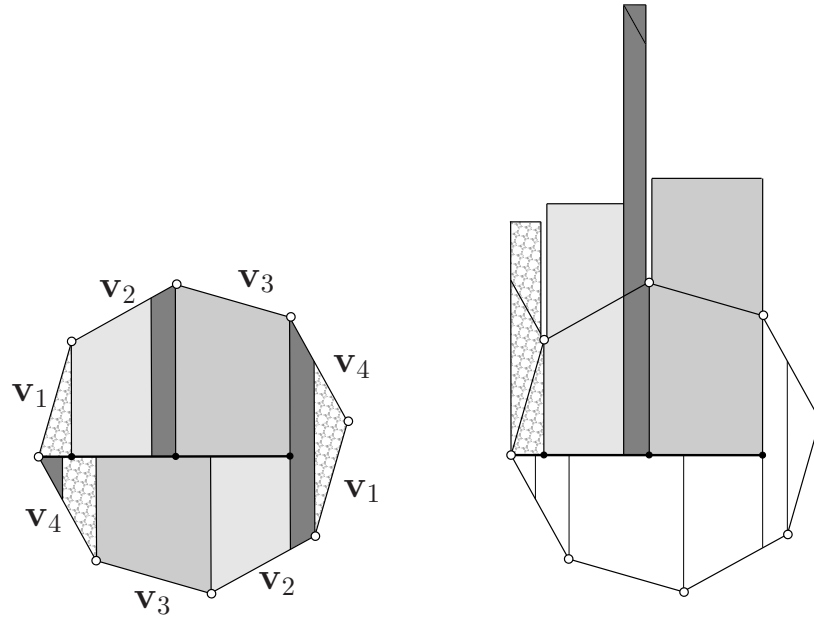


Fig. 21. The first return map $T : X \rightarrow X$ of a geodesic segment X defined by a directional flow decomposes the surface into four rectangles “zippered” along singular trajectories

along X to obtain a closed loop. Here $T : X \rightarrow X$ denotes the first return map to the transversal X induced by the vertical flow. Denote by $c(x, 1)$ the corresponding cycle in $H_1(S; \mathbb{Z})$. Following the vertical trajectory further on we shall return to X once again. Joining x and the point $T(T(x))$ of the second return to X along X we obtain the second cycle $c(x, 2)$. We want to describe the cycle $c(x, N)$ obtained after a very large number N of returns.

Actually, we prefer to close up a piece of trajectory going from $x \in X$ to the first return point $T(x) \in X$ in a slightly different way. Instead of completing the path joining the endpoints it is more convenient to close this piece of trajectory joining both points x and $T(x)$ to the left endpoint of X along X (see Fig. 22). This modified path defines the same homology cycle $c(x, 1)$ as the closed path for which the points x and $T(x)$ are joined directly.

Consider now the “first return cycle” $c(x, 1)$ as a function $c(x) = c(x, 1)$ of the starting point $x \in X$. Let the interval exchange transformation $T : X \rightarrow X$ decompose X into n subintervals $X_1 \sqcup \dots \sqcup X_n$. It is easy to see that the function $c(x)$ is piecewise constant: looking at Fig. 22 one can immediately verify that if two points x_1 and x_2 are not separated by a discontinuity point (i.e. if they belong to the same subinterval X_j) they determine homologous (and even homotopic) cycles $c(x_1) = c(x_2)$. Each subinterval X_j determines its own cycle $c(X_j)$.

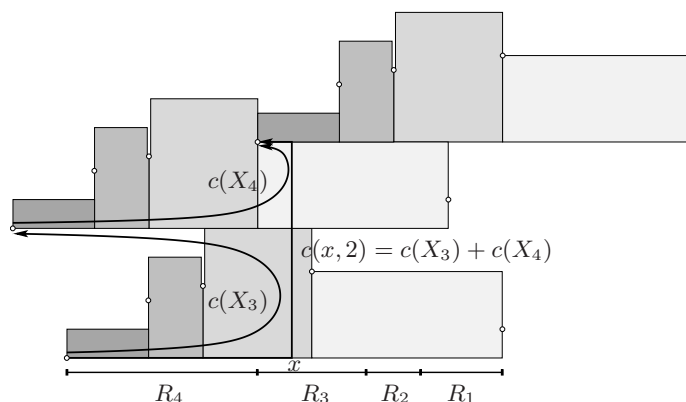


Fig. 22. Decomposition of a long cycle into the sum of basic cycles. (We have unfolded the flat surface along vertical trajectory emitted from the point x)

The vertical trajectory emitted from a point $x \in X$ returns to X at the points $T(x), T^2(x), \dots, T^N(x)$. It is easy to see that the cycle $c(x, 2)$ corresponding to the second return can be represented as a sum $c(x, 2) = c(x) + c(T(x))$, see Fig. 22. Similarly the cycle $c(x, N)$ obtained by closing up a long piece of vertical trajectory emitted from $x \in X$ and followed up to N -th return to X can be represented as a sum

$$c(x, N) = c(x) + c(T(x)) + \dots + c(T^{N-1}(x)) \quad (8)$$

According to the fundamental Theorem of S. Kerckhoff, H. Masur and J. Smillie [KMaS], for any flat surface the directional flow in almost any direction is ergodic, and even uniquely ergodic. Hence, the same is true for the corresponding interval exchange transformation. Applying the ergodic theorem (see Appendix A) to the sum (8) and taking into consideration that $c(x)$ is a piecewise-constant function we get

$$c(x, N) \sim N \cdot \frac{1}{|X|} \int_X c(x) dx = N \cdot \frac{1}{|X|} (\lambda_1 c(X_1) + \dots + \lambda_n c(X_n))$$

where $c(X_j)$ denotes the “first return cycle” for the points x in the subinterval X_j , see Fig. 22. This gives an explicit formula for the *asymptotic cycle*

$$c = \lim_{N \rightarrow \infty} \frac{c(x, N)}{N} = \frac{1}{|X|} (\lambda_1 c(X_1) + \dots + \lambda_n c(X_n)) \quad (9)$$

Note that the asymptotic cycle does not depend on the starting point $x \in X$.

Exercise. Show that the paths $\mathbf{v}_1, \dots, \mathbf{v}_4$ (see Fig. 21) represent a basis of cycles of the corresponding flat surface S of genus $g = 2$. Show that the first return cycles $c(X_j)$ determine another basis of cycles and that one can pass from one basis to the other using the following relations (see Fig. 21):

$$\begin{aligned} c(X_1) &= \mathbf{v}_1 - \mathbf{v}_4 & c(X_2) &= \mathbf{v}_1 - \mathbf{v}_3 - \mathbf{v}_4 \\ c(X_3) &= 2\mathbf{v}_1 + \mathbf{v}_2 - \mathbf{v}_4 & c(X_4) &= \mathbf{v}_1 + \mathbf{v}_2 + \mathbf{v}_3 - \mathbf{v}_4 \end{aligned}$$

Express the asymptotic cycle in the basis \mathbf{v}_j in terms of the lengths λ_j and then in terms of the angle by which the regular octagon is turned with respect to the standard presentation. Locally the vertical foliation goes to the North. And globally?

5.3 Time Acceleration Machine (Renormalization): Conceptual Description

In the previous section we have seen why all trajectories of a typical directional flow wind around the surface following the same asymptotic cycle. We have also found an effective way to evaluate this asymptotic cycle: we have seen that it is sufficient to find an interval exchange transformation $T : X \rightarrow X$ induced on any transverse segment X as the first return map of the directional flow, and then to determine the “first return cycles” $c(X_j)$, see Fig. 22. The linear combination of the cycles $c(X_j)$ taken with weights proportional to the lengths $\lambda_j = |X_j|$ of subintervals gives the asymptotic cycle, see (9).

Let us proceed now with a more delicate question of deviation of a trajectory of the directional flow from the asymptotic direction. Without loss of generality we may assume that the directional flow under consideration is the vertical flow. We know that a very long cycle $c(x, N)$ corresponding to a large number N of returns of the trajectory to the horizontal segment X stretches in the direction approaching the direction of the asymptotic cycle c . We want to describe how $c(x, N)$ deviates from this direction (see Sec. 4.2 and Sec. 4.3).

We have already seen that as soon as we have evaluated the “first return cycles” $c(X_j)$, complete information about cycles representing long pieces of trajectories of the directional flow is encoded in the corresponding trajectory $x, T(x), \dots, T^{N-1}(x)$ of the interval exchange transformation; see (8).

An interval exchange transformations gives an example of a parabolic dynamical system which is neither completely regular (like rotation of a circle) nor completely chaotic (like geodesic flow on a compact manifold of constant negative curvature, which is a typical example of a *hyperbolic* system). In some aspects interval exchange transformations are closer to rotations of a circle: say, as it was proved by A. Katok, an interval exchange transformation is never mixing [Kat2] (though, as it was very recently proved by A. Avila and G. Forni in [AvFor], generically it is weakly mixing). However, the behavior of deviation from the ergodic mean resembles the behavior of a chaotic system.

Our principal tool in the study of interval exchange transformations exploits certain self-similarity of these maps. Choosing a shorter horizontal interval X' we make the vertical flow wind for a long time before the first return to X' . However, the new first return map in a sense would not be more complicated than the initial one: it would be again an interval exchange

transformation $T' : X' \rightarrow X'$ of the same (or almost the same) number of subintervals.

To check the latter statement let us study the nature of the points of discontinuity of the first return map $T : X \rightarrow X$. An interior point $x \in X$ is a point of discontinuity either if the forward vertical trajectory of x hits one of the endpoints of X (as on Fig. 20) or if the forward vertical trajectory of x hits the conical point before coming back to X (see Fig. 21). A conical point having the cone angle $2\pi(d+1)$ has $d+1$ incoming vertical trajectories which land to this conical point. (Say, the flat surface represented on Fig. 21 has a single conical point with the cone angle 6π ; hence this conical point has 3 incoming vertical trajectories.) Following them at the backward direction till the first intersection with X we find $d+1$ points of discontinuity on X (see Fig. 21). Thus, all conical points taken together produce $\sum_j (d_j + 1)$ points of discontinuity on X .

Generically two more points of discontinuity come from the backward trajectories of the endpoints of X . However, in order to get as small number of discontinuity points as possible we can choose X in such way that either backward or forward trajectory of each of the two endpoints hits some conical point before coming back to X . This eliminates these two additional discontinuity points.

Convention 2. From now on we shall always choose any horizontal subinterval X in such way that the interval exchange transformation $T : X \rightarrow X$ induced by the first return of the vertical flow to X has the minimal possible number

$$n = \sum_j (d_j + 1) + 1 = 2g + (\text{number of conical points}) - 1$$

of subintervals under exchange.

In the formula above we used the Gauss–Bonnet formula telling that $\sum_j d_j = 2g - 2$, where g is the genus of the surface.

Following Convention 2 we shall usually place the left endpoint of the horizontal interval X at the conical singularity. This leaves a discrete choice for the position of the right endpoint.

Renormalization

We apply the following strategy in our study of cycles $c(x, N)$. Choose some horizontal segment X satisfying Convention 2. Consider vertical trajectories, which hit conical points. Follow them in backward direction till the first intersection with X . Consider the resulting decomposition $X = X_1 \sqcup \cdots \sqcup X_n$, the corresponding interval exchange transformation $T : X \rightarrow X$ and the “first return cycles” $c(X_j)$.

Consider a smaller subinterval $X' \subset X$ satisfying Convention 2. Apply the above procedure to X' ; let $X' = X'_1 \sqcup \cdots \sqcup X'_n$ be the corresponding

decomposition of X' . We get a new partition of our flat surface into a collection of n rectangles based over subintervals $X'_1 \sqcup \dots \sqcup X'_n$.

By construction the vertical trajectories of any two points $x_0, x \in X'_k$ follow the same high and narrow rectangle R'_k of the new building up to their first return to X' . This implies that the corresponding new “first return cycles” $c'(x_0) = c'(x)$ are the same and equal to $c'(X'_k)$.

Both vertical trajectories of $x_0, x \in X'_k$ intersect the initial interval X many times before first return to X' . However, since these trajectories stay together, they visit the same intervals X_{j_k} in the same order j_0, j_1, \dots, j_l (the length $l = l(k)$ of this trajectory depends on the subinterval X'_k).

This means that we can construct an $n \times n$ -matrix B_{jk} indicating how many times a vertical trajectory emitted from a point $x \in X'_k$ have visited subinterval X_j before the first return to X' . (By convention the starting point counts, while the first return point does not.) Here $X = X_1 \sqcup \dots \sqcup X_n$ is the partition of the initial “long” horizontal interval X and $X' = X'_1 \sqcup \dots \sqcup X'_n$ is the partition of the new “short” subinterval X' .

Having computed this integer matrix B we can represent new “first return cycles” $c'(X'_k)$ in terms of the initial “first return cycles” $c(X_j)$ as

$$c'(X'_k) = B_{1k}c(X_1) + \dots + B_{nk}c(X_n) \quad (10)$$

Moreover, it is easy to see that the lengths $\lambda'_k = |X'_k|$ of subintervals of the new partition are related to the lengths $|X_j|$ of subintervals of the initial partition by a similar relation

$$\lambda_j = B_{j1}\lambda'_1 + \dots + B_{jn}\lambda'_n. \quad (11)$$

Note that to evaluate matrix B we, actually, do not need to use the vertical flow: the matrix B is completely determined by the initial interval exchange transformation $T : X \rightarrow X$ and by the position of the subinterval $X' \subset X$.

What we gain with this construction is the following. To consider a cycle $c(x, N)$ representing a long piece of leaf of the vertical foliation we followed the trajectory $x, T(x), \dots, T^N(x)$ of the initial interval exchange transformation $T : X \rightarrow X$ and applied formula (8). Passing to a shorter horizontal interval $X' \subset X$ we can follow the trajectory $x, T'(x), \dots, (T')^{N'}(x)$ of the new interval exchange transformation $T' : X' \rightarrow X'$ (provided $x \in X'$). Since the subinterval X' is much shorter than X we cover the initial piece of trajectory of the vertical flow in a smaller number N' of steps. In other words, passing from T to T' we accelerate the time: it is easy to see that the trajectory $x, T'(x), \dots, (T')^{N'}(x)$ follows the trajectory $x, T(x), \dots, T^N(x)$ but jumps over many iterations of T at a time.

Of course this approach would be non efficient if the new first return map $T' : X' \rightarrow X'$ would be much more complicated than the initial one. But we know that passing from T to T' we stay within a family of interval exchange transformations of the fixed number n of subintervals, and, moreover, that the new “first return cycles” and the lengths of the new subintervals are expressed

in terms of the initial ones by means of the $n \times n$ -matrix B , which depends only on the choice of $X' \subset X$ and which can be easily computed.

Our strategy can be formalized as follows. In the next two sections we describe a simple explicit algorithm (generalizing Euclidean algorithm) called Rauzy–Veech induction which canonically associates to an interval exchange transformation $T : X \rightarrow X$ some specific subinterval $X' \subset X$ and, hence, a new interval exchange transformation $T' : X' \rightarrow X'$. This algorithm can be considered as a map from the *space of all interval exchange transformations* of a given number n of subintervals to itself. Applying recursively this algorithm we construct a sequence of subintervals $X = X^{(0)} \supset X^{(1)} \supset X^{(2)} \supset \dots$ and a sequence of matrices $B = B(X^{(0)}), B(X^{(1)}), \dots$ describing transitions from interval exchange transformation $T^{(r)} : X^{(r)} \rightarrow X^{(r)}$ to interval exchange transformation $T^{(r+1)} : X^{(r+1)} \rightarrow X^{(r+1)}$. Rewriting equations (10) and (11) in a matrix form we get:

$$\begin{pmatrix} c(X_1^{(r+1)}) \\ \dots \\ c(X_n^{(r+1)}) \end{pmatrix} = \begin{pmatrix} B(X^{(r)}) \end{pmatrix}^T \cdot \begin{pmatrix} c(X_1^{(r)}) \\ \dots \\ c(X_n^{(r)}) \end{pmatrix} \tag{12}$$

$$\begin{pmatrix} \lambda_1(X^{(r+1)}) \\ \dots \\ \lambda_n(X^{(r+1)}) \end{pmatrix} = \begin{pmatrix} B(X^{(r)}) \end{pmatrix}^{-1} \cdot \begin{pmatrix} \lambda_1(X^{(r)}) \\ \dots \\ \lambda_n(X^{(r)}) \end{pmatrix}$$

Taking a product $B^{(s)} = B(X^{(0)}) \cdot B(X^{(1)}) \cdot \dots \cdot B(X^{(s-1)})$ we can immediately express the “first return cycles” to a microscopic subinterval $X^{(s)}$ in terms of the initial “first return cycles” to X by a linear expression analogous to (12). Note, however, that before coming back to this microscopic subinterval $X^{(s)}$ the vertical flow has to travel for enormously long time. The first return cycle to this very short subinterval $X^{(s)}$ represents the cycle $c(x, N)$ corresponding to very long trajectory $x, T(x), \dots, T^N(x)$ of the initial interval exchange transformation with $N \sim \exp(\text{const} \cdot s)$. In other words, our renormalization procedure plays a role of a time acceleration machine: instead of following patiently the trajectory $x, T(x), \dots, T^N(x)$ of the initial interval exchange transformation for the exponential time $N \sim \exp(\text{const} \cdot s)$ we obtain the cycle $c(x, N)$ applying only s steps of renormalization!

One can argue that in this way we can describe only very special parts of vertical trajectories: those which start and end at the same microscopically small subinterval $X^{(s)} \subset X$. This can be overdone by the following technique. Consider an enormously long trajectory $x, T(x), \dots, T^N(x)$ which starts and finishes at some generic points of X . One can choose $s(N)$ in such way that the trajectory would get to $X^{(s)}$ relatively soon (in comparison with its length N); then would return back to $X^{(s)}$ many times; and would reach the last point $T^N(x)$ relatively fast after the last visit to $X^{(s)}$. That means that essentially (up to negligibly short starting part and ending part) one can assume that the

entire trajectory starts at $X^{(s)}$ and ends at $X^{(s)}$ (returning to this subinterval many times).

This simple idea can be developed and rigorously arranged (see [Zo4] for details). To avoid overloading of this survey with technicalities we consider only a simplified problem giving a comprehensive description of the first return cycles to $X^{(s)}$. The nature of the asymptotic flag is especially transparent in this case.

5.4 Euclidean Algorithm as a Renormalization Procedure in Genus One

To illustrate the idea of renormalization we start with the “elementary” case, when the Riemann surface is a torus, the foliation is a standard irrational foliation, and the initial transversal X is a meridian. We have seen at Fig. 19 that in this case the first return map $T : X \rightarrow X$ is just a rotation of a circle.

Consider rotation of a circle $T : S^1 \rightarrow S^1$ by an angle α . Let the length of the circle be normalized to one. Consider trajectory x, Tx, T^2x, \dots of a point x (see Fig. 23). Denote the length of the arc (x, Tx) by $\lambda = \alpha/(2\pi)$.

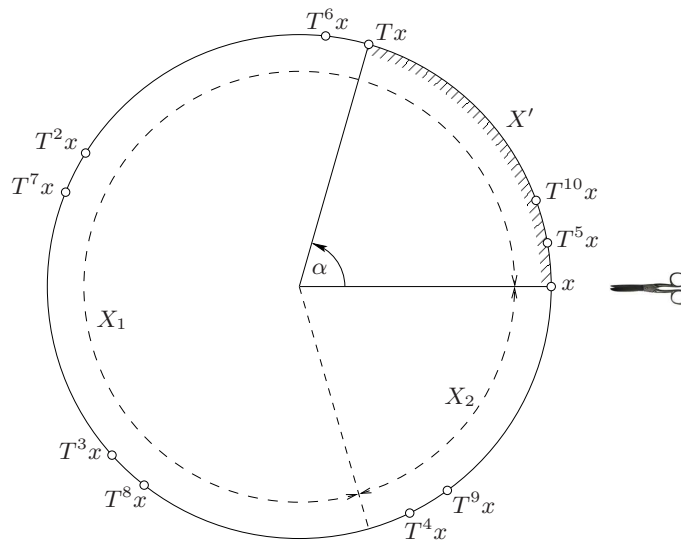


Fig. 23. Renormalization for rotation of a circle leads to Euclidean algorithm and to Gauss measure

Cutting the circle at the point x we get an interval X ; the rotation of the circle generates a map of the interval X to itself which we denote by the same symbol $T : X \rightarrow X$. Unbend X isometrically to get a horizontal interval of unit length in such way that the counterclockwise orientation of

the circle gives the standard positive orientation of the horizontal interval. The map T acts on X as follows: it cuts the unit interval X into two pieces $X_1 \sqcup X_2$ of lengths $|X_1| = 1 - \lambda$ and $|X_2| = \lambda$ and interchanges the pieces preserving the orientation, see Fig. 23. In other words, the map T is an interval exchange transformation of two subintervals. (To avoid confusion we stress that $X_2 = [T^{-1}x, x]$ and *not* $X = [x, Tx]$.)

Suppose now that we are looking at X in the microscope which shows only the subinterval $X' = [x, Tx[$ (corresponding to the sector of angle α at Fig. 23). Consider the trajectory x, Tx, T^2x, \dots of the point x which is the left extremity of X_1 . For the particular rotation represented at Fig. 23 the points Tx, T^2x, T^3x, T^4x are outside of the sector of our vision; the next point of the trajectory which we see in X' is the point T^5x . This is the first return point $T'x = T^5x$ to the subinterval X' . Following the trajectory T^5x, T^6x, \dots further on we would not see several more points and then we shall see $T^{10}x = T'(T'x)$. This is the second return to the subinterval X' .

Note that the distance between x and $T'x = T^5x$ is the same as the distance between $T'x = T^5x$ and $T'(T'x) = T^{10}x$; it equals $(1 - \{1/\lambda\}) \cdot \lambda$, where $\{ \}$ denotes the fractional part of a real number. It is easy to see that $T' : X' \rightarrow X'$ is again an interval exchange transformation of *two* subintervals $X'_1 \sqcup X'_2$. The lengths of subintervals are $|X'_1| = \{1/\lambda\} \cdot \lambda$ and $(1 - \{1/\lambda\}) \cdot \lambda$. After identification of the endpoints the segment X' becomes a circle and the map T' becomes a rotation of the circle T' . Having started with a rotation T in a *counterclockwise* direction by the angle $\alpha = 2\pi \cdot \lambda$ we get a rotation T' in a *clockwise* direction by the angle $\alpha' = 2\pi \cdot \left\{ \frac{1}{\lambda} \right\}$ (please verify).

One should not think that $T' = T^5$ identically. It is true for the points of first subinterval, $T'|_{X'_1} = T^5$. However, for the points of the second subinterval X'_2 we have $T'|_{X'_2} = T^4$. In other words, for the points of the sector α , which are close to the extremity Tx , *four* iterations of T bring them back to the sector. Thus, the matrix $B(X')$ of number of visits to subintervals has the form

$$\begin{pmatrix} B_{11} & B_{12} \\ B_{21} & B_{22} \end{pmatrix} = \begin{pmatrix} 4 & 3 \\ 1 & 1 \end{pmatrix}$$

(please draw $X_1 \sqcup X_2$ and $X'_1 \sqcup X'_2$ and verify). We remind that B_{jk} indicates how many times a vertical trajectory emitted from a point $x \in X'_k$ have visited subinterval X'_j before the first return to X' , where by convention the starting point counts, while the first return point does not.

Thus we get a renormalization procedure as described in the previous section: confine the map T to a smaller subinterval X' ; consider the resulting first return map T' ; rescale X' to have unit length. Having started with an interval exchange transformation T of two intervals of lengths $(1 - \lambda, \lambda)$, where $\lambda \in (0, 1)$ we get (after rescaling) an interval exchange transformation T' of two intervals of lengths $\{1/\lambda\}, 1 - \{1/\lambda\}$. Or, in terms of rotations, having

started with a *counterclockwise* rotation by the angle $\alpha = 2\pi\lambda$ we get a *clockwise* rotation by the angle $\alpha' = 2\pi \cdot \left\{ \frac{1}{\lambda} \right\}$.

One can recognize Euclidean algorithm in our renormalization procedure. Consider the “space of rotations”, where rotations are parametrized by the angle $2\pi\lambda$, $\lambda \in [0; 1[$. The map

$$g : \lambda \mapsto \left\{ \frac{1}{\lambda} \right\} \quad (13)$$

can be considered as a map from “the space of rotations” to itself, or what is the same, a map from “the space of interval exchange transformations of two subintervals” to itself. The map g is ergodic with respect to the invariant probability measure

$$d\mu = \frac{1}{\log 2} \cdot \frac{d\lambda}{(\lambda + 1)} \quad (14)$$

on the parameter space $\lambda \in [0; 1[$ which is called the *Gauss measure*. This map is intimately related with the development of λ into a continued fraction

$$\lambda = \frac{1}{n_1 + \frac{1}{n_2 + \frac{1}{n_3 + \dots}}}$$

We shall see another renormalization procedure related to map (13) in the next sections, in particular, in Sec. 5.9.

5.5 Rauzy–Veech Induction

In the previous section we have seen an example of a renormalization procedure for interval exchange transformations of two intervals. In this section we consider a similar renormalization procedure which now works for interval exchanges of any number of subintervals. As we have seen in the previous section, we do not need to keep information about the flat surface to describe the renormalization algorithm. Nevertheless, we prefer to keep track of zippered rectangles decomposition of the surface corresponding to the sequence of the horizontal subintervals $X = X^{(0)} \supset X^{(1)} \supset \dots$ in order to preserve geometric spirit of the algorithm.

Consider a flat surface S ; choose a horizontal interval X satisfying Convention 2; consider the corresponding decomposition of the surface into *zippered rectangles* as on Fig. 21. Let $X_1 \sqcup \dots \sqcup X_n$ be the corresponding decomposition of the horizontal segment X in the base; let $\lambda_j = |X_j|$ denote the widths of subintervals.

Convention 3. We associate to a decomposition of a flat surface into rectangles a permutation π in such way that the top horizontal segments of the rectangles are glued to the bottom side of the interval X in the order $\pi^{-1}(1), \dots, \pi^{-1}(n)$.

Example. In the example presented at Fig. 21 the four rectangles R_1, \dots, R_4 appear at the bottom side of X in the order R_3, R_1, R_4, R_2 , so we associate to this way of gluing a permutation

$$\begin{pmatrix} 1 & 2 & 3 & 4 \\ 3 & 1 & 4 & 2 \end{pmatrix} = (3, 1, 4, 2)^{-1} = (2, 4, 1, 3) = \pi$$

Exercise. Show that intersection indices $c(X_i) \circ c(X_j)$ of the “first return cycles” (see Sec. 5.2) are given by the following skew-symmetric matrix $\Omega(\pi)$ defined by the permutation π :

$$\Omega_{ij}(\pi) = \begin{cases} 1 & \text{if } i < j \text{ and } \pi^{-1}(i) > \pi^{-1}j \\ -1 & \text{if } i > j \text{ and } \pi^{-1}(i) < \pi^{-1}j \\ 0 & \text{otherwise} \end{cases} \quad (15)$$

Evaluate $\Omega(\pi)$ for the permutation in the Example above and compare the result with a direct calculation for the cycles $c(X_j)$, $j = 1, \dots, 4$, computed in the Exercise at the end of Sec. 5.2.

Compare now the width λ_n of the rightmost rectangle R_n with the width $\lambda_{\pi^{-1}(n)}$ of the rectangle which is glued to the rightmost position at the bottom of X . As a new subinterval $X' \subset X$ consider the subinterval X' , which has the same left extremity as X , but which is shorter than X by $\min(\lambda_n, \lambda_{\pi^{-1}(n)})$.

The situation when $\lambda_n > \lambda_{\pi^{-1}(n)}$ is represented at Fig. 24; the situation when $\lambda_n < \lambda_{\pi^{-1}(n)}$ is represented at Fig. 25.

By construction the first return map $T' : X \rightarrow X'$ has the same number n of subintervals in its decomposition. Observing Fig. 24 and 24 one can see that in the first case, when $\lambda_n > \lambda_{\pi^{-1}(n)}$, the new decomposition $X'_1 \sqcup \dots \sqcup X'_n$ is obtained from the original decomposition $X_1 \sqcup \dots \sqcup X_n$ by shortening the last interval by $\lambda_{\pi^{-1}(n)}$ from the right. In the second case, when $\lambda_n < \lambda_{\pi^{-1}(n)}$, the new decomposition $X'_1 \sqcup \dots \sqcup X'_n$ is obtained from the original decomposition $X_1 \sqcup \dots \sqcup X_n$ by eliminating the last subinterval X_n and by partitioning the subinterval $X_{\pi^{-1}(n)}$ into two ones of lengths $\lambda_{\pi^{-1}(n)} - \lambda_n$ and λ_n correspondingly.

The order in which the rectangles of the new building are glued to the bottom of the interval X' changes. The new permutation π' can be described as follows. Consider the initial permutation π as a pair of orderings of a finite set: a “top” ordering $1, 2, \dots, n$ (corresponding to the ordering of the rectangles along the top side of the base interval X) and a “bottom” ordering $\pi^{-1}(1), \dots, \pi^{-1}(m)$ (corresponding to the ordering of the rectangles along the bottom side of the base interval X). In the first case, when $\lambda_n > \lambda_{\pi^{-1}(n)}$, the new permutation π' corresponds to the modification of the *bottom* ordering

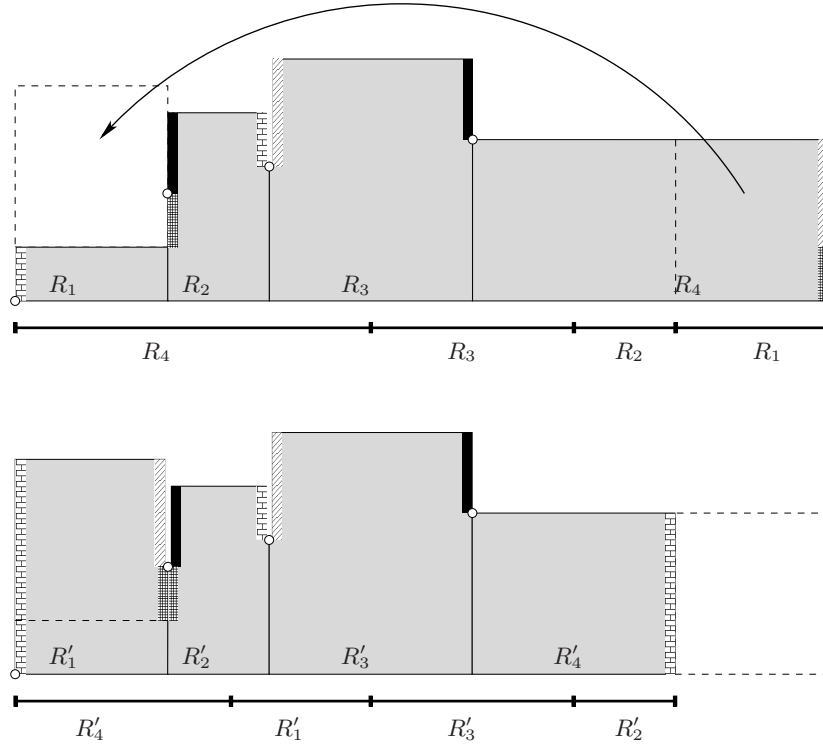


Fig. 24. Type I modification: the rightmost rectangle R_4 on top of X is wider than the rectangle $R_1 = R_{\pi^{-1}(4)}$ glued to the rightmost position at the bottom of X .

by cyclically moving one step forward those letters occurring after the image of the last letter in the bottom line, i.e., after the letter n . In the second case, when $\lambda_n < \lambda_{\pi^{-1}(n)}$, the new permutation π' corresponds to the modification of the *top* ordering by cyclically moving one step forward those letters occurring after the image of the last letter in the top line, i.e., after the letter $\pi^{-1}(n)$.

Example. For the initial buildings at both Figures 24 and 25 the permutation π corresponding to the initial interval exchange transformation $T : X \rightarrow X$ is the same and equals

$$\pi = \begin{pmatrix} 1 & 2 & 3 & 4 \\ 4 & 3 & 2 & 1 \end{pmatrix}$$

Our modification produces permutation

$$\begin{pmatrix} 1 & 2 & 3 & 4 \\ 4 & 3 \rightarrow 2 \rightarrow 1 \end{pmatrix} = \begin{pmatrix} 1 & 2 & 3 & 4 \\ 4 & 1 & 3 & 2 \end{pmatrix} = \pi'$$

in the first case (when $\lambda_n > \lambda_{\pi^{-1}(n)}$) and permutation

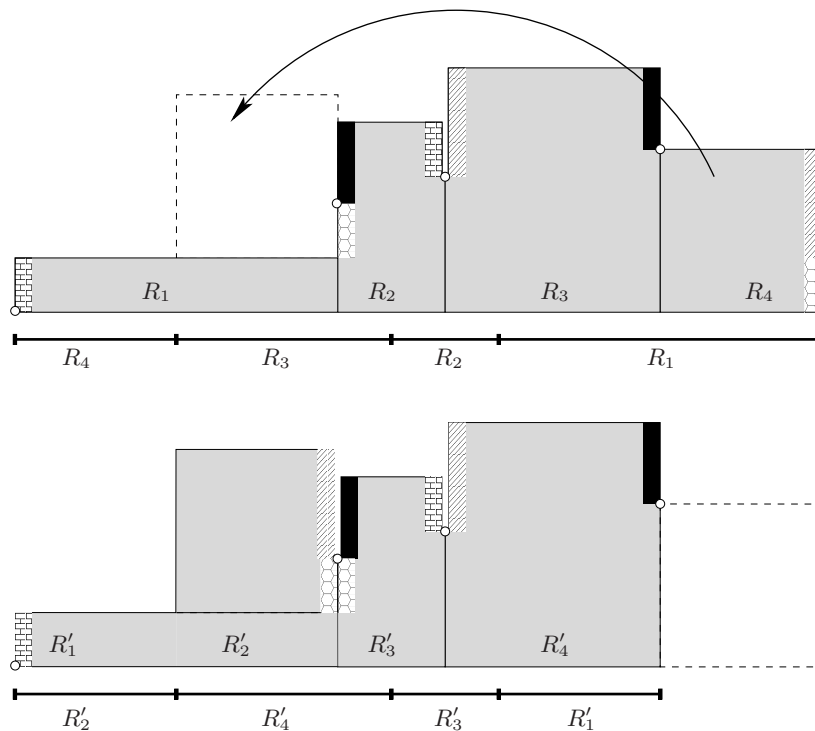


Fig. 25. Type II modification: the rightmost rectangle R_4 on top of X is narrower than the rectangle $R_1 = R_{\pi^{-1}(4)}$ glued to the rightmost position at the bottom of X .

$$\left(\begin{array}{cccc} 1 & \overbrace{2 \rightarrow 3 \rightarrow 4} & & \\ 4 & 3 & 2 & 1 \end{array} \right) = \begin{pmatrix} 1 & 4 & 2 & 3 \\ 4 & 3 & 2 & 1 \end{pmatrix} \sim \begin{pmatrix} 1 & 2 & 3 & 4 \\ 2 & 4 & 3 & 1 \end{pmatrix} = \pi'$$

in the second case (when $\lambda_n < \lambda_{\pi^{-1}(n)}$).

Note that in the second case (when $\lambda_n < \lambda_{\pi^{-1}(n)}$) passing to the new decomposition $X'_1 \sqcup \dots \sqcup X'_n$ we have to change the initial enumeration of the subintervals though physically all subintervals but one stay unchanged. Another choice would be to assign “names” to subintervals once and forever. Under the first choice the permutations

$$\begin{pmatrix} 1 & 4 & 2 & 3 \\ 4 & 3 & 2 & 1 \end{pmatrix} \text{ and } \begin{pmatrix} 1 & 2 & 3 & 4 \\ 2 & 4 & 3 & 1 \end{pmatrix}$$

coincide; under the latter choice they become different permutations. The article [Y] in the current volume adopts the second convention.

Similarly to the case of interval exchange transformations of two intervals the induction procedure described above can be described entirely in terms of

interval exchange transformations $T : X \rightarrow X$ and $T' : X' \rightarrow X'$. Historically it was proposed by G. Razy [Ra] in these latter form and then was interpreted by W. Veech [Ve3] in terms of zippered rectangles. (Actually, the zippered rectangles decomposition has appeared and was first studied in [Ve3].)

5.6 Multiplicative Cocycle on the Space of Interval Exchanges

The renormalization procedure constructed in Sec. 5.4 gives a map g from the space of rotations of a circle to itself, or, in other terms, from the space of interval exchange transformations of two subintervals to itself. The permutation π corresponding to an interval exchange transformations of two intervals $X_1 \sqcup X_2$ is always equal to $\pi = (2, 1)$, so such interval exchange transformation can be parametrized by a single real parameter $\lambda \in (0, 1)$, where $\lambda = |X_1|$. Here we assume that the total length $|X_1| + |X_2| = |X|$ of the interval X is normalized as $|X| = 1$.

An interval exchange transformation of n subintervals $X = X_1 \sqcup \dots \sqcup X_n$ is parametrized by a collection $\lambda_1, \dots, \lambda_n$ of positive numbers representing the lengths of subintervals and by a permutation $\pi \in \mathfrak{S}_n$. Assuming that the total length of the interval X is normalized as $|X| = 1$ we see that the *space of interval exchange transformations* is parametrized by a finite collection of $(n-1)$ -dimensional simplices $\Delta^{n-1} = \{(\lambda_1, \dots, \lambda_n) \mid \lambda_1 + \dots + \lambda_n = 1; \lambda_j > 0\}$, where each simplex corresponds to some fixed permutation π .

As a collection of permutations one can consider all permutations obtained from a given one by applying recursively the modifications described at the end of the previous section. Such collection of permutations is called a *Rauzy class* $\mathfrak{R} \subset \mathfrak{S}_n$. Figure 26 illustrates the Rauzy class of the permutation $(4, 3, 2, 1)$, where the arrows indicated modifications of the first and of the second type.

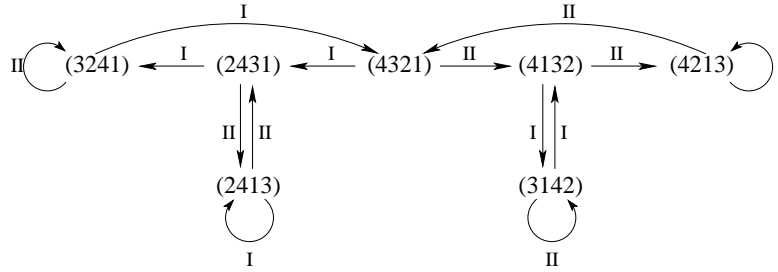


Fig. 26. Rauzy class of permutation $(4, 3, 2, 1)$

The renormalization procedure described in the previous section (combined with rescaling of the resulting interval X' to the unit length) defines a map

$$\mathcal{T} : \Delta^{n-1} \times \mathfrak{R} \rightarrow \Delta^{n-1} \times \mathfrak{R}$$

for each space of interval exchange transformations to itself. The following Theorem of W. A. Veech (see [Ve3]) is crucial in this story.

Key Theorem (W. A. Veech). *The map \mathcal{T} is ergodic with respect to absolutely continuous invariant measure.*

Remark. It is easy to see that the Rauzy class presented at Fig. 26 does not depend on the starting permutation. Actually, the same is true for any Rauzy class. Moreover, for almost any flat surface $S \in \mathcal{H}^{comp}(d_1, \dots, d_m)$ in any connected component of any stratum a finite set of all permutations realizable by first return maps to all possible horizontal segments X satisfying Convention 2 does not depend on the surface S . This set is a disjoint union of a finite collection of corresponding Rauzy classes $\mathfrak{R}_1, \dots, \mathfrak{R}_j$, where j is the number of distinct entries $d_{i_1} < d_{i_2} < \dots < d_{i_j}$. The union $\mathfrak{R}_{ex} = \mathfrak{R}_1 \sqcup \dots \sqcup \mathfrak{R}_j$ is called the *extended Rauzy class*; it depends only on the connected component $\mathcal{H}^{comp}(d_1, \dots, d_m)$. In particular, connected components of the strata are characterized by the extended Rauzy classes, where the latter ones can be described in purely combinatorial terms.

With the Theorem above we have almost accomplished our scheme for a renormalization procedure. There is only one trouble with the map \mathcal{T} : the measure mentioned in the Theorem is infinite (the total measure of the space of interval exchange transformations is infinite). This technical problem can be fixed by the following trick. We shall modify the renormalization algorithm described in the previous section by making several modifications of the zippered rectangle at a time. At a single step of the new algorithm \mathcal{G} we apply several steps of the previous one \mathcal{T} . Namely, we keep going as soon as we apply consecutive transformations \mathcal{T} of the same type I or of the same type II . Conceptually it does not change the renormalization procedure, but now the renormalization develops faster than before. The following example illustrates the correspondence between the renormalization procedures \mathcal{T} and \mathcal{G} :

$$\begin{array}{ccccccc}
 (\lambda, \pi) & \xrightarrow{I} & \mathcal{T}(\lambda, \pi) & \xrightarrow{I} & \mathcal{T}^2(\lambda, \pi) & \xrightarrow{I} & \mathcal{T}^3(\lambda, \pi) & \xrightarrow{II} & \mathcal{T}^4(\lambda, \pi) & \xrightarrow{II} & \mathcal{T}^5(\lambda, \pi) & \xrightarrow{I} & \dots \\
 \parallel & & & & & & \parallel & & & & \parallel & & \\
 (\lambda, \pi) & \longrightarrow & & \longrightarrow & \mathcal{G}(\lambda, \pi) & \longrightarrow & & \longrightarrow & \mathcal{G}^2(\lambda, \pi) & \longrightarrow & & \longrightarrow & \dots
 \end{array}$$

The accelerated procedure \mathcal{G} was introduced in [Zo2], where the following Theorem was proved.

Theorem. *The map \mathcal{G} is ergodic with respect to absolutely continuous invariant probability measure on each space of zippered rectangles.*

Now, when we have elaborated almost all necessary tools we are ready to give an idea of the proof of the Theorem from Sec. 4.3 concerning asymptotic flag. The last element which is missing is some analysis of the matrices $B(\lambda, \pi)$ in (12).

Multiplicative Cocycle

In our interpretation of a renormalization procedure as a map on the space of interval exchange transformations we have to consider matrix B as a matrix-valued function $B(\lambda, \pi)$ on the space $\Delta^{n-1} \times \mathfrak{R}$ of interval exchange transformations. Our goal (as it was outlined in Sec. 5.3) is to describe the properties of the products $B^{(s)} = B(X^{(0)}) \cdot B(X^{(1)}) \cdots B(X^{(s)})$ of matrices corresponding to successive steps of renormalization.

We shall keep the same notation $B(\lambda, \pi)$ for matrices corresponding to our fast renormalization procedure $\mathcal{G}(\lambda, \pi)$. Consider the product $B^{(s)}(\lambda, \pi)$ of values of $B(\cdot)$ taken along the orbit $(\lambda, \pi), \mathcal{G}(\lambda, \pi), \dots, \mathcal{G}^s(\lambda, \pi)$ of length s of the map \mathcal{G} :

$$B^{(s)}(\lambda, \pi) = B(\lambda, \pi) \cdot B(\mathcal{G}(\lambda, \pi)) \cdots B(\mathcal{G}^s(\lambda, \pi))$$

Such $B^{(s)}(\lambda, \pi)$ is called a *multiplicative cocycle* over the map \mathcal{G} :

$$B^{(p+q)}(\lambda, \pi) = B^{(p)}(\lambda, \pi) \cdot B^{(q)}(\mathcal{G}^p(\lambda, \pi))$$

Using ergodicity of \mathcal{G} we can apply multiplicative ergodic theorem (see Appendix B) to describe properties of $B^{(s)}$. Morally, the multiplicative ergodic theorem tells that for large values of s the matrix $B^{(s)}(\lambda, \pi)$ should be considered as a matrix conjugate to the s -th power of some *constant* matrix. (See Appendix B for a rigorous formulation.) The logarithms of eigenvalues of this constant matrix are called *Lyapunov exponents* of the multiplicative cocycle.

Recall that matrix $B^T(\lambda, \pi)$ was defined as a matrix representing the new “first return cycles” in terms of the old ones, see (12). Actually, it can be also interpreted as a matrix representing a change of a basis in the first relative cohomology $[\text{Re } \omega] = (\lambda_1, \dots, \lambda_n) \in H^1(S, \{\text{conical singularities}\}; \mathbb{R})$. It is easy to check that it respects the (degenerate) symplectic form: the intersection form (15). Note that symplectic matrices have certain symmetry of eigenvalues. In particular, it follows from the general theory that the corresponding Lyapunov exponents have the following symmetry:

$$\theta_1 > \theta_2 \geq \theta_3 \geq \dots \geq \theta_g \geq \underbrace{0 = 0 = \dots = 0}_{\text{number of conical points} - 1} \geq -\theta_g \geq \dots \geq -\theta_2 > -\theta_1$$

Note that the first return cycles actually belong to the absolute homology group $H_1(S; \mathbb{Z}) \subset H_1(S; \mathbb{R}) \simeq \mathbb{R}^{2g}$. Passing to this $2g$ -dimensional space we get matrices which already preserve a nondegenerate symplectic form. They define the following subcollection

$$\theta_1 > \theta_2 \geq \theta_3 \geq \dots \geq \theta_g \geq -\theta_g \geq \dots \geq -\theta_3 > -\theta_2 > -\theta_1$$

of Lyapunov exponents.

The rest is an elementary linear algebra. We want to describe how do the large powers s of a symplectic matrix with eigenvalues

$$\exp(\theta_1) > \exp(\theta_2) \geq \cdots \geq \exp(\theta_g) \geq \exp(-\theta_g) \geq \cdots \geq \exp(-\theta_2) \geq \exp(-\theta_1)$$

act on a $2g$ -dimensional symplectic space.

We know that the Lyapunov exponent $\theta_g \geq 0$ is nonnegative. Assume⁴ that it is actually strictly positive: $\theta_g > 0$. Then for half of dimensions our linear map is expanding and for half of dimensions it is contracting. In particular, under the assumption that $\theta_g > 0$ we conclude that the linear map $B^{(s)}(\lambda, \pi)$ projects all homology space to a Lagrangian subspace (spanned by eigenvectors corresponding to positive Lyapunov exponents).

Assuming that the spectrum of Lyapunov exponents is simple, that is assuming that

$$\theta_1 > \theta_2 > \theta_3 > \cdots > \theta_g$$

we get the entire picture of deviation. A generic vector in the homology space stretches along the principal eigenvector (the one corresponding to the eigenvalue θ_1) with a factor $\exp(s\theta_1)$; it expands along the next eigenvector with a factor $\exp(s\theta_2)$, etc, up to the order g ; its deviation from the Lagrangian subspace spanned by the first g eigenvectors tends to zero. Hence, the norm l of the image of a generic vector under s -th power of our linear map is of the order $l \sim \exp(s\theta_1)$; its deviation from the subspace \mathcal{V}_1 , which is spanned by the top eigenvector, is of the order $\exp(s\theta_2) = l^{\frac{\theta_2}{\theta_1}}$; its deviation from the subspace \mathcal{V}_2 spanned by the two top eigenvectors is of the order $\exp(s\theta_3) = l^{\frac{\theta_3}{\theta_1}}$, etc; there is no deviation from the Lagrangian subspace spanned by the top g eigenvectors. In particular, the exponent ν_j responsible for deviation from the subspace \mathcal{V}_{j-1} from the Theorem in Sec. 4.3 is obtained by normalization of the Lyapunov exponent θ_j by the leading Lyapunov exponent θ_1 :

$$\nu_j = \frac{\theta_j}{\theta_1}. \quad (16)$$

This completes the proof of the Theorem in the case when the vertical trajectory starts and ends at the same microscopic horizontal interval (in other words, when the piece of trajectory is “almost closed”). Applying some additional (relatively involved) ergodic machinery one can complete the proof of the Theorem for arbitrary long pieces of vertical trajectories; see [Zo4] for a complete proof.

I would like to stress that the original Theorem proved in [Zo4] is conditional: the statement about Lagrangian subspace was proved modulo conjecture that $\theta_g > 0$; the statement about a complete Lagrangian flag was proved modulo conjectural simplicity of the spectrum of Lyapunov exponents.

Positivity $\theta_g > 0$ was proved by G. Forni in [For1], and simplicity of the spectrum was recently proved by A. Avila and M. Viana [AvVi]; see more details in Sec. 5.8. As it was shown in [Zo2] the proof of the strict inequality $\theta_1 > \theta_2$ immediately follows from results of W. A. Veech.

⁴Actually, this assumption is a highly nontrivial Theorem of G. Forni [For1]; see below, see also Sec. 5.8

Exercise. In analogy with what was done in Sec. 5.4 consider the Rauzy–Veech induction in the torus case applying it to interval exchange transformations of two subintervals. We have seen that in this case the space of interval exchange transformations is just an interval $(0, 1)$. Find an explicit formulae for the Rauzy–Veech renormalization map $\mathcal{T} : (0, 1) \rightarrow (0, 1)$ and for the “fast” renormalization map $\mathcal{G} : (0, 1) \rightarrow (0, 1)$. Explain why the invariant measure is infinite for the map \mathcal{T} . Find a relation between \mathcal{G} and the Gauss map $g : x \mapsto \left\{ \frac{1}{x} \right\}$. Let

$$\frac{p_s}{q_s} = \frac{1}{n_1 + \frac{1}{n_2 + \frac{1}{\dots + \frac{1}{n_s}}}}$$

be the s -th best rational approximation of a real number $x \in (0, 1)$. In the torus case the spectrum of Lyapunov exponents reduces to a single pair $\theta_1 > -\theta_1$. Show that for almost all $x \in (0, 1)$ the Lyapunov exponent θ_1 (called in number theory the *Lévy constant*, see [Lv]) is responsible for the growth rate of the denominator of the continued fraction expansion of x :

$$\lim_{s \rightarrow \infty} \frac{\log q_s}{s} = \theta_1 = \frac{\pi^2}{12 \log 2}$$

5.7 Space of Zippered Rectangles and Teichmüller geodesic flow

We have proved the Theorem about an asymptotic Lagrangian flag of subspaces responsible for deviation of the cycles $c(x, N)$ from asymptotic direction. We have also proved that the exponents ν_j responsible for the quantitative description of the deviation are expressed in terms of the Lyapunov exponents of the multiplicative cocycle corresponding to our renormalization procedure: $\nu_j = \theta_j / \theta_1$.

There remains a natural question why should we choose this particular renormalization procedure and not a different one. One more natural question is what is the relation between renormalization procedure and the flow induced by the action of the diagonal subgroup $\begin{pmatrix} \exp(t) & 0 \\ 0 & \exp(-t) \end{pmatrix}$ on the space of flat surfaces which we agreed to call the *Teichmüller geodesic flow*; this relation was announced in Sec. 4.3. This section answers to these questions which are, actually, closely related.

In our presentation we follow the fundamental paper [Ve3] of W. A. Veech; the material at the end of the section is based on the paper [Zo2] developing the initial paper [Ve3].

Space of Zippered Rectangles

We have seen that locally a flat surface S can be parametrized by a collection of relative periods of the holomorphic 1-form ω representing the flat surface, i.e. we can choose a small domain containing $[\omega]$ in the relative cohomology group $H^1(S, \{P_1, \dots, P_m\}; \mathbb{C})$ as a coordinate chart in the corresponding stratum $\mathcal{H}(d_1, \dots, d_m)$.

Decomposition of a flat surface into zippered rectangles gives another system of local coordinates in the stratum. Namely, choose a horizontal segment X satisfying Convention 2 from Sec. 5.3 and consider the corresponding decomposition of S into zippered rectangles. Let $\lambda_1, \dots, \lambda_n$ be the widths of the rectangles, h_1, \dots, h_n their heights, and a_1, \dots, a_m be the altitudes responsible for the position of singularities (we zip the neighboring rectangles R_j and R_{j+1} from the bottom up to the altitude a_j and then the rectangles split at the singularity, see Figures 21, 24, 25). There is one more parameter describing a decomposition of a flat surface into zippered rectangles: a permutation $\pi \in \mathfrak{S}_n$. This latter parameter is discrete.

The vertical parameters h_j, a_k are not independent: they satisfy some linear equations and inequalities. Varying the continuous parameters λ, h, a respecting the linear relations between parameters h and a we get a new set of coordinates in the stratum. These coordinates were introduced and studied by W. A. Veech in [Ve3]. In particular, it was proved that for any $(\lambda, \pi) \in \Delta^{n-1} \times \mathfrak{R}$ in the space of interval exchange transformations there is an n -dimensional open cone of solutions (h, a) . In other words, having any interval exchange transformation $T : X \rightarrow X$ one can always construct a flat surface S and a horizontal segment $X \subset S$ inside it such that the first return of the vertical flow to X gives the initial interval exchange transformations. Moreover, there is a n -dimensional family of such flat surfaces – *suspensions* over the interval exchange transformation $T : X \rightarrow X$ (see [Ma3], [Ve3]).

Is there a canonical decomposition of a flat surface into zippered rectangles? A choice of horizontal segment $X \subset S$ completely determines a decomposition of a generic surface S into zippered rectangles, so our question is equivalent to the problem of a canonical choice of a horizontal segment X satisfying Convention 2. The choice which we propose is *almost* canonical; it leaves an arbitrariness of finite order which is the same for almost all S in the stratum. Here is the choice. Let us place the left extremity of the horizontal segment X at one of the conical singularities, and let us choose the length $|X|$ of the segment in such way that X would be the shortest possible interval satisfying Convention 2 and condition $|X| \geq 1$.

In practice the interval X can be constructed as follows: start with a sufficiently long horizontal interval having its left extremity at a conical point and satisfying Convention 2. Apply the “slow” Rauzy–Veech algorithm as long as the resulting subinterval has length at least 1. For almost all flat surfaces after finite number of steps we obtain the desired interval X .

The surface S has finite number of conical singularities; each conical singularity has finite number of horizontal prongs, so we get arbitrariness of finite order. Thus, the resulting *space of zippered rectangles* can be essentially viewed as a (ramified) covering over the corresponding connected component $\mathcal{H}^{comp}(d_1, \dots, d_m)$ of the stratum. Passing to a codimension one subspace Ω defined by the condition $\lambda \cdot h = 1$ we get a space of zippered rectangles of area one covering the space $\mathcal{H}_1^{comp}(d_1, \dots, d_m)$ of flat surfaces of area one. Consider a codimension-one subspace $\mathcal{Y} \subset \Omega$ of zippered rectangles which have unit area, and which have the base X of length one, $|X| = \lambda_1 + \dots + \lambda_n = 1$. The space \mathcal{Y} has a natural structure of a fiber bundle over the space $\Delta^{n-1} \times \mathfrak{R}$ of interval exchange transformations: we associate to a zippered rectangle $(\lambda, h, a, \pi) \in \mathcal{Y}$ the interval exchange transformation (λ, π) .

We would like to emphasize an interpretation of Ω as a *fundamental domain* in the space of *all* zippered rectangles of area one. As a fundamental domain Ω is defined by the additional condition on the base: X is the shortest possible interval satisfying Convention 2 such that $|X| \geq 1$. In this interpretation \mathcal{Y} is the boundary of the fundamental domain. Starting with an arbitrary zippered rectangle representation satisfying Convention 2 we can apply several steps of Rauzy–Veech algorithm (see Fig. 24 and Fig. 25), which does not change the surface S . After several iterations we get to the fundamental domain Ω .

We would use the same notation for Ω considered as a fundamental domain and for Ω considered as a quotient, when two boundary components of Ω are identified by the modification of zippered rectangles as on Fig. 24 and Fig. 25.

Teichmüller Geodesic Flow and its First Return Map to a Cross-section

Zippered rectangles coordinates are extremely convenient when working with the Teichmüller geodesic flow, which we identify with the action of the diagonal subgroup $g_t = \begin{pmatrix} \exp(t) & 0 \\ 0 & \exp(-t) \end{pmatrix}$. Namely, g_t expands the horizontal parameters λ by the factor $\exp(t)$ and contracts the vertical parameters h, a by the same factor.

Consider a zippered rectangle $S = (\lambda, h, a, \pi) \in \mathcal{Y}$ with the base X of unit length. Applying g_t to S with t continuously increasing from $t = 0$ we shall eventually make the length of the base of the deformed zippered rectangle $g_t S = (\exp(t)\lambda, \exp(-t)h, \exp(-t)a; \pi)$ too long and thus we shall get outside of the fundamental domain Ω . It is not difficult to determine an exact time t_0 when it will happen. We get to the boundary of the fundamental domain Ω at the time

$$t_0(S) = -\log(1 - \min(\lambda_n, \lambda_{\pi^{-1}(n)})). \quad (17)$$

The time t_0 is chosen in such way that applying to the zippered rectangle $g_{t_0} S$ one step of the Rauzy–Veech induction (see Fig. 24 and Fig. 25) we get a new zippered rectangle with the base X' of unit length. To verify formula (17) for t_0 it is sufficient to note that expansion-contraction commutes

with Rauzy–Veech induction. Thus, to evaluate t_0 we can *first* apply one step of the Rauzy–Veech induction and *then* apply expansion-contraction for an appropriate time, which would bring us back to \mathcal{Y} , i.e. which would make the length of the base of the new building of zippered rectangles equal to one.

In other words, starting at a point $S \in \mathcal{Y}$ and following the flow for the time $t_0(S)$ we get to the boundary of the fundamental domain in the space of zippered rectangles and we have to instantly jump back to the point of \mathcal{Y} identified with $g_{t_0}S$. One can recognize in this construction the first return map $\mathcal{S} : \mathcal{Y} \rightarrow \mathcal{Y}$ defined by the flow g_t on the section \mathcal{Y} : at the time $t_0(S)$ the flow g_t emitted from a point $S \in \mathcal{Y}$ returns back to the codimension-one subspace \mathcal{Y} transversal to the flow.

Morally one should consider the map \mathcal{S} as a map on some subspace of flat surfaces. Note, that \mathcal{S} is not applicable to points of flat surfaces, it associates to a flat surface taken as a whole another flat surface taken as a whole.

We see now that the Rauzy–Veech renormalization procedure $\mathcal{S} : \mathcal{Y} \rightarrow \mathcal{Y}$ performed on the level of zippered rectangles is nothing but discrete version of the Teichmüller geodesic flow. Namely \mathcal{S} is the first return map of the Teichmüller geodesic flow to a section \mathcal{Y} . By construction the Rauzy–Veech induction $\mathcal{T} : \Delta^{n-1} \times \mathfrak{R} \rightarrow \Delta^{n-1} \times \mathfrak{R}$ on the space of interval exchange transformations is just a projection of \mathcal{S} . In other words, the following diagram

$$\begin{array}{ccc} \mathcal{Y}(\mathfrak{R}) & \xrightarrow{\mathcal{S}} & \mathcal{Y}(\mathfrak{R}) \\ \downarrow & & \downarrow \\ \Delta^{n-1} \times \mathfrak{R} & \xrightarrow{\mathcal{T}} & \Delta^{n-1} \times \mathfrak{R} \end{array}$$

is commutative, and the invariant measure on the space $\Delta^{n-1} \times \mathfrak{R}$ of interval exchange transformations is a push forward of the natural invariant measure on the space \mathcal{Y} of zippered rectangles.

Choice of a Section

Now we can return to the questions addressed at the beginning of this section. Ignoring an algorithmic aspect of the choice of renormalization procedure we see that conceptually, it is defined by a section of the Teichmüller geodesic flow. In particular, the “fast” renormalization procedure $\mathcal{G} : \Delta^{n-1} \times \mathfrak{R} \rightarrow \Delta^{n-1} \times \mathfrak{R}$ defined in the previous section corresponds to a choice of a subsection $\mathcal{Y}' \subset \mathcal{Y}$. Luckily it has a simple algorithmic representation in terms of modification of the interval exchange transformation $T(\lambda, \pi)$, and, moreover, it has a simple description in terms of coordinates λ, h, a, π in the space of zippered rectangles given by an extra condition for the parameter a_n .

Recall that parameters a_j are responsible for the position of singularities: we zip the neighboring rectangles R_j and R_{j+1} from the bottom up to the altitude a_j , see Fig. 21. In particular, by construction all a_j for $j = 1, \dots, n-1$ are positive. Parameter a_n is, however, different from the others: the rectangle

R_n is the rightmost rectangle in the collection. If there is a conical singularity located at the right side of this rightmost rectangle (see, for example, the zippered rectangle decomposition of the flat surface on the top part of Fig. 24), then parameter a_m is positive; it indicates as usual at what height is located the singularity. However, the right side of the rightmost rectangle might contain no singularity. This means that the singularity is located on the corresponding vertical trajectory *below* the zero level of the base X . The rectangle which is glued to X from below at the rightmost position is the rectangle $R_{\pi^{-1}(n)}$; the singularity is located on the right side of this rectangle (see, for example, the zippered rectangle decomposition of the flat surface on the bottom part of Fig. 24). In this case we let a_n be negative indicating how low we have to descend along downward vertical trajectory emitted from the right endpoint of X to hit the singularity.

The subsection \mathcal{T}' is defined by the following extra condition

$$\begin{aligned} \mathcal{T}' = & \{ (\lambda, h, a, \pi) \in \mathcal{T} \mid a_n > 0 \text{ when } \lambda_n > \lambda_{\pi^{-1}(n)} \} \sqcup \\ & \sqcup \{ (\lambda, h, a, \pi) \in \mathcal{T} \mid a_n < 0 \text{ when } \lambda_n < \lambda_{\pi^{-1}(n)} \} \end{aligned}$$

Exercise. Check which zippered rectangles at Figures 21, 24, 25 satisfy the condition $a_n \cdot (\lambda_n - \lambda_{\pi^{-1}(n)}) > 0$ and which do not.

It can be verified (see [Zo2]) that the section \mathcal{T}' is still a fiber bundle over the space of zippered rectangles and that the corresponding first return map $\mathcal{S}' : \mathcal{T}' \rightarrow \mathcal{T}'$ projects to the map \mathcal{G} :

$$\begin{array}{ccc} \mathcal{T}'(\mathfrak{X}) & \xrightarrow{\mathcal{S}'} & \mathcal{T}'(\mathfrak{X}) \\ \downarrow & & \downarrow \\ \Delta^{n-1} \times \mathfrak{X} & \xrightarrow{\mathcal{G}} & \Delta^{n-1} \times \mathfrak{X} \end{array} \quad (18)$$

Exercise. Verify that the definition of the renormalization procedure \mathcal{G} as a projection of the first return map of the Teichmüller geodesic flow to \mathcal{T}' matches the intrinsic definition of \mathcal{G} given in Sec. 5.6.

Different choices of the section also explain why the invariant measure on the space of interval exchange transformations $\Delta^{n-1} \times \mathfrak{X}$ was infinite for the Rauzy–Veech induction \mathcal{T} while is finite for the “fast” renormalization procedure \mathcal{G} . As a model case consider a directional flow on a torus and two different sections to this flow. Taking as a section the line Y represented on the left picture of Fig. 27 we get a section of infinite measure though the measure of the torus is finite and the flow is very nice. Taking as a section a finite piece $Y' \subset Y$ as on the right side of Fig. 27 we get a section of finite measure.

Similarly, the component $\mathcal{H}_1^{\text{comp}}(d_1, \dots, d_m)$ of the stratum has finite volume and hence the space of zippered rectangles Ω which is a finite covering

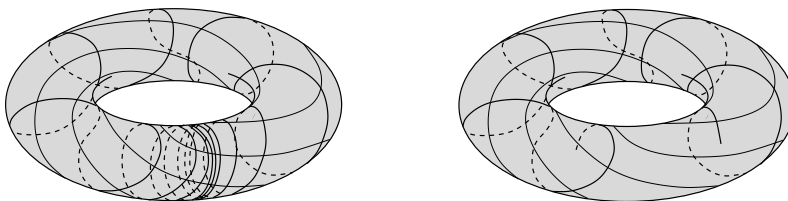


Fig. 27. The section Y on the left picture has infinite measure though the measure of the space is finite. The subsection $Y' \subset Y$ on the right picture has finite measure. In both cases the first return map of the ergodic flow to the section is ergodic, but the mean return time to the left subsection is zero

over $\mathcal{H}_1^{comp}(d_1, \dots, d_m)$ also has finite volume. However, the initial section \mathcal{Y} has infinite “hyperarea” while section \mathcal{Y}' already has finite “hyperarea”.

We complete this section with a several comments concerning Lyapunov exponents. Though these comments are too brief to give a comprehensive proof of the relation between exponents ν_j responsible for the deviation and the Lyapunov exponents of the Teichmüller geodesic flow, they present the key idea, which can be completed by an elementary calculation.

It is clear that the Lyapunov exponents of the Teichmüller geodesic flow g_t on the stratum $\mathcal{H}_1^{comp}(d_1, \dots, d_m)$ coincide with the Lyapunov exponents on its finite covering Ω . The Lyapunov exponents of the flow g_t differ from the Lyapunov exponents of the first return map \mathcal{S}' to the section \mathcal{Y}' only by a scaling factor representing the “hyperarea” of \mathcal{Y}' . The map \mathcal{G} on the space of zippered rectangles coincides with the restriction of the map \mathcal{S}' on the zippered rectangles restricted to horizontal parameters λ and discrete parameter π . Thus, the Lyapunov exponents of \mathcal{G} form a subcollection of the Lyapunov exponents of \mathcal{S}' corresponding to the subspace of horizontal parameters λ . It remains to note that the Lyapunov exponents of the map \mathcal{G} are related to the Lyapunov exponents of the cocycle $B(\lambda, \pi)$ just by the scaling factor, and that we have already expressed the exponents ν_j responsible for the deviation in terms of the Lyapunov exponents of the multiplicative cocycle B , see (16). Matching all the elements of this chain together we get a representation of the exponents ν_j in terms of the Lyapunov exponents of the Teichmüller geodesic flow given in Sec. 4.3.

Zippered rectangles and Lyapunov exponents: more serious reading. More details on Rauzy classes \mathfrak{R} , zippered rectangles, Lyapunov exponents of the Teichmüller geodesic flow and their relation might be found in original papers of G. Rauzy [Ra], W. Veech [Ve3], [Ve6] and the author [Zo2], [Zo4].

5.8 Spectrum of Lyapunov Exponents (after M. Kontsevich, G. Forni, A. Avila and M. Viana)

It should be mentioned that the statement that the subspace \mathcal{V}_g , such that $|dist(c(x, N), \mathcal{V}_g)| \leq const$ for any N , has dimension *exactly* g was formulated

in the original paper [Zo4] as a conditional statement. It was based on the conjecture that the Lyapunov exponent ν_g is strictly positive. This conjecture was later proved by G. Forni in [For1].

Theorem (G. Forni). *For any connected component $\mathcal{H}^{comp}(d_1, \dots, d_m)$ of any stratum of Abelian differentials the first g Lyapunov exponents of the Teichmüller geodesic flow are strictly greater than 1:*

$$1 + \nu_g > 1$$

As an indication why this positivity is not something which should be taken for granted we would like to give some precision about related results of G. Forni.

The Lyapunov exponents of the Teichmüller geodesic flow play the role of (logarithms of) eigenvalues of a virtual “average monodromy of the tangent bundle along the flow”. Instead of considering the tangent bundle to $\mathcal{H}(d_1, \dots, d_m)$ one can consider another vector bundle intimately related to the tangent bundle. This vector bundle has the space $H^1(S; \mathbb{R})$ as a fiber. Since we know how to identify the lattices $H^1(S; \mathbb{Z}) \subset H^1(S; \mathbb{R})$ and $H^1(S'; \mathbb{Z}) \subset H^1(S'; \mathbb{R})$ in the fibers over two flat surfaces S and S' which are close to each other in $\mathcal{H}(d_1, \dots, d_m)$, we know how to transport the fiber $H^1(S; \mathbb{R})$ over the “point” S in the base $\mathcal{H}(d_1, \dots, d_m)$ to the fiber $H^1(S'; \mathbb{R})$ over the “point” S' . In other words, we have a canonical connection (called Gauss–Manin connection) in the vector bundle. Hence we can again study the “average monodromy of the fiber along the flow”. It is not difficult to show that the corresponding Lyapunov exponents are related to the Lyapunov exponents of the Teichmüller flow. Namely, the new collection of Lyapunov exponents has the form:

$$1 \geq \nu_2 \geq \dots \geq \nu_g \geq -\nu_g \geq \dots \geq -\nu_2 \geq -1$$

In particular, the collection of Lyapunov exponents of the Teichmüller geodesic flow can be obtained as follows: take two copies of the collection above; add +1 to all the entries in one copy; add −1 to all entries in another copy; take the union of the resulting collections. The theorem of G. Forni tells that for any connected component of any stratum we have $\nu_g > 0$.

Consider now some $SL(2, \mathbb{R})$ -invariant subvariety $\mathcal{N} \subset \mathcal{H}(d_1, \dots, d_m)$. Consider the restriction of the vector bundle with the fiber $H^1(S; \mathbb{R})$ to \mathcal{N} . We can compute the “average monodromy of the fiber along the Teichmüller flow” restricted to \mathcal{N} . It gives a new collection of Lyapunov exponents. Since the “holonomy” preserves the natural symplectic form in the fiber, the collection will be again symmetric:

$$1 \geq \nu'_2 \geq \dots \geq \nu'_g \geq -\nu'_g \geq \dots \geq -\nu'_2 \geq -1$$

G. Forni has showed [For2] that there are examples of invariant subvarieties \mathcal{N} such that all ν'_j , $j = 2, \dots, g$, are equal to zero! Moreover, G. Forni explicitly

describes the locus where the monodromy does not change the fiber (or its exterior powers) too much, and where one may get multiplicities of Lyapunov exponents.

Another conditional statement in the original paper [Zo4] concerns *strict* inclusions $\mathcal{V}_1 \subset \mathcal{V}_2 \subset \dots \subset \mathcal{V}_g \subset H_1(S; \mathbb{R})$. It was based on the other conjecture claiming that the Lyapunov exponents have simple spectrum. The first strict inequality $\nu_1 > \nu_2$ is an elementary corollary of general results of Veech; see [Zo3]. The other strict inequalities are much more difficult to prove. Very recently A. Avila and M. Viana [AvVi] have announced a proof of simplicity of the spectrum (19) for any connected component of any stratum proving the conjecture which was open for a decade.

Theorem (A. Avila, M. Viana). *For any connected component of any stratum $\mathcal{H}^{comp}(d_1, \dots, d_m)$ of Abelian differentials the first g Lyapunov exponents are distinct:*

$$1 + \nu_1 > 1 + \nu_2 > \dots > 1 + \nu_g \quad (19)$$

Sum of the Lyapunov exponents

Currently there are no methods of calculation of Lyapunov exponents for general dynamical systems. The Teichmüller geodesic flow does not make an exception: there is some knowledge of approximate values of the numbers ν_j obtained by computer simulations for numerous low-dimensional strata, but there is no approach leading to explicit evaluation of these numbers with exception for some very special cases.

Nevertheless, for any connected component of any stratum (and, more generally, for any $GL^+(2; \mathbb{R})$ -invariant suborbifold) it is possible to evaluate the *sum* of the Lyapunov exponents $\nu_1 + \dots + \nu_g$, where g is the genus. The formula for this sum was discovered by M. Kontsevich in [Kon]; it is given in terms of the following natural structures on the strata $\mathcal{H}(d_1, \dots, d_m)$.

There is a natural action of \mathbb{C}^* on every stratum of the moduli space of holomorphic 1-forms: we can multiply a holomorphic form ω by a complex number. Let us denote by $\mathcal{H}_{(2)}(d_1, \dots, d_m)$ the quotient of $\mathcal{H}(d_1, \dots, d_m)$ over \mathbb{C}^* . The space $\mathcal{H}_{(2)}(d_1, \dots, d_m)$ can be viewed as the space of flat surfaces of unit area *without* choice of distinguished direction.

There are two natural holomorphic vector bundles over $\mathcal{H}_{(2)}(d_1, \dots, d_m)$. The first one is the \mathbb{C}^* -bundle $\mathcal{H}(d_1, \dots, d_m) \rightarrow \mathcal{H}_{(2)}(d_1, \dots, d_m)$. The second one is the \mathbb{C}^g -bundle, whose fiber is composed of all holomorphic 1-forms in the complex structure corresponding to a flat surface $S \in \mathcal{H}_{(2)}(d_1, \dots, d_m)$. Both bundles have natural curvatures; we denote by γ_1 and γ_2 the corresponding closed curvature 2-forms.

Finally, there is a natural closed codimension two form β on every stratum $\mathcal{H}_{(2)}(d_1, \dots, d_m)$. To construct β consider the natural volume form Ω on $\mathcal{H}(d_1, \dots, d_m)$. Four generators of the Lie algebra $\mathfrak{gl}(2; \mathbb{R})$ define four distinguished vectors in the tangent space $T_S \mathcal{H}(d_1, \dots, d_m)$ at any “point” $S \in \mathcal{H}(d_1, \dots, d_m)$. Plugging these four vectors in the first four arguments of

the volume form Ω we get a closed codimension four form on $\mathcal{H}(d_1, \dots, d_m)$. It is easy to check that this form can be pushed forward along the \mathbb{C}^* -fibers of the bundle $\mathcal{H}(d_1, \dots, d_m) \rightarrow \mathcal{H}_{(2)}(d_1, \dots, d_m)$ resulting in the closed codimension two form on the base of this fiber bundle.

Theorem (M. Kontsevich). *For any connected component of any stratum the sum of the first g Lyapunov exponents can be expressed as*

$$\nu_1 + \dots + \nu_g = \frac{\int \beta \wedge \gamma_2}{\int \beta \wedge \gamma_1},$$

where the integration is performed over the corresponding connected component of $\mathcal{H}_{(2)}(d_1, \dots, d_m)$.

As it was shown by G. Forni, this formula can be generalized for other $GL^+(2; \mathbb{R})$ -invariant submanifolds.

The proof is based on two observations. The first one generalizes the fact that dynamics of the geodesic flow on the hyperbolic plane is in some sense equivalent to dynamics of random walk. One can replace Teichmüller geodesics by geodesic broken lines consisting of geodesic segments of unit length. Having a broken line containing n geodesic segments with the endpoint at the point S_n we emit from S_n a new geodesic in a random direction and stop at the distance one from S_n at the new point S_{n+1} . This generalization suggested by M. Kontsevich was formalized and justified by G. Forni.

Consider the vector bundle over the moduli space of holomorphic 1-forms with the fiber $H^1(S; \mathbb{R})$ over the “point” S . We are interested in the sum $\nu_1 + \dots + \nu_g$ of Lyapunov exponents representing mean monodromy of this vector bundle along random walk. It follows from standard arguments concerning Lyapunov exponents that this sum corresponds to the top Lyapunov exponent of the exterior power of order g of the initial vector bundle. In other words, we want to measure the average growth rate of the norm of a g -dimensional subspace in $H^1(S; \mathbb{R})$ when we transport it along trajectories of the random walk using the Gauss–Manin connection.

Fix a Lagrangian subspace L in the fiber $H^1(S_0; \mathbb{R})$ over a “point” S_n . Consider the set of points located at the Teichmüller distance 1 from S_n . Transport L to each point S_{n+1} of this “unit sphere” along the corresponding geodesic segment joining S_n with S_{n+1} ; measure the logarithm of the change of the norm of L ; take the average over the “unit sphere”. The key observation of M. Kontsevich in [Kon] is that for an appropriate choice of the norm this average growth rate is the same for all Lagrangian subspaces L in $H^1(S_0; \mathbb{R})$ and depends only on the point S_n . A calculation based on this observation gives the formula above.

Actually, formula above can be rewritten in a much more explicit form (which is a work in progress). The values of the sum given by this more explicit formula perfectly match numerical simulations. The table below gives the values of the sums of Lyapunov exponents for some low-dimensional strata;

this computation uses the results of A. Eskin and A. Okounkov [EOk] for the volumes of the strata.

Conjectural values of $\nu_1 + \dots + \nu_g$ for some strata

$\mathcal{H}(2)$	$\mathcal{H}(1,1)$...	$\mathcal{H}(4,1,1)$...	$\mathcal{H}(1,1,1,1,1,1)$	$\mathcal{H}(1,1,1,1,1,1,1,1)$
$\frac{4}{3}$	$\frac{3}{2}$...	$\frac{1137}{550}$...	$\frac{839}{377}$	$\frac{235\,761}{93\,428}$

In particular, since $\nu_1 = 1$ this information gives the exact value of the only nontrivial Lyapunov exponent ν_2 for the strata in genus two. Some extra arguments show that $\nu_2 = 1/3$ for the stratum $\mathcal{H}(2)$ and for any $GL^+(2; R)$ -invariant submanifold in it; $\nu_2 = 1/2$ for the stratum $\mathcal{H}(1,1)$ and for any $GL^+(2; R)$ -invariant submanifold in it.

5.9 Encoding a Continued Fraction by a Cutting Sequence of a Geodesic

We have seen that renormalization for a rotation of a circle (or equivalently for an interval exchange transformation of two subintervals) leads to the Euclidean algorithm which can be considered in this guise as a particular case of the fast Rauzy–Veech induction.

The multiplicative cocycle

$$B^{(s)} = \begin{pmatrix} 1 & n_1 \\ 0 & 1 \end{pmatrix} \cdot \begin{pmatrix} 1 & 0 \\ n_2 & 1 \end{pmatrix} \cdots \begin{pmatrix} 1 & n_{2k-1} \\ 0 & 1 \end{pmatrix} \cdot \begin{pmatrix} 1 & 0 \\ n_{2k} & 1 \end{pmatrix} \cdots$$

considered in section 5.6 corresponds to the decomposition of a real number $x \in (0, 1)$ into continued fraction, $x = [0; n_1, n_2, \dots]$,

$$x = \frac{1}{n_1 + \frac{1}{n_2 + \frac{1}{\dots}}}$$

A flat surface which realizes an interval exchange transformation of two subintervals is a flat torus. The the moduli space of flat tori can be naturally identified with $SL(2, \mathbb{R})/SL(2, \mathbb{Z})$ which in its turn can be naturally identified with the unit tangent bundle to the modular surface $\mathbb{H}^2/SL(2, \mathbb{Z})$ see Sec. 3.2. Moreover, the Teichmüller metric on the space of tori coincides with the hyperbolic metric on \mathbb{H}^2 , and the Teichmüller geodesic flow on the moduli space of flat tori coincides with the geodesic flow on the modular surface.

Hence, the construction from the previous section suggests that the Euclidean algorithm corresponds to the following geometric procedure. There should be a section \mathcal{Y} in the (covering of) the unit tangent bundle to the modular surface and its subsection $\mathcal{Y}' \subset \mathcal{Y}$ such that the trajectory of the geodesic flow emitted from a point of \mathcal{Y}' returns to \mathcal{Y}' after n_1 intersections with \mathcal{Y} , then after n_2 intersections with \mathcal{Y} , etc. In other words there is a natural way to code a continued fraction by a sequence of intersections (so called “cutting sequence”) of the corresponding geodesic with some sections $\mathcal{Y}' \subset \mathcal{Y}$.

Actually, a geometric coding of a continued fraction by a cutting sequence of a geodesics on a surface is known since the works of J. Nielsen and E. Artin in 20s and 30s. The study of the geometric coding was developed in the 80s and 90s by C. Series, R. Adler, L. Flatto and other authors. We refer to the expository paper [Ser] of C. Series for detailed description of the following geometric coding algorithm.

Consider a tiling of the upper half plane with isometric hyperbolic triangles as at Fig. 29. A fundamental domain of the tiling is a triangle with vertices at $0, 1$ and ∞ ; the corresponding quotient surface is a triple cover over the standard modular surface (see Fig. 47). This triangulation of \mathbb{H}^2 by ideal triangles is also known as *Farey tessellation*.

Consider a real number $x \in (0, 1)$. Consider any geodesic γ landing to the real axis at x such that γ intersects with the imaginary axis; let iy be the point of intersection. Let us follow the geodesic γ starting from iy in direction of x . Each time when we cross a triangle of our tiling let us note by the symbol L the situation when we have a single vertex on the left and two vertices on the right (see Fig 28) and by the symbol R the symmetric situation.

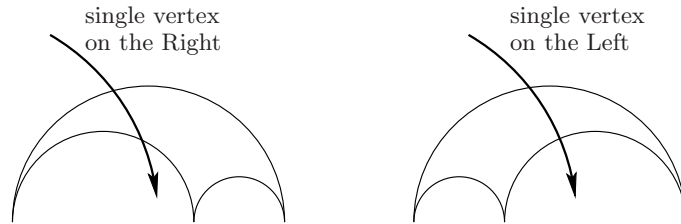


Fig. 28. Coding rule: when we cross a triangle leaving one vertex on the left and two on the right we write symbol L ; when there is one vertex on the right and two on the left we write symbol R

Example. Following the geodesic γ presented at Fig. 29 from some iy to $x = (\sqrt{85} - 5)/10 \approx 0.421954$ we get a sequence $R, R, L, L, R, L, L, R, R, L, \dots$ which we abbreviate as $R^2L^2R^1L^2R^2L^1 \dots$

Theorem (C. Series). *Let $x \in (0, 1)$ be irrational. Let γ be a geodesic emitted from some iy and landing at x ; let $R^{n_1}L^{n_2}R^{n_3}L^{n_4} \dots$ be the corresponding cutting sequence. Then $x = [0; n_1, n_2, n_3, n_4, \dots]$.*

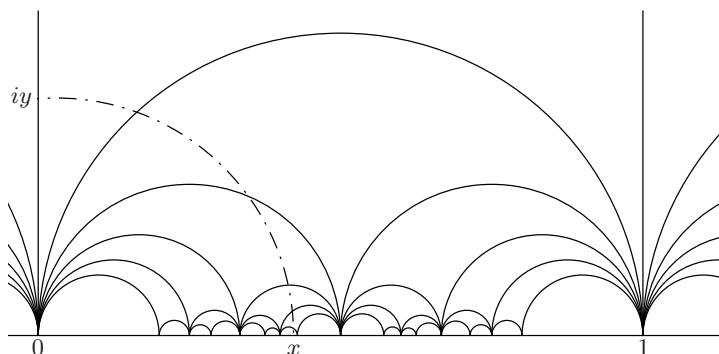


Fig. 29. (After C. Series.) The cutting sequence defined by this geodesic starts with $R, R, L, L, R, L, L, R, R, L, \dots$ which we abbreviate as $R^2L^2R^1L^2R^2L^1 \dots$. The real number $x \in (0, 1)$ at which lands the geodesic has continued fraction expansion $x = [0; 2, 2, 1, 2, 2, 1, \dots]$

Geometric symbolic coding: more serious reading. I can strongly recommend a paper of P. Arnoux [Arn] which clearly and rigorously explains the idea of suspension in the spirit of diagram (18) handling the particular case of Euclidean algorithm and of geodesic flow on the Poincaré upper half-plane. As a survey on geometric coding we can recommend the survey of C. Series [Ser] (as well as other surveys in this collection on related subjects).

6 Closed Geodesics and Saddle Connections on Flat Surfaces

Emitting a geodesic in an irrational direction on a flat torus we get an irrational winding line; emitting it in a rational direction we get a closed geodesic. Similarly, for a flat surface of higher genus a countable dense set of directions corresponds to closed geodesics.

In this section we study how many closed regular geodesics of bounded length live on a generic flat surface S . We consider also *saddle connections* (i.e. geodesic segments joining pairs of conical singularities) and count them.

We explain a curious phenomenon concerning saddle connections and closed geodesics on flat surfaces: they often appear in pairs, triples, etc of parallel saddle connections (correspondingly closed geodesics) of equal length.

When all saddle connections (closed geodesics) in such *configuration* become short the corresponding flat surface starts to degenerate and gets close to the boundary of the moduli space. Thus, a description of possible configurations of parallel saddle connections (closed geodesics) gives us a description of the multidimensional “cusps” of the strata.

6.1 Counting Closed Geodesics and Saddle Connections

Closed Regular Geodesics Versus Irrational Winding Lines

Consider a flat torus obtained by identifying pairs of opposite sides of a unit square. A geodesic emitted in an irrational direction (one with irrational slope) is an irrational winding line; it is dense in the torus. A geodesic emitted in a rational direction is closed; all parallel geodesics are also closed, so directional flow in a rational direction fills the torus with parallel periodic trajectories. The set of rational directions has measure zero in the set of all possible directions. In this sense directions representing irrational winding lines are typical and directions representing closed geodesics – nontypical.

The situation with flat surfaces of higher genera $g \geq 2$ is similar in many aspects, though more complicated in details. For example, for any flat surface S almost all directions are “irrational”; any geodesic emitted in an irrational direction is dense in the surface. Actually, even stronger statement is true:

Theorem (S. Kerckhoff, H. Masur, J. Smillie). *For any flat surface directional flow in almost any direction is uniquely ergodic.*

For the torus the condition that directional flow is *minimal* (that is any trajectory going in this direction is dense in the torus) is equivalent to the condition that the flow is *uniquely ergodic* (the natural Lebesgue measure induced by the flat structure is the only finite measure invariant under directional flow; see Appendix A for details). Surprisingly a directional flow on a surface of higher genus (already for $g = 2$) might be *minimal* but not *uniquely ergodic*! Namely, for some directions which give rise to a minimal directional flow it might be possible to divide the surface into two parts (of nonzero measure) in such way that some trajectories would mostly stay in one part while other trajectories would mostly stay in the other.

Closed geodesics on flat surfaces of higher genera also have some similarities with ones on the torus. Suppose that we have a regular closed geodesic passing through a point $x_0 \in S$. Emitting a geodesic from a nearby point x in the same direction we obtain a parallel closed geodesic of the same length as the initial one. Thus, closed geodesics also appear in families of parallel closed geodesics. However, in the torus case every such family fills the entire torus while a family of parallel regular closed geodesics on a flat surface of higher genus fills only part of the surface. Namely, it fills a flat cylinder having a conical singularity on each of its boundaries.

Exercise. Find several periodic directions on the flat surface from Fig. 12. Find corresponding families of parallel closed geodesics. Verify that each of the surfaces from Fig. 44 decomposes under the vertical flow into three cylinders (of different circumference) filled with periodic trajectories. Find these cylinders.

Counting Problem

Take an arbitrary loop on a torus. Imagine that it is made from a stretched elastic cord. Letting it contract we get a closed regular geodesic (may be winding several times along itself). Now repeat the experiment with a more complicated flat surface. If the initial loop was very simple (or if we are extremely lucky) we again obtain a regular closed geodesic. However, in general we obtain a closed broken line of geodesic segments with vertices at a collection of conical points.

Similarly letting contract an elastic cord joining a pair of conical singularities we usually obtain a broken line composed from several geodesic segments joining conical singularities. In this sense torus is very different from a general flat surface.

A geodesic segment joining two conical singularities and having no conical points in its interior is called *saddle connection*. The case when boundaries of a saddle connection coincide is not excluded: a saddle connection might join a conical point to itself.

Convention 4. In this paper we consider only saddle connections and closed regular geodesics. We never consider broken lines formed by several geodesic segments.

Now we are ready to formulate the Counting Problem. Everywhere in this section we normalize the area of flat surfaces to one.

Counting Problem. Fix a flat surface S . Let $N_{sc}(S, L)$ be the number of saddle connections on S of length at most L . Let $N_{cg}(S, L)$ be the number of maximal cylinders filled with closed regular geodesics of length at most L on S . Find asymptotics of $N_{sc}(S, L)$ and $N_{cg}(S, L)$ as $L \rightarrow \infty$.

It was proved by H. Masur (see [Ma5] and [Ma6]) that for any flat surface S counting functions $N(S, L)$ grow quadratically in L . Namely, there exist constants $0 < const_1(S) < const_2(S) < \infty$ such that

$$const_1(S) \leq N(S, L)/L^2 \leq const_2(S)$$

for L sufficiently large. Recently Ya. Vorobets has obtained in [Vb2] uniform estimates for the constants $const_1(S)$ and $const_2(S)$ which depend only on the genus of S .

Passing from *all* flat surfaces to *almost all* surfaces in a given connected component of a given stratum one gets a much more precise result; see [EMa].

Theorem (A. Eskin and H. Masur). For almost all flat surfaces S in a given connected component of a stratum $\mathcal{H}(d_1, \dots, d_m)$ the counting functions $N_{sc}(S, L)$ and $N_{cg}(S, L)$ have exact quadratic asymptotics

$$\lim_{L \rightarrow \infty} \frac{N_{sc}(S, L)}{\pi L^2} = const_{sc} \quad \lim_{L \rightarrow \infty} \frac{N_{cg}(S, L)}{\pi L^2} = const_{cg} \quad (20)$$

where Siegel–Veech constants $const_{sc}$ and $const_{cg}$ are the same for almost all flat surfaces in the component $\mathcal{H}_1^{comp}(d_1, \dots, d_m)$.

We multiply denominator by π to follow a conventional normalization.

Phenomenon of Higher Multiplicities

Let us discuss now the following problem. Suppose that we have a regular closed geodesic on a flat surface S . Memorize its direction, say, let it be the North-West direction. (Recall that by Convention 1 in Sec. 1.2 we can place a compass at any point of the surface and it will tell us what is the direction to the North.) Consider the maximal cylinder filled with closed regular geodesics parallel to ours. Take a point x outside this cylinder and emit a geodesic from x in the North-West direction. There are two questions.

- How big is the chance to get a closed geodesic?
- How big is the chance to get a closed geodesic of the same length as the initial one?

Intuitively it is clear that the answer to the first question is: “the chances are low” and to the second one “the chances are even lower”. This makes the following Theorem (see [EMaZo]) somehow counterintuitive:

Theorem (A. Eskin, H. Masur, A. Zorich). *For almost all flat surfaces S from any stratum different from $\mathcal{H}_1(2g - 2)$ or $\mathcal{H}_1(d_1, d_2)$ the function $N_{two_cyl}(S, L)$ counting the number of families of parallel regular closed geodesics filling two distinct maximal cylinders has exact quadratic asymptotics*

$$\lim_{L \rightarrow \infty} \frac{N_{two_cyl}(S, L)}{\pi L^2} = const_{two_cyl}$$

where Siegel–Veech constants $const_{two_cyl} > 0$ depends only on the connected component of the stratum.

For almost all flat surface S in any stratum one cannot find a single pair of parallel regular closed geodesics on S of different length.

There is general formula for the Siegel–Veech constant $const_{two_cyl}$ and for similar constants which gives explicit numerical answers for all strata in low genera. Recall that the *principal stratum* $\mathcal{H}(1, \dots, 1)$ is the only stratum of fill dimension in \mathcal{H}_g ; it is the stratum of holomorphic 1-forms with simple zeros (or, what is the same, of flat surfaces with conical angles 4π at all cone points). Numerical values of the Siegel–Veech constants for the principal stratum are presented in Table 2.

Comparing these values we see, that our intuition was not quite misleading. Morally, in genus $g = 4$ a closed regular geodesic belongs to a one-cylinder family with “probability” 97.1%, to a two-cylinder family with “probability” 2.8% and to a three-cylinder family with “probability” only 0.1% (where “probabilities” are calculated proportionally to Siegel–Veech constants).

	$g = 1$	$g = 2$	$g = 3$	$g = 4$
single cylinder	$\frac{1}{2} \cdot \frac{1}{\zeta(2)} \approx 0.304$	$\frac{5}{2} \cdot \frac{1}{\zeta(2)} \approx 1.52$	$\frac{36}{7} \cdot \frac{1}{\zeta(2)} \approx 3.13$	$\frac{3150}{377} \cdot \frac{1}{\zeta(2)} \approx 5.08$
two cylinders	–	–	$\frac{3}{14} \cdot \frac{1}{\zeta(2)} \approx 0.13$	$\frac{90}{377} \cdot \frac{1}{\zeta(2)} \approx 0.145$
three cylinders	–	–	–	$\frac{5}{754} \cdot \frac{1}{\zeta(2)} \approx 0.00403$

Table 2. Siegel–Veech constants $const_{n_cyl}$ for the principal stratum $\mathcal{H}_1(1, \dots, 1)$

In theorem above we discussed closed regular geodesics. A similar phenomenon is true for saddle connections. Recall that the cone angle at a conical point on a flat surface is an integer multiple of 2π . Thus, at a point with a cone angle $2\pi n$ every direction is presented n times. Suppose that we have found a saddle connection of length l going from conical point P_1 to conical point P_2 . Memorize its direction (say, the North-West direction) and its length l . Then with a “nonzero probability” (understood in the same sense as above) emitting a geodesic from P_1 in one of the remaining $n - 1$ North-West directions we make it hit P_2 at the distance l . More rigorously, the Siegel–Veech constant counting configurations of two parallel saddle connections of equal length joining P_1 to P_2 is nonzero.

The explicit formula for any Siegel–Veech constant from [EMaZo] can be morally described as the follows. Up to some combinatorial factor responsible for dimensions, multiplicities of zeroes and possible symmetries any Siegel–Veech constant can be obtained as a limit

$$c(\mathcal{C}) = \lim_{\varepsilon \rightarrow 0} \frac{1}{\pi \varepsilon^2} \frac{\text{Vol}(\text{“}\varepsilon\text{-neighborhood of the cusp } \mathcal{C} \text{”})}{\text{Vol } \mathcal{H}_1^{comp}(d_1, \dots, d_m)} \tag{21}$$

where \mathcal{C} is a particular *configuration* of saddle connections or closed geodesics.

Say, as a configuration \mathcal{C} one can consider a configuration of two maximal cylinders filled with parallel closed regular geodesics of equal lengths. The ε -neighborhood of the corresponding cusp is the subset of those flat surfaces $S \in \mathcal{H}_1^{comp}(d_1, \dots, d_m)$ which have at least one pair of cylinders filled with parallel closed geodesics of length shorter than ε .

As another example one can consider a configuration of three parallel saddle connections of equal lengths on $S \in \mathcal{H}_1(1, 1, 4, 8)$ joining zero P_1 of degree 4 (having cone angle 10π) to zero P_2 of degree 8 (having cone angle 18π) separated by angles $2\pi, 2\pi, 6\pi$ at P_1 and by angles $6\pi, 10\pi, 2\pi$ at P_2 . The ε -neighborhood $\mathcal{H}_1^\varepsilon(1, 1, 4, 8) \subset \mathcal{H}_1(1, 1, 4, 8)$ of the corresponding cusp is the subset of those flat surfaces in $\mathcal{H}_1(1, 1, 4, 8)$ which have at least one triple of saddle connections as described above of length shorter than ε .

We explain the origin of the key formula (21) in the next section. In section 6.4 we give an explanation of appearance of higher multiplicities.

Other counting problems (after Ya. Vorobets)

Having a flat surface S of unit area we have studied above the number of maximal cylinders $N_{cg}(S, L)$ filled with closed regular geodesics of length at most L on S . (In this setting when we get in some direction several parallel maximal cylinders of equal perimeter, we count each of them.) In the paper [Vb2] Ya. Vorobets considered other counting problems.

In particular, among all maximal periodic cylinders of length at most L (as above) he counted the number $N_{cg,\sigma}(S, L)$ of those ones, which have area greater than σ . He also counted the total sum $N_{area}(S, L)$ of areas of all maximal cylinders of perimeter at most L and the number $N_x(S, L)$ of regular periodic geodesics of length at most L passing through a given point $x \in S$.

Ya. Vorobets has also studied how the maximal cylinders filled with closed geodesics are distributed with respect to their direction and their area. He considered the induced families of probability measures on the circle S^1 , on the unit interval $[0, 1]$ and on their product $S^1 \times [0, 1]$. Given a subset $U \subset S^1$, $V \subset [0, 1]$, $W \subset S^1 \times [0, 1]$ the corresponding measures $dir_L(U)$, $ar_L(V)$, $pair_L(W)$ tell the proportion of cylinders of bounded perimeter having direction in U , area in V , or the pair (*direction*, *area*) in W correspondingly.

Using the general approach of A. Eskin and H. Masur, Ya. Vorobets has proved in [Vb2] existence of exact quadratic asymptotics for the counting functions introduced above. He has computed the corresponding Siegel–Veech constants in terms of the Siegel–Veech constant $const_{cg}$ in (20) and found the asymptotic distributions of directions and areas of the cylinders:

Theorem (Ya. Vorobets). *For almost any flat surface S of unit area in any connected component of any stratum $\mathcal{H}_1^{comp}(d_1, \dots, d_m)$ and for almost any point x of S one has*

$$\lim_{L \rightarrow \infty} \frac{N_{cg,\sigma}(S, L)}{\pi L^2} = c_{cg,\sigma} \quad \lim_{L \rightarrow \infty} \frac{N_{area}(S, L)}{\pi L^2} = c_{area} \quad \lim_{L \rightarrow \infty} \frac{N_x(S, L)}{\pi L^2} = c_x,$$

where $c_{cg,\sigma} = (1 - \sigma)^{2g-3+m} \cdot const_{cg}$ and $c_{area} = c_x = \frac{const_{cg}}{2g-2+m}$.

For almost any flat surface S of unit area one has the following weak convergence of measures:

$$dir_L \rightarrow \varphi \quad ar_L \rightarrow \rho \quad pair_L \rightarrow \varphi \times \rho,$$

where φ is the uniform probability measure on the circle and ρ is the probability measure on the unit interval $[0, 1]$ with the density $(2g-3+m)(1-x)^{2g-4+m} dx$.

Directional flow: more serious reading. Theorem of S. Kerckhoff, H. Masur and J. Smillie is proved in [KMaS]. An example of minimal but not uniquely ergodic interval exchange transformations is constructed by W. Veech in [Ve1] (using different terminology); an independent example (also using different terminology) was constructed at the same time by V. I. Oseledets. For flows such examples are constructed in the paper of A. Katok [Kat1] and developed by E. Sataev in [Sat]. Another example was discovered by M. Keane [Kea2]. For alternative approach to the study of unique ergodicity of interval exchange transformations see the paper of M. Boshernitzan [Ber2]. A very nice construction of minimal but not uniquely ergodic interval exchange transformations (in a language which is very close to the language of this paper) can be found in the survey of H. Masur and S. Tabachnikov [MaT] or in the survey of H. Masur [Ma7].

6.2 Siegel–Veech Formula

We start from a slight formalization of our counting problem. As usual we start with a model case of the flat torus. As usual we assume that our flat torus is glued from a unit square. We count closed regular geodesics on \mathbb{T}^2 of a bounded length. To mimic count of saddle connections we mark two points $P_1 \neq P_2$ on \mathbb{T}^2 and count geodesic segments of bounded length joining P_1 and P_2 .

Our formalization consists in the following construction. Consider an auxiliary Euclidian plane \mathbb{R}^2 . Having found a regular closed geodesic on \mathbb{T}^2 we note its direction α and length l and draw a vector in \mathbb{R}^2 in direction α having length l . We apply a similar construction to “saddle connections”. The endpoints of corresponding vectors form two discrete subsets in \mathbb{R}^2 which we denote by V_{cg} and V_{sc} .

It is easy to see that for the torus case a generic choice of P_1 and P_2 generates a set V_{sc} which is just a shifted square lattice, see Fig. 30. The set V_{cg} is a subset of *primitive* elements of the square lattice, see Fig. 30. Since we count only regular closed geodesics which do not turn many times around themselves we cannot obtain elements of the form (kn_1, kn_2) with $k, n_1, n_2 \in \mathbb{Z}$.

The corresponding counting functions $N_{sc}(\mathbb{T}^2, L)$ and $N_{cg}(\mathbb{T}^2, L)$ correspond to the number of element of V_{sc} and V_{cg} correspondingly which get to a disc of radius L centered in the origin. Both functions have exact quadratic asymptotics. Denoting by $\chi_L(v)$, where $v \in \mathbb{R}^2$ the indicator function of such disc we get

$$\begin{aligned} N_{sc}(\mathbb{T}^2, L) &= \sum_{v \in V_{sc}} \chi_L(v) \sim 1 \cdot \pi L^2 \\ N_{cg}(\mathbb{T}^2, L) &= \sum_{v \in V_{cg}} \chi_L(v) \sim \frac{1}{\zeta(2)} \cdot \pi L^2 \end{aligned} \tag{22}$$

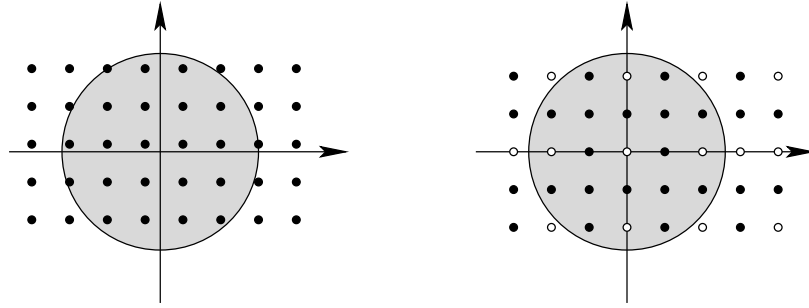


Fig. 30. Sets V_{sc} and V_{cg} for the flat torus

The coefficients in quadratic asymptotics define the corresponding Siegel–Veech constants $const_{sc} = 1$ and $const_{cg} = \frac{1}{\zeta(2)} = \frac{6}{\pi^2}$. (Note that here we count every geodesic twice: once with one orientation and the other one with the opposite orientation. This explains why in this normalization we obtain the value of $const_{cg}$ twice as much as $const_{cg}$ for genus one in Table 2.)

Consider now a more general flat surface S . Fix the geometric type of *configuration* \mathcal{C} of saddle connections or closed geodesics. By definition all saddle connections (closed geodesics) in \mathcal{C} are parallel and have equal length. Thus, similar to the torus case, every time we see a collection of saddle connections (closed geodesics) of geometric type \mathcal{C} we can associate to such collection a vector in \mathbb{R}^2 . We again obtain a discrete set $V(S) \subset \mathbb{R}^2$.

Now fix \mathcal{C} and apply this construction to every flat surface S in the stratum $\mathcal{H}_1(d_1, \dots, d_m)$. Consider the following operator $f \mapsto \hat{f}$ generalizing (22) from functions with compact support on \mathbb{R}^2 to functions on $\mathcal{H}_1(d_1, \dots, d_m)$:

$$\hat{f}(S) = \sum_{v \in V} f(v)$$

Lemma (W. Veech). *The functional*

$$f \mapsto \int_{\mathcal{H}_1^{comp}(d_1, \dots, d_m)} \hat{f}(S) d\nu_1$$

is $SL(2, \mathbb{R})$ -invariant.

Having proved convergence of the integral above the Lemma follows immediately from invariance of the measure $d\nu_1$ under the action of $SL(2, \mathbb{R})$ and from the fact that $V(gS) = gV(s)$ for any flat surface S and any $g \in SL(2, \mathbb{R})$.

Now note that there very few $SL(2, \mathbb{R})$ -invariant functionals on functions with compact support in \mathbb{R}^2 . Actually, there are two such functionals, and the other ones are linear combinations of these two. These two functionals are the value of $f(0)$ at the origin and the integral $\int_{\mathbb{R}^2} f(x, y) dx dy$. It is possible to see that the value $f(0)$ at the origin is irrelevant for the functional from the Lemma above. Hence it is proportional to $\int_{\mathbb{R}^2} f(x, y) dx dy$.

Theorem (W. Veech). *For any function $f : \mathbb{R}^2 \rightarrow \mathbb{R}$ with compact support one has*

$$\frac{1}{\text{Vol } \mathcal{H}_1^{\text{comp}}(d_1, \dots, d_m)} \int_{\mathcal{H}_1^{\text{comp}}(d_1, \dots, d_m)} \hat{f}(S) d\nu_1 = C \int_{\mathbb{R}^2} f(x, y) dx dy \quad (23)$$

Here the constant C in (23) *does not depend* on f ; it depends only on the connected component $\mathcal{H}_1^{\text{comp}}(d_1, \dots, d_m)$ and on the geometric type \mathcal{C} of the chosen configuration.

Note that it is an *exact* equality. In particular, choosing as $f = \chi_L$ the indicator function of a disc of radius L we see that for any given $L \in \mathbb{R}_+$ the *average* number of saddle connections not longer than L on flat surfaces $S \in \mathcal{H}_1^{\text{comp}}(d_1, \dots, d_m)$ is *exactly* $C \cdot \pi L^2$, where C does not depend on L .

It would be convenient to introduce a special notation for such \hat{f} . Let

$$\hat{f}_L(S) = \sum_{v \in V} \chi_L(v)$$

The Theorem of Eskin and Masur [EMa] cited above tells that for large values of L one gets $\hat{f}_L(S) \sim c(\mathcal{C})\pi L^2$ for almost all individual flat surfaces $S \in \mathcal{H}_1^{\text{comp}}(d_1, \dots, d_m)$ and that the corresponding constant $c(\mathcal{C})$ coincides with the constant C above.

Formula (23) can be applied to \hat{f}_L for any value of L . In particular, instead of considering large L we can choose a very small value $L = \varepsilon$. The corresponding function $\hat{f}_\varepsilon(S)$ counts how many collections of parallel ε -short saddle connections (closed geodesics) of the type \mathcal{C} we can find on the flat surface S .

Usually there are no such saddle connections (closed geodesics), so for most flat surfaces $\hat{f}_\varepsilon(S) = 0$. For some surfaces there is exactly one collection like this. We denote the corresponding subset by $\mathcal{H}_1^{\varepsilon, \text{thick}}(\mathcal{C}) \subset \mathcal{H}_1(d_1, \dots, d_m)$. Finally, for the surfaces from the remaining (very small) subset $\mathcal{H}_1^{\varepsilon, \text{thin}}(\mathcal{C})$ one has several collections of short saddle connections (closed geodesics) of the type \mathcal{C} . Thus,

$$\hat{f}_\varepsilon(S) = \begin{cases} 0 & \text{for most of the surfaces } S \\ 1 & \text{for } S \in \mathcal{H}_1^{\varepsilon, \text{thick}}(\mathcal{C}) \\ > 1 & \text{for } S \in \mathcal{H}_1^{\varepsilon, \text{thin}}(\mathcal{C}) \end{cases}$$

and we can rewrite (23) for \hat{f}_ε as

$$\begin{aligned}
c(\mathcal{C}) \cdot \pi \varepsilon^2 &= c(\mathcal{C}) \int_{\mathbb{R}^2} \chi_\varepsilon(x, y) dx dy = \\
&= \frac{1}{\text{Vol } \mathcal{H}_1^{\text{comp}}(d_1, \dots, d_m)} \int_{\mathcal{H}_1^{\text{comp}}(d_1, \dots, d_m)} \hat{f}_\varepsilon(S) d\nu_1 = \\
&= \frac{1}{\text{Vol } \mathcal{H}_1^{\text{comp}}(d_1, \dots, d_m)} \int_{\mathcal{H}_1^{\varepsilon, \text{thick}}(\mathcal{C})} 1 d\nu_1 + \\
&\quad + \frac{1}{\text{Vol } \mathcal{H}_1^{\text{comp}}(d_1, \dots, d_m)} \int_{\mathcal{H}_1^{\varepsilon, \text{thin}}(\mathcal{C})} \hat{f}_\varepsilon(S) d\nu_1
\end{aligned}$$

It can be shown that though $\hat{f}_\varepsilon(S)$ might be large on $\mathcal{H}_1^{\varepsilon, \text{thin}}(\mathcal{C})$ the measure of this subset is so small (it is of the order ε^4 that the last integral above is negligible in comparison with the previous one; namely it is $o(\varepsilon^2)$). (This is a highly nontrivial result of Eskin and Masur [EMa].) Taking into consideration that

$$\int_{\mathcal{H}_1^{\varepsilon, \text{thick}}(\mathcal{C})} 1 d\nu_1 = \text{Vol } \mathcal{H}_1^{\varepsilon, \text{thick}}(\mathcal{C}) = \text{Vol } \mathcal{H}_1^\varepsilon(\mathcal{C}) + o(\varepsilon^2)$$

we can rewrite the chain of equalities above as

$$c(\mathcal{C}) \cdot \pi \varepsilon^2 = \frac{\text{Vol } \mathcal{H}_1^\varepsilon(\mathcal{C})}{\text{Vol } \mathcal{H}_1^{\text{comp}}(d_1, \dots, d_m)} + o(\varepsilon^2)$$

which is equivalent to (21).

Baby Case: Closed Geodesics on the Torus

As an elementary application we can prove that proportion of primitive lattice points among all lattice points is $1/\zeta(2)$. In other words, applying (21) we can prove asymptotic formula (22) for the number of primitive lattice points in a disc of large radius L . As we have seen at Fig. 30 this number equals to the number $N_{cg}(\mathbb{T}^2, L)$ of families of oriented closed geodesics of length bounded by L on the standard torus \mathbb{T}^2 .

We want to apply (21) to prove the following formula for the corresponding Siegel–Veech constant c_{cg}^+ (where superscript + indicates that we are counting *oriented* geodesics on \mathbb{T}^2).

$$c_{cg}^+ = \lim_{L \rightarrow \infty} \frac{N_{cg}(\mathbb{T}^2, L)}{\pi L^2} = \frac{1}{\zeta(2)} = \frac{6}{\pi^2}$$

Note that the moduli space $\mathcal{H}_1(0)$ of flat tori is a total space of a unit tangent bundle to the modular surface (see Sec. 3.2, Fig. 13; see also (30) in Sec. 9.1 for geometric details). Modular surface can be considered as a space of flat tori of unit area without choice of direction to the North.

Measure on this circle bundle disintegrates to the product measure on the fiber and the hyperbolic measure on the modular curve. In particular, $\text{Vol}(\mathcal{H}_1(0)) = \pi \cdot \pi/3$, where $\pi/3$ is the hyperbolic area of the modular surface.

Similarly, $\text{Vol}(\mathcal{H}_1^\varepsilon(0)) = \pi \cdot \text{Area}(\text{Cusp}(\varepsilon))$, where $\text{Cusp}(\varepsilon)$ is a subset of the modular surface corresponding to those flat tori of unit area which have a geodesic shorter than ε (see Fig. 13).

Showing that $\text{Area}(\text{Cusp}(\varepsilon)) \approx \varepsilon^2$ we apply (21) to get

$$c_{cg} = \lim_{\varepsilon \rightarrow 0} = \frac{1}{\pi \varepsilon^2} \frac{\text{Area}(\text{Cusp}(\varepsilon))}{\text{Area}(\text{Modular surface})} = \frac{1}{\pi \varepsilon^2} \frac{\varepsilon^2 + o(\varepsilon^2)}{\pi/3} = \frac{1}{2\zeta(2)}.$$

Note that the Siegel–Veech constant c_{cg} corresponds to counting *nonoriented* closed geodesics on \mathbb{T}^2 . Thus, finally we obtain the desired value $c_{cg}^+ = 2c_{cg}$.

In the next section we give an idea of how one can compute $\text{Vol} \mathcal{H}_1^\varepsilon(\mathcal{C})$ in the simplest case, In Sec. 6.4 we describe the phenomenon of higher multiplicities and discuss the structure of typical cusps of the moduli spaces $\mathcal{H}(d_1, \dots, d_m)$.

6.3 Simplest Cusps of the Moduli Space

In this section we consider the simplest “cusp” \mathcal{C} on a stratum $\mathcal{H}(d_1, \dots, d_m)$ and evaluate $\text{Vol} \mathcal{H}_1^\varepsilon(\mathcal{C})$ for this cusp. Namely, we assume that the flat surface has at least two distinct conical points $P_1 \neq P_2$; let $2\pi(d_1 + 1), 2\pi(d_2 + 1)$ be corresponding cone angles. As a *configuration* \mathcal{C} we consider a configuration when we have a single saddle connection ρ joining P_1 to P_2 and no other saddle connections on S parallel to ρ . In our calculation we assume that the conical points on every $S \in \mathcal{H}(d_1, \dots, d_m)$ have names; we count only saddle connections joining P_1 to P_2 .

Consider some $S \in \mathcal{H}_1^{\varepsilon, \text{thick}}(\mathcal{C}) \subset \mathcal{H}(d_1, \dots, d_m)$, that is a flat surface S having a single saddle connection joining P_1 to P_2 which is not longer than ε and having no other short saddle connections or closed geodesics.

We are going to show that there is a canonical way to shrink the saddle connection on $S \in \mathcal{H}_1^{\varepsilon, \text{thick}}(\mathcal{C})$ coalescing two conical points into one. We shall see that, morally, this provides us with an (almost) fiber bundle

$$\begin{array}{c} \mathcal{H}_1^{\varepsilon, \text{thick}}(d_1, d_2, d_3, \dots, d_m) \\ \downarrow \tilde{D}_\varepsilon^2 \\ \mathcal{H}_1(d_1 + d_2, d_3, \dots, d_m) \end{array} \tag{24}$$

where \tilde{D}_ε^2 is a ramified cover of order $(d_1 + d_2 + 1)$ over a standard metric disc of radius ε . Moreover, we shall see that the measure on $\mathcal{H}_1^{\varepsilon, \text{thick}}(d_1, d_2, d_3, \dots, d_m)$ disintegrates into a product of the standard measure on \tilde{D}_ε^2 and the natural measure on $\mathcal{H}_1(d_1 + d_2, d_3, \dots, d_m)$. The latter would imply the following simple answer to our problem:

$$\begin{aligned} \text{Vol}(\text{“}\varepsilon\text{-neighborhood of the cusp } \mathcal{C}\text{”}) &= \\ &= \text{Vol} \mathcal{H}_1^\varepsilon(\mathcal{C}) = \text{Vol} \mathcal{H}_1^\varepsilon(d_1, d_2, d_3, \dots, d_m) \approx \\ &\approx (d_1 + d_2 + 1) \cdot \pi \varepsilon^2 \cdot \text{Vol} \mathcal{H}_1(d_1 + d_2, d_3, \dots, d_m) \end{aligned} \tag{25}$$

Instead of contracting an isolated short saddle connection to a point we prefer to create it breaking a conical point $P' \in S'$ of degree $d_1 + d_2$ on a surface $S' \in \mathcal{H}_1(d_1 + d_2, d_3, \dots, d_m)$ into two conical points of degrees d_1 and d_2 joined by a short saddle connections. We shall see that this surgery is invertible, and thus we shall get a coalescing construction. In the remaining part of this section we describe this surgery following [EMaZo].

Breaking up a Conical Point into Two

We assume that the initial surface $S' \in \mathcal{H}_1(d_1 + d_2, d_3, \dots, d_m)$ does not have any short saddle connections or short closed geodesics.

Consider a metric disc of a small radius ε centered at the point P' , i.e. the set of points Q' of the surface S' such that Euclidean distance from Q' to the point P' is less than or equal to ε . We suppose that $\varepsilon > 0$ is chosen small enough, so that the ε -disc does not contain any other conical points of the metric; we assume also, that the disc which we defined in the metric sense is homeomorphic to a topological disc. Then, metrically our disc has a structure of a regular cone with a cone angle $2\pi(d_1 + d_2 + 1)$; here $d_1 + d_2$ is the multiplicity of the zero P' . Now cut the chosen disc (cone) out of the surface. We shall modify the flat metric inside it preserving the metric at the boundary, and then paste the modified disc (cone) back into the surface.

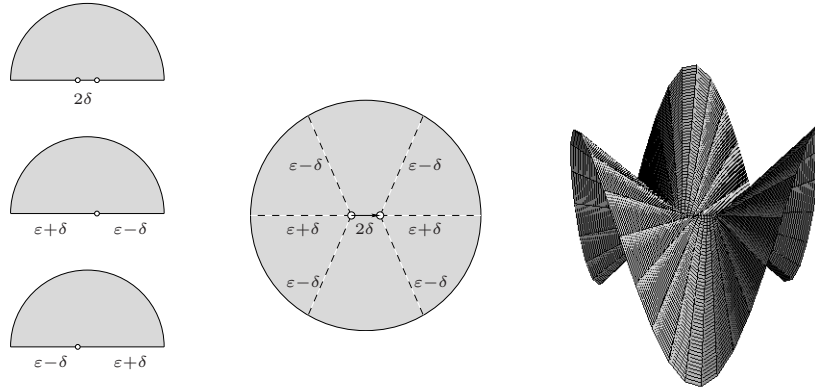


Fig. 31. Breaking up a conical point into two (after [EMaZo]).

Our cone can be glued from $2(k_i + 1)$ copies of standard metric half-discs of the radius ε , see the picture at the top of Fig. 31. Choose some small δ , where $0 < \delta < \varepsilon$ and change the way of gluing the half-discs as indicated on the bottom picture of Fig. 31. As patterns we still use the standard metric half-discs, but we move slightly the marked points on their diameters. Now we use two special half-discs; they have two marked points on the diameter at the distance δ from the center of the half disc. Each of the remaining $2k_i$ half-discs

has a single marked point at the distance δ from the center of the half-disc. We are alternating the half-discs with the marked point moved to the right and to the left from the center. The picture shows that all the lengths along identifications are matching; gluing the half-discs in this latter way we obtain a topological disc with a flat metric; now the flat metric has two cone-type singularities with the cone angles $2\pi(d_1 + 1)$ and $2\pi(d_2 + 1)$.

Note that a small tubular neighborhood of the boundary of the initial cone is isometric to the corresponding tubular neighborhood of the boundary of the resulting object. Thus we can paste it back into the surface. Pasting it back we can turn it by any angle φ , where $0 \leq \varphi < 2\pi(d_1 + d_2 + 1)$.

We described how to break up a zero of multiplicity $d_1 + d_2$ of an Abelian differential into two zeroes of multiplicities d_1, d_2 . The construction is local; it is parameterized by the two free real parameters (actually, by one complex parameter): by the small distance 2δ between the newborn zeroes, and by the direction φ of the short geodesic segment joining the two newborn zeroes. In particular, as a parameter space for this construction one can choose a ramified covering of degree $d_1 + d_2 + 1$ over a standard metric disc of radius ε .

6.4 Multiple Isometric Geodesics and Principal Boundary of the Moduli Space

In this section we give an explanation of the phenomenon of higher multiplicities, we consider typical degenerations of flat surfaces and we discuss how can one use configurations of parallel saddle connections or closed geodesics to determine the orbit of a flat surface S .

Multiple Isometric Saddle Connections

Consider a collection of saddle connections and closed geodesics representing a basis of relative homology $H_1(S, \{P_1, \dots, P_m\}; \mathbb{Z})$ on a flat surface S . Recall, that any geodesic on S goes in some constant direction. Recall also that by Convention 1 any flat surface is endowed with a distinguished direction to the North, so we can place a compass at any point of S and determine in which direction goes our geodesic. Thus, every closed geodesic or saddle connection determines a vector $\mathbf{v}_j \in \mathbb{R}^2 \simeq \mathbb{C}$ which goes in the same direction and have the same length as the corresponding geodesic element. Finally recall that collection of planar vectors $\{\mathbf{v}_1, \dots, \mathbf{v}_{2g+m-1}\}$ considered as complex numbers provide us with a local coordinate system in $\mathcal{H}(d_1, \dots, d_m)$. In complex-analytic language these coordinates are the *relative periods* of holomorphic 1-form representing the flat surface S , namely $\mathbf{v}_j = \int_{\rho_j} \omega$, where ρ_j is the corresponding geodesic element (saddle connection or closed geodesic).

We say that two geodesic elements γ_1, γ_2 (saddle connections or closed geodesics) are *homologous* on a flat surface S if they determine the same homology classes in $H_1(S, \{P_1, \dots, P_m\}; \mathbb{Z})$. In other words, γ_1 is homologous

to γ_2 if cutting S by γ_1 and γ_2 we break the surface S into two pieces. For example, the saddle connections $\gamma_1, \gamma_2, \gamma_3$ on the right surface at the bottom of Fig. 32 are homologous.

The following elementary observation is very important for the sequel. Since the holomorphic 1-form ω representing S is closed, homologous geodesic elements γ_1, γ_2 define the same period:

$$\int_{\gamma_1} \omega = \mathbf{v} = \int_{\gamma_2} \omega$$

We intensively used the following result of H. Masur and J. Smillie [MaS] in our considerations in the previous section.

Theorem (H. Masur, J. Smillie). *There is a constant M such that for all $\varepsilon, \kappa > 0$ the subset $\mathcal{H}_1^\varepsilon(d_1, \dots, d_m)$ of $\mathcal{H}_1(d_1, \dots, d_m)$ consisting of those flat surfaces, which have a saddle connection of length at most ε , has volume at most $M\varepsilon^2$.*

The volume of the set of flat surfaces with a saddle connection of length at most ε and a nonhomologous saddle connection with length at most κ is at most $M\varepsilon^2\kappa^2$.

Morally, this Theorem says that a subset corresponding to one complex parameter with norm at most ε has measure of order ε^2 , and a subset corresponding to two complex parameter with norm at most ε has measure of order ε^4 . In particular, this theorem implies that $\text{Vol } \mathcal{H}_1^{\varepsilon, \text{thin}}(d_1, \dots, d_m)$ is of the order ε^4 .

In the previous section we considered the subset of flat surfaces $S \in \mathcal{H}_1^\varepsilon(d_1, d_2, d_3, \dots, d_m)$ having a single short saddle connection joining zeroes of degrees d_1 and d_2 . We associated to such surface S a new surface $S' \in \mathcal{H}_1^\varepsilon(d_1 + d_2, d_3, \dots, d_m)$ in the smaller stratum. Note that, morally, surfaces S and S' have the same periods with a reservation that S has one more period than S' : the extra small period represented by our short saddle connection.

Metrically surfaces S and S' are almost the same: having a surface S we know how to contract our short saddle connection to a point; having a surface S' and an abstract short period $\mathbf{v} \in \mathbb{C} \simeq \mathbb{R}^2$ we know how to break the corresponding zero on S' into two zeroes joined by a single short saddle connection realizing period \mathbf{v} . (In the latter construction we have some additional discrete freedom: we can break the zeroes in direction \mathbf{v} in $d_1 + d_2 + 1$ different ways.)

Our construction does not work when we have two nonhomologous short geodesic elements on the surface S . But we do not care since according to the Theorem of H. Masur and J. Smillie the subset $\mathcal{H}_1^{\varepsilon, \text{thin}}(d_1, \dots, d_m)$ of such surfaces has very small measure (of the order ε^4).

Now consider a slightly more general surgery represented by Fig. 32. We take three distinct flat surfaces, we break a zero on each of them as it was done in the previous section. We do it coherently using the same direction

and the same distance δ on each surface (left part of Fig. 32). Then we slit each surface along the newborn saddle connection and glue the surfaces in a close compound surface as indicated on the right part of Fig. 32.

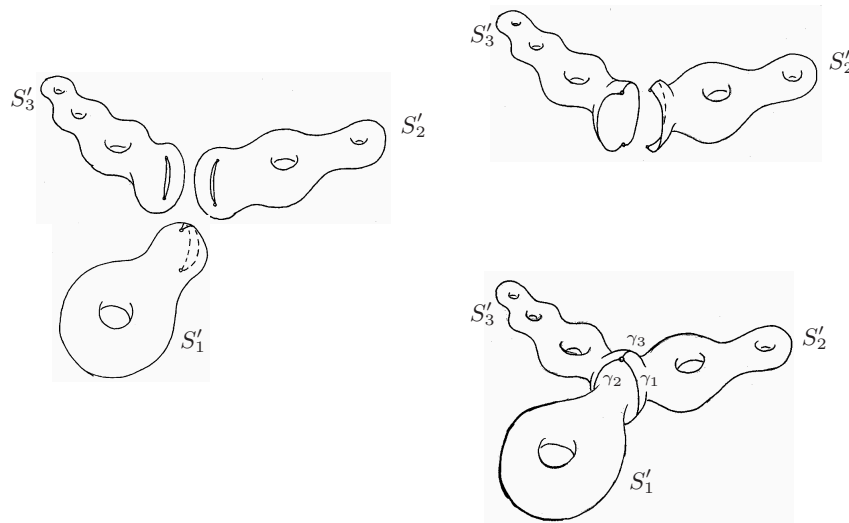


Fig. 32. Multiple homologous saddle connections; topological picture

The resulting surface has three short parallel saddle connections of equal length. By construction they are *homologous*: cutting along any two of them we divide the surface into two parts. Thus, the resulting surface again has only one short period! Note that a complete collection of periods of the compound surface can be obtained as disjoint union

$$\text{periods of } S'_1 \sqcup \text{periods of } S'_2 \sqcup \text{periods of } S'_3 \sqcup \text{newborn short period}$$

Hence, any flat surface S with three short homologous saddle connections and no other short geodesic elements can be viewed as a nonconnected flat surface $S'_1 \sqcup S'_2 \sqcup S'_3$ plus a memory about the short period $v \in \mathbb{C}$ which we use when we break the zeroes (plus some combinatorial arbitrariness of finite order).

The moduli space of disconnected flat surfaces of the same type as $S'_1 \sqcup S'_2 \sqcup S'_3$ has one dimension less than the original stratum $\mathcal{H}(d_1, \dots, d_m)$. Our considerations imply the following generalization of formula (25) for the volume of “ ε -neighborhood” of the corresponding cusp:

$$\begin{aligned} \text{Vol}(\text{“}\varepsilon\text{-neighborhood of the cusp } \mathcal{C}\text{”}) &= \text{Vol } \mathcal{H}_1^\varepsilon(\mathcal{C}) = \\ k \cdot \text{Vol } \mathcal{H}_1(\text{stratum of } S'_1) \cdot \text{Vol } \mathcal{H}_1(\text{stratum of } S'_2) \cdot \text{Vol } \mathcal{H}_1(\text{stratum of } S'_3) \cdot \pi \varepsilon^2 \end{aligned}$$

where the factor k is an explicit constant depending on dimensions, possible symmetries, and combinatorics of multiplicities of zeroes. In particular, we get a subset of order ε^2 .

Now for any flat surface $S_0 \in \mathcal{H}(d_1, \dots, d_m)$ we can state a counting problem, where we shall count only those saddle connections which appear in configuration \mathcal{C} of triples of homologous saddle connections breaking S_0 into three surfaces of the same topological and geometric types as S'_1, S'_2, S'_3 . Applying literally same arguments as in Sec. 6.2 and 6.3 we can show that such number of triples of homologous saddle connections of length at most L has quadratic growth rate and that the corresponding Siegel–Veech constant $c(\mathcal{C})$ can be expressed by the same formula as above:

$$\begin{aligned} c(\mathcal{C}) &= \lim_{\varepsilon \rightarrow 0} \frac{1}{\pi \varepsilon^2} \frac{\text{Vol}(\text{“}\varepsilon\text{-neighborhood of the cusp } \mathcal{C} \text{”})}{\text{Vol } \mathcal{H}_1^{\text{comp}}(d_1, \dots, d_m)} = \\ &= (\text{combinatorial factor}) \frac{\prod_{k=1}^n \text{Vol } \mathcal{H}_1(\text{stratum of } S'_k)}{\text{Vol } \mathcal{H}_1^{\text{comp}}(d_1, \dots, d_m)} \end{aligned}$$

Principal Boundary of the Strata

The results above give a description of typical degenerations of flat surfaces. A flat surface gets close to the boundary of the moduli space when some geodesic element (or a collection of geodesic elements) get short. Morally, we have described something like “faces” of the boundary, while there are still “edges”, etc, representing degenerations of higher codimension. Flat surfaces which are close to this “principal boundary” of a stratum $\mathcal{H}(d_1, \dots, d_m)$ have the following structure.

If the short geodesic element is a saddle connection joining two distinct zeroes, then the surface looks like the one at Fig. 32. It can be decomposed to several flat surfaces with slits glued cyclically one to another. The boundaries of the slits form short saddle connections on the compound surface. All these saddle connections join the same pair of points; they have the same length and direction. They represent homologous cycles in the relative homology group $H_1(S, \{P_1, \dots, P_m\}; \mathbb{Z})$.

Figure 33 represents a flat surface $S_0 \in \mathcal{H}(1, 1)$ unfolded to a polygon. The two short bold segments represent two homologous saddle connections. The reader can easily check that on any surface $S \in \mathcal{H}(1, 1)$ obtained from S_0 by a small deformation one can find a pair of short parallel saddle connections of equal length. Cutting S by these saddle connections we get a pair of tori with slits.

We did not discuss in the previous section the case when the short geodesic element is a regular closed geodesic (or a saddle connection joining a conical point to itself). Morally, it is similar to the case of saddle connections, but technically it slightly more difficult. A flat surface near the principal boundary of this type is presented on the right of Fig. 34.

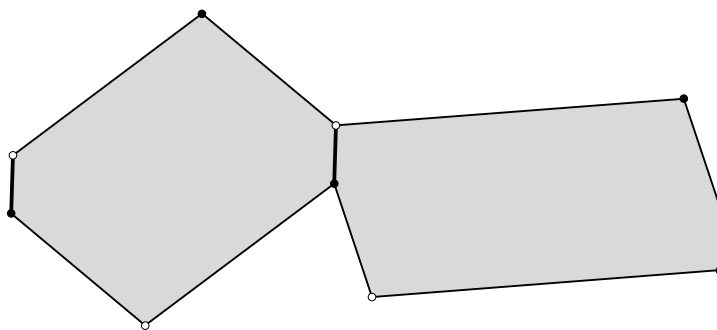


Fig. 33. Flat surface with two short homologous saddle connections. Any small deformation of this surface also has a pair of short homologous saddle connections.

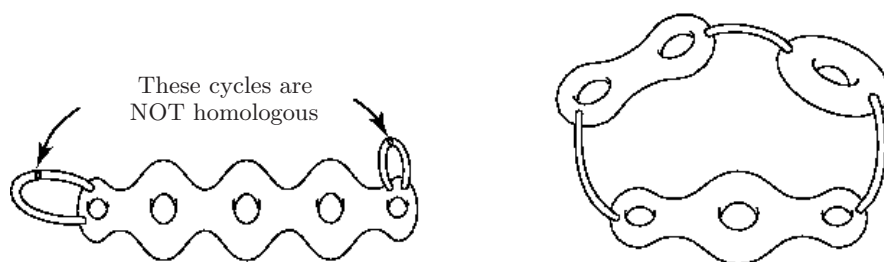


Fig. 34. A typical (on the right) and nontypical (on the left) degenerations of a flat surface. Topological picture

Similar to the case of saddle connections, the surface can be also decomposed to a collection of well-proportional flat surfaces S'_1, \dots, S'_n of lower genera. Each surface S'_k has a pair of holes. Each of these holes is realized by a saddle connection joining a zero to itself. The surfaces are cyclically glued to a “necklace”, where two neighboring surfaces might be glued directly or by a narrow cylinder. Since the waist curves of all these cylinders and all saddle connections representing boundaries of surfaces S'_k are homologous, the corresponding closed geodesics on S are parallel and have equal length. A more artistic⁵ image of a surface, which is located closed to the boundary of a stratum is represented on Fig. 35.

The surface on the left of Fig. 34 is close to an “edge” of the moduli space in the sense that it represents a “nontypical” degeneration: a degeneration of codimension two. This surface has two nonhomologous closed geodesics shorter than ε . Due to the Theorem of H. Masur and J. Smillie cited above, the subset $\mathcal{H}_1^{\varepsilon, thin}(d_1, \dots, d_m)$ of such surfaces has measure of the order ε^4 .



Fig. 35. Flat surface near the principal boundary⁵

Configurations of Saddle Connections and of Closed Geodesics as Invariants of Orbits

Consider a flat surface S_0 and consider its orbit under the action of $SL(2, \mathbb{R})$. It is very easy to construct this orbit locally for those elements of the group $GL^+(2, \mathbb{R})$ which are close to identity. It is a fairly complicated problem to construct this orbit globally in $\mathcal{H}(d_1, \dots, d_m)$ and to find its closure. Ergodic theorem of H. Masur and W. Veech (see Sec. 3.5) tells that for almost every surface S_0 the closure of the orbit of S_0 coincides with the emboding connected component of the corresponding stratum. But for some surfaces the closures of the orbits are smaller. Sometimes it is possible to distinguish such surfaces looking at the configurations of parallel closed geodesics and saddle connections. Say, for *Veech surfaces* which will be discussed in Sec. 9.5 the orbit of $SL(2, \mathbb{R})$ is already closed in the stratum, so Veech surfaces are very special. This property has an immediate reflection in behavior of parallel closed geodesics and saddle connections: as soon as we have a saddle connection or a closed geodesic in some direction on a Veech surface, *all* geodesics in this direction are either closed or (finite number of them) produce saddle connections.

Thus, it is useful to study configurations of parallel closed geodesics on a surface (which includes the study of proportions of corresponding maximal cylinders filled with parallel regular closed geodesics) to get information about the closure of corresponding orbit.

One can also use configurations of parallel closed geodesics on a flat surface to determine those connected component of the stratum, to which belongs our surface S_0 . Some configurations (say, $g - 1$ tori connected in a “necklace” by a chain of cylinders, compare to Fig. 35) are specific for some connected

⁵H. Matisse: La Danse. The State Hermitage Museum, St. Petersburg. (c) Succession H. Matisse/VG Bild-Kunst, Bonn, 2005

components and never appear for surfaces from other connected components. We return to this discussion in the very end of Sec. 9.4 where we use this idea to distinguish connected components of the strata in the moduli space of quadratic differentials.

6.5 Application: Billiards in Rectangular Polygons

Consider now a problem of counting *generalized diagonals* of bounded length or a problem of counting closed billiard trajectories of bounded length in a billiard in a rational polygon Π . Apply Katok–Zemliakov construction (see Sec. 2.1) and glue a very flat surface S from the billiard table Π . Every generalized diagonal (trajectory joining two corners of the billiard, possibly, after reflections from the sides) unfolds to a saddle connection and every periodic trajectory unfolds to a closed regular geodesic.

It is very tempting to use the results described above for the counting problem for the billiard. Unfortunately, the technique elaborated above is not applicable to billiards directly. The problem is that flat surfaces coming from billiards form a subspace of large codimension in any stratum of flat surfaces; in particular, this subspace has measure zero. Our “almost all” technique does not see this subspace.

However, the problems are related in some special cases; see [EMaScm] treating billiard in a rectangle with a barrier. As another illustration we consider billiards in “rectangular polygons”. These results represent the work [AthEZo] which is in progress. We warn the reader that we are extremely informal in the remaining part of this section.

Rectangular Polygons

Figure 36 suggests several examples of *rectangular polygons*. The “polygons” are allowed to have ramification points at the boundary, with restriction that the angles at ramification points are integer multiples of $\pi/2$. Note that we do not identify the side P_5P_6 with a part of the side P_4P_5 in the right polygon. This polygon should be considered with a cut along the side P_5P_6 . The corresponding billiard has a “barrier” along the side P_5P_6 .

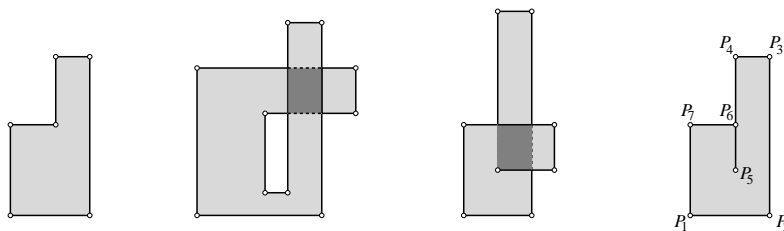


Fig. 36. Rectangular polygons

Formally speaking, by a *rectangular polygon* II we call a topological disc endowed with a flat metric, such that the boundary ∂II is presented by a finite broken line of geodesic segments and such that the angle between any two consecutive sides equals $k\pi/2$, where $k \in \mathbb{N}$.

Consider now our problem for a standard rectangular billiard table (the proportions of the sides do not matter). We emit a trajectory from some corner of the table and want it arrive to another corner after several reflections from the sides.

When our trajectory reflects from a side it is convenient to prolong it as a straight line by making a reflection of the rectangle with respect to the corresponding side (see Katok–Zemliakov construction in Sec. 2.1). Unfolding our rectangular table we tile the plane \mathbb{R}^2 with a rectangular lattice. Our problem can be reformulated as a problem of counting primitive lattice points (see the right part of Fig. 30).

We are emitting our initial trajectory from some fixed corner of the billiard. It means that in the model with a lattice in the plane we are emitting a straight line from the origin inside one of the four quadrants. Thus, we are counting the asymptotics for the number of primitive lattice points in the intersection of a coordinate quadrant with a disc of large radius L centered at the origin. This gives us $1/4$ of the number of all primitive lattice points. Note that in our count we have fixed the initial corner, but we let our trajectory hit any of the remaining three corners. Thus, if we count only those generalized diagonals which are launched from some prescribed corner P_i and arrive to a prescribed corner P_j (different from initial one) we get $1/3$ of the previous number. Hence, the number $N_{ij}(L)$ of generalized diagonals joining P_i with P_j is $1/12$ of the number $N_{cg}(\mathbb{T}^2, L) \sim (1/\zeta(2)) \cdot \pi L^2$ of primitive lattice points, see 22.

In our calculation we assumed that the billiard table has area one. It is clear that asymptotics for our counting function is homogeneous with respect to the area of the table. Adjusting our formula for a rectangular billiard table of the area different from 1 we get the following answer for the number of generalized diagonals of length at most L joining prescribed corner P_i to a prescribed corner P_j different from the first one:

$$N_{ij}(L) \approx \frac{1}{2\pi} \cdot \frac{L^2}{\text{Area of the billiard table}} \quad (26)$$

Now, having studied a model case, we announce two examples of results from [AthEZO] concerning rectangular polygons.

Consider a family of rectangular polygons having exactly $k \geq 0$ angles $3\pi/2$ and all other angles $\pi/2$ (see Fig. 37). Consider a generic billiard table in this family (in the measure-theoretical sense). Fix any two corners $P_i \neq P_j$ having angles $\pi/2$. The number $\tilde{N}_{ij}(L)$ of generalized diagonals of length at most L joining P_i to P_j is approximately the same as for a rectangle:

$$\tilde{N}_{ij}(L) \sim \frac{1}{2\pi} \cdot \frac{L^2}{\text{Area of the billiard table}}$$

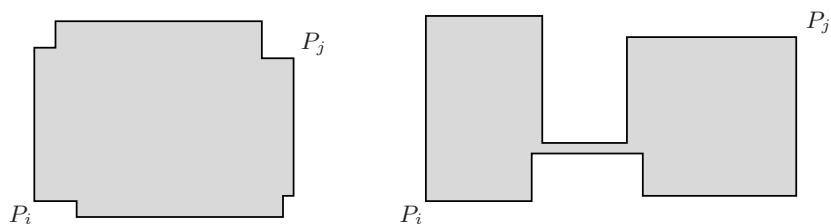


Fig. 37. Family of rectangular polygons of the same geometry and the same area. The shape of these polygons is quite different. Nevertheless for both billiard tables the number of trajectories of length at most L joining the right-angle corner P_i to the right-angle corner P_j is approximately the same as the number of trajectories of length at most L joining two right-angle corners of a rectangle of the same area.

We have to admit that we are slightly cheating here: the equivalence “ \sim ” which we can currently prove is weaker than “ \approx ” in (26); nevertheless, we do not want to go into technical details.

Note that the shape of the polygon within the family may vary quite considerably, see Fig. 37, and this does not affect the asymptotic formula. However, the answer changes drastically when we change the family. For rectangular polygons having several angles of the form $n\pi$ the constant in quadratic asymptotics is more complicated. This is why we do not expect any elementary proof of this formula (our proof involves evaluation of corresponding Siegel–Veech constant).

Actually, naive intuition does not help in counting problems of this type. Consider, for example, an L -shaped billiard table as on Fig. 38.



©Moon Duchin

Fig. 38. L -shaped billiard table

The angle at the vertex P_0 is $3\pi/2$ which is *three* times larger than the angle $\pi/2$ at the other five vertices P_1, \dots, P_5 . However, the number

$$\tilde{N}_{0j}(L) \sim \frac{2}{\pi} \cdot \frac{L^2}{\text{Area of the billiard table}}$$

of generalized diagonals of length at most L joining P_0 to P_j , where $1 \leq j \leq 5$, is *four* times bigger than the number $\tilde{N}_{ij}(L)$ of generalized diagonals joining two corners with the angles $\pi/2$.

7 Volume of Moduli Space

In Sec. 3.4 we defined a volume element in the stratum $\mathcal{H}(d_1, \dots, d_m)$. We used linear volume element in cohomological coordinates $H^1(S, \{P_1, \dots, P_m\}; \mathbb{C})$ normalized in such way that a fundamental domain of the lattice

$$H^1(S, \{P_1, \dots, P_m\}; \mathbb{Z} \oplus \sqrt{-1}\mathbb{Z}) \subset H^1(S, \{P_1, \dots, P_m\}; \mathbb{C})$$

has unit volume. The unit lattice does not depend on the choice of cohomological coordinates, its vertices play the role of *integer points* in the moduli space $\mathcal{H}(d_1, \dots, d_m)$. In Sec. 7.1 we suggest a geometric interpretation of flat surfaces representing integer points of the strata.

Using this interpretation we give an idea for counting the volume (“hyperarea”) of the hypersurface $\mathcal{H}_1(d_1, \dots, d_m) \subset \mathcal{H}(d_1, \dots, d_m)$ of flat surfaces of area one. We apply the strategy which can be illustrated in a model example of evaluation of the area of a unit sphere. We first count the asymptotics for the number $N(R)$ of integer points inside a ball of huge radius R . Clearly $N(R)$ corresponds to the volume of the ball, so if we know the asymptotics for $N(R)$ we know the formula for the volume $\text{Vol}(R)$ of the ball of radius R .

The derivative $\frac{d}{dR} \text{Vol}(R)|_{R=1}$ gives us the area of the unit sphere.

Similarly, to evaluate the “hyperarea of a unit hyperboloid” $\mathcal{H}_1(d_1, \dots, d_m)$ it is sufficient to count the asymptotics for the number of integer points inside a “hyperboloid” $\mathcal{H}_R(d_1, \dots, d_m)$ of huge “radius” R . The role of the “radius” R is played by the positive homogeneous real function $R = \text{area}(S)$ defined on $\mathcal{H}(d_1, \dots, d_m)$.

Note that the volume $\nu(\mathcal{H}_{\leq R}(d_1, \dots, d_m))$ of a domain bounded by the “hyperboloid” $\mathcal{H}_R(d_1, \dots, d_m)$ is a homogeneous function of R of the weight $\dim_{\mathbb{R}} \mathcal{H}(d_1, \dots, d_m)/2$ while the volume of a ball of radius R is a homogeneous function of R of the weight which equals the dimension of the space. This difference in weights explains the factor 2 in the formula below:

$$\begin{aligned} \text{Vol}(\mathcal{H}_1(d_1, \dots, d_m)) &= 2 \frac{d}{dR} \nu(\mathcal{H}_{\leq R}(d_1, \dots, d_m)) \Big|_{R=1} = \\ &= \dim_{\mathbb{R}}(\mathcal{H}_1(d_1, \dots, d_m)) \cdot \nu(\mathcal{H}_{\leq 1}(d_1, \dots, d_m)) \quad (27) \end{aligned}$$

This approach to computation of the volumes was suggested by A. Eskin and A. Okounkov and by M. Kontsevich and the author. However, the straightforward application of this approach, described in Sec. 7.1, gives the values of the volumes only for several low-dimensional strata. The general solution of the problem was found by A. Eskin and A. Okounkov who used in addition powerful methods of representation theory. We give an idea of their method in Sec. 7.2.

7.1 Square-tiled Surfaces

Let us study the geometric properties of the flat surfaces S represented by “integer points” $S \in H^1(S, \{P_1, \dots, P_m\}; \mathbb{Z} \oplus \sqrt{-1}\mathbb{Z})$ in cohomological coordinates. Let ω be the holomorphic one-form representing such flat surface S . Since $[\omega] \in H^1(S, \{P_1, \dots, P_m\}; \mathbb{Z} \oplus \sqrt{-1}\mathbb{Z})$ all periods of ω (including relative periods) belong to $\mathbb{Z} \oplus \sqrt{-1}\mathbb{Z}$. Hence the following map f_ω from the flat surface S to the standard torus $\mathbb{T}^2 = \mathbb{C}/(\mathbb{Z} \oplus \sqrt{-1}\mathbb{Z})$ is well-defined:

$$f_\omega : P \mapsto \left(\int_{P_1}^P \omega \right) \bmod \mathbb{Z} \oplus \sqrt{-1}\mathbb{Z},$$

where P_1 is one of the conical points. It is easy to check that f_ω is a ramified covering, moreover, it has exactly m ramification points, and the ramification points are exactly the zeros P_1, \dots, P_m of ω . Consider the flat torus \mathbb{T}^2 as a unit square with the identified opposite sides. The covering $f_\omega : S \rightarrow \mathbb{T}^2$ induces a tiling of the flat surface S by unit squares. Note that all unit squares are endowed with the following additional structure: we know exactly which edge is top, bottom, right, and left; adjacency of the squares respects this structure in a natural way: we glue vertices to vertices and edges to edges, moreover, the right edge of a square is always identified to the left edge of some square and top edge is always identified to the bottom edge of some square. We shall call a flat surface with such tiling a *square-tiled surface*. We see that the problem of counting the volume of $\mathcal{H}_1(d_1, \dots, d_m)$ is equivalent to the following problem: how many square-tiled surfaces of a given geometric type (determined by number and types of conical singularities) can we construct using at most N unit squares. Say, Fig. 46 gives the list of all square-tiled surfaces of genus $g > 1$ glued from at most 3 squares; they all belong to $\mathcal{H}(2)$.

In terms of the coverings our Problem can be formulated as follows. Consider the ramified coverings $p : S \rightarrow \mathbb{T}^2$ over the standard torus \mathbb{T}^2 . Fix the number m of branching points, and ramification degrees d_1, \dots, d_m at these points. Assume that all ramification points P_1, \dots, P_m project to the same point of the torus \mathbb{T}^2 . Enumerate ramified coverings of any given ramification type having at most $N \gg 1$ sheets. Here pairs of coverings forming commutative diagrams as below are identified:

$$\begin{array}{ccc} S & \longleftrightarrow & S \\ & \searrow & \swarrow \\ & \mathbb{T}^2 & \end{array} \quad (28)$$

Counting of Square-tiled Tori

Let us count the number of square-tiled tori tiled by at most $N \gg 1$ squares. In this case our square-tiled surface has no singularities at all: we have a flat torus tiled with the unit squares in a regular way. Cutting our flat torus by a horizontal waist curve we get a cylinder with a waist curve of length $w \in \mathbb{N}$ and a height $h \in \mathbb{N}$, see Fig. 39. The number of squares in the tiling equals $w \cdot h$. We can reglue the torus from the cylinder with some integer twist t , see Fig. 39. Making an appropriate Dehn twist along the waist curve we can reduce the value of the twist t to one of the values $0, 1, \dots, w - 1$. In other words, fixing the integer perimeter w and height h of a cylinder we get w different square-tiled tori.

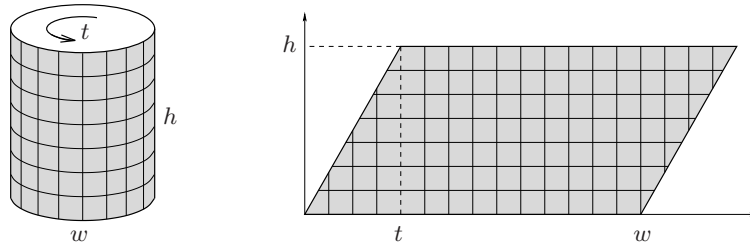


Fig. 39. A square-tiled surface is decomposed into several cylinders. Each cylinder is parametrized by its width (perimeter) w and height h . Gluing the cylinders together we get also a twist parameter t , where $0 \leq t < w$, for each cylinder

Thus the number of square tiled tori constructed by using at most N squares is represented as

$$\nu(\mathcal{H}_{\leq N}(0)) \sim \sum_{\substack{w, h \in \mathbb{N} \\ w \cdot h \leq N}} w = \sum_{\substack{w, h \in \mathbb{N} \\ w \leq \frac{N}{h}}} w \approx \sum_{h \in \mathbb{N}} \frac{1}{2} \cdot \left(\frac{N}{h}\right)^2 = \frac{N^2}{2} \cdot \zeta(2) = \frac{N^2}{2} \cdot \frac{\pi^2}{6}$$

Actually, some of the tori presented by the first sum are equivalent by an affine diffeomorphism, so we are counting them twice, or even several times. Say, the tori $w = 2; h = 1; t = 0$ and $w = 1; h = 2; t = 0$ are equivalent. However, this happens relatively rarely, and this correction does not affect the leading term, so we simply neglect it.

Applying the derivative $2 \frac{d}{dN} \Big|_{N=1}$ (see (27)) we finally get the following value for the volume of the space of flat tori

$$\text{Vol}(\mathcal{H}_1(0)) = \frac{\pi^2}{3}$$

Decomposition of a Square-Tiled Surface into Cylinders

Let us study the geometry of square-tiles surfaces. Note that all leaves of both horizontal and vertical foliation on every square-tiled surface are closed. In particular the union of all horizontal critical leaves (the ones adjacent to conical points) forms a finite graph Γ . The collection P_1, \dots, P_m of conical points forms the set of the vertices of this graph; the edges of the graph are formed by horizontal saddle connections. The complement $S - \Gamma$ is a union of flat cylinders.

For example, for the square-tiled surfaces from Fig. 46 we get the following decompositions into horizontal cylinders. We have one surface composed from a single cylinder filled with closed horizontal trajectories; this cylinder has width (perimeter) $w = 3$ and height $h = 1$. Two other surfaces are composed from two cylinders. The heights of the cylinders are $h_1 = h_2 = 1$, the widths are $w_1 = 1$ and $w_2 = 2$ correspondingly. Observing the two-cylinder surfaces at Fig. 46 we see that they differ by the *twist* parameter t_2 (see Fig. 39) of the wider cylinder: in one case $t_2 = 0$ and in the other case $t_2 = 1$. By construction the width w_i and height h_i of any cylinder are strictly positive integers; the value of the twist t_i is a nonnegative integer bounded by the width of the cylinder: $0 \leq t_i < w_i$.

Separatrix Diagrams

Let us study in more details the graphs Γ of horizontal saddle connections.

We start with an informal explanation. Consider the union of all saddle connections for the horizontal foliation, and add all critical points (zeroes of ω). We obtain a finite oriented graph Γ . Orientation on the edges comes from the canonical orientation of the horizontal foliation. Moreover, graph Γ is drawn on an oriented surface, therefore it carries so called *ribbon structure* (even if we forget about the orientation of edges), i.e. on the star of each vertex P a cyclic order is given, namely the counterclockwise order in which edges are attached to P . The direction of edges attached to P alternates (between directions toward P and from P) as we follow the counterclockwise order.

It is well known that any finite ribbon graph Γ defines canonically (up to an isotopy) an oriented surface $S(\Gamma)$ with boundary. To obtain this surface we replace each edge of Γ by a thin oriented strip (rectangle) and glue these strips together using the cyclic order in each vertex of Γ . In our case surface $S(\Gamma)$ can be realized as a tubular ε -neighborhood (in the sense of transversal measure) of the union of all saddle connections for sufficiently small $\varepsilon > 0$.

The orientation of edges of Γ gives rise to the orientation of the boundary of $S(\Gamma)$. Notice that this orientation is *not* the same as the canonical orientation of the boundary of an oriented surface. Thus, connected components of the boundary of $S(\Gamma)$ are decomposed into two classes: positively and negatively oriented (positively when two orientations of the boundary components coincide and negatively, when they are different). The complement to the tubular ε -neighborhood of Γ is a finite disjoint union of open

cylinders foliated by oriented circles. It gives a decomposition of the set of boundary circles $\pi_0(\partial(S(\Gamma)))$ into pairs of components having opposite signs of the orientation.

Now we are ready to give a formal definition:

A *separatrix diagram* is a finite oriented ribbon graph Γ , and a decomposition of the set of boundary components of $S(\Gamma)$ into pairs, such that

- the orientation of edges at any vertex is alternated with respect to the cyclic order of edges at this vertex;
- there is one positively oriented and one negatively oriented boundary component in each pair.

Notice that ribbon graphs which appear as a part of the structure of a separatrix diagram are very special. Any vertex of such a graph has even degree, and the number of boundary components of the associated surface with boundary is even. Notice also, that in general the graph of a separatrix diagram is *not* planar.

Any separatrix diagram $(\Gamma, \text{pairing})$ defines a closed oriented surface together with an embedding of Γ (up to a homeomorphism) into this surface. Namely, we glue to the surface with boundary $S(\Gamma)$ standard oriented cylinders using the given pairing.

In pictures representing diagrams we encode the pairing on the set of boundary components painting corresponding domains in the picture by some colors (textures in the black-and-white text) in such a way that every color appears exactly twice. We will say also that paired components have the *same color*.

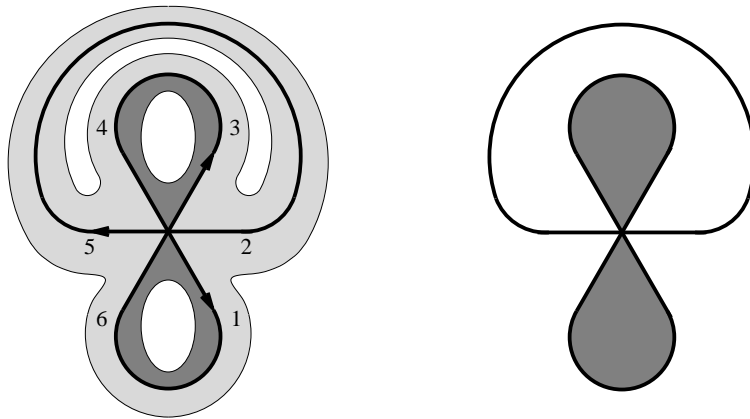


Fig. 40. An example of a separatrix diagram. A detailed picture on the left can be encoded by a schematic picture on the right.

Example. The ribbon graph presented at Figure 40 corresponds to the horizontal foliation of an Abelian differential on a surface of genus $g = 2$. The Abelian differential has a single zero of degree 2. The ribbon graph has two pairs of boundary components.

Any separatrix diagram represents an orientable measured foliation with only closed leaves on a compact oriented surface without boundary. We say that a diagram is *realizable* if, moreover, this measured foliation can be chosen as the horizontal foliation of some Abelian differential. Lemma below gives a criterion of realizability of a diagram.

Assign to each saddle connection a real variable standing for its “length”. Now any boundary component is also endowed with a “length” obtained as sum of the “lengths” of all those saddle connections which belong to this component. If we want to glue flat cylinders to the boundary components, the lengths of the components in every pair should match each other. Thus for every two boundary components paired together (i.e. having the same color) we get a linear equation: “the length of the positively oriented component equals the length of the negatively oriented one”.

Lemma. *A diagram is realizable if and only if the corresponding system of linear equations on “lengths” of saddle connections admits strictly positive solution.*

The proof is obvious.

Example. The diagram presented at Fig. 40 has three saddle connections, all of them are loops. Let p_{16}, p_{52}, p_{34} be their “lengths”. There are two pairs of boundary components. The corresponding system of linear equations is as follows:

$$\begin{cases} p_{34} = p_{16} \\ p_{16} + p_{52} = p_{34} + p_{52} \end{cases}$$

Exercise. Check that two separatrix diagrams at Fig. 41 are realizable, and one – not. Check that there are no other realizable separatrix diagrams for the surfaces from the stratum $\mathcal{H}(2)$. Find all realizable separatrix diagrams for the stratum $\mathcal{H}(1, 1)$.

Counting of Square-tiled Surfaces in $\mathcal{H}(2)$

To consider one more example we count square-tiled surfaces in the stratum $\mathcal{H}(2)$. We have seen that in this stratum there are only two realizable separatrix diagrams; they are presented on the left and in the center of Fig. 41.

Consider those square tiled surfaces from $\mathcal{H}(2)$ which correspond to the left diagram from Fig. 41. In this case the ribbon graph corresponding to the separatrix diagram has single “top” and single “bottom” boundary component, so our surface is glued from a single cylinder. The waist curve of the

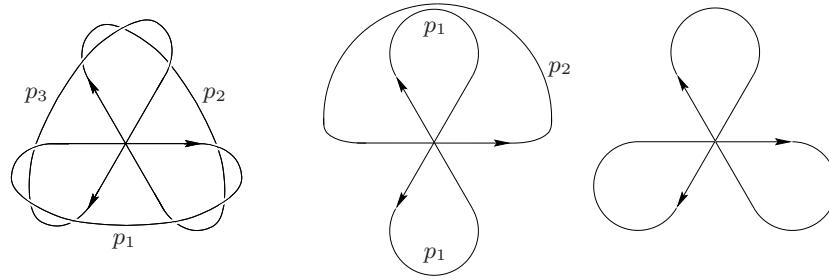


Fig. 41. The separatrix diagrams from left to right a) represent a square-tiled surface glued from one cylinder of width $w = p_1 + p_2 + p_3$; b) represent a square-tiled surface glued from two cylinder of widths $w_1 = p_1$ and $w_2 = p_1 + p_2$; c) do not represent any square-tiled surface

cylinder is of the length $w = p_1 + p_2 + p_3$, where p_1, p_2, p_3 are the lengths of the separatrix loops. As usual, denote the height of the cylinder by h . The twist t of the cylinder has an integer value in the interval $[0, w - 1]$. Thus the number of surfaces of this type of the area bounded by N is asymptotically equivalent to the sum

$$\frac{1}{3} \sum_{\substack{p_1, p_2, p_3, h \in \mathbb{N} \\ (p_1 + p_2 + p_3)h \leq N}} (p_1 + p_2 + p_3) \sim \frac{N^4}{24} \cdot \zeta(4) = \frac{N^4}{24} \cdot \frac{\pi^4}{90}$$

(see more detailed computation in [Zo5]). The coefficient $1/3$ compensates the arbitrariness of the choice of enumeration of p_1, p_2, p_3 preserving the cyclic ordering. Similar to the torus case we have neglected a small correction coming from counting equivalent surfaces several times.

Exercise. Check that for $p_1 = p_2 = p_3 = 1$ all possible values of the twist $t = 0, 1, 2$ give equivalent flat surfaces; see also Fig. 46

Consider now a ribbon graph corresponding to the middle diagram from Fig. 41. It has two “top” and two “bottom” boundary components. Thus, topologically, we can glue in a pair of cylinders in two different ways. However, to have a flat structure on the resulting surface we need to have equal lengths of “top” and “bottom” boundary components. These lengths are determined by the lengths of the corresponding separatrix loops. It is easy to check that one of the two possible gluings of cylinders is forbidden: it implies that one of the separatrix loops has zero length, and hence the surface is degenerate.

The other gluing is realizable. In this case there is a pair of separatrix loops of equal lengths p_1 , see Fig. 41. The square-tiled surface is glued from two cylinders: one having a waist curve $w_1 = p_1$, and the other one having waist curve $w_2 = p_1 + p_2$. Denote the heights and twists of the corresponding

cylinders by h_1, h_2 and t_1, t_2 . The twist of the first cylinder has the value in the interval $[0, w_1 - 1]$; the twist of the second cylinder has the value in the interval $[0, w_2 - 1]$. Thus the number of surfaces of 2-cylinder type of the area bounded by N is asymptotically equivalent to the sum

$$\sum_{\substack{p_1, p_2, h_1, h_2 \\ p_1 h_1 + (p_1 + p_2) h_2 \leq N}} p_1(p_1 + p_2) = \sum_{\substack{p_1, p_2, h_1, h_2 \\ p_1(h_1 + h_2) + p_2 h_2 \leq N}} p_1^2 + p_1 p_2$$

It is not difficult to represent these two sums in terms of the *multiple zeta values* $\zeta(1, 3)$ and $\zeta(2, 2)$ (see detailed computation in [Zo5]). Applying the relations $\zeta(1, 3) = \zeta(4)/4$ and $\zeta(2, 2) = 3\zeta(4)/4$ we get the following asymptotic formula for our sum:

$$\sum_{\substack{p_1, p_2, h_1, h_2 \\ p_1(h_1 + h_2) + p_2 h_2 \leq N}} p_1^2 + p_1 p_2 \sim \frac{N^4}{24} (2 \cdot \zeta(1, 3) + \zeta(2, 2)) = \frac{N^4}{24} \cdot \frac{5}{4} \cdot \zeta(4) = \frac{N^4}{24} \cdot \frac{5}{4} \cdot \frac{\pi^4}{90}$$

Joining the impacts of the two diagrams and applying $2 \cdot \frac{d}{dN} \Big|_{N=1}$ (see (27)) we get the following value for the volume of the stratum $\mathcal{H}(2)$:

$$\text{Vol}(\mathcal{H}_1(2)) = \frac{\pi^4}{120}$$

Separatrix diagrams: more serious reading. Technique of separatrix diagrams is extensively used by K. Strebel in [Str] and in some articles like [KonZo].

7.2 Approach of A. Eskin and A. Okounkov

It is time to confess that evaluation of the volumes of the strata by means of naive counting square-tiled surfaces suggested in the previous section is not efficient in general case. The number of realizable separatrix diagrams grows and it is difficult to express the asymptotics of the sums for individual separatrix diagrams in reasonable terms (say, in terms of multiple zeta values). In general case the problem was solved using the following approach suggested by A. Eskin and A. Okounkov in [EOk].

Consider a square-tiled surface $S \in \mathcal{H}(d_1, \dots, d_m)$. Enumerate the squares in some way. For the square number j let $\pi_r(j)$ be the number of its neighbor to the right and let $\pi_u(j)$ be the number of the square atop the square number j . Consider the commutator $\pi' = \pi_r \pi_u \pi_r^{-1} \pi_u^{-1}$ of the resulting permutations. When the total number of squares is big enough, for most of the squares

Geometrically the resulting permutation π' corresponds to the following path: we start from a square number j , then we move one step right, one step up, one step left, one step down, and we arrive to $\pi'(j)$. When the total number of squares is large, then for majority of the squares such path brings

us back to the initial square; for these values of index j we get $\pi'(j) = j$. However, we may have more than 4 squares adjacent to a conical singularity $P_k \in S$. For the squares adjacent to a singularity the path right-up-left-down does not bring us back to the initial square. It is easy to check that the commutator $\pi' = \pi_r \pi_u \pi_r^{-1} \pi_u^{-1}$ is represented as a product of m cycles of lengths $(d_1 + 1), \dots, (d_m + 1)$ correspondingly.

We conclude that a square-tiled surface $S \in \mathcal{H}(d_1, \dots, d_m)$ can be defined by a pair of permutations π_r, π_u , such that the commutator $\pi_r \pi_u \pi_r^{-1} \pi_u^{-1}$ decomposes into given number m of cycles of given lengths $(d_1 + 1), \dots, (d_m + 1)$. Choosing another enumeration of the squares of the same square-tiled surface S we get two new permutations $\tilde{\pi}_r, \tilde{\pi}_u$. Clearly the permutations in this new pair are conjugate to the initial ones by means of the same permutation ρ responsible for the change of enumeration of the squares: $\tilde{\pi}_r = \rho \pi_r \rho^{-1}, \tilde{\pi}_u = \rho \pi_u \rho^{-1}$.

We see that the problem of enumeration of square-tiled surfaces can be reformulated as a problem of enumeration of pairs of permutations of at most N elements such that their commutator decomposes into a given number of cycles of given lengths. Here the pairs of permutations are considered up to a simultaneous conjugation. This problem was solved by S. Bloch and A. Okounkov by using methods of representation theory. However, it is not directly applicable to our problem. Describing the square-tiled surfaces in terms of pairs of permutations one has to add an additional explicit constraint that the resulting square-tiled surface is *connected*! Taking a random pair of permutations of very large number $N \gg 1$ of elements realizing some fixed combinatorics of the commutator we usually get a disconnected surface!

The necessary correction is quite nontrivial. It was performed by A. Eskin and A. Okounkov in [EOk]. In the further paper A. Eskin, A. Okounkov and R. Pandharipande [EOkPnd] give the volumes of all individual connected components of the strata; see also very nice and accessible survey [E].

For a given square-tiled surface S denote by $Aut(S)$ its automorphism group. Here we count only those automorphisms which isometrically send each square of the tiling to another square. For most of the square-tiled surfaces $Aut(S)$ is trivial; even for those rare square-tiled surfaces, which have nontrivial inner symmetries the group $Aut(S)$ is obviously finite. We complete this section with the following arithmetic Theorem which confirms two conjectures of M. Kontsevich.

Theorem (A. Eskin, A. Okounkov, R. Pandharipande). *For every connected component of every stratum the generating function*

$$\sum_{N=1}^{\infty} q^N \sum_{\substack{N\text{-square-tiled} \\ \text{surfaces } S}} \frac{1}{|Aut(S)|}$$

is a quasimodular form, i.e. a polynomial in Eisenstein series $G_2(q), G_4(q), G_6(q)$.

Volume $\text{Vol}(\mathcal{H}_1^{\text{comp}}(d_1, \dots, d_m))$ of every connected component of every stratum is a rational multiple of π^{2g} , where g is the genus, $d_1 + \dots + d_m = 2g - 2$.

8 Crash Course in Teichmüller Theory

In this section we present the Teichmüller theorem about extremal quasiconformal map and define Teichmüller metric. This enables us to explain finally in what sense the “Teichmüller geodesic flow” (which we initially defined in terms of the action of the subgroup of diagonal matrices in $SL(2, \mathbb{R})$ on flat surfaces) is a *geodesic* flow.

8.1 Extremal Quasiconformal Map

Coefficient of Quasiconformality

Consider a closed topological surface of genus g and two complex structures on it. Let S_0 and S_1 be the corresponding Riemann surfaces. When the complex structures are different there are no conformal maps from S_0 to S_1 . A smooth map $f : S_0 \rightarrow S_1$ (or, being more precise, its derivative Df) sends an infinitesimal circle at $x \in S_0$ to an infinitesimal ellipse, see Fig. 42.

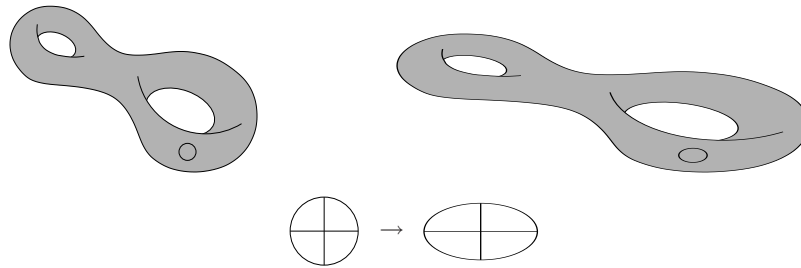


Fig. 42. Quasiconformal map

Coefficient of quasiconformality of f at $x \in S_0$ is the ratio

$$K_x(f) = \frac{a}{b}$$

of demi-axis of this ellipse. *Coefficient of quasiconformality* of f is

$$K(f) = \sup_{x \in S_0} K_x(f)$$

Though S_0 is a compact Riemann surface we use sup and not max since the smooth map f is allowed to have several isolated critical points where $Df = 0$ (and not only $\det(Df) = 0$) and where $K_x(f)$ is not defined.

Half-translation Structure

There is a class of flat metrics which is slightly more general than the *very flat* metrics which we consider in this paper. Namely, we can allow to a flat metric to have the most simple nontrivial linear holonomy which is only possible: we can allow to a tangent vector to change its sign after a parallel transport along some closed loops (see the discussion of linear holonomy in Sec. 1.2).

Surfaces endowed with such flat structures are called *half-translation surfaces*. A holomorphic one-form (also called a holomorphic differential or an Abelian differential) is an analytic object representing a *translation* surface (in our terminology, a *very flat* surface). A holomorphic *quadratic* differential is an analytic object representing a half-translation surface.

In local coordinate w a quadratic differential has the form $q = q(w)(dw)^2$. In other words, the tensor rule for q is

$$q = q(w)(dw)^2 = q(w(w')) \cdot \left(\frac{dw}{dw'}\right)^2 \cdot (dw')^2 \quad (29)$$

under a change of coordinate $w = w(w')$.

One should not confuse $(dw)^2$ with a wedge product $dw \wedge dw$ which equals to zero! It is just a tensor of the type described by the tensor rule (29). In particular, any holomorphic one-form defined in local coordinates as $\omega = \omega(w)dw$ canonically defines a quadratic differential $\omega^2 = \omega^2(w)(dw)^2$.

Reciprocally, a holomorphic quadratic differential $q = q(w)(dw)^2$ locally defines a pair of holomorphic one forms $\pm\sqrt{q(w)}dw$ in any simply-connected domain where $q(w) \neq 0$. However, for a generic holomorphic quadratic differential neither of these 1-forms is globally defined: trying to extend the local form $\omega_+ = \sqrt{q(w)}dw$ along a closed path we may get back with the form $\omega_- = -\sqrt{q(w)}dw$.

Recall that there is a bijection between *very flat* (=translation) surfaces and holomorphic 1-forms. There is a similar bijection between half-translation surfaces and holomorphic quadratic differentials, where similar to the “very flat” case a flat surface corresponding to a quadratic differential is polarized: it is endowed with canonical vertical and horizontal directions. (They can be defined locally using the holomorphic one-forms $\omega_{\pm} = \pm\sqrt{q(w)}dw$.) Note, however, that we cannot distinguish anymore between direction to the North and to the South, or between direction to the East and to the West unless the quadratic differential q is a global square of a holomorphic 1-form ω . In particular, the vertical and horizontal foliations are *nonorientable* for generic quadratic differentials.

Teichmüller Theorem

Choose any two complex structures on a topological surface of genus $g \geq 1$; let S_0 and S_1 be the corresponding Riemann surfaces. Developing ideas of Grötzsch Teichmüller has proved a Theorem which we adapt to our language.

Note that *flat structure* used in the formulation of the Theorem below is slightly more general than one considered in Sec. 1.2 and in Convention 1: it corresponds to a half-translation structure and to a holomorphic *quadratic* differential (see above in this section). In particular, speaking about a flat metric compatible with a given complex structure we mean a flat metric corresponding to a quadratic differential holomorphic in the given complex structure.

Theorem (Teichmüller). *For any pair S_0, S_1 of Riemann surfaces of genus $g \geq 1$ there exist an extremal map $f_0 : S_0 \rightarrow S_1$ which minimizes the coefficient of quasiconformality $K(f)$.*

For this extremal map f_0 the coefficient of quasiconformality is constant on S_0 (outside of a finite collection of singular points)

$$K_x(f_0) = K(f_0) \quad \forall x \in S_0 - \{P_1, \dots, P_m\}$$

One can choose a flat metric (half-translation structure) compatible with the complex structure in which foliation along big (correspondingly small) demi-axis of ellipses is the horizontal (correspondingly vertical) foliation in the flat metric.

In flat coordinates the extremal map f_0 is just expansion-contraction with coefficient \sqrt{K} .

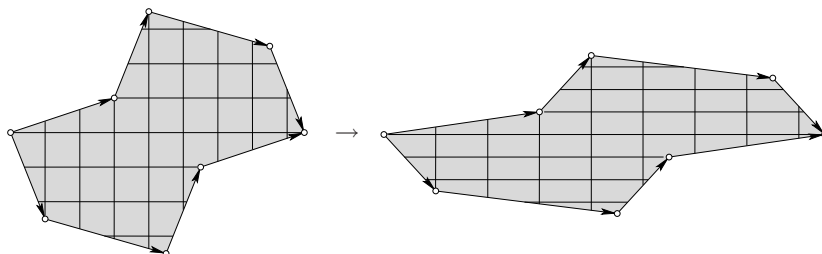


Fig. 43. In flat coordinates the extremal map f_0 is just an expansion-contraction linear map

8.2 Teichmüller Metric and Teichmüller Geodesic Flow

Now everything is ready to define the *Teichmüller metric*. In this metric we measure the distance between two complex structures as

$$\text{dist}(S_0, S_1) = \frac{1}{2} \log K(f_0),$$

where $f_0 : S_0 \rightarrow S_1$ is the extremal map.

It means that a holomorphic quadratic differential defines a direction of deformation of the complex structure and a geodesic in the Teichmüller metric.

Namely, a holomorphic quadratic differential defines a flat metric. A one-parameter family of maps which in the flat coordinates are defined by diagonal matrices

$$g_t = \begin{pmatrix} e^t & 0 \\ 0 & e^{-t} \end{pmatrix}$$

is a one-parameter family of extremal maps, so it forms a Teichmüller geodesic. According to the definition above we have

$$\text{dist}(S_0, g_t S_0) = t.$$

Remark. Note that the Teichmüller metric is not a Riemannian metric but a Finsler metric: it does not correspond to a quadratic form in the tangent space, but just to a norm which depends continuously on the point of the space of complex structures.

It is known that the space of complex structures on a surface of genus $g \geq 2$ has complex dimension $3g - 3$. We have seen, that the space of pairs (complex structure, holomorphic quadratic differential) can be identified with a tangent space to the space of complex structures, in particular, it has complex dimension $6g - 6$. Taking into consideration the functorial behavior of the space of pairs (complex structure, holomorphic quadratic differential) one can check, that it should be identified with a total space of a *cotangent* bundle.

9 Hope for a Magic Wand and Recent Results

This section is devoted to one of the most challenging problems in the theory of flat surfaces: to the problem of complete classification of the closures of *all* orbits of $GL^+(2, \mathbb{R})$ on the moduli spaces of Abelian (and quadratic) differentials. This problem was very recently solved for genus two in the works of K. Calta and of C. McMullen; we give a short survey of their results in Sec. 9.7 and 9.8.

9.1 Complex Geodesics

In this section we are following the geometric approach of C. McMullen developed in [McM2] and [McM3].

Fix the genus g of the surfaces. We have seen in the previous section that we can identify the space \mathcal{Q} of pairs (complex structure, holomorphic quadratic differential) with the total space of the (co)tangent bundle to the moduli space \mathcal{M} of complex structures. Space \mathcal{H} of pairs (complex structure, holomorphic quadratic differential) can be identified with a subspace in \mathcal{Q} of those quadratic differentials, which can be represented as global squares of holomorphic 1-forms. This subspace forms a vector subbundle of special directions in the (co)tangent space which we denote by the same symbol \mathcal{H} .

The “unit hyperboloid” $\mathcal{H}_1 \subset \mathcal{H}$ of holomorphic 1-forms corresponding to flat surfaces of unit area can be considered as a subbundle of *unit vectors* in \mathcal{H} . It is invariant under the Teichmüller geodesic flow – the geodesic flow for the Teichmüller metric.

One can check that an $SL(2; \mathbb{R})$ -orbit in \mathcal{H}_1 descends to a commutative diagram

$$\begin{array}{ccc}
 SL(2; \mathbb{R}) & \longrightarrow & \mathcal{H}_1 \\
 \downarrow & & \downarrow \\
 SL(2; \mathbb{R})/SO(2; \mathbb{R}) \simeq \mathbb{H}^2 & \longrightarrow & \mathcal{M},
 \end{array} \tag{30}$$

which we interpret as

$$\begin{array}{ccc}
 \left(\begin{array}{c} \text{Unit tangent} \\ \text{bundle to} \\ \text{hyperbolic plane} \end{array} \right) & \longrightarrow & \left(\begin{array}{c} \text{Unit tangent} \\ \text{subbundle to} \\ \text{moduli space} \end{array} \right) \\
 \downarrow & & \downarrow \\
 \left(\begin{array}{c} \text{Hyperbolic} \\ \text{plane} \end{array} \right) & \longrightarrow & \left(\begin{array}{c} \text{Moduli} \\ \text{space} \end{array} \right)
 \end{array}$$

Moreover, it can be checked that the map $\mathbb{H}^2 \rightarrow \mathcal{M}$ in this diagram is an isometry with respect to the standard hyperbolic metric on \mathbb{H}^2 and Teichmüller metric on \mathcal{M} . Thus, following C. McMullen it is natural to call the projections of $SL(2; \mathbb{R})$ -orbits to \mathcal{M} (which coincide with the images of \mathbb{H}^2) *complex geodesics*. Another name for these projections is *Teichmüller discs*.

9.2 Geometric Counterparts of Ratner’s Theorem

Though it is proved that the moduli space of complex structures is not a hyperbolic manifold (see [Ma1]) there is a strong hope that with respect to $SL(2, \mathbb{R})$ -action on \mathcal{H} and on \mathcal{Q} the moduli space behaves as if it is.

In this section we present several facts about group actions on homogeneous spaces and several related facts about geodesic submanifolds. We warn the reader that our selection is not representative; it opens only a narrow slit to the fascinating world of interactions of group actions, rigidity, hyperbolic geometry, dynamics and number theory.

We start with an informal formulation of part of Ratner’s Theorem (see much better exposition adopted to our subject in the survey of A. Eskin [E]).

A discrete subgroup Γ of a Lie group G is called a *lattice* if a homogeneous space G/Γ has finite volume.

Theorem (M. Ratner). *Let G be a connected Lie group and U a connected subgroup generated by unipotent elements. Then, for any lattice $\Gamma \subset G$ and any $x \in G/\Gamma$ the closure of the orbit Ux in G/Γ is an orbit of some closed algebraic subgroup of G .*

We would like to point out why this theorem is so remarkably powerful. Considering a dynamical system, even an ergodic one, it is possible to get a lot of information about a generic (in measure-theoretical sense) trajectory. However, usually there are plenty of trajectories having rather particular behavior. It is sufficient to consider geodesic flow on a surface with cusps to find trajectories with closures producing fairly wild sets. Ratner's theorem proves, that the closure of *any* orbit of a unipotent group acting on a homogeneous space is a nice homogeneous space.

Ratner's theorem has numerous important relations with geometry of homogeneous spaces. As an illustration we have chosen a result of N. Shah [Sh] and a generalization of his result for noncompact hyperbolic manifolds obtained by T. Payne [Pa].

Theorem (N. Shah). *In a compact manifold of constant negative curvature, the closure of a totally geodesic, complete (immersed) submanifold of dimension at least 2 is a totally geodesic immersed submanifold.*

Theorem (T. Payne). *Let $f : M_1 \rightarrow M_2$ be a totally geodesic immersion between locally symmetric spaces of noncompact type, with M_2 of finite volume. Then the closure of the image of f is an immersed submanifold. Moreover, when M_1 and M_2 have the same rank, the closure of the image is a totally geodesic submanifold.*

9.3 Main Hope

Main Conjecture and its Possible Applications

If only the moduli space of complex structures \mathcal{M} would be a homogeneous space we would immediately apply the Theorem above to diagram (30) and would solve considerable part of our problems. But it is not. Nevertheless, there is a strong hope for an analogous Theorem.

Problem. *Classify the closures of $GL^+(2, \mathbb{R})$ -orbits in \mathcal{H}_g and in \mathcal{Q}_g . Classify the orbit closures of the unipotent subgroup $\begin{pmatrix} 1 & t \\ 0 & 1 \end{pmatrix}_{t \in \mathbb{R}}$ on \mathcal{H}_g and on \mathcal{Q}_g .*

The following Conjecture is one of the key conjectures in this area.

Conjecture. *The closure $\mathcal{C}(S)$ of a $GL^+(2, \mathbb{R})$ -orbit of any flat surface $S \in \mathcal{H}$ (or $S \in \mathcal{Q}$) is a complex-algebraic suborbifold.*

Remark. We do not discuss here the problems related with possible *compactifications* of the moduli spaces \mathcal{H}_g and \mathcal{Q}_g . A complex-analytic description of a compactification of \mathcal{Q}_g can be found in the papers of J. Fay [Fay] and H. Masur [Ma2].

Recall that according to Theorem of M. Kontsevich (see Sec. 3.6) any $GL^+(2, \mathbb{R})$ -invariant complex suborbifold in \mathcal{H} is represented by an affine subspace in cohomological coordinates. Thus, if the Conjecture above is true, the structure of orbit closures of the action of $GL^+(2, \mathbb{R})$ on \mathcal{H} and on \mathcal{Q} (and of $SL(2, \mathbb{R})$ on \mathcal{H}_1 and on \mathcal{Q}_1) would be as simple as in the case of homogeneous spaces.

We have not discussed the aspects of Ratner's Theorem concerning the measures; it states more than we cited above. Actually, not only orbit closures have a nice form, but also invariant ergodic measures; namely, all such measures are just the natural measures supported on orbits of closed subgroups. Trying to make a parallel with Ratner's Theorem one should extend the Conjecture above to invariant measures.

In the most optimistic hopes the study of an individual flat surface $S \in \mathcal{H}(d_1, \dots, d_m)$ would look as follows. (Frankly speaking, here we slightly exaggerate in our scenario, but after all we are describing the dreams.) To describe all geometric properties of a flat surface S we first find the orbit closure $\mathcal{C}(S) = \overline{GL^+(2, \mathbb{R})S} \subset \mathcal{H}(d_1, \dots, d_m)$ (our optimistic hope assumes that there is an efficient way to do this). Then we consult a (conjectural) classification list and find $\mathcal{C}(S)$ in some magic table which gives all information about $\mathcal{C}(S)$ (like volume, description of cusps, Siegel–Veech constants, Lyapunov exponents, adjacency to other invariant subspaces, etc). Using this information we get answers to all possible questions which one can ask about the initial flat surface S .

Billiards in rational polygons give an example of possible implementation of this optimistic scenario. Fixing angles of the polygon which defines a billiard table we can change the lengths of its sides. We get a family \mathcal{B} of polygons which induces a family $\tilde{\mathcal{B}}$ of flat surfaces obtained by Katok–Zemlyakov construction (see Sec. 2.1). This family $\tilde{\mathcal{B}}$ belongs to some fixed stratum $\tilde{\mathcal{B}} \subset \mathcal{H}(d_1, \dots, d_m)$. However, it has a nontrivial codimension in the stratum, so $\tilde{\mathcal{B}}$ has measure zero and one cannot use ergodic theorem naively to get any information about billiards in corresponding polygons. Having a version of ergodic theorem which treats *all* orbits (like in Ratner's Theorem) presumably it would be possible to get a powerful tool for the study of rational billiards.

Exercise. Consider the family \mathcal{B} of billiard tables as on Fig. 37. Determine the stratum $\mathcal{H}(d_1, \dots, d_m)$ to which belong the corresponding flat surfaces and compute the codimension of the resulting family $\tilde{\mathcal{B}} \subset \mathcal{H}(d_1, \dots, d_m)$.

Content of Remaining Sections

The Conjecture above is trivial for genus one, since in this case the “Teichmüller space of Riemann surfaces of genus one” coincides with an upper half-plane, and the entire space coincides with a single Teichmüller disc (image of \mathbb{H}^2 in diagram (30)).

Very recently C. McMullen proved the Conjecture in genus two [McM2], [McM3], and this is a highly nontrivial result. We give a short report of revolutionary results of K. Calta [Clt] and of C. McMullen [McM2]–[McM6] in Sec. 9.7 below. However, their techniques, do not allow any straightforward generalizations to higher genera: Riemann surfaces of genus two are rather special, in particular, every such surface is hyperelliptic.

In the next two sections 9.4 and 9.5 we try to give an idea of what is known about invariant submanifolds in higher genera (which is an easy task since, unfortunately, little is known).

Having an invariant submanifold $\mathcal{K} \subset \mathcal{H}_g$ (or $\mathcal{K} \subset \mathcal{Q}_g$) in genus g one can construct a new invariant submanifold $\tilde{\mathcal{K}} \subset \mathcal{H}_{\tilde{g}}$ (correspondingly $\tilde{\mathcal{K}} \subset \mathcal{Q}_{\tilde{g}}$) in higher genus $\tilde{g} > g$ replacing every $S \in \mathcal{K}$ by an appropriate ramified covering \tilde{S} over S of some fixed combinatorial type. We do not want to specify here what does a “fixed combinatorial type” mean; what we claim is that having an invariant manifold \mathcal{K} there is some procedure which allows to construct a whole bunch of new invariant submanifolds $\tilde{\mathcal{K}}$ for higher genera $\tilde{g} > g$.

In some cases all quadratic differentials in the invariant submanifold $\tilde{\mathcal{K}}$ obtained by a ramified covering construction from some $\mathcal{K} \subset \mathcal{Q}_g$ might become global squares of Abelian differentials. Hence, using special ramified coverings one can construct $GL^+(2, \mathbb{R})$ -invariant submanifolds $\tilde{\mathcal{K}} \subset \mathcal{H}_{\tilde{g}}$ from invariant submanifolds $\mathcal{K} \subset \mathcal{Q}_g$.

What is really interesting to understand is what invariant manifolds form the “roots” of such constructions. Such invariant manifolds are often called the *primitive* ones.

In the following two sections 9.4 and 9.5 we consider the two extremal classes of primitive invariant submanifolds: the largest ones and the smallest ones. Namely, in Sec. 9.4 we present a classification of connected components of the strata $\mathcal{H}(d_1, \dots, d_m)$. It follows from ergodicity of $SL(2, \mathbb{R})$ -action on $\mathcal{H}_1(d_1, \dots, d_m)$ that the orbit closure of almost any flat surface in $\mathcal{H}(d_1, \dots, d_m)$ coincides with the embodying connected component of $\mathcal{H}(d_1, \dots, d_m)$.

In section 9.5 we consider the smallest possible $GL^+(2, \mathbb{R})$ -invariant submanifolds: those which correspond to closed orbits. Teichmüller discs obtained as projections of such orbits to the moduli space \mathcal{M} of complex structures form the “closed complex geodesics” — Riemann surfaces with cusps.

9.4 Classification of Connected Components of the Strata

In order to formulate the classification theorem for connected components of the strata $\mathcal{H}(d_1, \dots, d_m)$ we need to describe the classifying invariants. There are two of them: *spin structure* and *hyperellipticity*. Both notions are applicable only to part of the strata: flat surfaces from the strata $\mathcal{H}(2d_1, \dots, 2d_m)$ have *even* or *odd spin structure*. The strata $\mathcal{H}(2g-2)$ and $\mathcal{H}(g-1, g-1)$ have special *hyperelliptic connected component*.

Spin Structure

Consider a flat surface S from a stratum $\mathcal{H}(2d_1, \dots, 2d_m)$. Let $\rho : S^1 \rightarrow S$ be a smooth closed path on S ; here S^1 is a standard circle. Note that at any point of the surfaces S we know where is the “direction to the North”. Hence, at any point $\rho(t) = x \in S$ we can apply a compass and measure the direction of the tangent vector \dot{x} . Moving along our path $\rho(t)$ we make the tangent vector turn in the compass. Thus we get a map $G(\rho) : S^1 \rightarrow S^1$ from the parameter circle to the circumference of the compass. This map is called the *Gauss map*. We define the *index* $\text{ind}(\rho)$ of the path ρ as a degree of the corresponding Gauss map (or, in other words as the algebraic number of turns of the tangent vector around the compass) taken modulo 2.

$$\text{ind}(\rho) = \deg G(\rho) \pmod{2}$$

It is easy to see that $\text{ind}(\rho)$ does not depend on parameterization. Moreover, it does not change under small deformations of the path. Deforming the path more drastically we may change its position with respect to conical singularities of the flat metric. Say, the initial path might go on the left of P_k and its deformation might pass on the right of P_k . This deformation changes the $\deg G(\rho)$. However, if the cone angle at P_k is of the type $2\pi(2d_k + 1)$, then $\deg G(\rho) \pmod{2}$ does not change! This observation explains why $\text{ind}(\rho)$ is well-defined for a free homotopy class $[\rho]$ when $S \in \mathcal{H}(2d_1, \dots, 2d_m)$ (and hence, when all cone angles are odd multiples of 2π).

Consider a collection of closed smooth paths $a_1, b_1, \dots, a_g, b_g$ representing a symplectic basis of homology $H_1(S, \mathbb{Z}/2\mathbb{Z})$. We define the *parity of the spin-structure* of a flat surface $S \in \mathcal{H}(2d_1, \dots, 2d_m)$ as

$$\phi(S) = \sum_{i=1}^g (\text{ind}(a_i) + 1) (\text{ind}(b_i) + 1) \pmod{2} \quad (31)$$

Lemma. *The value $\phi(S)$ does not depend on the choice of symplectic basis of cycles $\{a_i, b_i\}$. It does not change under continuous deformations of S in $\mathcal{H}(2d_1, \dots, 2d_m)$.*

Lemma above shows that the parity of the spin structure is an invariant of connected components of strata of those Abelian differentials, which have zeroes of even degrees.

Exercise. Consider two flat surfaces presented at Fig. 44. They are obtained by a surgery which attaches a handle to a flat surface obtained from a regular octagon. Note, however, that the handles are attached in two different ways (see the identifications of vertical sides). Check that both surfaces belong to the same stratum $\mathcal{H}(4)$.

Consider a symplectic basis of cycles of the initial surface (corresponding to the regular octagon) realized by paths which do not pass through the

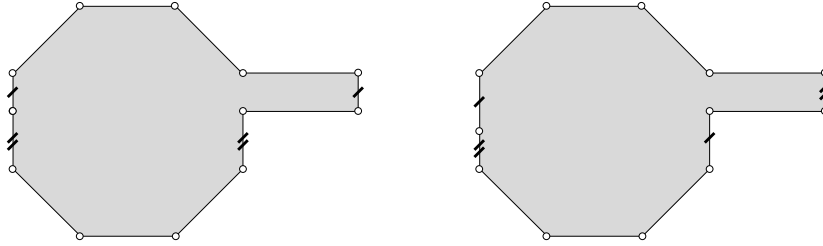


Fig. 44. Attaching a handle to the flat surface $S_0 \in \mathcal{H}(2)$ in two different ways we get two flat surfaces in $\mathcal{H}(4)$ with different parities of spin structure. Hence the resulting flat surfaces live in different connected components of $\mathcal{H}(4)$

conical singularity. Show that a symplectic basis of cycles for each of two new surfaces can be obtained by completion of the initial basis with a pair of cycles a, b representing the attached handle, where the cycle a is the waist curve of the handle. Calculate $\text{ind}(a)$ and $\text{ind}(b)$ for each of two surfaces. Check that $\text{ind}(b)$ are different, and thus our two flat surfaces have different parities of spin structure and hence belong to different connected components of $\mathcal{H}(4)$.

Spin structure: more serious reading. We have hidden under the carpet geometry of the “spin structure” defining the “parity-of-the-spin-structure”. The reader can find details in [KonZo] and in original papers of M. Atiyah [At], J. Milnor [Mil], D. Mumford [Mum] and D. Johnson [J]. Recent paper of C. McMullen [McM4] contains further applications of spin structures to flat surfaces.

Hyperellipticity

A flat surface S may have a symmetry; one specific family of such flat surfaces, which are “more symmetric than others” is of a special interest for us. Recall that there is a one-to-one correspondence between flat surfaces and pairs (Riemann surface M , holomorphic 1-form ω), see Sec. 3.3. When the corresponding Riemann surface is *hyperelliptic* the *hyperelliptic involution* $\tau : M \rightarrow M$ acts on any holomorphic 1-form ω as $\tau^*\omega = -\omega$.

We say that a flat surface S is a *hyperelliptic flat surface* if there is an isometry $\tau : S \rightarrow S$ such that τ is an involution, $\tau \circ \tau = \text{id}$, and the quotient surface S/τ is a topological sphere. In flat coordinates differential of such involution obviously satisfies $D\tau = -\text{Id}$.

Exercise. Check that the flat surface S from Fig. 12 is hyperelliptic, and that the central symmetry of the polygon induces the hyperelliptic involution of S .

In a general stratum $\mathcal{H}(d_1, \dots, d_m)$ hyperelliptic surfaces form a small subspace of nontrivial codimension. However, there are two special strata, namely $\mathcal{H}(2g-2)$ and $\mathcal{H}(g-1, g-1)$, for which hyperelliptic surfaces form entire *hyperelliptic connected components* $\mathcal{H}^{\text{hyp}}(2g-2)$ and $\mathcal{H}^{\text{hyp}}(g-1, g-1)$ correspondingly.

Note that in the stratum $\mathcal{H}(g-1, g-1)$ there are hyperelliptic flat surfaces of two different types. A hyperelliptic involution $\tau S \rightarrow S$ may fix the conical points or might interchange them. It is not difficult to show that for surfaces from the *connected component* $\mathcal{H}^{hyp}(g-1, g-1)$ the hyperelliptic involution *interchanges* the conical singularities.

The remaining family of those hyperelliptic flat surfaces in $\mathcal{H}(g-1, g-1)$, for which the hyperelliptic involution keeps the saddle points fixed, forms a subspace of nontrivial codimension in the complement $\mathcal{H}(g-1, g-1) - \mathcal{H}^{hyp}(g-1, g-1)$. Thus, the hyperelliptic connected component $\mathcal{H}^{hyp}(g-1, g-1)$ does not coincide with the space of all hyperelliptic flat surfaces.

Classification Theorem for Abelian Differentials

Now, having introduced the classifying invariants we can present the classification of connected components of strata of Abelian differentials.

Theorem (M. Kontsevich and A. Zorich). *All connected components of any stratum of Abelian differentials on a curve of genus $g \geq 4$ are described by the following list:*

The stratum $\mathcal{H}(2g-2)$ has three connected components: the hyperelliptic one, $\mathcal{H}^{hyp}(2g-2)$, and two nonhyperelliptic components: $\mathcal{H}^{even}(2g-2)$ and $\mathcal{H}^{odd}(2g-2)$ corresponding to even and odd spin structures.

The stratum $\mathcal{H}(2d, 2d)$, $d \geq 2$ has three connected components: the hyperelliptic one, $\mathcal{H}^{hyp}(2d, 2d)$, and two nonhyperelliptic components: $\mathcal{H}^{even}(2d, 2d)$ and $\mathcal{H}^{odd}(2d, 2d)$.

All the other strata of the form $\mathcal{H}(2d_1, \dots, 2d_m)$ have two connected components: $\mathcal{H}^{even}(2d_1, \dots, 2d_m)$ and $\mathcal{H}^{odd}(2d_1, \dots, 2d_m)$, corresponding to even and odd spin structures.

The stratum $\mathcal{H}(2d-1, 2d-1)$, $d \geq 2$, has two connected components; one of them: $\mathcal{H}^{hyp}(2d-1, 2d-1)$ is hyperelliptic; the other $\mathcal{H}^{nonhyp}(2d-1, 2d-1)$ is not.

All the other strata of Abelian differentials on the curves of genera $g \geq 4$ are nonempty and connected.

In the case of small genera $1 \leq g \leq 3$ some components are missing in comparison with the general case.

Theorem. *The moduli space of Abelian differentials on a curve of genus $g = 2$ contains two strata: $\mathcal{H}(1, 1)$ and $\mathcal{H}(2)$. Each of them is connected and coincides with its hyperelliptic component.*

Each of the strata $\mathcal{H}(2, 2)$, $\mathcal{H}(4)$ of the moduli space of Abelian differentials on a curve of genus $g = 3$ has two connected components: the hyperelliptic one, and one having odd spin structure. The other strata are connected for genus $g = 3$.

Since there is a one-to-one correspondence between connected components of the strata and *extended Rauzy classes* (see Sec. 5.6 and paper [Y] in this

collection) the Classification Theorem above classifies also the extended Rauzy classes.

Classification Theorem for Quadratic Differentials

Note that for any partition $d_1 + \dots + d_m = 2g - 2$ of a positive even integer $2g - 2$ the stratum $\mathcal{H}(d_1, \dots, d_m)$ of Abelian differentials is nonempty. For meromorphic quadratic differentials with at most simple poles there are four *empty* strata! Namely,

Theorem (H. Masur and J. Smillie). *Consider a partition of the number $4g - 4$, where $g \geq 0$ into integers $d_1 + \dots + d_m$ with all $d_j \in \mathbb{N} \cup \{-1\}$. The corresponding stratum $\mathcal{Q}(d_1, \dots, d_m)$ is non-empty with the following four exceptions:*

$$\mathcal{Q}(\emptyset), \mathcal{Q}(1, -1) \text{ (in genus } g = 1) \quad \text{and} \quad \mathcal{Q}(4), \mathcal{Q}(1, 3) \text{ (in genus } g = 2)$$

Classification of connected components of the strata of meromorphic quadratic differentials with at most simple poles was recently obtained by E. Laneeau [Lan].

Theorem (E. Laneeau). *Four exceptional strata $\mathcal{Q}(-1, 9)$, $\mathcal{Q}(-1, 3, 6)$, $\mathcal{Q}(-1, 3, 3, 3)$ and $\mathcal{Q}(12)$ of meromorphic quadratic differentials contain exactly two connected components; none of them hyperelliptic.*

Three series of strata

$$\begin{aligned} \mathcal{Q}(2(g-k) - 3, 2(g-k) - 3, 2k+1, 2k+1) & \quad k \geq -1, g \geq 1, g-k \geq 2 \\ \mathcal{Q}(2(g-k) - 3, 2(g-k) - 3, 4k+2) & \quad k \geq 0, g \geq 1 \text{ and } g-k \geq 1 \\ \mathcal{Q}(4(g-k) - 6, 4k+2) & \quad k \geq 0, g \geq 2 \text{ and } g-k \geq 2 \end{aligned}$$

contain hyperelliptic connected components. The strata from these series in genera $g \geq 3$ and the strata $\mathcal{Q}(-1, -1, 3, 3)$, $\mathcal{Q}(-1, -1, 6)$ in genus $g = 2$ contain exactly two connected components; one of them – hyperelliptic, the other one – not.

The remaining strata from these series, namely, $\mathcal{Q}(1, 1, 1, 1)$, $\mathcal{Q}(1, 1, 2)$, $\mathcal{Q}(2, 2)$ in genus $g = 2$ and $\mathcal{Q}(1, 1, -1, -1)$, $\mathcal{Q}(-1, -1, 2)$ in genus $g = 1$ coincide with their hyperelliptic connected component.

All other strata of meromorphic quadratic differentials with at most simple poles are connected.

Recall that having a meromorphic quadratic differential with at most simple poles one can associate to it a surface with a flat metric which is slightly more general than our usual *very* flat metric (see Sec. 8.1 for a discussion of half-translation structures).

It is easy to verify whether a half-translation surface belongs to a hyperelliptic component or not. However, currently there is no simple and efficient way to distinguish half-translation surfaces from the four exceptional components.

Problem. Find an invariant of the half-translation structure which would be easy to evaluate and which would distinguish half-translation surfaces from different connected components of the four exceptional strata $\mathcal{Q}(-1, 9)$, $\mathcal{Q}(-1, 3, 6)$, $\mathcal{Q}(-1, 3, 3, 3)$ and $\mathcal{Q}(12)$.

Currently there are two ways to determine to which of the two connected components of an exceptional stratum belongs a flat surface S .

The first approach suggests to find a “generalized permutation” for an analog of the first return map of the vertical flow to a horizontal segment and then to find it in one of the two extended Rauzy classes (see Sec. 5.6) corresponding to two connected components. Note, however, that already for the stratum $\mathcal{Q}(-1, 9)$ the corresponding Rauzy classes contain 97 544, and 12 978 generalized permutations; the Rauzy classes for the components of $\mathcal{Q}(12)$ contain already 894 117 and 150 457 elements.

In the second approach one studies configurations of saddle connections (see Sec. 6.4) on the surface S and tries to find a configuration which is forbidden for one of the two connected components of the corresponding stratum.

For example, for surfaces from one of the two connected components of $\mathcal{Q}(-1, 9)$ as soon as we have a saddle connection joining the simple pole with the zero we necessarily have a closed geodesic going in the same direction. Thus, if we manage to find on a surface $S \in \mathcal{Q}(-1, 9)$ a saddle connection which is not accompanied by a parallel closed geodesic, S belong to the other connected component of $\mathcal{Q}(-1, 9)$.

9.5 Veech Surfaces

For almost every flat surface S in any stratum $\mathcal{H}_1(d_1, \dots, d_m)$ the orbit $SL(2, \mathbb{R}) \cdot S$ is dense in the stratum and for any $g_1 \neq g_2 \in SL(2, \mathbb{R})$ we have $g_1 S \neq g_2 S$. However, some flat surfaces have extra symmetries. When a flat surface S_0 has an affine automorphism, i.e. when for some $g_0 \in SL(2, \mathbb{R})$ we get $g_0 S = S$ the orbit of S_0 is smaller than usual.

The stabilizer $Stab(S) \in SL(2; \mathbb{R})$, that is a subgroup of those $g \in SL(2, \mathbb{R})$ for which $gS = S$, is called the *Veech group* of the flat surface S and is denoted $SL(S)$. In representation of the flat surface S in terms of a pair (Riemann surface X , holomorphic 1-form ω on it) the Veech group is denoted as $SL(X, \omega)$ following the notation of C. McMullen [McM2].

Some exceptional flat surfaces S possess very large group of symmetry and their orbits are very small. The flat surfaces having the largest possible symmetry group are called *Veech surfaces*. More precisely, a flat surface is called a *Veech surface* if its Veech group $SL(S)$ is a lattice in $SL(2, \mathbb{R})$ (that is the quotient $SL(2, \mathbb{R})/SL(S)$ has finite volume).

Theorem (J. Smillie). An $SL(2, \mathbb{R})$ -orbit of a flat surface S is closed in $\mathcal{H}_1(d_1, \dots, d_m)$ if and only if S is a Veech surface.

Forgetting polarization (direction to the “North”) of a flat surface we get a *Teichmüller disc* of S (see (30) and the comments below it)

$$SO(2, \mathbb{R}) \backslash SL(2, \mathbb{R}) / SL(S) = \mathbb{H} / SL(S)$$

A flat surface S is a Veech surface if its Teichmüller disc $\mathbb{H}^2 / SL(S)$ has finite volume. However, even for a Veech surface the Teichmüller disc is never compact: it necessarily contains at least one cusp. The Teichmüller discs of Veech surfaces can be considered as *closed complex geodesics* (see discussion at the end of Sec. 9.1).

Consider an elementary example. As a flat surface take a flat torus obtained from a unit square. Fig. 45 shows why the element $g_+ = \begin{pmatrix} 1 & 1 \\ 0 & 1 \end{pmatrix} \in SL(2, \mathbb{Z})$ belongs to a stabilizer of S .

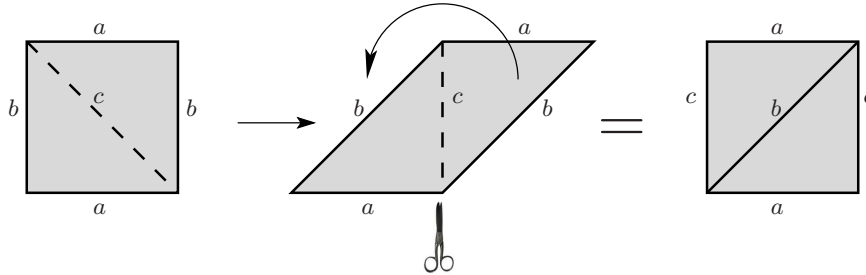


Fig. 45. This linear transformation belongs to the Veech group of \mathbb{T}^2

Similarly the element $g_- = \begin{pmatrix} 1 & 0 \\ 0 & 1 \end{pmatrix} \in SL(2, \mathbb{R})$ also belongs to the Veech group $SL(\mathbb{T}^2)$ of \mathbb{T}^2 . Since the group $SL(2, \mathbb{Z})$ is generated by g_+ and g_- we conclude that $SL(2, \mathbb{Z}) \subset SL(\mathbb{T}^2)$. It is easy to check that, actually, $SL(2, \mathbb{Z}) = SL(\mathbb{T}^2)$. As the Teichmüller disc of \mathbb{T}^2 we get the modular curve $\mathbb{H}^2 / SL(2, \mathbb{Z})$ (see Fig. 13) which, actually, coincides with the moduli space of complex structures on the torus.

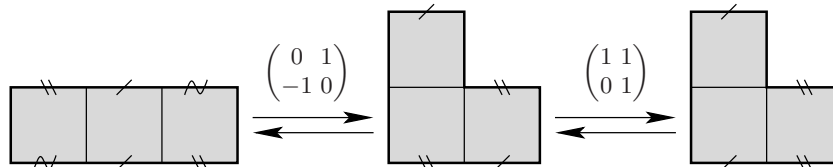


Fig. 46. There are three 3-square-tiled surfaces in $\mathcal{H}(2)$. Our picture shows that they all belong to the same $SL(2; \mathbb{Z})$ -orbit

Consider a slightly more complicated example.

Exercise. Verify that square-tiled surfaces presented at Fig. 46 belong to the stratum $\mathcal{H}(2)$. Show that there are no other 3-square-tiled surfaces. Verify that the linear transformations indicated at Fig. 46 act as it is described on the Figure; check that the surfaces belong to the same $SL(2, \mathbb{R})$ -orbit. Find Veech groups of these three surfaces. Show that these flat surfaces are Veech surfaces. Verify that the corresponding Teichmüller disc is a triple cover over the modular curve (see Fig. 47).

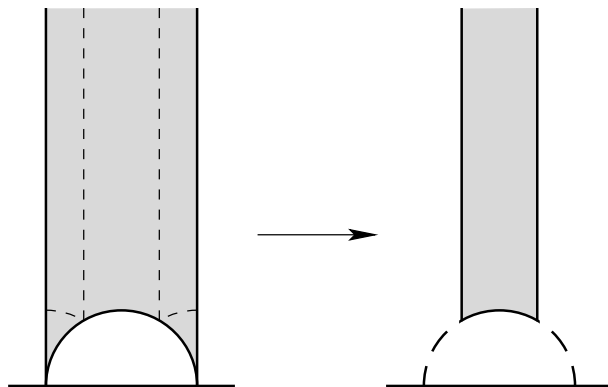


Fig. 47. Teichmüller discs of a 3-square-tiled surface is a triple cover over the modular curve

Primitive Veech Surfaces

It is not difficult to generalize the Exercise above and to show that any *square-tiled surface* (see Sec. 7.1) is necessarily a Veech surface.

A square-tiled surface is a ramified covering over a flat torus, such that all ramification points project to the same point on the flat torus, which is a Veech surface. One can generalize this observation. Having a Veech surface S one can construct a ramified covering $\tilde{S} \rightarrow S$ such that all ramification points on \tilde{S} project to conical singularities on S . One can check that any such \tilde{S} is a Veech surface. Thus, having a Veech surface we can construct a whole bunch of Veech surfaces in higher genera.

Veech surfaces which cannot be obtained from simpler Veech surfaces by the covering construction are called *primitive*. For a long time (and till recent revolution in genus two, see Sec. 9.7, the list of known primitive Veech surfaces was very short. Very recently C. McMullen has found infinitely many Veech surfaces in genera 3 and 4 as well, see [McM7]. All other known primitive Veech surfaces of genus $g > 2$ can be obtained by Katok–Zemlyakov construction (see Sec. 2.1) from triangular billiards of the first three types in the list below:

$$\begin{aligned}
& \left(\frac{\pi}{n}, \frac{n-1}{2n} \pi, \frac{n-1}{2n} \pi \right), \text{ for } n \geq 6 && \text{(discovered by W. Veech)} \\
& \left(\frac{\pi}{n}, \frac{\pi}{n}, \frac{n-2}{n} \pi \right), && \text{for } n \geq 7 \text{ (discovered by W. Veech)} \\
& \left(\frac{\pi}{n}, \frac{\pi}{2n}, \frac{2n-3}{2n} \pi \right), && \text{for } n \geq 4 \text{ (discovered by Ya. Vorobets)} \\
& \left(\frac{\pi}{3}, \frac{\pi}{4}, \frac{5\pi}{12} \right) && \text{(discovered by W. Veech)} \\
& \left(\frac{\pi}{3}, \frac{\pi}{5}, \frac{7\pi}{15} \right) && \text{(discovered by Ya. Vorobets)} \\
& \left(\frac{2\pi}{9}, \frac{3\pi}{9}, \frac{4\pi}{9} \right) && \text{(discovered by R. Kenyon} \\
& && \text{and J. Smillie)} \\
& \left(\frac{\pi}{3}, \frac{\pi}{12}, \frac{7\pi}{12} \right) && \text{(discovered by W. P. Hooper)}
\end{aligned}$$

— The flat surface corresponding to the isosceles triangle with the angles $\pi/n, (n-1)\pi/(2n), (n-1)\pi/(2n)$ belongs to the hyperelliptic component $\mathcal{H}^{hyp}(2g-2)$ when $n = 2g$ and to the hyperelliptic component $\mathcal{H}^{hyp}(g-1, g-1)$ when $n = 2g + 1$. The surface can be unwrapped to the regular $2n$ -gon with opposite sides identified by parallel translations, see Fig. 21.

— The flat surface corresponding to the isosceles triangle with the angles $\pi/n, \pi/n, (n-2)\pi/(2n)$ belongs to the hyperelliptic component $\mathcal{H}^{hyp}(2g-2)$ when $n = 2g + 1$ and to the hyperelliptic component $\mathcal{H}^{hyp}(g-1, g-1)$ when $n = 2g + 2$. The surface can be unwrapped to a pair of regular n -gons glued by one side. Each side of one polygon is identified by a parallel translation with the corresponding side of the other polygon, see Fig. 7.

— The flat surface corresponding to the obtuse triangle with the angles $\pi/n, \pi/(2n), (2n-3)\pi/(2n)$ belongs to one of two nonhyperelliptic components of the stratum $\mathcal{H}(2g-2)$ where $n = g + 1$.

— The flat surface corresponding to the acute triangle $\pi/3, \pi/4, 5\pi/12$ belongs to the nonhyperelliptic component $\mathcal{H}^{odd}(4)$; here $g = 3$.

— The flat surface corresponding to the acute triangle $\pi/3, \pi/5, 7\pi/15$ belongs to the nonhyperelliptic component $\mathcal{H}^{even}(6)$; here $g = 4$.

— The flat surface corresponding to the acute triangle $2\pi/9, 3\pi/9, 4\pi/9$ belongs to the stratum $\mathcal{H}(3, 1)$; here $g = 3$.

— The flat surface corresponding to the obtuse triangle $\pi/3, \pi/12, 7\pi/12$ belongs to the stratum $\mathcal{H}(6)$; here $g = 4$ (the information that this is a Veech surface is taken from [McM7]).

The details on unwrapping of these surfaces and on cylinder decompositions of some of them can be found in the paper of Ya. Vorobets [Vb1].

It is proved that unwrapping triangular billiards in other acute, rectangular or isosceles triangles does not give new Veech surfaces in genera $g > 2$ (see [KenS], [Pu], [Vb1] and further references in these papers). For obtuse triangles the question is open.

We discuss genus $g = 2$ separately in the next section: very recently K. Calta [Clt] and C. McMullen [McM2] have found a countable family of primitive Veech surfaces in the stratum $\mathcal{H}(2)$ and proved that the list is complete. However, even in genus $g = 2$ the situation with the stratum $\mathcal{H}(1, 1)$ is drastically different: using the results of M. Moeller [Mo1]–[Mo3] very recently C. McMullen has proved [McM6] the following result.

Theorem (C. McMullen). *The only primitive Veech surface in the stratum $\mathcal{H}(1, 1)$ is the surface represented by the regular decagon with identified opposite sides.*

Thus, it is not clear, what one should expect as a solution of the following general problem.

Problem. *Find all primitive Veech surfaces.*

An algebro-geometric approach to Veech surfaces suggested by M. Möller in [Mo1] and [Mo2] might help to shed some light on this Problem.

Veech surfaces: more serious reading. I recommend the survey paper [HuSdt5] of P. Hubert and T. Schmidt as an introduction to Veech surfaces. A canonical reference for square-tiled surfaces (also called *arithmetic Veech surfaces*) is the paper of E. Gutkin and C. Judge [GuJg]. More information about Veech surfaces can be found in the pioneering paper of W. Veech [Ve7] and in the paper of Ya. Vorobets [Vb1]. For the most recent results concerning Veech groups and geometry of the Teichmüller discs see the original papers of P. Hubert and T. Schmidt [HuSdt1], [HuSdt2], [HuSdt3], [HuSdt4], of C. McMullen [McM1], [McM7] and of P. Hubert and S. Lelièvre [HuLe1], [HuLe2].

9.6 Kernel Foliation

In this section we describe some natural holomorphic foliation on the moduli space of Abelian differentials. In higher genera little is known about this foliation (though it seems to be worth of study). We use this foliation in the next section to describe $GL(2, \mathbb{R})$ -invariant submanifolds of “intermediate type” discovered by K. Calta and by C. McMullen in genus two.

We have seen that any stratum $\mathcal{H}(d_1, \dots, d_m)$ can be locally parameterized by a collection of basic *relative periods* of the holomorphic one-form ω , or, in other words, that a neighborhood $\mathcal{U}([\omega]) \subset H^1(S; \{P_1, \dots, P_m\}; \mathbb{C})$ gives a local chart in $\mathcal{H}(d_1, \dots, d_m)$.

Let $S \in \mathcal{H}(1, 1)$. Let closed paths a_1, a_2, b_1, b_2 represent a basis of cycles in $H_1(S; \mathbb{Z})$. Any path c joining conical singularities P_1 and P_2 represents a *relative cycle* in $H_1(S, \{P_1, P_2\}; \mathbb{Z})$. Let $A_1, A_2, B_1, B_2, C \in \mathbb{C}$ be the *periods* of ω : the integrals of ω over a_1, a_2, b_1, b_2, c correspondingly.

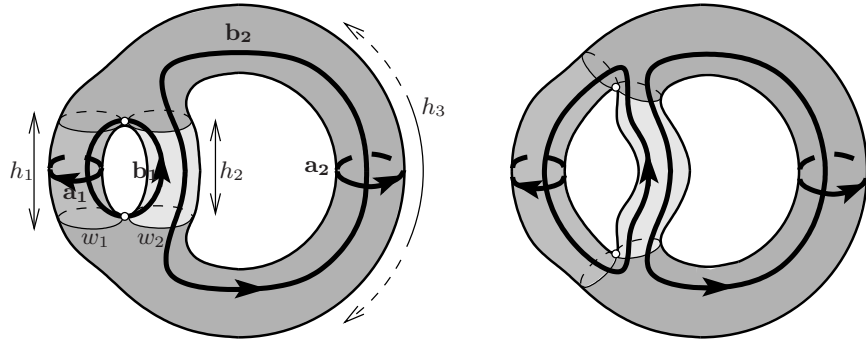


Fig. 48. A deformation of a flat surface inside the kernel foliation keeps the absolute periods unchanged

Example. The collection of cycles $a_i, b_i, i = 1, 2$, on the surfaces from Fig. 48 represent a basis of cycles in $H_1(S; \mathbb{Z})$. All horizontal geodesics on these surfaces are closed; each surface can be decomposed into three cylinders filled with horizontal geodesics. Let $w_1, w_2, w_3 = w_1 + w_2$ be the widths (perimeters) of these cylinders; h_1, h_2, h_3 be their heights; t_1, t_2, t_3 their twists, see Fig. 39. It is easy to check that

$$\begin{aligned} A_1 &= \int_{a_1} \omega = -w_1 & B_1 &= \int_{b_1} \omega = (t_1 - t_2) + \sqrt{-1}(h_2 - h_1) \\ A_2 &= \int_{a_2} \omega = -(w_1 + w_2) & B_2 &= \int_{b_2} \omega = (t_2 + t_3) - \sqrt{-1}(h_2 + h_3) \end{aligned}$$

The *kernel foliation* in $\mathcal{H}(1, 1)$ is the foliation defined in local coordinates by equations

$$\begin{cases} A_1 = \text{const}_{11} \\ A_2 = \text{const}_{21} \end{cases} \quad \begin{cases} B_1 = \text{const}_{12} \\ B_2 = \text{const}_{22} \end{cases}$$

In other words, this is a foliation which is obtained by fixing *all* absolute periods and changing the relative period $C = \int_{P_1}^{P_2} \omega$. Similarly, the *kernel foliation* in arbitrary stratum $\mathcal{H}(d_1, \dots, d_m)$ is a foliation which in cohomological coordinates is represented by parallel complex $(m-1)$ -dimensional affine subspaces obtained by changing all relative periods while fixing the absolute ones.

Passing to a finite cover over $\mathcal{H}(d_1, \dots, d_m)$ we can assume that all zeroes P_1, \dots, P_m are *named* (i.e. having two zeroes P_j, P_k of same degrees, we know exactly which of the two is P_j and which is P_k). Now we can fix an arbitrary subcollection of zeroes and define a kernel “subfoliation” along relative periods corresponding to chosen subcollection.

Recall that the area of a flat surface is expressed in terms of the absolute periods (see Riemann bilinear relation in Table 1 in Sec. 3.3). Thus, moving along leaves of kernel foliation we do not change the area of the surface. In

particular, we can consider the kernel foliation as a foliation of the “unit hyperboloid” $\mathcal{H}_1(d_1, \dots, d_m)$.

Exercises on Kernel Foliation

Exercise. To deform the flat surface on the left of Fig. 48 along the kernel foliation we have to keep all A_1, A_2, B_1, B_2 unchanged. Hence, we cannot change the widths (perimeters) of the cylinders, since they are expressed in terms of A_1 and A_2 . Increasing the height of the second cylinder by ε we have to *increase* the height of the first cylinder by the same amount ε to keep $B_1 = (t_1 - t_2) + \sqrt{-1}((h_2 + \varepsilon) - (h_1 + \varepsilon))$ unchanged; we also have to *decrease* the height h_3 of the third cylinder by ε to preserve the value of B_2 . Similarly, *increasing* the twist t_1 by δ we have to *increase* the twist t_2 by the same amount δ and to *decrease* t_3 by δ .

Exercise. It is convenient to consider the kernel foliation in the total moduli space \mathcal{H}_g of all holomorphic 1-forms without subdivision of \mathcal{H}_g into strata $\mathcal{H}(d_1, \dots, d_m)$, where $\sum_j d_j = 2g - 2$. In particular, to deform a surface $S \in \mathcal{H}(2) \subset \mathcal{H}_2$ along the kernel foliation we have to break the double zero into two simple zeroes preserving the absolute periods. The corresponding surgery is presented at Fig. 31.

The leaves of the kernel foliation are naturally endowed with a flat structure, which has conical singularities at the points of intersection of the leaf with the smaller strata and with degenerate strata.

Assuming that the zeroes P_1, P_2 of a surface $S \in \mathcal{H}(1, 1)$ are *named* show that the intersection of the kernel foliation with the stratum $\mathcal{H}(2)$ corresponds to a conical point with the cone angle 6π , while the intersections with the two strata of degenerate flat surfaces (determine which ones) are just the regular points of the flat structure.

In the exercise below we use a polygonal representation of a flat surface (compare to Fig. 8 in the paper [Clt] of K. Calta).

Exercise. Consider a regular decagon. Imagine that there are springs inside its sides so that we can shrink or expand the sides keeping them straight segments. Imagine that we hammer a nail in the center of each side. Though the centers of the sides are now fixed our decagon is still flexible: we can pull a vertex and the whole frame will follow, see Fig. 49b. We assume that under any such deformation each nail stays exactly in the middle of the corresponding side.

Prove that the deformed polygon is again centrally symmetric with the same center of symmetry. Prove that the opposite sides of the deformed polygon are parallel and have equal length. Prove that the resulting flat surface lives in the same leaf of the kernel foliation. Show that the “nails” (the centers of the sides) and the center of symmetry are the Weierstrass points of the corresponding Riemann surface (fixed points of the hyperelliptic involution).

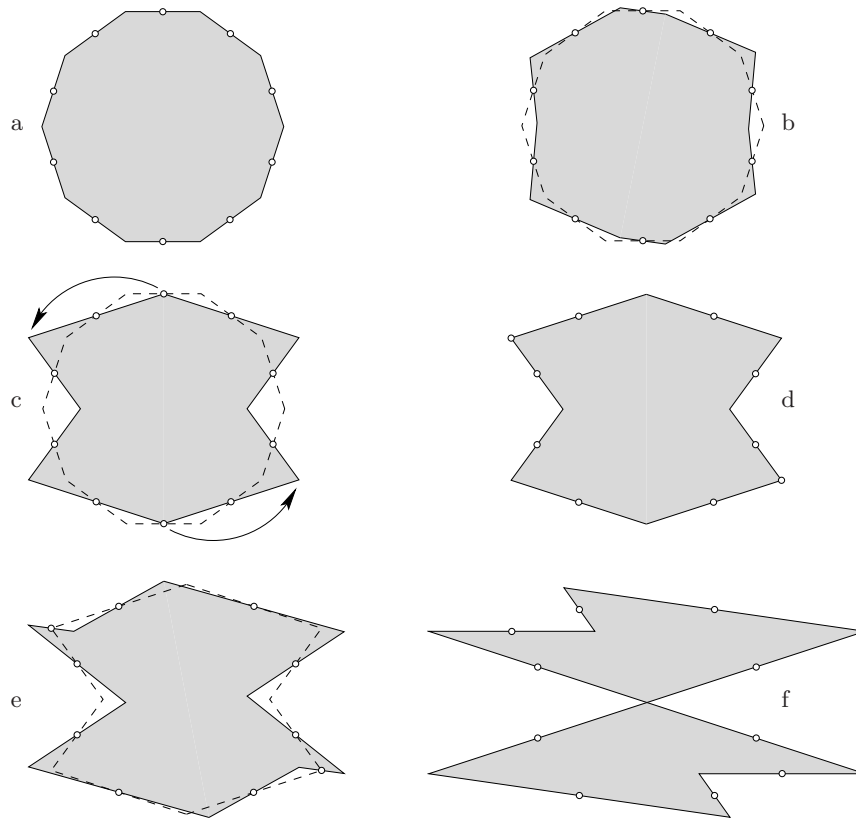


Fig. 49. This cartoon movie represents a path living inside a leaf of the kernel foliation. When at the stage c it lands to a surface from the stratum $\mathcal{H}(2)$ we remove the nails from one pair of vertices and hammer them in the other symmetric pair of vertices (stage d). Then we continue the trip inside the kernel foliation

Move a vertex towards the center of the side which this vertex bounds. The side becomes short (see the upper side on Fig. 49b) and finally contracts to a point (Fig. 49c). What flat surface do we get?

Show that the deformation presented at Fig. 49c brings us to a surface S_0 in the stratum $\mathcal{H}(2)$. Remove the pair of clues, which is hammered at the vertices of the resulting octagon. Hammer them to another pair of symmetric vertices (see Fig. 49d). We can declare that we have a new centrally-symmetric decagon with a pair of sides of zero lengths. Stretching this pair of sides and making them have positive length (see Fig. 49e) we continue our trip inside the kernel foliation. Show that for a given small value $\mathbf{v} \in \mathbb{C}$ of the saddle connection joining two conical singularities, there are exactly three different surfaces obtained as a small deformation of the surface $S_0 \in \mathcal{H}(2)$ as on

Fig. 49c along the leaf of the kernel foliation and having a saddle connection \mathbf{v} . (Use previous Exercise and Fig. 31.)

Following our path in the kernel foliation we get to the surface S_1 as on Fig. 49f. Is this surface singular? To what stratum (singular stratum) it belongs?

Compact Leaves of the Kernel Foliation

Let us show that the leaf \mathcal{K} of the kernel foliation passing through a square-tiled surface $S(\omega_0)$ of genus two is a compact square-tiled surface. To simplify notations suppose that the absolute periods of the holomorphic 1-form ω_0 , representing the flat surface $S(\omega_0)$, generate the entire integer lattice $\mathbb{Z} + \sqrt{-1}\mathbb{Z}$.

Consider the “relative period” map $p : \mathcal{K} \rightarrow \mathbb{T}^2$ from the corresponding leaf \mathcal{K} of the kernel foliation containing $S(\omega_0)$ to the torus. The map p associates to a flat surface $S(\omega) \in \mathcal{K}$ the relative period C taken modulo integers,

$$\mathcal{K} \ni S(\omega) \xrightarrow{p} C = \int_{P_1}^{P_2} \omega \pmod{\mathbb{Z} + \sqrt{-1}\mathbb{Z}} \in \mathbb{C}/(\mathbb{Z} + \sqrt{-1}\mathbb{Z}) = \mathbb{T}^2$$

Since the flat surface $S(\omega)$ belongs to the same leaf \mathcal{K} as the square-tiled surface $S(\omega_0) \in \mathcal{K}$, the absolute periods of ω are the same as the ones of ω_0 , and hence the integral above taken modulo integers does not depend on the path on $S(\omega)$ joining P_1 and P_2 . It is easy to check that the map p is a finite ramified covering over the torus \mathbb{T}^2 , and thus the leaf \mathcal{K} is a square-tiled surface.

Those flat surfaces $S(\omega) \in \mathcal{K}$, which have integer relative period $C \in \mathbb{Z} + \sqrt{-1}\mathbb{Z}$, have *all* periods in $\mathbb{Z} + \sqrt{-1}\mathbb{Z}$. Hence, these flat surfaces are square-tiled. Since $S(\omega)$ and $S(\omega_0)$ have the same area, the number N of squares tiling $S(\omega)$ and $S(\omega_0)$ is the same. Thus, \mathcal{K} has a structure of a square-tiled surface such that the vertices of the tiling are represented by N -square-tiled surfaces $S(\omega) \in \mathcal{K}$.

To discuss the geometry of \mathcal{K} we need to agree about enumeration of zeroes P_1, P_2 of a surface $S \in \mathcal{H}(1, 1)$. We choose the convention where the zeroes are *named*. That is, given two zeroes of order 1 we know which of them is P_1 and which of them is P_2 . Under this convention the square-tiled surface \mathcal{K} is a translation surface; it is represented by a *holomorphic one-form*. (Accepting the other convention we would obtain the quotient of \mathcal{K} over the natural involution exchanging the names of the zeroes. In this latter case the zeroes of $S \in \mathcal{H}(1, 1)$ are not distinguishable; the leaf of the kernel foliation gives a flat surface represented by a *quadratic differential*.)

The lattice points of the square-tiled surface \mathcal{K} are represented by N -square-tiled surfaces $S \in \mathcal{K}$ of several types. We have the lattice points represented by N -square tiled surfaces from $\mathcal{H}(1, 1)$. These points are the regular points of the flat metric on \mathcal{K} .

There are points of intersection of \mathcal{K} with $\mathcal{H}(2)$. Such point $S(\omega) \in \mathcal{K} \cap \mathcal{H}(2)$ is always represented by a square-tiled surface, and hence gives a vertex of the tiling of \mathcal{K} . We have seen (see Fig. 31) that given a surface $S(\omega) \in \mathcal{H}(2)$ and a small complex period C one can construct three different flat surfaces $S(\omega_1), S(\omega_2), S(\omega_3) \in \mathcal{H}(1, 1)$ with the same absolute periods as ω and with the relative period C . Thus, the points $S(\omega) \in \mathcal{K} \cap \mathcal{H}(2)$ correspond to conical points of \mathcal{K} with the cone angles $3 \cdot 2\pi$ when the zeroes are named (and with the cone angle 3π , when they are not named). The total number of such points was computed in the paper of A. Eskin, H. Masur and M. Schmol [EMaScm]; it equals

$$\text{number of conical points on } \mathcal{K} = \frac{3}{8}(N - 2)N^2 \prod_{p|N} \left(1 - \frac{1}{p^2}\right) \quad (32)$$

There remain vertices of the tiling of \mathcal{K} represented by degenerate square-tiled surfaces $S(\omega)$. It is not difficult to show that these points are regular for the flat metric on $\mathcal{K}(\omega)$ when the zeroes are named. (They correspond to conical singularities with the cone angle π , when the zeroes are not named). The degenerate N -square-tiled surfaces $S(\omega)$ are of two types. It might be an N -square-tiled torus with two points of the tiling identified. It might be a pair of square-tiled tori with a vertex of the tiling on one torus identified with a vertex of the tiling on the other torus. Here the total number of squares used to tile these two tori is N . The total number of the vertices of the tiling of \mathcal{K} of this type is computed in the paper [Schl1]; it equals

$$\text{number of special points on } \mathcal{K} = \frac{1}{24}(5N + 6)N^2 \prod_{p|N} \left(1 - \frac{1}{p^2}\right)$$

Summarizing we conclude that the translation surface \mathcal{K} lives in the stratum $\mathcal{H}(\underbrace{2, \dots, 2}_k)$, where the number k of conical points is given by formula (32).

We complete this section with an interpretation of a compact leaf \mathcal{K} as a space of torus coverings; this interpretation was introduced by A. Eskin, H. Masur and M. Schmol in [EMaScm] and developed by M. Schmol in [Schl1], [Schl2].

We have seen that a nondegenerate flat surface $S(\omega_0) \in \mathcal{H}(1, 1)$ representing a vertex of the square tiling of \mathcal{K} is an N -square-tiled surface. Hence, $S(\omega)$ is a ramified covering over the standard torus \mathbb{T}^2 of degree N having two simple ramification points, which project to the same point of the torus. A non vertex point $S(\omega) \in \mathcal{K}$ is also a ramified covering over the standard torus \mathbb{T}^2 . To see this consider once more the period map, but this time applied to $S(\omega)$:

$$S(\omega) \ni P \xrightarrow{proj} \int_{P_1}^P \omega \pmod{\mathbb{Z} + \sqrt{-1}\mathbb{Z}} \in \mathbb{C}/(\mathbb{Z} + \sqrt{-1}\mathbb{Z}) = \mathbb{T}^2.$$

Since all absolute periods of ω live in $\mathbb{Z} + \sqrt{-1}\mathbb{Z}$ the integral taken modulo integers does not depend on the path joining the marked point (conical singularity) P_1 with a point P of the flat surface $S(\omega)$. The map *proj* is a ramified covering.

The degree of the covering can be computed as the ratio of areas of $S(\omega)$ and of the torus \mathbb{T}^2 , which gives N . The covering has precisely two simple ramification points, which are the conical points P_1, P_2 of $S(\omega)$. This time they project to two different points of the torus.

Recall that by convention we assume that the absolute periods of ω generate the entire lattice $\mathbb{Z} + \sqrt{-1}\mathbb{Z}$. They corresponds to primitive covers: the ones which do not quotient through a larger torus.

Proposition (M. Schmoll). *Consider primitive branched covers over the standard torus \mathbb{T}^2 . Fix the degree N of the cover. Let the cover have exactly two simple branch points.*

The space of such covers is connected; its natural compactification coincides with the corresponding leaf \mathcal{K} of the kernel foliation. The Veech group of the square-tiled surface \mathcal{K} coincides with $SL(2, \mathbb{Z})$.

Connectedness of the space of covers is not quite obvious (actually, it was proved earlier in other terms by W. Fulton [Ful]). An observation above shows, that the leaf \mathcal{K} coincides with a connected component of the space of covers. Thus, connectedness of the space of covers implies that this space coincides with \mathcal{K} . The group $SL(2, \mathbb{Z})$ acts naturally on the space of covers; in particular it maps the space of covers to itself. This implies that $SL(2, \mathbb{Z})$ belongs to the Veech group of the square-tiled surface \mathcal{K} . It is easy to show, that it actually coincides with $SL(2, \mathbb{Z})$.

Corollary (M. Schmoll). *Consider square-tiled surfaces $S(\omega)$ of genus two such that the absolute periods of ω span the entire integer lattice $\mathbb{Z} + \sqrt{-1}\mathbb{Z}$. For any given $N > 3$ all such N -square tiled surfaces belong to the same compact connected leaf $\mathcal{K}(N)$ of the kernel foliation.*

For more information on kernel foliation of square-tiled surfaces in genus two see the papers of A. Eskin, H. Masur and M. Schmol [EMaScm] and of M. Schmoll [Schl1], [Schl2]. In particular, the latter papers propose a beautiful formula for Siegel–Veech constants of any flat surface $S \in \mathcal{K}(N)$ in terms of geometry of the cylinder decomposition of the square-tiled surface $\mathcal{K}(N)$.

9.7 Revolution in Genus Two (after K. Calta and C. McMullen)

In this section we give an informal survey of recent revolutionary results in genus $g = 2$ due to K. Calta [Clt] and to C. McMullen [McM2].

Using different methods they found a countable collection of primitive Veech surfaces in the stratum $\mathcal{H}(2)$, proved that this collection describes

all Veech surfaces, and gave efficient algorithms which recognize and classify Veech surfaces in $\mathcal{H}(2)$.

This result is in a sharp contrast with the Theorem of C. McMullen [McM6] cited above, which tells that in the other stratum $\mathcal{H}(1, 1)$ in genus $g = 2$ there is *only one* primitive Veech surface.

This discovery of an infinite family of primitive Veech surfaces in the stratum $\mathcal{H}(2)$ is also in a sharp contrast with our poor knowledge of primitive Veech surfaces in higher genera: as we have seen in the previous section, primitive Veech surfaces in higher genera $g \geq 3$ are currently known only in some special strata (mostly hyperelliptic), and even in these special strata we know only finite number of primitive Veech surfaces (basically, only one).

Another remarkable result is a discovery by K. Calta and by C. McMullen of nontrivial examples of invariant submanifolds of intermediate dimension: larger than closed orbits and smaller than the entire stratum.

One more revolutionary result in genus two is a Classification Theorem due to C. McMullen [McM3] which proves that a closure of *any* $GL^+(2, \mathbb{R})$ -orbit is a nice complex-analytic variety which is either an entire stratum, or which has one of the types mentioned above.

Algebraic-geometric Approach To avoid overloading of this survey I had to sacrifice beautiful algebraic-geometric part of this story developed by C. McMullen; the reader is addressed to original papers [McM2]–[McM6] and to a short overview presented in [HuSdt5].

Periods of Veech Surfaces in Genus $g = 2$

If S is a Veech surface then the flat surface gS is also a Veech surface for any $g \in GL^+(2, \mathbb{R})$. Thus, speaking about a finite or about a countable collection of Veech surfaces we, actually, choose some family of representatives $\{S_k\}$ of the orbits $GL^+(2, \mathbb{R}) \cdot S$ of Veech surfaces.

The question, which elements of our collection $\{S_k\}$ belong to the same $GL^+(2, \mathbb{R})$ -orbit and which ones belong to different orbits is a matter of a separate nontrivial study. A solution was found by C. McMullen in [McM4]; it is briefly presented in the next Sec. 9.8. In this section we present effective algorithm due to K. Calta and to C. McMullen which enables to determine whether a given flat surface in $\mathcal{H}(2)$ is a Veech surface.

Following K. Calta we say that a flat surface S can be *rescaled* to a flat surface S' if S and S' belong to the same $GL^+(2, \mathbb{R})$ -orbit. We say that a flat surface S is *quadratic* if for any homology cycle $c \in H_1(S; \mathbb{Z})$ we have

$$\int_c \omega = (p + q\sqrt{d}) + i(r + s\sqrt{d}), \quad \text{where } d \in \mathbb{N}, \quad p, q, r, s \in \mathbb{Q}$$

In other words, we say that a flat surface S defined by a holomorphic 1-form ω is *quadratic* if all periods of ω live in $\mathbb{Q}(\sqrt{d}) + i\mathbb{Q}(\sqrt{d})$.

We can considerably restrict the area of our search using the following Lemma of W. Thurston.

Lemma (W. Thurston). *Any Veech surface in genus $g = 2$ (no matter primitive or not, in the stratum $\mathcal{H}(2)$ or $\mathcal{H}(1, 1)$) can be rescaled to a quadratic surface.*

Using this Lemma K. Calta suggest the following algorithm deciding whether a given flat surface $S \in \mathcal{H}(2)$ is a Veech surface or not.

Algorithm of Calta

Recall, that if S is a Veech surface (of arbitrary genus), then by Veech alternative (see Sec. 3.7) a directional flow in any direction is either minimal or completely periodic, that is a presence of a closed geodesic going in some direction implies that all geodesics going in this direction are periodic. Moreover, it was proved by Veech that as soon as there a saddle connection going in some direction, this direction is also completely periodic. In both cases the surface decomposes into a finite collection of cylinders; each boundary component of each cylinder contains a conical singularity (see Sec. 7.1).

The algorithm works as follows. Having a flat surface $S \in \mathcal{H}(2)$ it is easy to find *some* closed geodesic on S (which is allowed to be a closed geodesic saddle connection). Since “rescaling” the surface S (i.e. applying a linear transformation from $GL^+(2, \mathbb{R})$) we replace a Veech surface by a Veech surface, we can turn S in such way that the direction of the closed geodesic will become horizontal. We denote the resulting surface by the same symbol S .

Since S lives in $\mathcal{H}(2)$ it has a single conical point P with the cone angle 6π . In particular, there are exactly three geodesics leaving the conical point in the positive horizontal direction (to the East). If at least one of these three horizontal geodesics does not come back to P the surface S is *not* a Veech surface. Otherwise our test continues.

As we have seen in Sec. 7.1 there are two possible ways in which three horizontal geodesics emitted from P to the East can return to P . Either all three geodesics return at the angle 3π , or one of them returns at the angle 3π and two others return at the angle π , see Fig. 41. In both cases all horizontal geodesics are closed. In the first case the surface decomposes into a single cylinder; in the second case the surface is glued from two cylinders, see Sec. 7.1.

If the surface is decomposed into a single cylinder, it is sufficient to compare the lengths p_1, p_2, p_3 of three horizontal saddle connections, see Fig. 41. The flat surface S is a Veech surface if and only if p_1, p_2, p_3 are commensurable. Moreover, if p_1, p_2, p_3 are commensurable, we can rescale S to a square-tiled surface. It can be done in several elementary steps. First we rescale S in the horizontal direction making p_1, p_2, p_3 rational and then integer. Then we rescale S in the vertical direction making the height h of the cylinder integer. Finally, we apply an appropriate parabolic linear transformation $\begin{pmatrix} 1 & s \\ 0 & 1 \end{pmatrix}$. It does not change neither p_1, p_2, p_3 nor h , but when $s \in \mathbb{R}$ varies the twist t

also varies continuously (see Fig. 39) taking all values in \mathbb{R} ; in particular, we can achieve $t = 0$. We get a square-tiled surface.

Consider the second case, when the surface decomposes into two cylinders. Let $w_1, w_2, h_1, h_2, t_1, t_2$ be the widths (perimeters), heights and twists of this cylinders correspondingly (compare to Sec. 7.1). In a complete analogy with the one-cylinder case we can rescale the surface horizontally, then vertically, and finally apply an appropriate parabolic linear transformation in order to make the width (perimeter) w_1 and height h_1 of the first cylinder equal to one, $h_1 = w_1 = 1$, and the twist $t_1 = 0$ equal to zero. Applying an appropriate Dehn twist to the second cylinder we can assure $0 \leq t_2 < w_2$.

If after our rescaling all parameters w_2, h_2, t_2 characterizing the second cylinder do not get to the same quadratic field $\mathbb{Q}(\sqrt{d})$ for some $d \in \mathbb{N}$, the surface S is not a Veech surface.

If w_2, h_2, t_2 are rational (i.e. if d is a complete square), the surface S can be rescaled to a square-tiled surface.

The remaining case is treated by one of the key Theorems in the paper of K. Calta [Clt].

Theorem (K. Calta). *Let all parameters w_j, h_j, t_j , $j = 1, 2$ of a two-cylinder decomposition of a flat surface $S \in \mathcal{H}(2)$ belong to the same quadratic field $\mathbb{Q}(\sqrt{d})$ with $d \in \mathbb{N}$ not a complete square. Then S is a Veech surface if and only if the parameters satisfy the following system of equations:*

$$\begin{cases} w_1 \bar{h}_1 & = -w_2 \bar{h}_2, \\ \bar{w}_1 t_1 + \bar{w}_2 t_2 & = w_1 \bar{t}_1 + w_2 \bar{t}_2, \end{cases} \quad (33)$$

(where the bar denotes conjugation $\overline{p + q\sqrt{d}} = p - q\sqrt{d}$ in $\mathbb{Q}(\sqrt{d})$ with $p, q \in \mathbb{Q}$).

Actually, we kept the system of equation above as it is written in the original paper [Clt]. In this form it can be adopted to a more general normalization of parameters: it is sufficient to rescale surface S to bring all w_j, h_j, t_j , $j = 1, 2$ to a quadratic field.

Remark. Similar *necessary* conditions for Veech surfaces in $\mathcal{H}(2)$ were obtained by D. Panov independently of K. Calta and of C. McMullen.

Since by Lemma of Thurston any Veech surface in $\mathcal{H}(2)$ can be rescaled to a quadratic surface, taking a collection of all quadratic surfaces decomposed into two horizontal cylinders satisfying the condition above, we get representatives of the $GL^+(2, \mathbb{R})$ -orbits of *all* flat surfaces in $\mathcal{H}(2)$.

Exercise. Show that the Katok–Zemlyakov construction applied to an L -shaped billiard as on Fig. 50 (see also Fig. 38) generates a surface $S \in \mathcal{H}(2)$. Show that this surface is decomposed into two cylinders filled by closed horizontal geodesics and that these cylinders have parameters $w_1 = 2, h_1 =$

$2a - 2, t_1 = 0$ for the first cylinder and $w_2 = 2b, h_2 = 2, t_2 = 0$ for the second cylinder. Using the condition above prove the following Theorem of C. McMullen [McM2]:

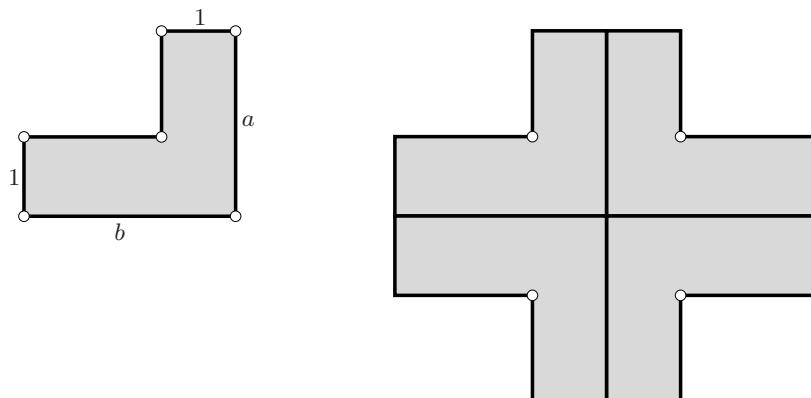


Fig. 50. L-shaped billiard table $P(a, b)$ and its unfolding into a flat surface $S \in \mathcal{H}(2)$ (after C. McMullen [McM2])

Theorem (C. McMullen). *The L-shaped billiard table $P(a, b)$ as on Fig. 50 generates a Veech surface if and only if a and b are rational or*

$$a = x + z\sqrt{d} \quad \text{and} \quad b = y + z\sqrt{d}$$

for some $x, y, z \in \mathbb{Q}$ with $x + y = 1$ and $d \geq 0$ in \mathbb{Z} .

Kernel Foliation in Genus 2

The following elementary observation explains our interest to kernel foliation in the content of our study of $GL^+(2, \mathbb{R})$ -invariant subvarieties. Let $\mathcal{N} \subset \mathcal{H}(d_1, \dots, d_n)$ be a $GL^+(2, \mathbb{R})$ -invariant submanifold. The “germ” of the kernel foliation at \mathcal{N} is equivariant with respect to the action of $GL^+(2, \mathbb{R})$.

In other words this statement can be described as follows. Denote by $t(\delta)$ a translation by δ along kernel foliation defined in a neighborhood of $S \in \mathcal{H}(1, 1)$. Here $\delta \in \mathbb{C}$ is a small parameter. Let $g \in GL^+(2, \mathbb{R})$ be close to identity. Then

$$g \circ t(\delta) \cdot S = t(g\delta) \circ gS$$

where g acts on a complex number δ as on a vector in \mathbb{R}^2 . Moving along the kernel foliation, and then applying an element g of the group is the same as applying first the same element of the group and then moving along an appropriate translation along the kernel foliation. A similar construction works in a general stratum.

We get the following very tempting picture. Suppose, that we have a closed $GL^+(2, \mathbb{R})$ -orbit \mathcal{N} in $\mathcal{H}(1, 1)$ or in $\mathcal{H}(2)$. For example, suppose that \mathcal{N} is an orbit of a Veech surface. Consider a union of leaves of the kernel foliation passing through \mathcal{N} . Due to the remark above this is a $GL^+(2, \mathbb{R})$ -invariant subset!

The weakness of this optimistic picture is that there is no *a priori* reason to hope that the resulting invariant subset in $\mathcal{H}(1, 1)$ would be closed. And here the magic comes. The following statement was proved independently by K. Calta [Clt] and by C. McMullen [McM2].

Theorem (K. Calta; C. McMullen). *For any Veech surface $S_0 \in \mathcal{H}(2)$ the union of leaves of the kernel foliation passing through the $GL^+(2, \mathbb{R})$ -orbit of S_0 is a closed $GL^+(2, \mathbb{R})$ -invariant complex orbifold \mathcal{N} of complex dimension 3.*

In particular, the complex dimension of the resulting orbifold is the sum of the complex dimension of the $GL^+(2, \mathbb{R})$ -orbit of S_0 and of the complex dimension of the kernel foliation $3 = 2 + 1$.

K. Calta has found the following beautiful geometric characterization of flat surfaces living in an invariant subvariety \mathcal{N} as above. Surfaces in any such \mathcal{N} are *completely periodic*: as soon as there is a single closed trajectory in some direction, *all* geodesics going in this direction are closed. This condition is necessary and sufficient condition for a surface to live in an invariant subvariety \mathcal{N} as above. In particular, this shows that not only Veech surfaces have this property.

An algorithm analogous to the algorithm determining Veech surfaces in $\mathcal{H}(2)$ (see above) allows to K. Calta to determine whether a given surface $S \in \mathcal{H}(1, 1)$ is completely periodic or not (and hence, whether it belongs to an invariant subvariety \mathcal{N} as above or not). As before one starts with finding *some* closed geodesic or *some* saddle connection. If the surface is completely periodic in the corresponding direction, then all other geodesics going in this direction are periodic and the surface decomposes into cylinders. After an appropriate rotation this periodic direction becomes horizontal. Without loss of generality, we may assume that S decomposes into three cylinders. By w_i , h_i and t_i with $1 \leq i \leq 3$, we denote the widths, heights and twists. After renumbering, we may assume that $w_3 = w_1 + w_2$. Define $s_1 = h_1 + h_3$, $s_2 = h_2 + h_3$, $\tau_1 = t_1 + t_3$, $\tau_2 = t_2 + t_3$. If the surface is completely periodic its absolute periods can be rescaled to get to $\mathbb{Q}(\sqrt{d}) + i\mathbb{Q}(\sqrt{d})$ (compare to the algorithm for Veech surfaces). Leaving the elementary case when $d \in \mathbb{N}$ is a complete square, the following characteristic equations obtained by K. Calta (analogous to equations (33) above) tell whether our flat surface is completely periodic or not:

$$\begin{aligned} w_1 \bar{s}_1 &= -w_2 \bar{s}_2, \\ \bar{w}_1 \tau_1 + \bar{w}_2 \tau_2 &= w_1 \bar{\tau}_1 + w_2 \bar{\tau}_2, \quad 0 \leq \tau_i < w_i + w_3. \end{aligned}$$

Note that we consider any invariant subvariety \mathcal{N} as above as a subvariety in $\mathcal{H}_2 = \mathcal{H}(1, 1) \sqcup \mathcal{H}(2)$. Clearly, the intersection $\mathcal{N} \cap \mathcal{H}(1, 1)$ and $\mathcal{N} \cap \mathcal{H}(2)$ results in close $GL^+(2, \mathbb{R})$ -invariant subvarieties in the corresponding strata. Note that $\dim_{\mathbb{C}} \mathcal{N} = 3$. Since \mathcal{N} is a union of leaves of the kernel foliation this implies that $\dim_{\mathbb{C}} \mathcal{N} \cap \mathcal{H}(2) = 2$. This means that *any* surface $S \in \mathcal{N} \cap \mathcal{H}(2)$ is a Veech surface!

Classification Theorem of McMullen

We complete this section with a description of the wonderful result of C. McMullen [McM3] realizing a dream of a complete classification of closures of $GL^+(2, \mathbb{R})$ -orbits in genus $g = 2$. The classification is astonishingly simple. We slightly reformulate the original Theorem using the notions of kernel foliation and of completely periodic surface (and, hence, using implicitly results of K. Calta [Clt]).

Theorem (C. McMullen).

- If a surface $S \in \mathcal{H}(2)$ is a Veech surface, its $GL^+(2, \mathbb{R})$ -orbit is a closed complex 2-dimensional subvariety;
- Closure of $GL^+(2, \mathbb{R})$ -orbit of any surface $S \in \mathcal{H}(2)$ which is not a Veech surface is the entire stratum $\mathcal{H}(2)$;
- If a surface $S \in \mathcal{H}(1, 1)$ is a Veech surface, its $GL^+(2, \mathbb{R})$ -orbit is a closed complex 2-dimensional subvariety;
- If a surface $S \in \mathcal{H}(1, 1)$ is not a Veech surface but is a completely periodic surface, then the closure of its $GL^+(2, \mathbb{R})$ -orbit is a closed complex 3-dimensional subvariety \mathcal{N} foliated by leaves of the kernel foliation as described above;
- If a surface $S \in \mathcal{H}(1, 1)$ is not completely periodic, then the closure of its $GL^+(2, \mathbb{R})$ -orbit is the entire stratum $\mathcal{H}(1, 1)$.

Actually, the Theorem above is even stronger: connected components of these invariant submanifolds are basically also classified. We have seen that the $GL^+(2, \mathbb{R})$ -orbit of any Veech surfaces in $\mathcal{H}(2)$ has a representative with all periods in a quadratic field. The *discriminant* $D = b^2 - 4c > 0$ is a positive integer: a discriminant of the corresponding quadratic equation $x^2 + bx + c = 0$ with integer coefficients. The discriminant is an invariant of an $GL^+(2, \mathbb{R})$ -orbit. Since for any integer b the number $b^2 \pmod{4}$ can be either 0 or 1, the discriminant $D \pmod{4} = 0, 1$. The values $D = 1, 4$ are not realizable, so the possible values of D are 5, 8, 9, 12, 13, ...

We postpone the description of results of P. Hubert and S. Lelièvre [HuLe1] and of C. McMullen [McM4] on classification of the orbits of Veech surfaces in $\mathcal{H}(2)$ to the next section. Here we state the following result of C. McMullen [McM3]. By $\mathcal{N}(D)$ denote the 3-dimensional invariant submanifold obtained as a union of leaves of the kernel foliation passing through the orbits of all Veech surfaces corresponding to the given discriminant D .

Theorem (C. McMullen). *The invariant subvariety $\mathcal{N}(D)$ is nonempty and connected for any $D = 0, 1 \pmod{4}$, $D \in \mathbb{N}$, $D \geq 5$.*

Ergodic Measures

Actually, the Classification Theorem of C. McMullen is even stronger: it also classifies the invariant measures. Consider the “unit hyperboloids” $\mathcal{H}_1(2)$ and $\mathcal{H}_1(1, 1)$: the subvarieties of real codimension one representing flat surfaces of area 1. The group $SL(2, \mathbb{R})$ acts on $\mathcal{H}_1(2)$ and $\mathcal{H}_1(1, 1)$ preserving the measure induced on these “unit hyperboloids”, see Sec. 3.4. Let us discuss what other $SL(2, \mathbb{R})$ -invariant measures do we know.

When we have an $SL(2, \mathbb{R})$ -invariant subvariety, we can get an invariant measure concentrated on this subvariety. For example, as we know an $SL(2, \mathbb{R})$ -orbit of a Veech surface S is closed; it is isomorphic to the quotient $SL(2, \mathbb{R})/\Gamma(S)$, where, by definition of a Veech surface, this quotient has finite volume. Thus, Haar measure on $SL(2, \mathbb{R})$ induces a finite invariant measure on the $SL(2, \mathbb{R})$ -orbit of a Veech surface S .

Consider now a “unit hyperboloid” $\mathcal{N}_1 \subset \mathcal{N}$ in the manifold \mathcal{N} obtained as a union of leaves of the kernel foliation passing through $SL(2, \mathbb{R})$ -orbit of a Veech surface S . Note that by Riemann bilinear relations the area of a flat surface can be expressed in terms of absolute periods. Thus, moving along the kernel foliation we do not change the area of the surface. We have seen that every leaf of the kernel foliation is flat. Consider the corresponding Euclidean volume element in each leaf. The group $SL(2, \mathbb{R})$ maps leaves of the kernel foliation to leaves and respects this volume element. Thus we get an invariant measure on $\mathcal{N}_1 \subset \mathcal{N}$; near an $SL(2, \mathbb{R})$ -orbit of a Veech surface it disintegrates to a product measure.

We have associated to any connected invariant subvariety of each of four types as above a natural $SL(2, \mathbb{R})$ -measure supported on it. One more result of C. McMullen in [McM3] tells that there are no other ergodic measures.

Other Properties

The invariant subvarieties have numerous wonderful geometric properties. In particular, their projections to the moduli space \mathcal{M} of complex structures on a surface of genus two are also nice subvarieties. C. McMullen has showed that the $GL^+(2, \mathbb{R})$ -orbit of a Veech surface projects to an isometrically immersed algebraic curve and $\mathcal{N}(D)$ projects to a complex surface. Such surfaces (of complex dimension two) are called *Hilbert modular surfaces*.

One more surprising phenomenon proved by C. McMullen in [McM3] concerns Veech groups of flat surfaces in genus $g = 2$.

Theorem (C. McMullen). *If the Veech group $\Gamma(S)$ of a flat surface $S \in \mathcal{H}(2)$ contains a hyperbolic element, the flat surface S is a Veech surface; in particular, its Veech group $\Gamma(S)$ is a lattice in $SL(2, \mathbb{R})$.*

If the Veech group $\Gamma(S)$ of a flat surface $S \in \mathcal{H}(1,1)$ contains a hyperbolic element, and the flat surface S is not a Veech surface, then S is completely periodic. In this case the Veech group $\Gamma(S)$ is infinitely generated.

The Veech group of a flat surface S contains a hyperbolic element if and only if S admits an affine pseudoanosov diffeomorphism.

We complete this section with the following natural problem for higher genera $g \geq 3$.

Problem. Let \mathcal{K} be a $GL^+(2, \mathbb{R})$ -invariant subvariety in some stratum of holomorphic one-forms $\mathcal{H}(d_1, \dots, d_m) \subset \mathcal{H}_g$. Consider the union \mathcal{U} of leaves of the kernel foliation passing through \mathcal{K} . Is \mathcal{U} a closed subvariety in $\mathcal{H}(1, \dots, 1)$? Similar question for other strata.

9.8 Classification of Teichmüller Discs of Veech Surfaces in $\mathcal{H}(2)$

It is easy to check that any square-tiled surface (see Sec. 7.1) is a Veech surface, and thus an $SL(2, \mathbb{R})$ -orbit of any square-tiled surface is closed. Such orbit contains other square-tiled surfaces. Since the $SL(2, \mathbb{R})$ -action does not change the area of a surface these other square-tiled surfaces are tiled with the same number of squares, see Fig. 46 in Sec. 9.5 and the Exercise related to this Figure.

For a fixed integer n the number of n -square-tiled surfaces is finite. It would be interesting to know (and this is certainly a part of general Problem from Sec. 9.3) how the square-tiled surfaces are arranged into orbits of $SL(2, \mathbb{R})$. Say, we have seen in the previous section that there are exactly three 3-square-tiled surfaces in $\mathcal{H}(2)$ (see Fig. 46) and that they belong to the same orbit. For $n = 4$ there are already nine 4-square-tiled surfaces in $\mathcal{H}(2)$ and they still belong to the same $SL(2, \mathbb{R})$ -orbit. The corresponding Teichmüller disc is a 9-fold cover over the modular curve. For $n = 5$ there are twenty seven 5-square-tiled surfaces in $\mathcal{H}(2)$ and they split into two different orbits of $SL(2, \mathbb{R})$.

Generalizing a result of P. Hubert and S. Lelièvre [HuLe1] obtained for prime number n C. McMullen has recently proved the following conjecture of P. Hubert and S. Lelièvre.

Theorem (C. McMullen). All n -square-tiled surfaces in $\mathcal{H}(2)$, which cannot be tiled with $p \times q$ -rectangles with p or q greater than 1, get to the same $SL(2, \mathbb{R})$ -orbit when $n \geq 4$ is even and get to exactly two distinct orbits when $n \geq 5$ is odd.

Actually, C. McMullen has classified in [McM4] the orbits of all Veech surfaces in $\mathcal{H}(2)$. As we have seen in the previous section Veech surfaces in $\mathcal{H}(2)$ are characterized by an integer parameter, called the *discriminant* D . For n -square-tiled surfaces the discriminant equals $D = n^2$.

Veech surfaces which cannot be rescaled to a square-tiled surface are called *nonarithmetic* Veech surfaces. Any nonarithmetic Veech surface in $\mathcal{H}(2)$ can be rescaled to a flat surface having all periods in a quadratic field (see the Lemma of W. Thurston in the previous section). The discriminant corresponding to a nonarithmetic Veech surface is the discriminant of this quadratic field. Of course a $GL^+(2, \mathbb{R})$ -orbit of a nonarithmetic Veech surface might have different representatives S , such that all periods of S belong a quadratic field. Nevertheless, for Veech surfaces in genus $g = 2$ the discriminant is well-defined: it is an invariant of a $GL^+(2, \mathbb{R})$ -orbit. The discriminant is a positive integer $D = 0, 1 \pmod{4}$, $D \geq 5$.

C. McMullen has proved the following classification Theorem [McM4]:

Theorem (C. McMullen). *For $D = 1 \pmod{8}$, $D > 9$, all Veech surfaces in $\mathcal{H}(2)$ corresponding to discriminant D get to exactly two distinct $GL^+(2, \mathbb{R})$ -orbits. For other values $D = 0, 1 \pmod{4}$, $D \geq 5$, they belong to the same $GL^+(2, \mathbb{R})$ -orbit.*

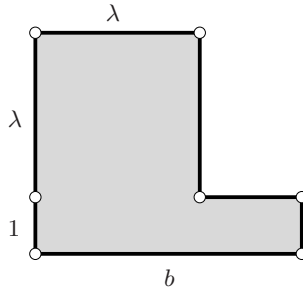


Fig. 51. The L -shaped billiard table $L(b, e)$ generating a “canonical” Veech surface

Moreover, C. McMullen proposed the following canonical representative for any such $GL^+(2, \mathbb{R})$ -orbit, see [McM4]. Consider an L -shaped billiard $L(b, e)$ as on Fig. 51, where

$$\begin{cases} b, e \in \mathbb{Z}; & \lambda = (e + \sqrt{e^2 + 4b})/2 \\ e = -1, 0 \text{ or } 1 \\ e + 1 < b \\ \text{if } e = 1 \text{ then } b \text{ is even} \end{cases} \quad (34)$$

The billiard table $L(b, e)$ generates a flat surface $S(b, e)$ in $\mathcal{H}(2)$, see Fig. 50.

Theorem (C. McMullen). *The flat surface $S(b, e)$ generated by the L -shaped billiard table $L(b, e)$ with parameters b, e satisfying (34) is a Veech surface. Any closed $GL^+(2, \mathbb{R})$ -orbit in $\mathcal{H}(2)$ is represented by one of such $S(b, e)$ and this representation is unique. The discriminant D of $S(b, e)$ equals $D = e^2 + 4b$.*

Exercise. Using linear transformations and scissors rescale the flat surface obtained from the “double pentagon” (see Fig. 7) to the flat surface obtained from a “golden cross” $P(a, b)$, with $a = b = \frac{1 + \sqrt{5}}{2}$; see Fig. 50 for the definition of $P(a, b)$. Using linear transformations and scissors rescale any of these flat surfaces to a surface obtained from the billiard table $L(1, -1)$, see Fig. 51, proving that these Veech surfaces have discriminant $D = 5$. (For solutions see Fig. 4 in [McM2]; see also and [McM5]).

Exercise (T. Schmidt). Using linear transformations and scissors rescale the flat surface obtained from the regular octagon to a surface obtained from the billiard table $L(2, 0)$, see Fig. 51, proving that these Veech surfaces have discriminant $D = 8$. (See [McM5]).

Stratum $\mathcal{H}(1, 1)$

We have discussed in details Veech surfaces in $\mathcal{H}(2)$. We did not discuss the Veech surface for the stratum $\mathcal{H}(1, 1)$ because for square-tiled surfaces in $\mathcal{H}(1, 1)$ (also called *arithmetic Veech surfaces*) the classification of the $GL^+(2, \mathbb{R})$ -orbits is not known yet...

The classification of *nonarithmetic* Veech surfaces in $\mathcal{H}(1, 1)$ is, however, known (since very recently), and is quite surprising. Using the results of M. Moeller [Mo1]–[Mo3] C. McMullen has proved in [McM6] the following Theorem.

Theorem (C. McMullen). *Up to a rescaling the only primitive nonarithmetic Veech surface in $\mathcal{H}(1, 1)$ is the one obtained from the regular decagon by identification of opposite sides. In other words, any primitive nonarithmetic Veech surface in $\mathcal{H}(1, 1)$ belongs to the $GL^+(2, \mathbb{R})$ -orbit of the surface obtained from the regular decagon.*

For higher genera nothing is known neither about the number of $SL(2, \mathbb{R})$ -orbits of n -square-tiled surfaces, nor about their geometry.

Problem. *Classify orbits of square-tiled surfaces in any stratum, in particular in $\mathcal{H}(1, 1)$.*

Square-tiled Surfaces: more serious reading. An elementary introduction can be found in [Zo5]. Paper [HuLe1] of P. Hubert and S. Lelièvre and [McM4] of C. McMullen classify orbits of square-tiled surfaces in $\mathcal{H}(2)$. See also the paper of G. Schmihüsen [Schn] for an algorithm of evaluation of the Veech group of a square-tiled surface and for examples of square-tiled surfaces having $SL(2, \mathbb{R})$ as a Veech group. Another such example due to M. Möller is presented in the survey [HuSdt5] of P. Hubert and T. Schmidt.

10 Open Problems

Flat surfaces with nontrivial holonomy and billiards in general polygons

Problem 1 (Geodesics on general flat surfaces; Sec. 1.1).

Describe behavior of geodesics on general flat surfaces with nontrivial holonomy. Prove (or disprove) that geodesic flow is ergodic on a typical (in any reasonable sense) flat surface.

Does any (almost any) flat surface has at least one closed geodesic which does not pass through singular points?

If yes, are there many regular closed geodesics? Namely, find the asymptotics for the number of closed geodesics of bounded length as a function of the bound.

Problem 2 (Billiards in general polygons; Sec. 2.1).

Describe the behavior of a generic regular billiard trajectory in a generic triangle, in particular, prove (or disprove) that the billiard flow is ergodic.

Does any (almost any) billiard table has at least one regular periodic trajectory? If the answer is affirmative, does this trajectory survive under deformations of the billiard table?

If a periodic trajectory exists, are there many periodic trajectories like that? Namely, find the asymptotics for the number of periodic trajectories of bounded length as a function of the bound.

More problems on billiards can be found in the survey of E. Gutkin [Gu2].

Problem 3 (Renormalization of billiards in polygons; Sec. 2.1 and Sec. 5).

Is there a natural dynamical system (renormalization procedure) acting on the space of billiards in polygons?

Classification of orbit closures in \mathcal{H}_g and \mathcal{Q}_g

Problem 4 (Orbit closures for moduli spaces; Sec. 9.3).

Is it true that the closures of $GL^+(2, \mathbb{R})$ -orbits in \mathcal{H}_g and \mathcal{Q}_g are always complex-analytic (complex-algebraic?) orbifolds? Classify these closures. Classify ergodic measures for the action of $SL(2, \mathbb{R})$ on “unit hyperboloids”.

Suppose that these orbit closures are described by an explicit list. Find natural intrinsic invariants of a flat surface S which would allow to determine the closure of the orbit of S in the list.

To be honest, even having obtained a conjectural classification above, one would need to develop a serious further machinery to get full variety of interesting applications. The situation with the problem below is quite different: a reasonable solution of this problem would immediately give a burst of applications since such a machinery already exists. For the experts interested in ergodic aspects, counting problems, etc, the measure-theoretic analogue of Ratner’s Theorem discussed below is the biggest open problem in the area.

Problem 5 (A. Eskin: “Ratner’s theorem” for moduli spaces; Sec. 9.3).

Does the unipotent subgroup of $SL(2, \mathbb{R})$ act nicely on \mathcal{H}_g and \mathcal{Q}_g or not? Are the orbit closures always nice (for example, real-analytic) orbifolds or one can get complicated closures (say, Kantor sets)?

If the action is “nice”, classify the closures of orbits of the unipotent subgroup $\begin{pmatrix} 1 & t \\ 0 & 1 \end{pmatrix}_{t \in \mathbb{R}}$ in \mathcal{H}_g and \mathcal{Q}_g . Classify ergodic measures for the action of the unipotent subgroup on “unit hyperboloids”.

Solve the problem for genus $g = 2$.

The problem above is solved in the particular case when the unipotent flow acts on a $SL(2, \mathbb{R})$ -invariant submanifold in \mathcal{H}_g obtained by a ramified covering construction from a Veech surface; see the papers of A. Eskin, H. Masur and M. Schmoll [EMaScm] and of A. Eskin, J. Marklof, D. Witte Morris [EMkWt].

The next problem concerns possibility of construction of $GL^+(2, \mathbb{R})$ -invariant submanifolds in higher genera using kernel foliation.

It follows from the results of K. Calta and C. McMullen that for *any* Veech surface $S_0 \in \mathcal{H}(2)$ the union of complex one-dimensional leaves of the kernel foliation passing through the complex two-dimensional $GL^+(2, \mathbb{R})$ -orbit $\mathcal{O}(S_0)$ of S_0 is a closed complex orbifold \mathcal{N} of complex dimension 3, see Sec. 9.7. By construction it is $GL^+(2, \mathbb{R})$ -invariant.

Problem 6 (Kernel foliation; Sec. 9.7).

Let $\mathcal{O} \subset \mathcal{H}(d_1, \dots, d_m) \subset \mathcal{H}_g$ be a $GL(2, \mathbb{R})$ -invariant submanifold (sub-orbifold). Let $\mathcal{H}(d'_1, \dots, d'_n) \subset \mathcal{H}_g$ be a bigger stratum adjacent to the first one, $d_j = d'_{k_1} + \dots + d'_{k_j}$, $i = 1, \dots, m$.

Consider the closure of the union of leaves of the kernel foliation in $\mathcal{H}(d'_1, \dots, d'_n)$ (or in \mathcal{H}_g) passing through \mathcal{O} . We get a closed $GL^+(2, \mathbb{R})$ -invariant subset $\mathcal{N} \subset \mathcal{H}(d'_1, \dots, d'_n)$ (correspondingly $\mathcal{N} \subset \mathcal{H}_g$).

Is \mathcal{N} a complex-analytic (complex-algebraic) orbifold? When \mathcal{N} does not coincide with the entire connected component of the stratum $\mathcal{H}(d'_1, \dots, d'_n)$ (correspondingly \mathcal{H}_g)? When $\dim_{\mathbb{C}} \mathcal{N} = \dim_{\mathbb{C}} \mathcal{O} + (n - m)$ (correspondingly $\dim_{\mathbb{C}} \mathcal{N} = \dim_{\mathbb{C}} \mathcal{O} + (2g - 2 - m)$)? Here $(n - m)$ and $(2g - 2 - m)$ is the complex dimension of leaves of the kernel foliation in $\mathcal{H}(d'_1, \dots, d'_n)$ and in \mathcal{H}_g correspondingly.

Particular cases of classification problem

Problem 7 (Exceptional strata of quadratic differentials; Sec. 9.4).

Find an invariant which would be easy to evaluate and which would distinguish half-translation surfaces from different connected components of the four exceptional strata $\mathcal{Q}(-1, 9)$, $\mathcal{Q}(-1, 3, 6)$, $\mathcal{Q}(-1, 3, 3, 3)$ and $\mathcal{Q}(12)$.

Problem 8 (Veech surfaces; Sec. 9.5).

Classify primitive Veech surfaces.

Problem 9 (Orbits of square-tiled surfaces; Sec 9.8).

Classify orbits of square-tiled surfaces in any stratum. Describe their Teichmüller discs.

Same problem for the particular case $\mathcal{H}(1, 1)$.

Geometry of individual flat surfaces

Problem 10 (Quadratic asymptotics for any surface; Sec. 6.1).

Is it true that *any* very flat surface has exact quadratic asymptotics for the number of saddle connections and for the number of regular closed geodesics?

Problem 11 (Error term for counting functions; Sec. 6.1).

What can be said about the error term in quadratic asymptotics for counting functions $N(S, L) \sim c \cdot L^2$ on a generic flat surface S ? In particular, is it true that the limit

$$\limsup_{L \rightarrow \infty} \frac{\log |N(S, L) - c \cdot L^2|}{\log L} \stackrel{?}{<} 2$$

is strictly less than two? Is it the same for almost all flat surfaces in a given connected component of a stratum?

One of the key properties used by C. McMullen for the classification of the closures of orbits of $GL(2, \mathbb{R})$ in $\mathcal{H}(1, 1)$ was the knowledge that on *any* flat surface in this stratum one can find a pair of homologous saddle connections. Cutting the surface along these saddle connections one decomposes the surface into two tori and applies machinery of Ratner theorem.

Problem 12 (A. Eskin; C. McMullen: Decomposition of surfaces; Sec. 6.4).

Given a connected component of the stratum $\mathcal{H}(d_1, \dots, d_m)$ of Abelian differentials (or of quadratic differentials $\mathcal{Q}(d_1, \dots, d_m)$) find those configurations of homologous saddle connections (or homologous closed geodesics), which are presented at *any* very flat surface S in the stratum.

For quadratic differentials the notion of “homologous” saddle connections (closed geodesics) should be understood in terms of homology with local coefficients, see [MaZo].

Topological, geometric, and dynamical properties of the strata

Problem 13 (M. Kontsevich: Topology of strata; Sec. 3).

Is it true that strata $\mathcal{H}(d_1, \dots, d_m)$ and $\mathcal{Q}(q_1, \dots, q_n)$ are $K(\pi, 1)$ -spaces (i.e. their universal covers are contractible)?

Problem 14 (Compactification of moduli spaces; Sec. 6.3 and 6.4).

Describe natural compactifications of the moduli spaces of Abelian differentials \mathcal{H}_g and of the moduli spaces of meromorphic quadratic differentials with at most simple poles \mathcal{Q}_g . Describe natural compactifications of corresponding strata $\mathcal{H}(d_1, \dots, d_m)$ and $\mathcal{Q}(q_1, \dots, q_n)$.

Problem 15 (Dynamical Hodge decomposition; Sec. 4.3, 5.7 and Appendix B).

Study properties of distributions of Lagrangian subspaces in $H^1(S; \mathbb{R})$ defined by the Teichmüller geodesic flow, in particular, their continuity. Is there any topological or geometric way to define them?

Problem 16 (Lyapunov exponents; Sec. 5.7 and Appendix B).

Study *individual* Lyapunov exponents of the Teichmüller geodesic flow

- for all known $SL(2; \mathbb{R})$ -invariant subvarieties;
- for strata in large genera.

Are they related to characteristic numbers of some natural bundles over appropriate compactifications of the strata?

Some other open problems can be found in [HuMSdtZ].

A Ergodic Theorem

We closely follow the presentation in Chapter 1 of [CFSin]. However, for the sake of brevity we do not consider flows; for the flows the theory is absolutely parallel.

Ergodic Theorem

Consider a manifold M^n with a measure μ . We shall assume that the measure comes from a volume form on M^n , and that the total volume (total measure) of M^n is finite. We shall consider only measurable subsets of M^n .

Let $T : M^n \rightarrow M^n$ be a smooth map. We do not assume that T is a bijection unless it is explicitly specified. We say that T *preserves measure* μ if for any subset $U \subset M^n$ measure $\mu(T^{-1}U)$ of the preimage coincides with measure $\mu(U)$ of the set. For example the double cover $T : S^1 \rightarrow S^1$ of the circle $S^1 = \mathbb{R}/\mathbb{Z}$ over itself defined as $T : x \mapsto 2x \pmod{1}$ preserves the Lebesgue measure on S^1 . In this section we consider only measure preserving maps.

We say that some property is valid *for almost all* points of M^n if it is valid for a subset $U \subset M^n$ of complete measure $\mu(U) = \mu(M^n)$.

A subset $U \subset M^n$ is *invariant* under the map T if the preimage $T^{-1}U$ coincides with U . Thus, a notion of an invariant subset is well-defined even when T is not a one-to-one map. The measure-preserving map $T : M^n \rightarrow M^n$ is *ergodic* with respect to μ if any invariant subset has measure 0 or 1. The measure-preserving map $T : M^n \rightarrow M^n$ is *uniquely ergodic* with respect to μ if there is no other invariant probability measure.

Note that if T has a fixed point or, more generally, a periodic orbit (that is $T^k(x_0) = x_0$ for some $x_0 \in M^n$ and some $k \in \mathbb{N}$), one can consider an invariant probability measure concentrated at the points of the orbit. Thus, such map T cannot be uniquely ergodic with respect to any Lebesgue equivalent measure.

Now we are ready to formulate the keystone theorem. Consider an integrable function f on M^n and some point x . Consider an orbit of T of length n starting at x . Let us evaluate the values of f at the points of the orbit, and let us calculate the “mean value” $\frac{1}{n}(f(x) + f(Tx) + \dots + f(T^{n-1}x))$ with respect to the discrete time k of our dynamical system $\dots, T^{k-1}x, T^kx, T^{k+1}x, \dots$.

Ergodic Theorem. *Let $T : M^n \rightarrow M^n$ preserve a finite measure μ on M^n . Then for any integrable function f on M^n and for almost all point $x \in M^n$ there exists the time mean: there exist the following limit:*

$$\lim_{n \rightarrow \infty} \frac{1}{n} \sum_{k=0}^{n-1} f(T^k x) = \bar{f}(x).$$

The function $\bar{f}(x)$ is integrable and invariant under the map $\bar{f}(Tx) = \bar{f}(x)$. In particular, if T is ergodic, \bar{f} is constant almost everywhere. Moreover,

$$\int_{M^n} \bar{f} d\mu = \int_{M^n} f d\mu$$

First Return Map

The following theorem allows to construct numerous *induced* dynamical systems which are closely related to the initial one.

Theorem (Poincaré Recurrence Theorem). *For any subset $U \subset M^n$ of positive measure and for almost any starting point $x \in U$ the trajectory x, Tx, \dots eventually returns to U , i.e. there is some $n \geq 1$ such that $T^n x \in U$.*

The minimal $n = n(x) \in \mathbb{N}$ as above is called the *first return time*. According to Poincaré Recurrence Theorem integer-valued function $n(x)$ is defined almost everywhere in U . Consider the *first return map* $T|_U : U \rightarrow U$ defined as $T|_U : x \mapsto T^{n(x)}x$, where $x \in U$. In other words, the map $T|_U$ maps a point $x \in U$ to the point where trajectory Tx, T^2x, \dots first meets U .

Lemma. *For any subset $U \subset M^n$ of positive measure the first return map $T|_U : U \rightarrow U$ preserves measure μ restricted to U . If $T : M^n \rightarrow M^n$ is ergodic than $T|_U : U \rightarrow U$ is also ergodic.*

The first return time induced by an ergodic map T has the following geometric property.

Kac Lemma. For an ergodic diffeomorphism $T : M^n \rightarrow M^n$ and for any subset $U \in M^n$ of positive measure the mean value of the first return time equals to the volume of entire space:

$$\int_U n(x) d\mu = \mu(M^n)$$

Ergodic Theory: more serious reading. There are numerous nice books on ergodic theory. I can recommend a classical textbook of I. P. Cornfeld, S. V. Fomin and Ya. G. Sinai [CFSin] and a recent survey of B. Hasselblatt and A. Katok [HaKat].

B Multiplicative Ergodic Theorem

In this section we discuss multiplicative ergodic theorem and the notion of *Lyapunov exponents* and then we present some basic facts concerning Lyapunov exponents. As an alternative elementary introduction to this subject we can recommend beautiful lectures of D. Ruelle [Ru]. A comprehensive information representing the state-of-the-art in this subject can be found in the very recent survey [BP2].

B.1 A Crash Course of Linear Algebra

Consider a linear transformation $A : \mathbb{R}^n \rightarrow \mathbb{R}^n$ represented by a matrix $A \in SL(n, \mathbb{R})$. Assume that A has n distinct eigenvalues $e^{\lambda_1}, \dots, e^{\lambda_n}$; let $\mathbf{v}_1, \dots, \mathbf{v}_n$ be the corresponding eigenvectors. Note that since $\det A = 1$ we get $\lambda_1 + \dots + \lambda_n = 0$; in particular, $\lambda_1 > 0$ and $\lambda_n < 0$.

Consider now a linear transformation $A^N : \mathbb{R}^n \rightarrow \mathbb{R}^n$, where N is a very big positive integer. For almost all vectors $\mathbf{v} \in \mathbb{R}^n$ the linear transformation A^N acts roughly as follows: it takes the projection \mathbf{v}_{proj} of \mathbf{v} to the line $\mathcal{V}_1 = \text{Vec}(\mathbf{v}_1)$ spanned by the top eigenvector \mathbf{v}_1 and then expands it with a factor $e^{N\lambda_1}$. So, roughly, A^N smashes the whole space to the straight line \mathcal{V}_1 and then stretches this straight line with an enormous coefficient of expansion $e^{N\lambda_1}$. (Speaking about projection to $\mathcal{V}_1 = \text{Vec}(\mathbf{v}_1)$ we mean a projection along the hyperplane spanned by the remaining eigenvectors $\mathbf{v}_2, \dots, \mathbf{v}_n$.)

To be more precise, we have to note that the image of \mathbf{v} would not have exactly the direction of \mathbf{v}_1 . A better approximation of $A^N(\mathbf{v})$ would give us a vector in a two-dimensional subspace $\mathcal{V}_2 = \text{Vec}(\mathbf{v}_1, \mathbf{v}_2)$ spanned by the two top eigenvectors $\mathbf{v}_1, \mathbf{v}_2$. When $\lambda_2 > 0$ the direction of $A^N(\mathbf{v})$ would be very close to the direction of \mathcal{V}_1 though the endpoint of $A^N(\mathbf{v})$ might be at a distance of order $e^{N\lambda_2}$ from \mathcal{V}_1 , which is very large. However, this distance is small in comparison with the length of $A^N(\mathbf{v})$ which is of order $e^{N\lambda_1} \gg e^{N\lambda_2}$.

Further terms of approximation give us subspaces \mathcal{V}_j spanned by the top j eigenvectors, $\mathcal{V}_j = \text{Vec}(\mathbf{v}_1, \dots, \mathbf{v}_j)$. Note that starting with some $k \leq n$ the eigenvalues e^{λ_k} become strictly smaller than one. This means that the image $A^N(\mathbf{v})$ of *any* fixed vector \mathbf{v} gets exponentially close to the subspace \mathcal{V}_{k-1} .

Going into details we have to admit that vectors \mathbf{v} from a subspace of measure zero in the set of directions expose different behavior. Namely, vectors \mathbf{v} from the hyperplane \mathcal{L}_2 spanned by $\mathbf{v}_2, \dots, \mathbf{v}_n$ have smaller coefficient of distortion than the generic ones. From this point of view vectors from linear subspaces $\mathcal{L}_j = \text{Vec}(\mathbf{v}_j, \mathbf{v}_{j+1}, \dots, \mathbf{v}_n)$ expose more and more exotic behavior;

in particular, all vectors from the subspace $\mathcal{L}_k = \text{Vec}(\mathbf{v}_k, \mathbf{v}_{j+1}, \dots, \mathbf{v}_n)$ get exponentially contracted.

B.2 Multiplicative Ergodic Theorem for a Linear Map on the Torus

Consider a linear transformation $A : \mathbb{R}^n \rightarrow \mathbb{R}^n$ this time represented by an integer matrix $A \in SL(n, \mathbb{Z})$ as above. Consider the induced map $F : \mathbb{T}^n \rightarrow \mathbb{T}^n$ of the torus $\mathbb{T}^n = \mathbb{R}^n / \mathbb{Z}^n$. This map preserves the natural linear measure on the torus. Consider the N -th iterate F^N of the map F , where N is a *very large* number.

Note, that the differential of F in the natural coordinates on the torus is represented by the constant matrix $D_{x_0}F = A$ for any $x_0 \in \mathbb{T}^n$. Note also that the differential of the N -th iterate of F is represented as a product of N differentials of F along the trajectory $x_0, F(x_0), F(F(x_0)) \dots, F^{N-1}(x_0)$ of x_0 :

$$D_x(F^N) = D_{F^{N-1}(x_0)}F \circ \dots \circ D_{F(x_0)}F \circ D_{x_0}F \quad (35)$$

Hence, in “linear” coordinates we get $D_x(F^N) = A^N$. Thus, the results of the previous section are literally applicable to the local analysis of the map F^N , where now vector \mathbf{v} should be interpreted as a tangent vector to the torus \mathbb{T}^n . In particular, these results have the following interpretation. If we consider the trajectory $x_0, F(x_0), \dots, F^N(x_0)$ of the initial point and the trajectory $x, F(x), \dots, F^N(x)$ of a point x obtained from x_0 by a very small deformation in direction \mathbf{v} , then for *most* of the vectors \mathbf{v} trajectories would deviate exponentially fast one from the other; while for *some special* vectors they would approach each other exponentially fast.

Namely, we get a distribution of linear subspaces \mathcal{L}_k in the tangent space to the torus such that deforming the starting point of trajectory in any direction in \mathcal{L}_k we get two exponentially converging trajectories. The subspace $\mathcal{L}_k = \text{Vec}(\mathbf{v}_k, \mathbf{v}_{k+1}, \dots, \mathbf{v}_n)$ is spanned by the eigenvectors of the matrix A having eigenvalues, which are smaller than one. This distribution is integrable; it defines a so-called *stable* foliation.

There is also a complementary *unstable* foliation corresponding to the distribution of subspaces $\mathcal{V}_{k-1} = \text{Vec}(\mathbf{v}_1, \dots, \mathbf{v}_{k-1})$ spanned by the eigenvectors of the matrix A having eigenvalues, which are greater than one. Passing from the map F to the map F^{-1} the stable and unstable foliations change the roles: stable foliation of F becomes unstable for F^{-1} and vice versa.

When matrix A has an eigenvalue (or several eigenvalues) equal to ± 1 , we get also a *neutral* foliation corresponding to the distribution spanned by the corresponding eigenvectors.

Exercise. Evaluate the limit

$$\lim_{N \rightarrow \infty} \frac{\log \|D_x(F^N)(\mathbf{v})\|}{N} \quad (36)$$

for a tangent vector $\mathbf{v} \in T_{x_0} \mathbb{T}^n$ having a generic direction. What are the possible values of this limit for *any* tangent vector $\mathbf{v} \in T_{x_0} \mathbb{T}^n$? Show that vectors leading to different values of this limit are organized into a flag of subspaces $\mathcal{L}_1 \supset \mathcal{L}_2 \supset \cdots \supset \mathcal{L}_n$, where we assume that all eigenvalues of the matrix A are positive and distinct. How would this flag change if some eigenvalues would have multiplicities? Would we have a flag of subspaces defined by different values of the limit above for the most general matrix $A \in SL(n, \mathbb{Z})$ (which may have Jordan blocks, complex eigenvalues, multiplicities, ...)?

B.3 Multiplicative Ergodic Theorem

Consider now a smooth measure-preserving map $F : M^n \rightarrow M^n$ on a manifold M^n . We consider the case when that the total measure of M^n is finite, and when the map F is *ergodic* with respect to this measure.

Consider some generic point x_0 . Let us study, whether we have convergence of the limit (36) for tangent vectors $\mathbf{v} \in T_{x_0} M^n$ in this more general situation. We can always trivialize the tangent bundle to M^n on an open subset of full measure. Using this trivialization we can reduce our problem to the study of product of matrices (35). This study is now much more difficult than in the previous case since the matrices $D_{F^k(x_0)} F$ are not constant anymore. The following *multiplicative ergodic theorem* formulated for general mappings of general manifolds mimics the simplest situation with a linear map on the torus.

Theorem (Oseledets). *Let a smooth map $F : M^n \rightarrow M^n$ be ergodic with respect to a finite measure. Then, there exists a collection of numbers*

$$\lambda_1 > \lambda_2 > \cdots > \lambda_k,$$

such that for almost any point $x \in M$ there is an equivariant filtration

$$\mathbb{R}^n \simeq T_x M^n = \mathcal{L}_1 \supset \mathcal{L}_2 \supset \cdots \supset \mathcal{L}_k \supset \mathcal{L}_{k+1} = \{0\}$$

in the fiber $T_x M^n$ of the tangent bundle at x with the following property. For every $\mathbf{v} \in \mathcal{L}_j - \mathcal{L}_{j+1}$, $j = 1, \dots, k$, one has

$$\lim_{N \rightarrow +\infty} \frac{1}{N} \log \|(DF^N)_x(\mathbf{v})\| = \lambda_j$$

The multiplicative ergodic theorem was proved by V. I. Oseledets [O2]; a similar statement for products of random matrices was proved earlier by H. Furstenber [Fur].

Multiplicative ergodic theorem has several natural generalizations. The theorem essentially describes the behavior of products (35) of matrices along trajectories of the map F . Actually, matrices $D_x F$ are not distinguished by any special property. One can consider any matrix-valued function $A : M^n \rightarrow GL(m, \mathbb{R})$ and study the products of matrices

$$A(F^{N-1}(x)) \cdots A(F(x)) \cdot A(x)$$

along trajectories $x, F(x), \dots, F^{N-1}(x)$ of F . A statement completely analogous to the above Theorem is valid in this more general case provided the matrix-valued function $A(x)$ satisfy some very moderate requirements. Namely, we do not assume that $A(x)$ is continuous or even bounded. The only requirement is that

$$\int_{M^n} \log_+ \|A(x)\| \mu < +\infty,$$

where $\log_+(y) = \max(\log(y), 0)$. When this condition is satisfied one says that $A(x)$ defines an *integrable cocycle*. The numbers $\lambda_1 > \dots > \lambda_k$ are called the *Lyapunov exponents* of the corresponding cocycle.

Exercise. Formulate a “continuous-time” version of multiplicative ergodic theorem when instead of a map $F : M^n \rightarrow M^n$ we have a flow F_t which is ergodic with respect to a finite measure on M^n . Show that under the natural normalization the corresponding Lyapunov exponents coincide with the Lyapunov exponents of the map F_1 obtained as an action of the flow at the time $t = 1$.

Consider a vector bundle over M^n ; suppose that the vector bundle is endowed with a flat connection. Formulate a version of multiplicative ergodic Theorem for the natural action of the flow on such vector bundle.

Note that in the latter case the Lyapunov exponents are responsible for the “mean holonomy” of the fiber along the flow. Namely, we take a fiber of the vector bundle and transport it along a very long piece of trajectory of the flow. When the trajectory comes close to the starting point we identify the fibers using the flat connection and we study the resulting linear transformation of the fiber.

Note that the choice of a norm in the fibers V_x is in a sense irrelevant. Consider two norms $\| \cdot \|$ and $\| \cdot \|'$ and let

$$c(x) = \min_{\|\mathbf{v}\|=1} \|\mathbf{v}\|' \quad C(x) = \max_{\|\mathbf{v}\|=1} \|\mathbf{v}\|'.$$

If

$$\int_M \max(|\log(c(x))|, |\log(C(x))|) \mu < +\infty,$$

then neither the filtration $\mathcal{L}_k(x)$ nor the Lyapunov exponents λ_k do not change when we replace the norm $\| \cdot \|$ by the norm $\| \cdot \|'$. In particular, when M is a compact manifold all nonsingular norms are equivalent.

In general, even for smooth maps $F : M \rightarrow M$ (flows F_t) the subspaces defined by the terms $\mathcal{L}_k(x) \subset V_x$ of the filtration do not change continuously with respect to a deformation of the base point x . However, these subspaces behave nicely for maps (flows) which have strong hyperbolic behavior (see [Po] for a short introduction; a recent quite accessible textbook [BP1] and a survey [BP2] describing the contemporary status of *Pesin theory*).

Currently there are no general methods of computation of Lyapunov exponents other than numerically. There are some particular situations, say, when the vector bundle has a one-dimensional equivariant subspace, or when F_t is a homogeneous flow on a homogeneous space; in these rather special cases the corresponding Lyapunov exponents can be computed explicitly. However, in general it is extremely difficult to obtain any nontrivial information (positivity, simplicity of spectrum) about Lyapunov exponents.

References

- [AGLP] N. E. Alekseevskii, Yu. P. Gaidukov, I. M. Lifshits, V. G. Peschanskii: *JETPh*, **39** (1960)
- [Ald1] V. I. Arnold: Small denominators and problems of stability of motion in classical and celestial mechanics. *Russian Math. Surveys* **18** no. 6, 85–191 (1963)
- [Ald2] V. I. Arnold: Topological and ergodic properties of closed 1-forms with rationally independent periods. *Functional Anal. Appl.*, **25**, no. 2, 81–90 (1991)
- [Arn] P. Arnoux: Le codage du flot géodésique sur la surface modulaire. *L’Enseignement Mathématique*, **40**, 29–48 (1994)
- [At] M. Atiyah: Riemann surfaces and spin structures. *Ann. scient. ÉNS 4^e série*, **4**, 47–62 (1971)
- [AthEZO] J. Athreya, A. Eskin, A. Zorich: Rectangular billiards and volumes of spaces of quadratic differentials. In preparation.
- [AvFor] A. Avila, G. Forni: Weak mixing for interval exchange transformations and translation flows. To appear in *Annals of Math. Eprint*, [arXiv.math.DS/0406326](https://arxiv.org/abs/math/0406326), 21 pp (2004)
- [AvVi] A. Avila, M. Viana: Simplicity of Lyapunov spectra: proof of the Zorich–Kontsevich conjecture. *Eprint math.DS/0508508*, 36 pp (2005)
- [AzLK] M. Ya. Azbel, I. M. Lifshits, M. I. Kaganov: *Elektronnaiia Teoriya Metallov*. “Nauka”, 1971; English translation: *Electron Theory of Metals*. Consultants Bureau (1973)
- [BP1] L. Barreira and Ya. Pesin: *Lyapunov Exponents and Smooth Ergodic Theory*. Univ. Lect. Series 23, Amer. Math. Soc. (2002)
- [BP2] L. Barreira and Ya. Pesin: Smooth ergodic theory and nonuniformly hyperbolic dynamics. In: B. Hasselblatt and A. Katok (ed) *Handbook of Dynamical Systems*, Vol. 1B. Elsevier Science B.V., Amsterdam, 57–264 (2006)
- [Ber1] L. Bers: Quasiconformal mappings and Teichmüller’s theorem. In collection: R. Nevanlinna et al. (ed) *Analytic Functions*. Princeton Math. Ser. 24, Princeton University Press, NJ, 89–119 (1960)
- [Ber2] L. Bers: Finite dimensional Teichmüller spaces and generalizations. *Bull. Amer. Math. Soc.* **5**, 131–172 (1981)
- [Ber2] M. Boshernitzan: A condition for minimal interval exchange maps to be uniquely ergodic. *Duke Math. J.* **52**, no. 3, 723–752 (1985)
- [Clb] E. Calabi: An intrinsic characterization of harmonic 1-forms, *Global Analysis*. In: D. C. Spencer and S. Iyanaga (ed) *Papers in Honor of K. Kodaira*. 101–117 (1969)

- [Clt] K. Calta: Veech surfaces and complete periodicity in genus two. *J. Amer. Math. Soc.*, **17** 871-908 (2004)
- [CFSin] I. P. Corndeld, S. V. Fomin, Ya. G. Sinai: *Ergodic Theory*. Springer Verlag New York (1982)
- [D1] I. A. Dynnikov: Surfaces in 3-Torus: Geometry of Plane Sections. *Progress in Math.*, Vol. 168, 162–177 Birkhäuser Verlag. Basel (1998)
- [D2] I. A. Dynnikov: Geometry of stability zones in S.P. Novikov’s problem on semi-classical motion of an electron. *Russian Math. Surveys*, **54**, no. 1, 21–60 (1999)
- [E] A. Eskin: Counting problems in moduli space. In: B. Hasselblatt and A. Katok (ed) *Handbook of Dynamical Systems*, Vol. 1B. Elsevier Science B.V., Amsterdam, 581–595 (2006)
- [EMa] A. Eskin, H. Masur: Asymptotic formulas on flat surfaces. *Ergodic Theory and Dynamical Systems*, **21**:2, 443–478 (2001)
- [EMaScm] A. Eskin, H. Masur, M. Schmoll; Billiards in rectangles with barriers, *Duke Math. J.*, **118** (3), 427–463 (2003)
- [EMkWt] A. Eskin, J. Marklof, D. Witte Morris; Unipotent flows on the space of branched covers of Veech surfaces, submitted to *Ergod. Theory and Dyn. Syst.*, **26** (1), 129–162 (2006)
- [EMaZo] A. Eskin, H. Masur, A. Zorich: Moduli spaces of Abelian differentials: the principal boundary, counting problems, and the Siegel–Veech constants. *Publications de l’IHES*, **97**:1, pp. 61–179 (2003)
- [EOk] A. Eskin, A. Okounkov: Asymptotics of number of branched coverings of a torus and volumes of moduli spaces of holomorphic differentials. *Inventiones Mathematicae*, **145**:1, 59–104 (2001)
- [EOkPnd] A. Eskin, A. Okounkov, R. Pandharipande: The theta characteristic of a branched covering, [math.AG/0312186](https://arxiv.org/abs/math/0312186), 22 pp (2003)
- [Fay] J. Fay: Theta functions on Riemann surfaces. *Lecture Notes in Mathematics*, **352**. Springer-Verlag (1973)
- [For1] G. Forni: Deviation of ergodic averages for area-preserving flows on surfaces of higher genus. *Annals of Math.*, **155**, no. 1, 1–103 (2002)
- [For2] G. Forni: On the Lyapunov exponents of the Kontsevich–Zorich cocycle. In: B. Hasselblatt and A. Katok (ed) *Handbook of Dynamical Systems*, Vol. 1B. Elsevier Science B.V., Amsterdam, 549–580 (2006)
- [Ful] W. Fulton: Hurwitz Schemes and Moduli of Curves. *Annals of Math.*, **90**, 542–575 (1969)
- [FxFKr] R. H. Fox, R. B. Kershner: Geodesics on a rational polyhedron. *Duke Math. J.*, **2**, 147–150 (1936)
- [Fur] H. Furstenberg: Non-commuting random products. *Trans. Amer. Math. Soc.*, **108**, 377–428 (1963)
- [GaStVb1] G. Galperin, Ya. B. Vorobets, A. M. Stepin: Periodic billiard trajectories in polygons. *Russian Math. Surveys* **46**, no. 5, 204–205 (1991)
- [GaStVb2] G. Galperin, Ya. B. Vorobets, A. M. Stepin: Periodic billiard trajectories in polygons: generation mechanisms. *Russian Math. Surveys* **47**, no. 3, 5–80 (1992)
- [GaZe] G. Galperin and A. N. Zemliakov: Mathematical billiards. Billiard problems and related problems in mathematics and mechanics. Library “Kvant”, **77**. “Nauka”, Moscow (in Russian) 288 pp. (1990)
- [Gu1] E. Gutkin: Billiards in polygons: survey of recent results. *J. Stat. Phys.*, **83**, 7–26 (1996)

- [Gu2] E. Gutkin: Billiards dynamics: a survey with the emphasis on open problems. *Regular and Chaotic Dynamics*, **8**, no.1, 1–13 (2003)
- [GuJg] E. Gutkin, C. Judge: Affine mappings of translation surfaces: geometry and arithmetic. *Duke Math. J.*, **103**, no. 2, 191–213 (2000)
- [HaKat] B. Hasselblatt and A. B. Katok: Principal structures, In: B. Hasselblatt and A. Katok (ed) *Handbook of Dynamical Systems*, Vol. 1A, Elsevier Science B.V., 1–203, (2002)
- [HbMa] J. Hubbard and H. Masur: Quadratic differentials and measured foliations. *Acta Math.*, **142**, 221–274 (1979)
- [HuLe1] P. Hubert, S. Lelièvre: Prime arithmetic Teichmüller discs in $\mathcal{H}(2)$. *Israel Journal of Math.*, **151**, 281–321 (2006)
- [HuLe2] P. Hubert, S. Lelièvre: Noncongruence subgroups in $\mathcal{H}(2)$, *Internat. Math. Research Notes* **2005:1**, 47–64 (2005)
- [HuMSdtZ] P. Hubert, H. Masur, T. A. Schmidt, A. Zorich: Problems on billiards, flat surfaces and translation surfaces. In: B. Farb (ed) *Problems on Mapping Class Groups and Related Topics*, Proc. Symp. Pure Math., Amer. Math. Soc. (2006)
- [HuSdt1] P. Hubert, T. A. Schmidt: Veech groups and polygonal coverings. *J. Geom. and Phys.* **35**, 75–91 (2000)
- [HuSdt2] P. Hubert, T. A. Schmidt: Invariants of translation surfaces. *Ann. Inst. Fourier (Grenoble)* **51**, no. 2, 461–495 (2001)
- [HuSdt3] P. Hubert, T. A. Schmidt: Infinitely generated Veech groups. *Duke Math. J.* **123**, 49–69 (2004)
- [HuSdt4] P. Hubert, T. A. Schmidt: Geometry of infinitely generated Veech groups. *Conform. Geom. Dyn.* **10**, 1–20 (2006)
- [HuSdt5] P. Hubert and T. Schmidt: An Introduction to Veech Surfaces. In: B. Hasselblatt and A. Katok (ed) *Handbook of Dynamical Systems*, Vol. 1B. Elsevier Science B.V., Amsterdam, 501–526 (2006)
- [J] D. Johnson: Spin structures and quadratic forms on surfaces. *J. London Math. Soc.*, (2) **22**, 365–373 (1980)
- [Kat1] A. Katok: Invariant measures of flows on oriented surfaces. *Soviet Math. Dokl.*, **14**, 1104–1108 (1973)
- [Kat2] A. Katok: Interval exchange transformations and some special flows are not mixing, *Israel Journal of Mathematics* **35**, no. 4, 301–310 (1980)
- [KatZe] A. Katok, A. Zemlyakov: Topological transitivity of billiards in polygons. *Math. Notes*, **18**, 760–764 (1975)
- [Kea1] M. Keane: Interval exchange transformations. *Math. Z.*, **141**, 25–31 (1975)
- [Kea2] M. Keane: Non-ergodic interval exchange transformations. *Israel J. Math.* **26**, no. 2, 188–196 (1977)
- [KenS] R. Kenyon and J. Smillie: Billiards in rational-angled triangles, *Comment. Mathem. Helv.* **75**, 65–108 (2000)
- [Ker1] S. P. Kerckhoff: The Asymptotic geometry of Teichmüller space. *Topology*, **19**, 23–41 (1980)
- [Ker2] S. P. Kerckhoff: Simplicial systems for interval exchange maps and measured foliations. *Ergod. Th. & Dynam. Sys.* **5**, 257–271 (1985)
- [KMaS] S. Kerckhoff, H. Masur, and J. Smillie: Ergodicity of billiard flows and quadratic differentials. *Annals of Math.*, **124**, 293–311 (1986)
- [KhSin] K. M. Khanin, Ya. G. Sinai: Mixing of some classes of special flows over rotations of the circle. *Functional Anal. Appl.* **26**, no. 3, 155–169 (1992)

- [Kon] M. Kontsevich: Lyapunov exponents and Hodge theory. “The mathematical beauty of physics” (Saclay, 1996), (in Honor of C. Itzykson) 318–332, *Adv. Ser. Math. Phys.*, 24. World Sci. Publishing, River Edge, NJ (1997)
- [KonZo] M. Kontsevich, A. Zorich: Connected components of the moduli spaces of Abelian differentials. *Invent. Math.*, **153:3**, 631–678 (2003)
- [Lan] E. Lanneau: Connected components of the moduli spaces of quadratic differentials. Eprint, [arXiv.math.GT/0506136](https://arxiv.org/abs/math/0506136), 41 pp (2005)
- [Lv] P. Lévy: Sur le développement en fraction continue d’un nombre choisi au hasard. *Compositio Mathematica*, **3**, 286–303 (1936)
- [MmMsY] S. Marmi, P. Moussa, J.-C. Yoccoz: The cohomological equation for Roth-type interval exchange maps. *J. Am. Math. Soc.* **18**, No.4, 823–872 (2005)
- [Ma1] H. Masur: On a class of geodesics in Teichmüller space. *Ann. of Math.*, **102**, 205–221 (1975)
- [Ma2] H. Masur: Extension of the Weil-Petersson metric to the boundary of Teichmüller space. *Duke Math. Jour.*, **43**, no. 3, 623–635 (1976)
- [Ma3] H. Masur: Interval exchange transformations and measured foliations. *Ann. of Math.*, **115**, 169–200 (1982)
- [Ma4] H. Masur: Closed Trajectories for Quadratic Differentials with an Application to Billiards. *Duke Math. Jour.* **53**, 307–314 (1986)
- [Ma5] H. Masur: Lower bounds for the number of saddle connections and closed trajectories of a quadratic differential. In: *Holomorphic Functions and Moduli*, Vol. I (Berkeley, CA, 1986), 215–228. *Math. Sci. Res. Inst. Publ.*, **10** Springer, New York – Berlin (1988)
- [Ma6] H. Masur: The growth rate of trajectories of a quadratic differential. *Ergodic Theory and Dynamical Systems*, **10**, no. 1, 151–176 (1990)
- [Ma7] H. Masur: Ergodic Theory of Translation Surfaces. In: B. Hasselblatt and A. Katok (ed) *Handbook of Dynamical Systems*, Vol. 1B Elsevier Science B.V., Amsterdam, 527–547 (2006)
- [MaS] H. Masur, J. Smillie: Hausdorff dimension of sets of nonergodic foliations. *Ann. of Math.* **134**, 455–543 (1991)
- [MaT] H. Masur and S. Tabachnikov: Rational Billiards and Flat Structures. In: B. Hasselblatt and A. Katok (ed) *Handbook of Dynamical Systems*, Vol. 1A, Elsevier Science B.V., 1015–1089 (2002)
- [MaZo] H. Masur and A. Zorich: Multiple Saddle Connections on Flat Surfaces and Principal Boundary of the Moduli Spaces of Quadratic Differentials, Preprint [math.GT/0402197](https://arxiv.org/abs/math/0402197) 73pp (2004)
- [McM1] C. McMullen: Teichmüller geodesics of infinite complexity, *Acta Math.* **191**, 191–223 (2003)
- [McM2] C. McMullen: Billiards and Teichmüller curves on Hilbert modular surfaces. *J. Amer. Math. Soc.*, **16**, no. 4, 857–885 (2003)
- [McM3] C. McMullen: Dynamics of $SL_2(\mathbb{R})$ over moduli space in genus two. *Annals of Math.* (to appear)
- [McM4] C. McMullen: Teichmüller curves in genus two: Discriminant and spin. *Math. Ann.*, **333**, no.1, 87–130 (2005)
- [McM5] C. McMullen: Teichmüller curves in genus two: The decagon and beyond. *J. Reine Angew. Math.*, **582**, 173–199 (2005)
- [McM6] C. McMullen: Teichmüller curves in genus two: Torsion divisors and ratios of sines. *Invent. Math.* (to appear).

- [McM7] C. McMullen: Prym varieties and Teichmüller curves. *Duke Math. J.*, to appear.
- [Mil] J. Milnor: Remarks concerning spin manifolds. In: *Differential and Combinatorial Topology (in Honor of Marston Morse)*, Princeton (1965)
- [Mo1] M. Möller: Teichmüller curves, Galois actions and GT-relations. *Math. Nachrichten* **278:9**, 1061–1077 (2005)
- [Mo2] M. Möller: Variations of Hodge structures of a Teichmüller curve. *Journal of the AMS*, **19**, 327–344 (2006)
- [Mo3] M. Möller: Periodic points on Veech surfaces and the Mordell–Weil group over a Teichmüller curve. *Invent. Math.* (to appear). Eprint [math.AG/0410262](https://arxiv.org/abs/math.AG/0410262), 13 pages (2004)
- [Mum] D. Mumford: Theta-characteristics of an algebraic curve. *Ann. scient. Éc. Norm. Sup. 4^e série*, **2**, 181–191 (1971)
- [NgRd] A. Nogueira, D. Rudolph: Topological weak-mixing of interval exchange maps. *Ergodic Theory Dynam. Systems* **17**, no. 5, 1183–1209 (1997)
- [N] S. P. Novikov: The Hamiltonian formalism and a multi-valued analogue of Morse theory. *Russian Math. Surveys*, **37:5**, 1–56 (1982)
- [NM] S. P. Novikov, A. Ya. Maltsev: Topological phenomena in normal metals. *Letters to JETPh*, **63**, No. 10, 809–813 (1996)
- [O1] V. I. Oseledets (Oseledec): The spectrum of ergodic automorphisms. *Dokl. Akad. Nauk SSSR (Soviet Math. Dokl.)* **168**, 1009–1011 (1966)
- [O2] V. I. Oseledets: A Multiplicative Ergodic Theorem. Ljapunov characteristic numbers for dynamical systems. *Trans. Moscow Math. Soc.* **19**, 197–231 (1968)
- [Pa] T. Payne: Closures of totally geodesic immersions into locally symmetric spaces of noncompact type. *Proc. Amer. Math. Soc.* **127**, no. 3, 829–833 (1999)
- [Po] M. Pollicott: *Lectures on ergodic theory and Pesin theory on compact manifolds*. London Mathematical Society Lecture Note Series, **180**. Cambridge University Press, Cambridge (1993)
- [Pu] J.-Ch. Puchta: On triangular billiards, *Comment. Mathem. Helv.* **76**, 501–505 (2001)
- [Ra] G. Rauzy: Echanges d’intervalles et transformations induites. *Acta Arith.* **34**, 315–328 (1979)
- [Ru] D. Ruelle: *Chaotic Evolution and Strange Attractors*. Cambridge University Press (1989)
- [Sat] E. Sataev: The number of invariant measures for flows on orientable surfaces. *Izv. Akad. Nauk SSSR Ser. Mat.* **39**, no. 4, 860–878 (1975)
- [Schn] G. Schmihüsen: An algorithm for finding the Veech group of an origami. *Experimental Mathematics* **13:4**, 459–472 (2004)
- [Schl1] M. Schmoll: Spaces of elliptic differentials. In: “Algebraic and Topological Dynamics”, S. Kolyada, Yu. I. Manin and T. Ward (Editors), *Contemporary Math.*, Vol. 385, Amer. Math. Soc., Providence, RI, 303–320 (2005)
- [Schl2] M. Schmoll: Moduli spaces of branched covers of Veech surfaces I, II. Eprint, [arXiv.math.GT/0602396](https://arxiv.org/abs/math.GT/0602396), 40 pp, (2006)
- [Schw] S. Schwartzman: Asymptotic cycles. *Annals of Math.*, **66**, 270–284 (1957)

- [Ser] C. Series: Geometric methods of symbolic coding. In: T. Bedford, M. Keane, C. Series (ed) *Ergodic Theory, Symbolic Dynamics and Hyperbolic Spaces*. Oxford University Press, Oxford, 125–151 (1991)
- [Sin] Ya. G. Sinai: Dynamical systems with elastic reflections, *Russ. Math. Surveys*, **68**, 137–189 (1970)
- [S] J. Smillie: Dynamics of billiard flow in rational polygons. In: Ya. G. Sinai (ed) *Dynamical Systems. Encyclopedia of Math. Sciences. Vol. 100. Math. Physics 1*. Springer Verlag, 360–382 (2000)
- [Sh] N. Shah: Closures of totally geodesic immersions in manifolds of constant negative curvature. In: *Group theory from a geometrical viewpoint (Trieste, 1990)*, 718–732, World Sci. Publishing, River Edge, NJ (1991)
- [Str] K. Strebel: *Quadratic Differentials*. Springer-Verlag (1984)
- [T] S. Tabachnikov: *Billiards. Panoramas and Synthèses*. SMF (1995)
- [Ve1] W. A. Veech: Strict ergodicity in zero dimensional dynamical systems and the Kronecker-Weyl theorem mod 2. *Trans. Amer. Math. Soc.* **140**, 1–33 (1969)
- [Ve2] W. Veech: Interval exchange transformations. *Journ. Anal. Math.*, **33** 222–278 (1978)
- [Ve3] W. A. Veech: Gauss measures for transformations on the space of interval exchange maps. *Annals of Math.*, **115**, 201–242 (1982)
- [Ve4] W. A. Veech: The metric theory of interval exchange transformations I. Generic spectral properties. *Amer. Journal of Math.*, **106**, 1331–1359 (1984)
- [Ve5] W. A. Veech: The metric theory of interval exchange transformations II. Approximation by primitive interval exchanges. *Amer. Journal of Math.*, **106**, 1361–1387 (1984)
- [Ve6] W. A. Veech: Teichmüller geodesic flow. *Annals of Math.*, **124**, 441–530 (1986)
- [Ve7] W. A. Veech: Teichmüller curves in modular space, Eisenstein series, and an application to triangular billiards, *Inv. Math.* **97**, 553–583 (1989)
- [Ve8] W. A. Veech: Flat surfaces. *Amer. Journal of Math.*, **115**, 589–689 (1993)
- [Ve9] W. A. Veech: *Geometric realization of hyperelliptic curves*. *Chaos, Dynamics and Fractals*. Plenum (1995)
- [Vb1] Ya. Vorobets: Planar structures and billiards in rational polygons: the Veech alternative. *Russian Math. Surveys*, **51:5**, 779–817 (1996)
- [Vb2] Ya. Vorobets: Periodic geodesics on generic translation surfaces. In: “Algebraic and Topological Dynamics”, S. Kolyada, Yu. I. Manin and T. Ward (Editors), *Contemporary Math.*, Vol. 385, Amer. Math. Soc., Providence, RI, 205–258 (2005)
- [WYa] S. Wakon, J. Yamashita: *J. Phys. Soc. Japan*, **21**, 1712 (1966)
- [Y] J.-C. Yoccoz: Continuous fraction algorithms for interval exchange maps: an introduction. “Frontiers in Number Theory, Physics and Geometry Vol. 1”, P. Cartier; B. Julia; P. Moussa; P. Vanhove (Editors), Springer Verlag, 403–437 (2006)
- [Zo1] A. Zorich: The S. P. Novikov problem on the semiclassical motion of an electron in homogeneous Magnetic Field. *Russian Math. Surveys*, **39:5**, 287–288 (1984)

- [Zo2] A. Zorich: Finite Gauss measure on the space of interval exchange transformations. Lyapunov exponents. *Annales de l'Institut Fourier*, **46:2**, 325–370 (1996)
- [Zo3] A. Zorich: Deviation for interval exchange transformations. *Ergodic Theory and Dynamical Systems*, **17**, 1477–1499 (1997)
- [Zo4] A. Zorich: How do the leaves of a closed 1-form wind around a surface. In the collection: “Pseudoperiodic Topology”, *AMS Translations*, Ser. 2, vol. 197, AMS, Providence, RI, 135–178 (1999)
- [Zo5] A. Zorich: Square tiled surfaces and Teichmüller volumes of the moduli spaces of Abelian differentials. In collection “Rigidity in Dynamics and Geometry”, M. Burger, A. Iozzi (Editors), Springer Verlag, 459–471 (2002)

Index

- $GL^+(2, \mathbb{R})$ -action on the moduli space, 11, 28–30, 102, 104–106, 122–132
- \mathcal{H}_g – moduli space of holomorphic 1-forms, 26, 72, 104, 117, 132–134
- $\mathcal{H}(d_1, \dots, d_m)$ – stratum in the moduli space, 26, 27, 29–32, 59, 64–66, 71, 79, 81, 83, 84, 86, 90, 106, 108, 110, 134
- $\mathcal{H}_1(d_1, \dots, d_m)$ – “unit hyperboloid”, 28, 29, 31, 32, 38, 76, 82, 90, 91, 111
- \mathcal{M}_g – moduli space of complex structures, 11, 26, 32, 102–104, 106, 128
- \mathcal{Q} – moduli space of quadratic differentials, 102–106, 110, 111, 132–134
- \mathfrak{R} – (extended) Rauzy class, 54–56, 59–63, 109
- $SL(2, \mathbb{R})$ -action on the moduli space, 8, 28–30, 76, 99, 103–106, 111–113, 121, 128–134
- $d\nu$ – volume element in the moduli space, 27, 90
- $d\nu_1$ – volume element on the “unit hyperboloid”, 28, 29, 76
- ν_1, \dots, ν_g – Lyapunov exponents related to the Teichmüller geodesic flow, 36, 38, 57, 63–67
- $\theta_1, \dots, \theta_g$ – Lyapunov exponents of the Rauzy–Veech cocycle, 56–58
- Abelian differential, *see* Holomorphic 1-form
- Action on the moduli space
of $GL^+(2, \mathbb{R})$, 11, 28–30, 102, 104–106, 122–132
of $SL(2, \mathbb{R})$, 8, 28–30, 76, 99, 103–106, 111–113, 121, 128–134
- Asymptotic
cycle, 9, 33–38, 43
flag, 38, 48, 55, 139
- Billiard
counting of periodic trajectories, 13, 87–90, 132
in polygon, 7, 8, 13, 132
in rational polygon, 8, 15–17
in rectangular polygon, 87–90
table, 12, 132
L-shaped, 89, 124, 125, 130
trajectory, 8, 13–15
generic, 13, 132
periodic, 13, 17, 87–90, 132
triangular, 13, 113, 132
- Cocycle
multiplicative, 9, 56
- Cone angle, 4, 6, 14, 16, 25, 73, 79, 80
- Configuration of saddle connections or of closed geodesics, 79, 84, 86
- Conical
point, *see* Conical singularity
singularity, 4, 6, 14, 16, 20, 21, 25, 27, 80–81, 120
- Connected component of a stratum, *see* Moduli space: connected components of the strata

- Connection
 - saddle connection, *see* Saddle connection
- Continued fraction, 10, 50, 58, 67–69
- Cusp of the moduli space, *see also* Moduli space; principal boundary, 10, 24, 31, 69, 79, 83–87
- Cycle
 - asymptotic, *see* Asymptotic cycle
 - relative, 25
- Degree of zero, 25
- Diagonal
 - generalized, 13, 87
- Diagram
 - separatrix diagram, 94
- Differential
 - Abelian, *see* Holomorphic 1-form
 - quadratic, *see* Holomorphic quadratic differential
- Dimension of a stratum, 26
- Direction
 - completely periodic, 32
 - vertical, 7, 25, 38
- Discriminant, 129
- Ergodic, 5, 13, 29, 132, 135
 - multiplicative ergodic theorem, 9, 11, 56, 138–140
 - uniquely ergodic, 8, 32, 70, 135
- Exponent
 - Lyapunov exponent, 9, 11, 36, 38, 56–58, 63–67, 137
- Fagnano trajectory, 13
- Fermi-surface, 8, 12, 18, 20
- Flag
 - asymptotic, 38, 48, 55, 139
 - Lagrangian, 38, 57
 - of subspaces, *see* Flag; asymptotic
- Flat surface, 7
- Flow
 - ergodic, 31
 - minimal, 31, 70
 - Teichmüller geodesic flow, *see* Teichmüller geodesic flow
 - uniquely ergodic, 70
- Foliation
 - defined by a closed 1-form on a surface, *see* Foliation: measured foliation
 - horizontal, 21
 - kernel foliation, 116
 - measured foliation, 8, 19–21
- Form
 - holomorphic 1-form, *see* Holomorphic 1-form
- Formula
 - of Gauss–Bonnet, 25
 - of Siegel–Veech, 10, 77
- Gauss–Bonnet formula, 25
- Generalized diagonal, 13
- Geodesic, 5
 - closed, 5, 17, 69–79, 81–87
 - complex geodesic, 11, 103, 106, 112
 - counting of periodic geodesics, 5, 69–79
 - generic, 5, 33
 - in flat metric, 8, 14
- Half-translation surface, 7, 100–101, 110, 133
- Holomorphic
 - 1-form, 8, 27
 - differential, *see* Holomorphic 1-form
 - quadratic differential, 100, 101
- Holonomy, 4–7, 14, 15, 100
- Hyperelliptic
 - connected component, 108
 - involution, 108
 - surface, 108
- Integer point of the moduli space, *see* Lattice in the moduli space
- Interval exchange map, *see* Interval exchange transformation
- Interval exchange transformation, 9, 40–55
 - space of, 47, 50, 54–56, 58, 59, 61, 62
- Katok–Zemliakov construction, 16, 87
- Kernel foliation, 116
- Lagrangian
 - flag, 38, 57
- Lattice
 - in the moduli space, 10, 90, 91
 - subgroup, 103

- Lyapunov exponent, 9, 11, 36, 38, 56–58, 63–67, 137
- Metric
 - flat, *see* Surface: flat; very flat
 - Teichmüller metric, 10, 101
- Moduli space
 - connected components of the strata, 38, 55, 87, 111, 133
 - integer point of, *see* Lattice in the moduli space
 - of Abelian differentials, *see* Moduli space of holomorphic 1-forms
 - of complex structures, 11, 26, 32, 102–104, 106, 128
 - of holomorphic 1-forms, 8, 10, 26, 72, 103, 104, 117, 132–134
 - of quadratic differentials, 10, 87, 102–106, 110, 111, 132–134
 - principal boundary of the moduli space, *see also* Cusp of the moduli space, 10, 84–87
 - volume of the moduli space, 10, 28, 90–92, 97–99
- Multiplicative cocycle, *see* Cocycle: multiplicative
- Multiplicative ergodic theorem, 9, 11, 56, 138–140
- Period, 26, 81
 - absolute, 26
 - relative, 27, 32, 115, 119
- Pesin theory, 140
- Polygon
 - rational, 8, 15
 - rectangular, 87–90
- Polygonal billiard, *see* Billiard in polygon
- Principal boundary of the moduli space, *see* Moduli space: principal boundary
- Quadratic differential, *see* Holomorphic quadratic differential
- Quasiconformal
 - coefficient of quasiconformality, 99, 101
 - extremal quasiconformal map, 10, 99, 101
- Rational polygon, *see* Polygon: rational
- Rauzy class, 54, 55, 63, 109, 111
 - extended Rauzy class, 55
- Rauzy–Veech induction, 9, 50
- Relative
 - cycle, 25
 - homology group, 25
- Renormalization, 9, 44–50, 132
- Saddle
 - connection, 21, 32, 69–79, 81–87
 - point, *see* Conical singularity
- Separatrix, 21
 - diagram, 94
- Siegel–Veech
 - constant, 72–79, 89
 - formula, 10
- Singularity
 - conical, *see* Conical singularity
- Space of interval exchange transformations, *see* Interval exchange transformation: space of
- Square-tiled surface, 10, 91, 112, 113, 115, 119, 121, 123, 129–131, 134
- Stratum
 - connected component, *see* Moduli space: connected components of the strata
 - in the moduli space, 26–29, 31, 32, 38, 59, 64–66, 71, 76, 79, 81–84, 86, 90, 91, 106, 108, 110, 111, 134
- Stratum in the moduli space, 8
- Surface
 - Fermi-surface, 8, 12, 18, 20
 - flat, 7, 21, 23
 - half-translation, 7, 100–101, 110, 133
 - square-tiled, 10, 91, 112, 113, 115, 119, 121, 123, 129–131, 134
 - translation, *see* Very flat
 - Veech, 10, 11, 86, 111–115, 121–131, 133
 - very flat, 6, 15–17, 21
- Teichmüller
 - disc, 11, 103, 105, 112
 - geodesic flow, 9, 10, 29, 31, 32, 38, 58–67, 99, 102, 103, 135
 - metric, 10, 101
 - theorem, 10

- Theorem
 - multiplicative ergodic, 9, 11, 56, 138–140
 - Teichmüller, 10
- Theory
 - Pesin theory, 140
- Trajectory
 - billiard trajectory, 13, 87–90, 132
 - Fagnano trajectory, 13
- Translation surface, *see* Surface: very flat
- Unit hyperboloid, 28, 29, 31, 32, 38, 76, 82, 90, 91, 103, 111
- Veech
 - group, 111, 112
 - surface, 10, 11, 111–115, 121–131, 133
 - nonarithmetic, 130
- Vertical direction, *see* Direction: vertical
- Very flat surface, *see* Surface: very flat
- Volume element
 - in the moduli space, 27
 - on the “unit hyperboloid”, 28
- Volume of a stratum, *see* Moduli space: volume of the moduli space
- Zero, 25, 27
 - degree of zero, 25
- Zippered rectangle, 9, 42, 50, 54, 55, 59–63

